

**Toll-like Receptor (TLR)7 and TLR8 Stimulation of Mucosal-Associated Invariant T cells
and Gamma Delta T cells: A Role in HIV Susceptibility**

by

Zipporah Bosibori Richard

A Thesis Submitted to the Faculty of Graduate Studies of

The University of Manitoba

in partial fulfilment of the requirements of the degree of

Doctor of Philosophy

Department of Medical Microbiology and Infectious Diseases,

University of Manitoba

Winnipeg

Copyright © 2022 by Zipporah Richard

Abstract

Host inflammation has been shown to increase the risk of HIV-1 acquisition. Innate T cells are positioned to respond early to infections and produce proinflammatory cytokines associated with end-organ inflammation and increased risk of HIV infection. Therefore, understanding activation of innate T lymphocytes and their role in immune modulation and HIV infection is important for the development of an effective intervention against HIV transmission. The response of mucosal-associated invariant T (MAIT) cells to toll-like receptor (TLR) 7/8 stimulation may lead to the increased activation, depletion, and impaired functionality of MAIT cells observed during acute HIV infection. Stimulation of MAIT cells after TLR8 stimulation may also have implications to the reduced acquisition of HIV in HIV-exposed seronegative (HESN) subjects: it was reported that peripheral blood mononuclear cells (PBMCs) from HESN were hyporesponsive to TLR7 (resulting in reduced cytokine responses to the corresponding ligands) but hyperresponsive to TLR8 following stimulation with ssRNA40. Proinflammatory cytokines have been shown to increase the numbers of HIV target cells in the mucosa, reduce mucosal integrity, and increase HIV replication in infected cells, resulting in effective transmission and acquisition of the virus. This Thesis is a comparison of TLR 7 and TLR8, both which have been shown to recognize HIV genetic material, responses in innate T cells in PBMCs from healthy blood donors. Here is the hypothesis tested that TLR7 or TLR8 stimulation of PBMCs or monocyte-derived dendritic cells (MDDC) will lead to increased major histocompatibility complex (MHC) related protein 1 (MR1), which is a ligand for MAIT cell recognition on the membrane of antigen-presenting cells (APCs), and/or the expression of IL-12 and IL-18. Further, TLR7 and TLR8 stimulation of PBMCs will lead to stimulation of innate T cells, leading to an increase in proinflammatory cytokines, increased immune activation, and increased HIV infection *in vitro*.

The results demonstrated that MAIT cells were highly activated by both TLR7 and TLR8, as evidenced by increased CD69 expression, but only TLR8 stimulation resulted in elevated cytokine responses. Gamma/delta ($\gamma\delta$) T cells were found to be hyporesponsive to both TLR7 and TLR8 stimulation, as evidenced by reduced CD69 and cytokine responsiveness. MAIT and $\gamma\delta$ T cells therefore differed in their ability to respond to TLR7/8 stimulation. In contrast, TLR8 stimulation of PBMCs in the presence of interleukin 7 (IL-7) led to expression of interferon gamma (IFN- γ),

suggesting TLR responses mediated via MAIT/ $\gamma\delta$ may be a key component in reduced susceptibility to HIV.

These results demonstrate that although innate T cells are known to respond and protect against bacterial infections, they may also be activated during HIV infection, and their response may result in the activation of other immune cells resulting in enhanced HIV infection in vitro, supporting the overall hypothesis tested. This Thesis contributes to growing knowledge of the outcomes of TLR7 and TLR8 stimulation and the role of MAIT and $\gamma\delta$ T cell activation with respect to HIV infection, which could be critical information in the design of HIV vaccines, microbicides, or other interventions.

Acknowledgements

I would like to express my deep and sincere gratitude to my advisor Dr. Blake T. Ball for the continuous support of my PhD studies and research and his immense knowledge, patience, and motivation. His guidance and patience with me have helped in all the times of research and writing. I also wish to show my sincere and deep appreciation to my committee, Dr. Keith Fowke and Dr. Abdelilah Soussi Gounni, for their encouragement, support, and insightful questions and comments. The helpful professional editing of Karen Limbert Rempel is acknowledged with appreciation.

I thank current and past members of the Ball lab for their direct or indirect contributions to this project through physical, intellectual, or moral support. Especially Dr. Ruey Su, Dr. Catherine Card, Dr. Xufen Yang, Dr. Sandra Gonzales and Bernard Abrenica, Sue Ramdahin, Dr. Jennifer Juno, Dr. Were Omango, and Christine Mesa, for their time and patience in teaching me different techniques. I also thank Margot Plews and Winnie Apidi, Andrew Plesniarski, Abu Sadik, Dr. Florence Mutua, Max Abou, and all the other members of our lab. I would like to specifically thank Jude Zieske, Angela Nelson, Sharon Tardi, Eva Lindsey, Cheryl Reimer, Natasha Hollett, Carmen Lopez, and all the Department of Medical Microbiology staff, who made my learning enjoyable and my stay in Winnipeg pleasant, often by extending a hand of friendship over and above their duty.

I thank all members of the UNITID Nairobi lab, particularly; Dr. Joshua Kimani, Dr. Julius Oyugi, Dinah Amwayi, Maureen Njoga, Festus Kiogora, Erastus Irungu, Anne Maingi, Jemimah v Nyakio, Nancy Kayere, Cecilia Olangida, Ernest Lutomia, Marion Makobe, Peter Wambugu, Keneth Oduor, Dominic Ouma, Lucy Mwangi, Antony Kariri, Ricky Kitsao, Kevin Kamau, and the entire IT and data team.

I thank my fellow trainees of the International Infectious Diseases and Global Health training program (IID and GHTP). They enriched my learning experience and broadened my perspectives during joint presentations and day-to-day interactions within the program.

Last but not least, I would like to thank my family for their support, encouragement, and constant motivation that made it possible to complete this PhD, including my parents, Hebisibah Machuki and Billy Stephens Machuki, my brothers and sisters Irene, Denis, and Ayorah.

Dedication

This Thesis is dedicated to my children, Esther, Mary-Shine, and Mauwa, who have been my inspiration. You have made me stronger, better, and more fulfilled than ever imagined.

Table of Contents

Abstract.....	i
Acknowledgements.....	iii
Dedication.....	v
List of Figures.....	x
List of Tables.....	xiii
Chapter 1: Introduction and Literature Review.....	1
1.1 Human immunodeficiency virus.....	1
1.1.1 Origin and history of HIV.....	1
1.1.2 Epidemiology of HIV.....	1
1.1.3 HIV structure and genome.....	2
1.1.4 HIV life cycle.....	4
1.1.5 Correlates of protection against HIV.....	5
1.2 Human immune system.....	6
1.2.1 Innate immunity.....	7
1.2.2 Adaptive immune system.....	26
Chapter 2: Rationale, Hypothesis, and Objectives.....	51
2.1 Hypothesis.....	51
2.1.1 Sub-hypotheses.....	52
2.2 Objectives.....	52
Chapter 3: Materials and Methods.....	53
3.1 Study participants.....	53
3.2 Ethics statement.....	53
3.3 General reagents.....	53
3.3.1 TLR agonists and other stimulants.....	53
3.3.2 Culture media and tissue processing reagents.....	54
3.3.3 Flow cytometry reagents.....	55
3.3.4 Monocyte isolation kit.....	55
3.3.5 HIV p24 Enzyme Linked Immunosorbent Assay (ELISA) reagents Kit (Cat# 5447, Advanced Bioscience Laboratories (ABL), Rockville, MD).....	56
3.3.6 Human IL-18 duo set ELISA kit (R&D Systems Cat# DV318, Minneapolis, MN)....	57
3.3.7 IL-12(p70) reagents and kit.....	58
3.4 Routine procedures.....	59

3.4.2	PBMC isolation.....	59
3.4.3	TLR stimulation and cell culture	60
3.4.5	Flow cytometry.....	60
	74
3.4.6.	Monocyte enrichment.....	75
3.4.7.	HIV assays.....	75
3.5	Data and statistical analysis.....	80
3.5.1	tSNE analysis.....	80
Chapter 4	Results	81
4.1	Defining MAIT cells by surrogate markers	81
4.1.1	Confirmation of MAIT cells by MR1 tetramer	83
4.1.2	MAIT cell subsets.....	86
4.1.3	Gamma delta T cells were gated as CD3+ $\gamma\delta$ TCR+ cell.....	89
4.1.4	Frequency of MAIT cells in healthy donors.....	92
4.1.5	Frequency of $\gamma\delta$ T cells in health adult peripheral blood	94
4.2.	Differential response of MAIT and $\gamma\delta$ T cells in bulk PBMC culture to TLR7 and TLR8 stimulation.....	96
4.2.1.	Rationale.....	96
4.2.2.	Hypothesis	96
4.2.3.	Time course and establishing MAIT cell culture conditions.....	96
4.2.4.	MAIT cells are highly activated following TLR 7/8 stimulation.....	99
4.2.5	Heterogeneity of MAIT cell activation as revealed by tSNE, UMAP and TriMap analysis	102
4.2.6.	MAIT cells express IFN- γ following TLR8 stimulation.....	105
4.2.7	Analysis of cytokine expression on MAIT cells by tSNE.....	108
4.3	Time course and establishing $\gamma\delta$ T cell culture conditions	111
4.3.1.	TLR7 and TLR8 lead to activation of $\gamma\delta$ T cells.....	113
4.3.2.	Analysis of $\gamma\delta$ T cell CD69 expression after stimulation by tSNE	116
4.3.3.	TLR8 but not TLR7 stimulates IFN- γ expression by $\gamma\delta$ T cells.....	118
4.3.4	Analysis of $\gamma\delta$ T cell cytokine expression after stimulation by tSNE	121
4.4	MAIT cells supplemented with IL-7 express high IFN- γ , TNF- α , IL-17a and GM-CSF after TLR8 stimulation.....	124

4.4.1 $\gamma\delta$ T cells in media supplemented with IL-7 express high IFN- γ , IL-17a, and GM-CSF after TLR8 stimulation	127
4.4.2 MAIT and $\gamma\delta$ T cells cultured in media supplemented with IL-7 express higher levels of IFN- γ , IL-17a, and GM-CSF after TLR8 stimulation compared to conventional CD4+ and CD8+ T cells.....	129
4.4.3. Analysis of cytokine expression by MAIT cells by tSNE.....	133
4.4.4 Analysis of $\gamma\delta$ T cells cytokine expression by tSNE.....	136
4.4.5 Frequency of IFN- γ +, TNF- α +, IL-17a+ and GM-CSF+ $\gamma\delta$ T cells by different subsets of $\gamma\delta$ T cells in IL-7 supplemented media	138
4.4.6 Frequency of CD69+ $\gamma\delta$ T cells in different subsets of $\gamma\delta$ T cells.....	141
4.5 MAIT cells and $\gamma\delta$ T cells express high chemokine receptors.....	143
4.5.1. Downregulation of surface CCR5 on MAIT cells after TLR8 stimulation.....	146
4.5.2. CCR5 is downregulated on MAIT cells and CD4+ T cells after stimulation	148
4.6 Summary	150
Chapter 5: TLR8 Stimulation Results in Higher Maturation Markers on Monocyte-derived Dendritic Cells Compared to TLR7 Stimulation	151
5.1 Rationale.....	151
5.2 Hypothesis.....	151
5.3 Objectives.....	151
5.4 Results	152
5.4.1 Monocyte enrichment.....	152
5.4.2 Monocyte differentiation	154
5.4.3 Monocyte-derived maturation	154
5.4.4 Analysis by tSNE	158
5.4.5 MDDCs matured by TLR8 stimulation express high IL-12p70 compared to TLR7 stimulation	160
Chapter 6: HIV Infection Assay	162
6.1 Rationale.....	162
6.1.1 Pure MAIT and CD4+ cells sorted from blood of healthy blood donors.....	162
6.2 Lower HIV-1p24+ CD4+ T cells in unstimulated CD4+ T cell co-cultured with activated MAIT cells	164
6.2.1 No effect on HIV-1 infection in CD4+ T cells co-cultured with MAIT cells	167
Chapter 7 General Discussion, Conclusion, Limitations, and Significance	169
7.1 Discussion	169

surrogate 7.1.1 Use of markers to identify MAIT cells leads to overestimation of MAIT cells compared to use of MR1 Ag-loaded tetramers.....	169
7.1.2 MAIT cells and $\gamma\delta$ T cells express high levels of chemokine receptors	178
7.1.3 TLR8 stimulation results in higher MDSC maturation markers compared to TLR7 stimulation	181
7.1.4 Lower HIV-1p24+ CD4+ T cells in unstimulated CD4+ T cell co-cultured with activated MAIT cells	183
7.1.5 A proposed role for unconventional MAIT and $\gamma\delta$ T cell stimulation in immune activation and HIV infection	184
7.2 Conclusion.....	188
7.3 Limitations	188
7.4 Significance.....	189
7.5 Future directions.....	190
Appendix 1: List of Abbreviations	xiv
Appendix 2 : IL-12p70 ELISA Analysis	xix
Appendix 3: IL-18 ELISA analysis	xx
Appendix 4 : HIV-1 p24 ELISA analysis.....	xxi

List of Figures

Figure 1.	Human immunodeficiency virus.....	4
Figure 2.	TLR signaling pathway.....	21
Figure 3.	TCR-dependent and -independent activation of MAIT cells.....	43
Figure 4.	Expression of a wide range receptors by $\gamma\delta$ T cells.....	46
Figure 5.	Fluorescence minus one (FMO) gating for: $\gamma\delta$ TCR PE Cy5, BV650 CD8, BV605 CD4, BV421 CD161, and PerCP-/Cyanine5.5 V α 7.2TCR	64
Figure 6.	Fluorescence minus one (FMO) gating for CCR5+, CCR4+, CCR6+, CXCR3+ and CXCR6+ -MAIT cells and - $\gamma\delta$ T cells.....	67
Figure 7.	Fluorescence minus one (FMO) gating for CD69+, CCR5+ and CCR6+ MAIT cells and CD69+, CCR5+ and CCR6+ $\gamma\delta$ T cells.....	70
Figure 8.	Fluorescence minus one (FMO) MAIT and CD4+ T cells.....	72
Figure 9.	Fluorescence minus one (FMO) gating strategy for MDDCs	74
Figure 10.	MAIT cells defined by surrogate markers.....	82
Figure 11.	Ag-specific identification of MAIT cells.....	85
Figure 12.	MAIT cells are predominantly CD8+ and CD4-CD8-(DN)	88
Figure 13.	Two subsets of $\gamma\delta$ T cells defined by $\gamma\delta$ TCR as $\gamma\delta$ TCR ^{high} and $\gamma\delta$ TCR ^{low}	91
Figure 14.	Variability in peripheral blood mucosal-associated invariant T (MAIT) cells frequency in healthy blood donors.....	93
Figure 15.	Proportion of Variability in $\gamma\delta$ T cells frequency in peripheral blood between different donors.....	95
Figure 16.	Increasing CD69+ MAIT cells with time over the course of a 24 h stimulation	98
Figure 17.	MAIT cells are highly activated following stimulation compared to CD4 and CD8 cells.....	101
Figure 18.	Heterogeneity in MAIT cell activation. Heatmap of MAIT cell expression of CD69 after stimulation represented by t-SNE, UMAP, and TriMap	104
Figure 19.	Expression of cytokines by circulating MAIT cells in PBMC after stimulation.....	107
Figure 20.	TLR8 stimulation of PBMC with highest dose of ssRNA40 used resulted in a small subset of MAIT cell expressing IFN- γ	110

Figure 21.	21Increasing frequency of CD69+ $\gamma\delta$ T cells over the course of 24 h stimulation	112
Figure 22.	Highly activated $\gamma\delta$ T cells following stimulation compared to CD4 and CD8 cells.....	115
Figure 23.	Heterogeneity in $\gamma\delta$ T cells activation. Heatmap of CD69 expression by $\gamma\delta$ T cells after TLR7, TLR8, <i>E. coli</i> and PMA/Ion stimulation.....	117
Figure 24.	Cytokine expression by $\gamma\delta$ T cells after stimulation.....	120
Figure 25.	TLR8 stimulation of PBMC with highest dose of ssRNA40 used resulted in a small subset of $\gamma\delta$ T cell expressing IFN- γ	123
Figure 26.	Increased frequency of IFN- γ + IL-17a, and GM-CSF+ MAIT cells after TLR8 stimulation	126
Figure 27.	Increased frequency of IFN- γ + and GM-CSF+ $\gamma\delta$ T cells following TLR8 stimulation.	128
Figure 28.	MAIT cells and $\gamma\delta$ T cells express higher IFN- γ , TNF- α , IL-17a and GM-CSF following stimulation compared to conventional T cells.....	132
Figure 29.	Heatmap of MAIT cell cytokine expression after stimulation, with tSNE analysis.....	135
Figure 30.	Heatmap of tSNE analysis of $\gamma\delta$ T cells cytokine expression after stimulation.	137
Figure 31.	IFN- γ + CD161+ $\gamma\delta$ T cells trending after TLR8 stimulation.....	140
Figure 32.	Higher CD69 frequency of CD161+ $\gamma\delta$ T cells after stimulation.....	142
Figure 33.	Frequency of chemokine expressing MAIT cells is high compared to conventional CD4 and CD8 T cells.....	145
Figure 34.	MAIT cell surface expression of CCR5 is significantly downregulated after 14h stimulation.....	147
Figure 35.	Frequency of CCR5+ MAIT cells downregulated following stimulation.....	149
Figure 36.	CD14+ staining of <i>ex vivo</i> PBMCs and enriched monocytes.....	153
Figure 37.	Light microscope images of monocyte differentiation day 0, day 2 and 4.....	154
Figure 38.	Increased expression of maturation markers on MDDCs after stimulation	157
Figure 39.	Heatmap of tSNE analysis of MDDCs.....	159
Figure 40.	High IL-12p70 expression after DC maturation with TLR8 compared to TLR7 stimulation.....	161
Figure 41.	Gating strategy for sorting pure populations of MAIT cells and CD4+ T cells	163

Figure 42. Downmodulation of CD4 receptor following HIV infection..... 166

Figure 43. HIV-1 p24 expression by CD4+ T cells co-cultured with MAIT cells..... 168

Figure 44. Proposed role for MAIT and $\gamma\delta$ T cell stimulation in immune activation and HIV susceptibility..... 187

List of Tables

Table 1.	Subsets of gamma delta T cells	47
Table 2.	Flow cytometry antibody panel	60
Table 2.1	T cell activation and chemokine receptor panel	61
Table 2.2.	ICS cytokine panel	61
Table 2.3.	Chemokine receptor surface staining panel	61
Table 2.4.	MAIT cell and CD4+ T cells sorting panel	62
Table 2.5.	Monocyte purity panel	62
Table 2.6.	Monocyte-derived dendritic cell (MDDC) maturation panel	62
Table 3.	HIV-p24 ELISA results	76
Table 4.	Cell mortality ratio calculation	76

Chapter 1: Introduction and Literature Review

1.1 Human immunodeficiency virus

1.1.1 Origin and history of HIV

Human immunodeficiency virus (HIV) type 1 and 2 are lentiviruses that cause acquired immunodeficiency syndrome (AIDS) (1).

AIDS was first described in 1981 in a group of men who had sex with men (MSM), who presented with opportunistic infection caused by *Pneumocystis carinii* and a relatively rare cancer called Kaposi sarcoma in New York and San Francisco (2,3). Thus, AIDS was initially associated with men who have sex with men (3–5), then with drug users (6), people who had received blood transfusions (5), and finally, the general population (7). The causative agent, HIV-1 and HIV-2, resulted from cross-species transmission of a closely related simian immunodeficiency virus (SIV) into humans, probably due to the hunting and butchering of primates for bushmeat, which likely led to infectious viruses present in raw primate meat coming into contact with human mucosal tissues (8).

HIV-1 occurs globally, while HIV-2 is found primarily in West Africa (8). HIV-1 is further grouped into four groups (M, N, O, and P) (9). HIV-1 groups M, N, and O came about likely due to cross-species transmission of SIV from chimpanzees (10), and P came from gorillas (11). The HIV-1 group major (M) consists of 11 clades – A, B, C, D, E, F, G, H, I, J, and K – and is responsible for most HIV infection globally (12). HIV-1 groups outlier (O), nonmajor, nonoutlier (N), and P mainly occur in West Africa (9). For this Thesis, HIV-1 will be referred to only as HIV, unless otherwise stated.

1.1.2 Epidemiology of HIV

According to UNAIDS, by the end of 2020 there were 1.7 million (1.2 million–2.2 million) new HIV infections per year worldwide (13). Despite new HIV cases of infection having been reduced to the lowest level since the peak in 1989 and declining by 23% since 2010, the rate per year of new infections has remained consistent. Furthermore, the estimated new infection rate per year is still three times higher than the UNAIDS 90-90-90 target of less than 500,000 new infections per

year needed to end the AIDS epidemic by 2020. Although many countries are making remarkable progress, many fail or are unable to adopt proven methods for preventing HIV infection at the required scale (13), suggesting that novel HIV prevention methods are still urgently required.

Some populations have made better progress than others in reducing the number of new HIV infections, e.g., the annual number of new infections among women and girls (a 27% decrease since 2010) declined more rapidly than among men and boys (an 18% decrease) worldwide. Globally, in 2019, 48% of total infections were among women and girls compared to 52% among men and boys. Most of these new infections were still occurring in sub-Saharan Africa. Although only 9% of new infections occurred in children (aged 0 to 14 years) in 2019, most of these (84%) occurred also in sub-Saharan Africa (13).

Nevertheless, the reduction of new infections worldwide is primarily due to a decrease of new infections in eastern and southern Africa (a 38% reduction since 2010), in the Caribbean (29%), western and central Africa (25%), western and central Europe and North America (15%), and Asia and the Pacific (12%). However, the epidemic has continued to grow in eastern Europe and central Asia, with new HIV infections rising by 72% between 2010 and 2019, in the Middle East and North Africa (22%), and in Latin America (21%) (13). Due to the success of HIV treatment programs, progress has also been made in reducing AIDS-related deaths from 1.7 million (1.3 million–2.4 million) in 2004 and 1.2 million (860,000–1.6 million) in 2010 to 770,000 (570,000–1.1 million) in 2018. However, HIV/AIDS still was the leading cause of death among all infectious diseases (14). Further, the progress made so far in reducing AIDS-related deaths could be easily reversed due to the COVID-19 pandemic seriously disrupting the AIDS response. Even a 20% disruption of HIV care and treatment programs could cause an additional 110,000 deaths; alarmingly, a six-month complete disruption in HIV care and treatment could generate more than 500,000 other deaths in sub-Saharan Africa over the next year (2020–2021), bringing the region back to 2008 AIDS mortality levels (15).

1.1.3 HIV structure and genome

HIV is a member of the Retroviridae family, subfamily orthoretroviridae, in the genus of lentivirus (16). HIV is spherical with a diameter of 100 nm and has a lipid envelope derived from the host

cell plasma membrane during budding (17). The virus envelope is embedded with trimeric transmembrane proteins gp41 (stalk) (Figure 1) and gp120 (head), forming projections (18). Beneath the envelope are matrix protein p17 (19) and core proteins p24 and p6, and nucleocapsid protein p7 (20). Inside the virus core are two copies of positive-sense viral RNA genome together with three enzymes: integrase (IN), reverse transcriptase (RT), and protease (PR) and five accessory proteins; viral infectivity protein (Vif), viral protein R (vpr), transactivator of transcription (tat), regulator of viral protein expression (Rev), and negative regulatory factor (Nef). An additional protein found in HIV-1 but not HIV 2 is viral protein u (vpu) (21–23).

The HIV genome contains nine open reading frames (ORF) – *gag*, *pol*, *vif*, *vpr*, *vpu*, *env*, *nef*, *rev*, and *tat*, encoding 19 different proteins (24). Three genes, *gag*, *pol*, and *env*, encode structural proteins for new virus particles (25). An example of gene that encodes structural proteins is the *gag* gene, which encodes the Gag protein that is cleaved to produce four structural proteins: p17, p24 (capsid), p7 (nucleocapsid), and p6 (26). The *env* gene encodes a polyprotein, gp160, that is later cleaved by PR into gp120 and gp41 (27), and the *pol* gene encodes three viral enzymes, PR, IN, and RT (28). The remaining six genes, *vif*, *vpr*, *vpu*, *nef*, *rev*, and *tat*, are regulatory genes that encode for proteins involved in controlling the ability of HIV to infect cells, replicate, and cause disease (20,29,30).

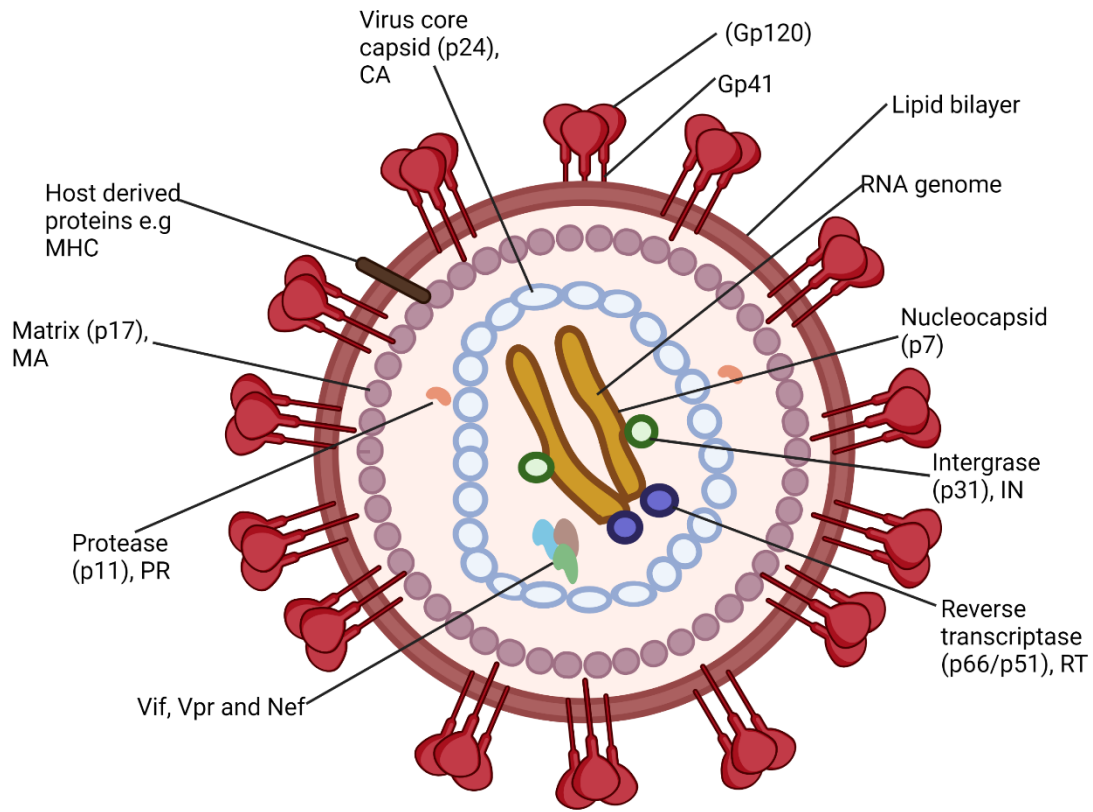


Figure 1. Human immunodeficiency virus. HIV is a roughly spherical and enveloped virus with trimeric projections consisting of gp120 (head) and gp41 (stalk) and specific host proteins such as MHC molecules incorporated into the viral envelope. A layer of matrix protein (p17 or MA) found beneath the envelope bilayer surrounds a cone-shaped virus core made up of p24 protein. The virus core contains two positive-sense RNA strands encapsulated by a nucleocapsid (p7 protein), enzymes: integrase (p31, IN), reverse transcriptase (p66/p51, RT) and protease (p11, PR), and accessory proteins (Vif, Vpu, Vpr, Tat, and Nef). **Adapted from (31)**

1.1.4 HIV life cycle

HIV replication begins when HIV encounters CD4⁺ host cells and is divided into 10 distinct steps: (i) binding, (ii) fusion and entry, (iii) uncoating, (iv) reverse transcription, (v) nuclear entry, (vi) integration, (vii) transcription of viral DNA, (viii) viral protein synthesis, (ix) budding, and (x) virion maturation. The first step in replication is HIV entry into the target cells which begins with gp120, on the virus's surface, binding to a CD4 receptor, which is primarily expressed on CD4⁺ T cells or macrophages. This leads to conformational changes on gp120, thus exposing a chemokine binding domain on gp120 and enabling interaction between the host CCR5 and the viral gp120-CD4 complex for HIV strains that utilize CCR5 as co-receptor (also known as R5 HIV

virus) or between CXCR4 and gp120-CD4 complex for HIV-1 strains that utilize CXCR4 as co-receptor (also known as X4 HIV) (32). The gp120-CD4 complex is stable, allowing the N-terminal end of gp41 to penetrate the plasma membrane (33). The conformational change in gp41 leads to the interaction of the viral envelope and plasma membrane of the target cell, fusion of viral and host membrane, and insertion of the viral core into the cytoplasm (34,35). Uncoating of the capsid proteins follows, thus releasing the viral RNA (36–38). Reverse transcription begins with the viral ssRNA being converted into a double-stranded DNA that enters the nucleus. The proviral DNA is integrated into the host genome to form a provirus by the viral enzyme integrase (36,39). After successful integration, transcription of the proviral DNA is initiated at a promoter site termed the long terminal repeat (LTR) through a complex process involving a viral transactivator of transcription (Tat) and several host transcription factors, including NF- κ B leading to new progeny virions and viral mRNA transcripts (40).

The viral mRNA transcripts are exported out of the nucleus, with the help of the Rev protein, as spliced, partially spliced, or unspliced RNA (41). They are translated by cellular ribosomes, giving rise to different viral proteins. Once in the cytosol, Rev is released from the mRNA and transported back into the host nucleus (42,43). The Gag-derived protein MA initiates viral packaging and assembly on the inner surface of the plasma membrane (44). The virus core is assembled from the gag-pol protein by incorporating Vif, Vpr, and Nef and genomic viral RNA to form the immature virion, which then buds off the plasma membrane, producing new but immature virions (45). The budding of the new virion is followed by the initiation of virus maturation, during which the Gag-Pol polyprotein is cleaved by viral protease (PR) to produce structural proteins MA, CA, and NC, which then make up the viral core, and viral enzymes IN, RT and PR (46,47). The mature virion can then infect a new target cell, thereby initiating a new replication cycle.

1.1.5 Correlates of protection against HIV

Like any other infectious disease, exposure to HIV leads to different outcomes. Some individuals who are infected after repeated exposure and without treatment show varying progression rates to AIDS (48). Others may get infected, but they develop a markedly prolonged course of infection that does not show signs or symptoms of AIDS despite the absence of therapy and are referred to as long-term non-progressors (LTNP) (49). Finally, some individuals are not infected despite

repeated exposure and are referred to as HIV-exposed seronegative (HESN); these include the women from the well-described Majengo cohort, who can be epidemiologically defined as relatively resistant to HIV (50,51). HESN individuals have been identified in different cohorts, including intravenous drug users (52), health care workers accidentally exposed to HIV (53), homosexuals or heterosexual subjects that have unprotected sex with their seropositive partners (54,55), children born to HIV-infected mothers exposed through natural birth and/or breast feeding (56–58), and hemophiliacs who had received HIV-contaminated anti-clotting factors (59). Thus, understanding the factors responsible for resistance to HIV acquisition and progression would be critically important in offering new insights into HIV transmission as they would facilitate the design of preventive measures, including effective vaccines to protect against HIV infection.

Understanding strategies to prevent and reduce susceptibility to HIV-1 infection is paramount in controlling the pandemic. However, defining immune protection correlations against HIV has proved difficult due to the diversity of the exposure routes and varied epidemiological backgrounds of HIV-exposed, uninfected subjects (60). Individuals meeting the HESN definition are individuals who lack anti-HIV immunoglobulin (IgG) seropositivity or evidence of infection despite being repeatedly exposed to HIV and/or are frequently involved in high-risk behavior in high HIV prevalence areas (61). Thus, HESN subjects may have mucosal IgA responses to HIV, but they must be HIV IgG seronegative systemically and HIV-negative by ultrasensitive polymerase chain reaction (PCR) testing (55). Exposure to HIV may be quantified in some studies of HIV-discordant couples and hemophiliacs (60,62). However, other studies, primarily in commercial sex workers and IV drug users, have inferred exposure to HIV based on mathematical models of high-risk activity frequency and the prevalence of HIV in the community being studied (63–65).

1.2 Human immune system

The human immune system is classified into two general types, depending on the response speed and specificity: the innate and adaptive immune systems (66). Both the innate and adaptive immune systems work together to protect the body from harmful microorganisms. The innate immune system informs the development of the adaptive immune system (67). Although the term innate immunity may refer to physical, chemical, and microbiological barriers, in many cases, it is used to imply the elements of the immune system (e.g., neutrophils, monocytes, macrophages,

complement, cytokines, and acute-phase proteins) that provide immediate host defense (68). The innate immune system is essential for survival, as it is found even in single-celled organisms as well as invertebrates and vertebrates (69). The adaptive immune system is present in higher animals and consists of antigen-specific reactions through T lymphocytes and B lymphocytes (70). Although the innate immune system can also have aspects similar to adaptive immune system, such as memory in natural killer (NK) cells and trained immunity in macrophages and other cell types, it is more rapid and may cause damage to the tissue due to a lack of specificity. The adaptive immune system takes longer to develop, is more specific and has memory (71,72). Bridging the innate and adaptive immune system are the innate-like lymphocytes, consisting mainly of gamma delta ($\gamma\delta$) T cells, mucosal-associated invariant T (MAIT) cells, and invariant natural killer T (iNKT) cells (73–76). Innate T lymphocytes utilize restricted T cell receptor rearrangements, which recognize conserved microbial elements presented on MHC-like molecules instead of the peptide-MHC complexes that activate classical $\alpha\beta$ T cells. Thus, innate T lymphocytes are essential in recognizing nonpeptide antigens, resulting in the immune response and linking the innate and adaptive immune response (77).

1.2.1 Innate immunity

The innate immune system is an evolutionarily older line of defense found in all plants and animals, including single-celled organisms (78). The innate system is strategically placed in a position where it becomes the first to encounter intruding pathogens and is rapid to respond but does not maintain memory. Components of the innate immune system include anatomic (e.g., skin and mucus membrane), which prevents entry of pathogenic and commensal bacteria (normal flora). The innate immune system also comprises mucus found on the surface of the mucosa, which traps microbes and limits their access into underlying tissues. It further includes enzymes like lysozyme found in tears and digestive enzymes in the gut that can lyse microbial membranes and finally consists of a variety of immune cells (e.g., granulocytes including neutrophils, eosinophils and basophils as well as mast cells, monocytes, dendritic cells (DCs), NK cells, and innate T lymphocytes and innate lymphoid cells (ILCs)) that are phagocytic or cytotoxic to infected cells or release a broad array of inflammatory mediators, such as cytokines, chemokines, and proteases.

1.2.1.1 Innate and genetic immunity and HIV

1.2.1.1.1 Immunogenetic correlates of protection against HIV infection

Genetic variations among human beings can influence susceptibility to HIV infection by influencing multiple steps in the viral replication, such as viral entry, packaging, and maturation. However, only individuals homozygous for the $\Delta 32$ allelic variant of the CCR5 protein, due to a 32 base pair deletion in the CCR5 (*ckr5*) gene, which results in the expression of a truncated and non-functional CCR5 receptor, display a complete, even if not absolute, protection to sexually transmitted HIV infection (79–81). The *ccr5 δ 32* allele is abundant in Caucasian ethnicities, being present in 4–15% of the population, although higher frequencies can be observed in Northern Europeans (82). The *ccr5 δ 32* variant is absent from people of other ethnicities, including sub-Saharan African populations, where it is lacking, yet these populations are where most HIV infection occurs (82). Only individuals homozygous for *ccr5 δ 32* mutation are wholly protected against mucosal HIV transmission (80,81). Although individuals heterozygous for the *ccr5 δ 32* allele can be infected with HIV, they are characterized by a delayed progression towards clinical stages of AIDS. Individuals heterozygous for *ccr5 δ 32* express low levels of functional CCR5 molecules on their cell surfaces, resulting in a reduced ability of HIV to bind its co-receptor and, ultimately, in diminished viral replication (79,83). The *ccr5 δ 32* homozygous genotype has been identified in several HESN cohorts, but this genotype is absent in African populations (84). Other polymorphisms exist in the regulatory region of the CCR5 gene, but none has been associated with HESN individuals (83).

The CC-chemokines have been shown to play a role in the modulation of susceptibility to HIV infections and include regulated on activation normal T cell expressed and secreted (RANTES) (CCL5), MIP-1 α (CCL3), MIP-1 β (CCL4), and MIP1 α P (CCL3L1). These bind to CCR5, thus competing for receptor binding with R5-tropic virus (85). High expression of RANTES in genital mucosa has been observed among HESN, suggesting a role for RANTES in preventing HIV infection. A possible explanation for the observed differences detected in RANTES expression comes from identifying genetic variants in its promoter region (86–88). Another CC-chemokine, CCL3L1, considered the most potent agonist of CCR5, can also limit HIV infection in target cells. The gene for CCL3L1, together with those for CCL3, CCL4, and CCL5, came about due to a duplication of a common ancestral gene. These nonallelic copies are found in variable numbers in the human population. Gene duplication may contribute to the overexpression of the corresponding

protein, which is likely to modulate immune responses (89). Increased CCL3L1 secretion has also been associated with reduced CCR5 expression on CD4+ T cells (89). Although CCL3L1 may reduce HIV target cells, it has been associated with increased susceptibility to HIV in South African women, suggesting that higher expression of the *CCL3L1* gene may not be protective against HIV acquisition (90). Analysis of single nucleotide polymorphisms (SNP) on chromosome 17 led to the discovery of the *ccl2-ccl7-ccl11* or the *h7* haplotype in HESN of Caucasian ethnicity. Since the proteins encoded by these genes do not bind to CCR5 or CXCR4, they do not modulate virus entry. However, the authors suggested that their role in the immune mechanism, including the chemokine-mediated recruitment of monocytes, eosinophils, and dendritic cells to the inflammation site, could mediate the protective effect of the *h7* haplotype (91). Similarly, an SNP in the stromal-cell-derived factor-1 (SDF-1) gene, was reportedly overrepresented in a group of HESN (92) but failed to be associated with HIV resistance in other cohorts (93). SDF-1 is a natural ligand for CXCR4, which is a co-receptor for X4 HIV strains, SDF-1 3'A, results in increased transcript stability and, thus, enhances SDF1 production.

The human leukocyte antigen (HLA) genes encode cell surface molecules responsible for antigen presentation to T lymphocytes (94), are ligands for inhibitory NK cells (95) and are highly polymorphic. Several HLA genotypes, including HLA-B*57:01, HLA-B*58:01, HLA-B27, and HLA-B51, have been associated with delayed HIV disease progression. The HLA-B*57:01, HLA-B*58:01, HLA-B27, and HLA-B51 genotypes enable cytotoxic T lymphocyte (CTL) to target multiple HIV peptides and recognize conserved HIV-Gag epitopes in individuals who express them (96). There are two groups of HLA-B*35 antigens: Py and Px. Only B*35Px is associated with more rapid HIV disease progression (97,98). Some DQB1 alleles and haplotypes in the Pumwani sex worker cohort have been associated with HIV resistance (99). Discordance in HLA class I alleles between the HIV-infected subject and the uninfected sexual partner was also associated with reduced HIV transmission (100,101). Likewise, a study of pregnant mothers in Nairobi found that incompatibility in HLA class I alleles between mothers and their newborns decreased the risk of perinatal HIV transmission to the newborns (102). Soluble factors expressed by CD8+ T cells have also been shown to protect against HIV infection in newborn babies who remain HIV seronegative although they are born to HIV+ mothers(103).

Interferon regulatory factors (IRF) are transcription factors that have been shown to play a central role as transcriptional regulators of type I interferon (IFN- α and - β) biology (104). IRF-1 is expressed in all cell types except early embryonal cells and plays a pivotal role in many aspects of the immune response, including immune cell development and differentiation as well as regulation of the response to pathogens (105,106). Given their role, IRFs have been implicated in the pathology of several autoimmune and autoinflammatory conditions, including systemic lupus erythematosus (SLE), in which overexpression of type I IFNs is thought to be a major contributor to pathology. IRF-1/NF- κ B are essential facilitators of the early transactivation of the HIV-1 genome (107,108). The presence of SNPs 619A and 6516G on the IRF-1 gene has been shown to reduce the IRF-1 protein expression and protect against HIV infection. Binding of IRF-1 to an interferon-stimulated response element (ISRE)-like sequence of the HIV 5'-LTR results in Tat-independent initiation of the transcription of HIV genes. Thus, reduced IRF-1 expression downregulates HIV transcription and replication at the initial stages of infection, possibly allowing the immune response to respond effectively (109).

Interferon-stimulated genes (ISGs) are expressed in response to stimulation with interferons (IFN) (110), which are antiviral cytokines that are mainly classified into two: type I and type II (111,112). In humans, type I IFN binds a common cell surface receptor, known as the type I IFN receptor, and they include IFN- α , IFN- β , IFN- ϵ , IFN- κ , and IFN- ω (111–113). However, only one type II IFN, IFN- γ , binds to the type II IFN receptor (114–116). Recently, a new class of IFNs known as IFN- λ has emerged (111,117). Both the type I IFN receptor and the type II IFN receptor have multichain structures composed of at least two distinct “subunits”, which interact with a member of the Janus-activated kinase (JAK) family: IFNAR1 and IFNAR2 for the type I IFN receptor interacts with tyrosine kinase 2 (TYK2) and JAK1, respectively. In the case of type II IFN receptor, the IFNGR1 subunit binds to JAK1, whereas IFNGR2 binds to JAK2 (118,119). The binding of IFN to its receptor leads to type-I- and type-II-IFN-mediated signalling activation of receptor-associated JAKs, followed by autophosphorylation and activation of the associated JAKs as well as activation of the classical JAK–STAT (signal transducer and activator of transcription) signalling pathway (120). The STAT proteins homo- or heterodimerize and form complexes with other transcription factors to activate the transcription of ISGs (121). The gene products regulated by IFNs are the primary effectors of the IFN response. ISGs are commonly expressed in response

to viral infection, but also during bacterial infection and in the presence of parasites (110,122). Although the functions of most ISGs remain to be elucidated, some of the best-studied ISGs play pivotal roles in host defense (123). ISGs function to inhibit virus replication through viral RNA degradation, viral translation inhibition, or both (123). Several innate ISGs have been described that can interfere directly with HIV replication. These ISGs, including apolipoprotein B editing complex (APOBEC3), sterile alpha motif histidine aspartate domain containing protein 1 (SAMHD1), tripartite motif 5 alpha (TRIM5 α), tetherin, and serine incorporator 5 (SERINC5), restrict HIV replication at multiple stages in the replication cycle (124). The expression of high levels of several of these host restriction factors, including APOBEC3G and myxovirus resistance 2 (MX2/MXB) is associated with reduced susceptibility to HIV infection *in vitro* (125,126).

1.2.1.1.2 Mucosal immunity and HIV susceptibility

The vagina and ectocervix epithelia in women are composed of a multilayer of keratin-containing cells, the stratified squamous epithelium, that does not have a polarized plasma membrane or tight junctions. Thus, this barrier is permissive to passage of small particles less than 30 nm in diameter. Therefore, HIV being 80–100 nm in diameter, is physically barred from crossing the genital mucosa (127). However, the lack of tight junctions in the genital mucosa allows CD4⁺ T cells, macrophages, and DC migration into the vaginal and ectocervical epithelium, where the cells may take up HIV that has gained access to “leaky” epithelium (128),(129). The anal mucosa, endocervix uterus, and Fallopian tubes are a single layer of polarized, columnar epithelial cells with tight junctions (127)(130). Adult human foreskin is a stratified epithelium consisting of the highly keratinized outer foreskin, a “wet” mucosal epithelium, and less keratinized inner foreskin. The inner foreskin is enriched with HIV target cells such as CD4⁺ T lymphocytes, macrophages, and DCs (131–134). Thus, the inner foreskin is more susceptible to HIV infection than the outer foreskin (134–136). Circumcision in men has been shown to lower the risk of HIV infection by 60% (137). Also, *in vitro* studies have demonstrated that mucosal foreskin epithelium removal leaves a dry keratinized epithelial surface, which is more resistant to HIV infection (137,138). The penile urethra in both non-circumcised and circumcised men has the potential for HIV transmission. It too has stratified squamous epithelia and contains immune cells such as macrophages and T cells but not Langerhans cells, which are target cells for HIV (131,132,135). Thus, the risk of HIV acquisition depends on the characteristic of the mucosal epithelial layer, with

anal intercourse having a high risk of HIV transmission (0.3–5%) per coital act (139) followed by the female genital epithelium (0.05–0.5%) per coital act (139) and male genital epithelium (0.04–0.14%) per coital act (139,140). The oral mucosa has the lowest risk of HIV transmission (0.01%) per coital act (139), probably due to the highly stratified epithelium with tight junctions observed between the more superficial monolayers, obstructing viral access particles to the submucosa. These tight junctions are formed due to dimerization of transmembrane proteins, such as occludin and claudins, with the cytoplasmic protein zonula occludens (ZO)-1; these together maintain the polarized structure of the epithelium (141).

HIV mucosal transmission also depends on the surface area. Thus, women have a higher per-act risk of HIV acquisition after virus exposure than men because the surface area of cervicovaginal mucosa is larger than that of the penis and foreskin (142). However, circumcision in men may lower the risk of HIV acquisition by reducing the susceptible surface area (143).

Cell-free or cell-associated HIV can penetrate the epithelium into the subepithelial lamina propria due to the disruption of cervicovaginal mucosa caused by trauma or infection-associated mucosal inflammation, ulceration, and erosions (144). Mechanical micro-abrasions induced by sexual intercourse, chemical use (e.g., topical microbicides), and genital ulcers caused by sexually transmitted diseases (e.g., syphilis, chancroid, and those caused by herpes simplex virus) may allow HIV to directly access target cells, such as DCs, T cells, and macrophages, at the basal epithelium and stroma (145).

Although cell-free or cell-associated HIV can penetrate the epithelium, the transmission of cell-associated HIV seems to be more efficient than cell-free virions in the male and female genital mucosa and anorectal mucosa (146)(147). A virus can cross the mucosal epithelium by either paracellular passage or transcytosis. The choice of method is determined by the type and the intrinsic characteristic of the epithelium (148). Paracellular passage can happen in all mucosal surfaces, mainly due to disruption of mucosal integrity. For instance, HIV gp120 proteins can disrupt tight junctions and lead to the formation of gaps at the epithelial monolayers through which the virus may reach the submucosa (149–151). This is mainly due to gp120 binding to either the coreceptors CCR5, CXCR4, or galactosylceramide (GalCer), which are expressed on epithelial cells, leading to a reduction of the expression of occludin, claudins, and ZO-1. This may increase

calcium ion (Ca²⁺) levels and activation of the mitogen-activated protein (MAPK) and phosphatidylinositol 3-kinase (PI3K) pathways, resulting in disruption of ZO-1 and Claudins/Occludin interactions and tight junctions, internalization of surface proteins, and disruption of epithelial monolayers (151–153). Other effects, such as stimulation of TLR2 and TLR4 on endometrial and endocervical epithelial cells by gp120 may lead to NF-κB activation and increased proinflammatory cytokines, including tumor necrosis factor (TNF)-α (154). Proinflammatory cytokines expressed by HIV-infected cells, including, TNF-α, IFN-γ, IFN-α, and IL-1β, have been shown to disrupt epithelial junctions (141). Paracellular passage of HIV may be responsible for transmitting 0.1% of virus *in vitro* (150). However, their impact on HIV transmissions *in vivo* is not known. HIV can also cross the mucosal epithelial by transcytosis. The viral particles bind to molecules expressed on epithelial cells such as heparan sulfate proteoglycans (HSPGs) or Glacier, followed by transportation into the intracellular compartment (155,156). However, this mechanism is less efficient, as it results in transcytosis of only 0.01% of the initial inoculum of HIV (156).

Despite the low transmission rate per sexual act, sexual intercourse still accounts for most HIV infections worldwide, making it the main transmission route (157). For HIV sexual transmission to occur, the HIV has to cross the mucosal epithelium barrier, produce a productive infection in subepithelial mononuclear cells, and be delivered to lymph nodes to initiate systemic infection (158). As discussed, the structure of the exposed epithelium is crucial in terms of susceptibility to viral entry. Since not all episodes of sexual intercourse result in HIV infection, the efficiency of HIV transmission depends on the infectiousness of the HIV-infected partner and the susceptibility of the uninfected person (159). If the infected person has high blood viral load, it increases the probability of transmission (160). Sexually transmitted diseases (STDs; e.g., herpes outbreaks) have been associated with increased blood HIV viral load and may result in increased HIV transmission (161). Other STDs including bacterial vaginosis (BV), herpes simplex virus (HSV), human papillomavirus (HPV), Chlamydia trachomatis, Neisseria gonorrhoeae, Candida, genital ulceration and vaginal discharge have been shown to correlate with increased HIV shedding and may increase HIV transmission (162). STDs also increase the HIV susceptibility of the uninfected partner of an HIV-infected individual. For instance, infections in the female genital tract, including HPV, C. trachomatis, and N. gonorrhoeae, may lead to upregulation of proinflammatory cytokines

(e.g., IL-1, IL-6, TNF- α) and immunoregulatory cytokines (e.g., IL-12, IL-10) that modulate HIV replication (163). Proinflammatory cytokines can increase HIV replication by activating the LTR sequence of HIV, especially the HIV clade C virus, as it has been shown to have additional LTR-binding sites for TNF- α (164). This implies that increased levels of proinflammatory cytokines in the mucosal area would be associated with increased HIV acquisition (165). Thus, a proinflammatory environment such as the one created by STDs encourages HIV acquisition (166). In support of this, the HESN individual's natural resistance to HIV acquisition has been hypothesised to be linked to immune quiescence in the mucosa (167). The establishment of HIV infection at the mucosa depends on the availability of susceptible target cells, particularly memory CD4⁺ T cells (168). Thus the presence of CD4⁺ cells in the mucosa, especially those expressing CCR5, is associated with increased susceptibility to HIV infection (169). Therefore, HIV can gain direct access to the mucosal microcirculation in cases of mucosal trauma, inflammation, and ulceration. This may disrupt the epithelial barrier and provide directional signals to recruit highly susceptible and activated inflammatory monocytes and T cells (170).

With respect to mucosal secretions, proteins of small molecular weight with anti-HIV activity have been described in several HESN cohorts including, the saliva protein, a secretory leukocyte protease inhibitor (SLP1) (171), lactoferrin (172), defensin (173), and elafin/ trappin-2 (174). The Pumwani sex workers who were HIV resistant also expressed high levels of antiprotease inhibitors, including serpins (serine protease inhibitors), elafin, alpha-2-microglobulin 1 (A2ML1), cystatin A, and cystatin B in the genital mucosa (175).

1.2.1.2 Monocytes

Monocytes make up to 10% of circulating leukocytes (176). In inflammatory conditions, monocytes are recruited to tissue sites to differentiate into monocyte-derived macrophage or monocyte-derived dendritic cells (MDDCs) (177–179). They also express a wide range of scavenging receptors that can recognize lipids and bind to microorganisms and apoptotic cells, enabling monocytes to play an essential role in the phagocytosis of pathogens and clearance of apoptotic cells and toxic compounds at the end of an inflammatory process (180).

Human monocytes can be classified based on CD14 and CD16 expression as classical (CD14⁺ CD16⁻), intermediate (CD14⁺ CD16⁺) or nonclassical (CD14^{dim}/- CD16⁺) monocytes (181). Although monocytes act as antigen-presenting cells (APCs), they are not as efficient as DCs in presenting antigens to T cells (182). Monocytes are the precursor cells to “professional” APCs, such as macrophages and DCs (177,183,184). Therefore, monocytes patrol the bloodstream and tissues to replenish dying APCs or, in case of infection, to provide enough of these cells for the body to respond to invading pathogens effectively (185). Although undifferentiated monocytes may live for only a few days in the bloodstream once activated or differentiated, their lifespan is significantly prolonged for up to several months (186). DCs, B cells, and monocytes can act as APCs by presenting bacterial vitamin B metabolites intermediates by MR1 to MAIT T cells (which are key innate lymphocytes), leading to T-cell receptor (TCR)- mediated MAIT cell activation (187). Toll-like receptor (TLR) stimulation of DCs and monocytes may also lead to cytokine production, including IL-12 and IL-18, which activate MAIT cells (187). Activation of MAIT cells can lead to induction of proinflammatory cytokines (188,189) which may modulate and increase immune activation. Thus, this Thesis focuses on understanding whether and how the differentiation of monocytes into MDDC and maturation of MDDCs with TLR7 and TLR8 may lead to activation of MAIT cells and expression of proinflammatory cytokines.

1.2.1.2.1 Monocytes in HIV infection

Although HIV can infect monocytes, in some cases leading to latent infection, the infection of monocytes, macrophages, and DCs by HIV is relatively rare compared to the infection of CD4⁺ T cells. Monocytes and macrophages express host restriction factors such as SAMHD1 as well as VIPERIN (virus-inhibitory protein, endoplasmic reticulum-associated, interferon-inducible) and APOBEC3G, reducing their susceptibility to HIV (190,191). Infected monocytes can disseminate the virus as they migrate into peripheral tissues (192,193) and are likely to differentiate into MDMs, which transforms them into a long-lived reservoir for the virus (194–196). Furthermore, differentiated MDMs are more susceptible to new infection compared to freshly isolated monocytes due to increased expression of the HIV co-receptor CCR5 (197).

1.2.1.3 Dendritic cells

DCs are a heterogeneous family of innate cells that act as potent APCs linking the innate and adaptive immune responses (184). Thus, DCs play an essential role in initiating and regulating the immune response (198). Depending on the subtype and anatomical location, DCs can survive for a few weeks, and they can be replaced through proliferating hematopoietic progenitors, monocytes, or tissue-resident cells (199). DCs in the human blood lack lineage (lin) markers for T cells (CD3), B cells (CD19 or CD20), and NK cells (CD56). However, they express very high levels of MHC class II markers, including HLA-DR, -DP, -DQ antigens, and high levels of MHC class I markers, including HLA-A, -B, and -C surface antigens (200,201). Human DCs make up to 1% of human blood mononuclear cells and can be classified as plasmacytoid DCs (pDCs) or myeloid or conventional DCs (cDCs) (202). The pDCs are lin-HLA-DR+, CD123+, CD300+ blood DC antigen 2 (BDCA2) CD304+ blood DC antigen 4 (BDCA4). The cDCs are lin-HLA-DR+, and just like macrophages and monocytes, they express CD11C (198,200). pDCs and cDCs express unique pattern recognition receptors (PRR), such as TLRs, C-type lectins, and intracellular nucleic acid sensors, enabling them to recognize different PAMPs (203–205). DCs play a central role in immune surveillance whereby upon exposure to antigens (Ags), they home into lymphoid organs through the lymphatic system to localize in the T-cell zone. In the T-cell zone, DCs process and then present Antigens to the resident T cells, leading to potent CTL responses (206). The cDCs produce IL-12, IL-15, and IL-18 crucial for developing T helper 1 (Th1) responses, and promoting CTL development critical during viral infections (207).

1.2.1.3.1 DCs in HIV infection

In the mucosa, DCs are, in most cases, the first immune cell to encounter HIV (208). One of their prime functions is immunosurveillance at mucosal surfaces capturing incoming pathogens, then migrating to secondary lymphoid organs for antigen presentation to T cells (209). Once the HIV enters the submucosa, it can be captured by DCs, which act as a trojan horse carrying the virus to the lymph nodes, resulting in systemic infection (210,211). Although HIV can directly infect different DC subtypes (known as cis infection), this infection efficiency is thought to be lower than infection of activated CD4+ T cells. Therefore, only a small percentage of circulating DCs get infected with HIV. The lifespan of DCs in the lymph nodes is prolonged due to cytokine stimulation in the microenvironment (212), which may help spread HIV-1 infection and maintain viral reservoirs.

Langerhans cells are a specialized DC subset that populate the epidermis or mucosal epithelia as immune sentinels (209). Interestingly, Langerhans cells are resistant to HIV infection due to the expression of Langerin, which causes internalization and break-down of HIV particles, thus blocking viral transmission (213). However, in the case of skin abrasion (214) or co-infection with other sexually transmitted organisms such as the bacterium *Neisseria gonorrhoeae* and/or the fungus *Candida albicans* (215), Langerhans cells can become more susceptible to HIV and can transmit HIV to CD4+ T cells effectively.

1.2.1.4 Innate recognition

The innate immune system comprises germ-Line-encoded PRRs that recognize pathogen-associated molecular patterns (PAMPs) on pathogenic microorganisms (216). Innate recognition enables the immune system to distinguish self from non-self (217). PAMP recognition by PRR leads to an intracellular signalling cascade resulting in the activation of transcription factors encoding inflammatory cytokines, chemokines, co-stimulatory, and antimicrobial peptides (218). The PRRs can be classified into three categories: secreted, transmembrane, and cytosolic. The secreted family of PRRs include collectins, ficolins, and pentraxins (219). The transmembrane family of PRRs includes TLRs and C-type lectins; the cytosolic family of proteins includes nucleotide binding oligomerization domain (NOD) like receptors (NLRs) and retinoic acid-inducible gene (RIG)-like receptors (RLRs) (220).

1.2.1.4.1 Toll-like receptors

TLRs are transmembrane proteins characterized by an extracellular domain containing varying numbers of leucine-rich-repeat (LRR) motifs that mediate recognition of PAMPs via transmembrane domains and an intracellular signalling domain homologous to that of the interleukin-1 receptor (IL-1R), termed the Toll/IL-1R homology (TIR) domain (220). In humans, 10 TLRs have been discovered that recognize several PAMPs, including lipids, lipoproteins, proteins, and nucleic acids derived from a wide range of microbes such as bacteria, viruses, parasites, and fungi (220). TLR can be categorized into two groups depending on cellular location and the PAMPs they recognize. TLR1, TLR2, TLR4, TLR5, TLR6, and TLR10 are expressed on the cell surface and recognize mainly lipids, lipoproteins, and proteins. TLR3, TLR7, TLR8, and

TLR9 are expressed intracellularly and recognize viral, bacterial, and self nucleic acids, typically RNA or DNA (220). TLR2 forms a heterodimer with TLR1 or TLR6 (221). The ligand for the TLR2-TLR1 heterodimer is triacylated lipopeptides from Gram-negative bacteria and mycoplasma (222). The TLR2-TLR6 heterodimer ligates diacylated lipopeptides from Gram-positive bacteria and mycoplasma (223,224). TLR4 complexes with myeloid differentiation factor 2 (MD2) to respond to bacterial lipopolysaccharide (LPS), a component of the outer membrane of Gram-negative bacteria (225). TLR5 is highly expressed in CD11c+CD11b+ lamina propria DCs in the small intestine, and it recognizes the bacterial flagellin (216). TLR3 recognizes double-stranded RNA (dsRNA) from reoviruses, self RNAs from damaged cells, and dsRNA produced during the replication of positive-sense single-stranded RNA (ssRNA), e.g., respiratory syncytial virus (RSV) (216,226). TLR7 is highly expressed in DCs, and it recognizes ssRNA leading to high type I IFN expression during viral infections (216,220). TLR8 that also senses ssRNA is expressed in various tissues, with its highest expression in monocytes, and is upregulated after bacterial infection (220,227). Although TLR7 and TLR8 are closely related and both recognize ssRNA, TLR7 and TLR8 agonists have been shown to differ in their target cell selectivity and cytokine induction profile. Although TLR7 agonists directly activated purified pDCs and, to a lesser extent, monocytes, TLR8 agonists directly activated purified cDCs, monocytes, and MDDC. Furthermore, TLR7-selective agonists were more effective than TLR8-selective agonists at inducing IFN- α and IFN-regulated chemokines such as IFN-inducible protein and IFN-inducible T cell chemoattractant from human PBMC. In contrast, TLR8 agonists were more effective than TLR7 agonists at inducing proinflammatory cytokines and chemokines, such as TNF- α , IL-12, and MIP-1 (228). Furthermore, human TLR7 was shown to recognize guanosine-uridine (GU)-rich and human TLR8 recognize both GU-rich and uridine (U)-rich ssRNA (229). TLR9 recognizes unmethylated 2'-deoxyribo (cytidine-phosphate guanosine) (CpG) DNA motifs present in bacteria and viruses but rare in mammalian cells. Synthetic ligands of TLR9 have been shown to stimulate DCs, macrophages, and B cells and drive strong TH1 responses.

1.2.1.4.1.1 TLR signalling

TLR recognition of PAMPs triggers a signalling cascade leading to the induction of genes involved in antimicrobial host defense. Once TLR ligand binding occurs, the receptor undergoes dimerization and conformational changes, leading to the recruitment of TIR-domain-containing

adaptor molecules to the TIR domain of the TLR. There are four adaptor molecules: myeloid differentiation primary response 88 (MyD88), TIR-associated protein (TIRAP) / MyD88-adaptor-like (MAL), TIR-domain-containing adaptor protein-inducing IFN- β (TRIF)/TIR-domain-containing molecule 1 (TICAM1) (230,231), and TRIF-related adaptor molecule (TRAM). The differential responses mediated by distinct TLR ligands can be explained in part by the selective usage of these adaptor molecules. There are two major pathways involved in TLR signalling: MyD88 or TRIF. The MyD88-dependent pathway predominantly leads to the production of inflammatory cytokines (e.g., TNF- α , IL-6, IL-1) and chemokines (e.g., C-C motif ligand 4, CCL4), while the TRIF-mediated pathway leads to type I IFNs production e.g., IFN α/β (232).

1.2.1.4.1.1.1 MyD88 dependent signalling pathway

All TLRs except TLR3 use the MyD88 signalling pathway. TLR ligation leads to stimulation of MyD88, thus leading to binding to the TIR domain and then recruitment of IL-1R-associated kinase 4 (IRAK-4) and IRAK-1. In TLR2 and TLR4 signalling, another adaptor, the TIRAP/MAL, is required for recruiting MyD88 to the receptor (233). After IRAK-1 associates with MyD88, it is phosphorylated by the activated IRAK-4 and subsequently associates with TNF receptor-associated factor 6 (TRAF6), which acts as a ubiquitin protein ligase (E3) (234). This then catalyzes the formation of an Lys63 (K63) polyubiquitin chain on IRAK1, NF- κ B modulator (NEMO), and on the TRAF6 itself (**Figure 2**). The K63-linked polyubiquitin chain recruits transforming growth factor beta (TGF- β)-activated kinase 1 (TAK-1), and the TAK-1 binding proteins (TAB)1, TAB2, and TAB3, are also recruited to TRAF6 (235). TAK1 then phosphorylates I kappa B (I κ B) kinase (IKK)- β , an NF- κ B inhibitory protein, which then undergoes proteasome degradation, releasing the NF- κ B. NF- κ B will then translocate into the nucleus to induce proinflammatory gene expression (**Figure 2**). TAK1 activation also results in phosphorylation of MAPK6, thus initiating the MAPK signalling cascade resulting in the inactivation of MAPK family members such as ERK1/2, p38, and JNK. The phosphorylated MAPK6 mediates activation of transcription factor activator protein 1 (AP-1) leading to inflammatory responses (**Figure 2**) (236).

1.2.1.4.1.1.2. TRIF-mediated signalling

TRIF is a MyD88 independent pathway utilized by TLR3 and TLR4 leading to the expression of IFN- β (237). Although TLR3 and TLR4 signal through the adaptor TRIF, TLR3 can directly associate with TRIF, whereas TLR4 requires the bridging adaptor TRAM to interact with TRIF (231,232,238). TLR3 interaction with TRIF leads to recruitment of the enzyme 3 ubiquitin (E3 Ub) ligase TRAF3, which then activates TRAF family member-associated NF-kB activator (TANK)-binding kinase 1 (TBK1). This leads to IRF3 phosphorylation, dimerization, and translocation to the nucleus, to mediate the expression of type I IFNs (**Figure 2**). The TLR3-TRIF interaction may also lead to the recruitment of TRAF6, which interacts with receptor-interacting serine/threonine-protein kinase 1 (RIPK1) via their respective RIP homotypic interaction motif (RHIM) domains. This leads to the formation of Ub scaffold for the formation of the TAK1 complex. The TAK1 complex then drives NF-kB activation and MAPK pathways (239).

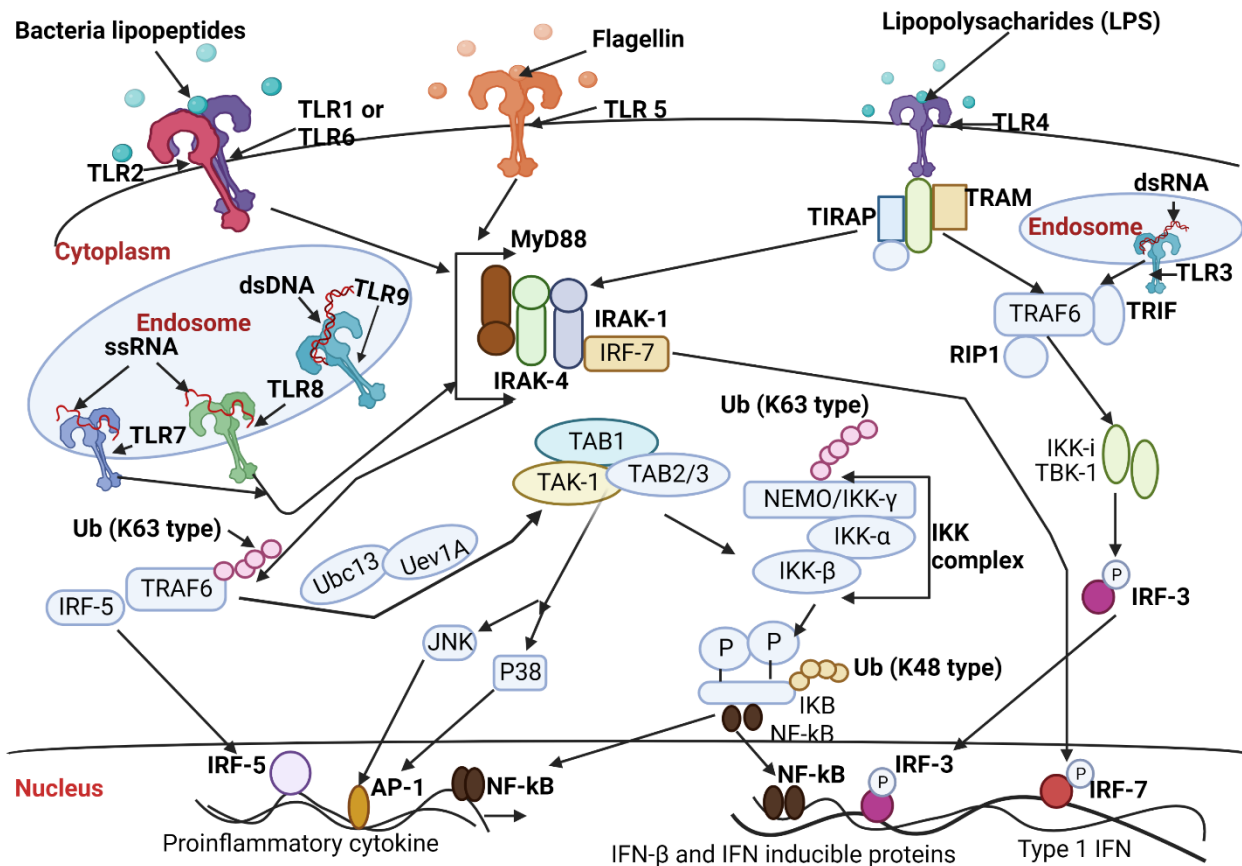


Figure 2: TLR signaling pathway. TLRs have a specific ectodomain that recognize different pathogen-associated molecular patterns (PAMPs) and a conserved cytoplasmic Toll/IL-1 receptor domain. TLR signalling pathways. TLR1, 2, 5, and 6 are located on the cell surface, while TLR 7, 8, and 9 are in the endosomal vesicles. TLR1-TLR2 heterodimer senses triacylated lipopeptides; TLR2-TLR6 heterodimer senses diacylated lipopeptides; TLR4 senses lipopolysaccharide; TLR5 senses bacterial flagellin; TLR7 senses imidazoquinolines or guanine rich ssRNA TLR8 senses uridine rich ssRNA and TLR9 senses bacterial CpG. TLR engagement, leads to recruitment of TIR-domain-containing adaptors including MyD88 and TIRAP to the receptor. MyD88 forms a complex with IRAK kinase family members, referred to as the Myddosome. During Myddosome formation, IRAK-4 activates IRAK-1, which is then autophosphorylated at several sites and released from MyD88. IRAK-1, TRAF6 and IRF-5 form a complex and TRAF6 acts as an E3 ubiquitin ligase and catalyzes the K63-linked polyubiquitin chain on TRAF6 itself and NEMO with E2 ubiquitin ligase complex of Ubc13 and Uev1A. This ubiquitination activates the TAK-1 complex, resulting in the phosphorylation of NEMO and activation of the IKK complex. Phosphorylated IκB undergoes K48-linked ubiquitination and degradation by the proteasome. Freed NF-κB translocates into the nucleus and initiates the expression of proinflammatory cytokine genes. Simultaneously, TAK1 activates the MAP kinase cascades, leading to the activation of AP-1, which is also critical for the induction of cytokine genes. Stimulation with TLRs recruits a complex of MyD88, IRAK-4, IRAK-1, TRAF6, and IRF-7. Phosphorylated IRF-7 translocates into the nucleus and upregulates the expression of type I IFN genes. TLR4 triggers the MyD88-independent, TRIF-dependent signaling pathway via TRAM to induce type I IFNs. TRIF activates NF-κB and IRF-3, resulting in the induction of proinflammatory cytokine genes

and type I IFNs. TRAF6 and RIP1 induce NF- κ B activation and TBK1/IKK-i phosphorylate IRF-3, which induces the translocation of IRF-3. **Adapted from (216)**

1.2.1.4.1.1.3 TLR recognition of bacteria

Most bacteria can be broadly classified as Gram-positive or Gram-negative (240). Gram-positive bacterial cell walls are composed of thick layers of peptidoglycan and stain purple when subjected to a Gram stain procedure (241). Gram-negative bacteria have cell walls with a thin layer of peptidoglycan and stain pink when subjected to a Gram stain procedure. The cell wall of Gram-negative bacteria is also embedded with lipopolysaccharide (LPS) molecules (241). Although both Gram-positive and Gram-negative bacteria produce exotoxins, only Gram-negative bacteria produce endotoxins (242). Some bacterial cell wall components act as PAMPs and are recognized by individual TLRs to stimulate immune cells (243). The most potent PAMP is LPS, also known to be an endotoxin expressed by Gram-negative bacteria. LPS associates with LPS binding protein (LBP), an acute-phase protein present in the bloodstream, and then binds to CD14, a glycosylphosphatidylinositol (GPI)-linked protein expressed on the cell surface of monocytes. LPS binds to MD2, which then associates with the extracellular portion of TLR4 followed by oligomerization of TLR4. The LPS in different bacteria is structurally different due to variations in acyl chains and fatty-acid composition. This results in the varied biological activities of lipid A, with monophosphoryl having less toxicity. Lipid A is the portion of LPS responsible for most of the pathogenic phenomena associated with Gram-negative bacterial infection, e.g., endotoxin shock (216).

TLR2 detects lipoproteins and lipoteichoic acid (LTA) in Gram-positive bacteria and peptidoglycan (PG) in Gram-positive and Gram-negative bacteria. TLR2 interacts physically and functionally with TLR1 and TLR6, which appear to be involved in the discrimination of subtle changes in the lipid portion of lipoproteins. TLR2/TLR6 is also activated by LTA, an amphiphilic, negatively charged glycolipid that contains a diacylated moiety (244,245). TLR5 detects both Gram-positive and Gram-negative bacteria that have flagellin. Flagellin detected by TLR5 has C-terminal helix chains (D0), the major helix chains (D1), and the hypervariable central region with β sheets (D2 and D3) (246). The central portion of flagellin detected by TLR5 is domain D1, which is relatively conserved among different bacterial species (247). TLR5 is expressed by epithelial cells, monocytes, and immature DCs. Since TLR5 is basolaterally expressed on intestinal epithelia, flagellin is recognized by the host only when bacteria have invaded across the epithelia. TLR5 is highly expressed in the lungs and seems to play an essential role in the defense against the

pathogens in the respiratory tract. Up to 10% of individuals with impaired TLR5-mediated signalling are susceptible to pneumonia caused by the flagellated bacterium *L. pneumophila*. These individuals have a point mutation that introduces a stop codon within the ligand-binding domain of TLR5, referred to as TLR5392STOP. The TLR5392STOP mutant protein functions as a dominant-negative receptor that severely impairs TLR5-mediated signalling (248). Some bacteria may escape the flagellin-specific host immune response, e.g., *Helicobacter pylori* and *Campylobacter jejuni*, which produce flagellins that lack proinflammatory properties (249).

TLR9 detects unmethylated CpG dinucleotides that are abundant in bacterial genomes but suppressed and highly methylated in mammalian genomes (250), preventing self-recognition by TLR9 (216). The CpG-DNA ligation with TLR9 leads to the induction of inflammatory cytokine production and Th1 immune responses. Bacterial species differ in their cytosine and guanine (CG) frequencies, resulting in differences in DNA-dependent immunostimulatory capacity (251). TLR7 is also expressed in other immune cells, including cDCs, where it functions by sensing RNA species from bacteria such as group B Streptococcus and induces type I IFN (252).

1.2.1.4.1.1.4 TLR recognition of virus

Viral nucleic acid, whether DNA, double-stranded RNA (dsRNA), or single-stranded RNA (ssRNA), can act as PAMPs for TLR9, TLR3, and TLR7/TLR8, respectively. DNA viruses contain genomes rich in CpG-DNA motifs. Therefore, they are recognized by TLR9, leading to activation of immune cells and inflammatory cytokines and type I IFN secretion. This has also been shown for DNA-containing viruses including herpes simplex virus 1 (HSV-1), HSV-2, and murine cytomegalovirus (MCMV) (216,253). The type I IFN expression mediated by TLR9 stimulation by DNA virus is limited to pDCs (254). However, other cells also express TLR9, including macrophages, but these secrete less IFN- α , TNF- α and RANTES compared to pDCs (253).

TLR3 is activated by dsRNA expressed during viral infection by dsRNA viruses or as a replication intermediate for ssRNA viruses. The TLR3 ectodomain has a large horseshoe-like shape that may be necessary to increase its surface area and facilitate dsRNA recognition. The TLR3 ectodomain has N and C termini that bind dsRNA and provides enough stability to allow TLR3 to form a homodimer through the C-terminal region (255). The synthetic analog for dsRNA is

polyinosinic:polycytidylic acid (poly I:C) and when poly I:C is recognized by TLR3, type I IFN is produced (256). TLR3 engagement leading to the production of type I IFN, and inflammatory cytokines is crucial in antiviral immunity. Evidence shows that TLR3-deficient mice are susceptible to lethal infection with murine cytomegalovirus (257), and in humans, TLR3 deficiency may increase susceptibility to herpes simplex virus type 1 (HSV-1) (258).

TLR7 was initially demonstrated to recognize synthetic analogs of ssRNA with antiviral and antitumor properties, including imidazoquinoline derivatives such as imiquimod and resiquimod (R-848) and guanine analogs such as loxoribine (107,259). TLR7 was also shown to respond to ssRNA following infection with RNA viruses such as vesicular stomatitis virus, influenza A virus, and HIV (227). TLR7 is mostly expressed in pDCs that can produce large amounts of type I interferon after virus infection. This induction of cytokines by pDCs in response to RNA viruses is dependent on TLR7 (227,260). TLR7 expressed by pDCs can also recognize replicating vesicular stomatitis virus that enters the cytoplasm via autophagy (261). Antiviral responses are initiated after the viruses are internalized and recruited to the endolysosomes, where TLR7 detects their ssRNA. Thus, pDC autophagy may be essential for delivering cytosolic viral replication intermediates to the lysosome where they are recognized by TLR7, thus initiating an antiviral response.

TLR8 phylogenetically resembles TLR7. Human TLR8, like TLR7, can mediate the recognition of HIV-derived ssRNA. Although both TLR7 and TLR8 recognize ssRNA, they are expressed within the endosomal membrane, indicating that the accessibility of ssRNA may be a key factor for cell activation via these receptors. Enveloped viruses are trafficked into the cytosol through the endosomal compartment, where they are degraded, releasing the ssRNA, which TLR7 and TLR8 then recognize. Furthermore, phagocytosed apoptotic cells that are virus-infected release viral RNAs (216). Although both TLR7 and TLR8 recognize ssRNA, TLR7 responds to GU-rich ssRNA, while TLR8 can sense both GU-rich and U-rich ss RNA (262).

TLR7 and TLR8 stimulation in APC may lead to expression of proinflammatory cytokines including IL-12, and IL-18 (263), which further stimulate innate T cells leading to expression of IFN- γ , IL-17, and GM-CSF as well as cytolytic molecules like granzyme B (GrzB) and perforin (264,265). During the early stages of infection, IFN- γ and TNF- α antiviral response may protect

against HIV infection (266). However, proinflammatory cytokines may also increase immune activation and HIV susceptibility (165,267).

1.2.2 Adaptive immune system

The adaptive immune responses depend on host derived custom-tailored receptors. They are selected through somatic recombination of an extensive array of gene segments that arose by means of gene duplication early in vertebrate evolution to generate highly specific and flexible immune responses. The evolution of the adaptive immune system resulted from the overwhelming variability of antigenic structures and the ability of pathogens to mutate to avoid host detection (268). The adaptive immune system's main features that are absent from the innate immune system include specificity and memory (269). After the initial pathogen encounters, cells expressing these immune receptors may persist in the host for life, providing immunologic memory and rapid response capacity in the event of re-exposure.

The adaptive immune system is generally classified into two components: the antibody response mediated through B lymphocytes and cellular responses mediated through T lymphocytes. Lymphocytes develop in the primary lymphoid organs (thymus and bone marrow). The early progenitors of T and B lymphocytes come from multipotent hematopoietic stem cells (270). In their early developmental stages, T and B lymphocyte progenitors undergo rearrangement of different sets of prototypic immunoglobulins (Ig) variable (V), diversity (D), and joining (J) gene segments to generate the antigen-binding regions of their TCRs and B cell receptors (BCRs). Further diversification of the antigen-binding regions of the different V(D)J combinations occurs through a random enzymatic addition of non-encoded nucleotides in the joints created during V(D)J segment assembly. These may result in the generation of some receptors that recognize self-antigens. T and B lymphocytes bearing potentially harmful, self-reactive receptors may be deleted in their thymic and bone marrow birthplaces or otherwise inactivated. The selected populations of long-lived T and B lymphocytes then enter the bloodstream to begin their patrol of the body and migrate from the blood into strategically located lymphoid tissues, where they may engage invading pathogens and subsequently return to the circulation via lymphatic channels.

TCRs recognize peptide fragments of antigens presented by other cells, usually innate DCs and macrophages, by cell surface molecules encoded by the major histocompatibility complex (MHC) *class I and class II* genes. The T cells then traffic to secondary lymphoid organs, including lymph nodes and the spleen, to capture circulating antigens from lymph and blood, respectively. Adaptive immune responses originate in the secondary lymphoid organs, often under the influence of innate immune system signals provided either directly by circulating pathogens or indirectly by pathogen-activated cutaneous or mucosal APCs migrating to the secondary lymphoid organs. Lymphocytes emigrating from the spleen and lymph nodes can then travel to many sites in the body to exert effector functions. Thus, lymphocytes are highly mobile, and their movement is regulated by an array of adhesion molecules and chemokine receptors. For example, the cutaneous lymphocyte-associated antigen 1 positive (CLA1+) CC-chemokine receptor 4 (CCR4)-bearing lymphocytes traffic to the skin, whereas cells bearing the $\alpha 4\beta 7$ integrin binds to mucosal addressin cellular adhesion molecule-1 (MadCAM-1) on gut endothelial cells and therefore preferentially home to the gastrointestinal tract.

1.2.2.1 B lymphocytes

B lymphocytes are cells that express clonally diverse cell surface Ig receptors that recognize specific antigenic epitopes. B cells arise from hemopoietic stem cells in the bone marrow, referred to as progenitor B cells (Pro-B cells). Commitment to the B-cell lineage depends on several transcription factors including PU.1, IKAROS family zinc finger 1 (IKAROS), early B cell factor 1 (E2A, EBF), paired box gene 5 (PAX5), and interferon regulatory factor (IRF8) (271,272). The B cells undergo different developmental stages in the bone marrow in the absence of exogenous antigens. Following lineage commitment, further differentiation depends on the successful rearrangement of Ig gene loci. The genes coding for the heavy chain of Ig are assembled from 4 segments, mainly V_H , D, J_H , and C_H , while the genes encoding the light chain are assembled from 3 segments, mainly V_L , J_L , and C_L . There are 9 different heavy chain types (*IgM*, *IgD*, *IgG1-4*, *IgA1* and *IgA2*, and *IgE*) and 2 light chains, kappa and lambda.

Mature B cells expressing IgD and IgM traffic throughout the blood. Activation of B cells can be T-cell dependent or T-cell independent. Certain molecules mediate the T-cell independent activation of B cells, such as some plant lectins (e.g., pokeweed mitogen), which can induce

proliferation and antibody production from mature B cells (273). However, most B cell responses to proteins and glycoproteins require T cell participation, and these antigens are called T dependent. As the mature B cells recirculate to lymph nodes, the spleen, and mucosal-associated lymphoid tissues, they may encounter antigens presented on the surface of APCs. This will lead to crosslinking of the Ig receptor with antigen on the APC surface, which will result in the activation of intracellular signalling pathways that render the cell capable of interacting with T cells and thereby receiving a second maturation signal (274). B cells can act as APCs by internalizing antigens and presenting them to T cells along with MHC-II. If the B cell, which an APC previously activated, contacts a CD4⁺ T cell-specific for such a peptide with self-MHC class II, the T cell can activate the B cell for further differentiation into memory cells or plasma cells (275). The activated B cells can either become short-lived plasma cells secreting low-affinity antibodies without somatic mutation or enter a follicle to establish a germinal center (276). B cells can undergo class switching in the germinal center whereby they change from IgM and IgD to other isotypes, such as IgG, IgA, and IgE (277). The process of class switching is partly controlled by cytokines. For example, IL-4 and IL-13 promote switching to IgE (278), but IFN- γ can antagonize this effect. Switching to IgA is encouraged by IL-10 and TGF- β (279).

1.2.2.1.1 B cells and HIV infection

HIV has been shown to activate B cells in a T cell-independent manner leading to proliferation and differentiation of normal human peripheral blood B lymphocytes in vitro (280). Although B cells do not express CD4⁺ receptors, they can be infected with HIV via complement receptor 2 (CR2) or CD21, establishing latent infection (281). HIV can also bind to CD21 expressed on B cells leading to stimulation and activation of B cells. The HIV bound to CD21 may be passed to nearby activated CD4⁺ T cells, leading to increased HIV infection (282). HIV has been detected in B cells of HIV-infected patients (283). In the same way that follicular DCs (FDCs) infected with HIV serve as a source of infection of CD4⁺ T cells, these B cells containing HIV then can migrate into lymphoid tissue germinal centers (284), B cells complexed with virus can also be presented to activated CD4⁺ T cell targets. Furthermore, since B cells circulate through peripheral blood and migrate within lymphoid tissues to the border of follicles for cognate B–T interactions (285), they may have even better opportunities than FDCs to transmit the virus to CD4⁺ T cells. B cells are

dysregulated during acute HIV infection due to the high level of HIV replication and the inflammatory environment (286).

Infection with HIV-1 may lead to antibody responses of multiple isotypes to proteins encoded by HIV *env*, *gag*, and *pol* genes (287). The first HIV specific antibodies are antibodies directed to HIV-1 *env*, and they appear in a sequential order, with anti-gp41 IgM appearing in the first 13 days, and the initial binding antibody response to gp120 is appearing at 28 days after detectable viral RNA (288). IgG antibodies to Gag may appear 33 days following detectable plasma viral RNA. Antibodies to p31 (integrase) are elicited at a median time of 53 days. However, these antibodies generally do not control virus replication in most patients. They are not responsible for the initial decline in plasma viral load, as evident through mathematical modelling of the early HIV-1-specific IgM and IgG antibody responses. Furthermore, the antibodies elicited during the first 40 days after detectable plasma viremia did not inhibit virus in standard TZM-bl neutralization assays and did not mediate antibody-dependent cell-mediated virus inhibition (ADCVI) (289).

There is evidence that both neutralizing and non-neutralizing HIV-specific antibodies can contribute to protection or exert immune pressure on the virus leading to escape. Moreover, HIV-specific broadly neutralizing antibodies (NAbs) have been shown to prevent the virion from infecting the host cells by binding cell-free virus, thereby disrupting subsequent rounds of replication (290,291). However, the first neutralizing antibodies are detected at approximately 13 weeks post infection in acute clade B-infected patients and at 3–8 weeks post infection for clade C-infected patients (292). In macaques, the passive transfer of modest titers of potent and broadly neutralizing anti-HIV monoclonal antibodies has been shown to block simian human immunodeficiency virus (SHIV) infection (291).

Non-neutralizing antibodies that bind to HIV antigens on the surface of HIV-infected cells by their Fab fragments can recruit by their Fc fragment innate immune cells that possess an Fc-gamma receptors (FcγR), including APCs, NK cells, or monocyte/macrophages. Such FcγR-mediated recruitment of innate immune cells can lead to either killing of the infected cell, referred to as antibody-dependent cellular cytotoxicity (ADCC), or to inhibition of viral replication, referred to as ADCVI, AD cellular phagocytosis, AD cellular trogocytosis, and AD complement deposition (293).

Two kinds of HIV-specific antibody-mediated immune responses have been described in HESN individuals: antibodies to self cellular proteins involved in HIV infection or entry process, and HIV-specific mucosal antibodies. These self antibodies to cellular proteins involved in HIV infection are directed to CD4⁺ T cells and HLA class I molecules. Anti-HLA class I antibodies were first associated with long-lasting exposure to blood derivatives, as observed in hemophiliacs (294,295). These anti-HLA class I antibodies cross-react with gp120 and have also been found in sera of other HESN individuals, including people who inject drugs (PWID) (296). Although HIV-seropositive individuals and some healthy blood donors may have anti-CD4 antibodies, their anti-CD4 antibodies recognized epitopes different from those seen by antibodies found in sera of HESN individuals (297). HIV-specific IgA and IgG antibodies expressed at the mucosal and systemic level target CCR5, leading to downregulation of CCR5 (298). Although both anti-CD4 and anti-CCR5 antibodies have been observed as specific HIV-exposure markers in Asian and Caucasian HESN, it has not been described in African HESN individuals (299). Thus, differences in the genetic background, in the route of exposure, or the different environmental conditions, and modulating immune responses to microbes may determine the antibody response to HIV in HESN (300–302). Neutralization of HIV by IgA that recognizes epitopes on gp41 has been described in multiple HESN cohorts (303–308). In *ex vivo* assays, IgA from HESN has been shown to neutralize HIV with the most neutralizing epitopes found in gp41 and gp120 (303,309). HIV-specific IgA responses may also inhibit transcytosis across epithelial barriers and trigger ADCC of infected target cells in conjunction with innate immune cells bearing the IgA-specific Fc receptor CD89 (310,311).

1.2.2.2 T lymphocytes

T lymphocytes develop in the thymus from common lymphoid progenitors originating from the bone marrow or fetal liver (312,313). Progenitor movement into the thymus is promoted by the interaction of platelet selectin glycoprotein 1 on the progenitors with the adhesion molecule P-selectin on the thymic epithelium. Newly arrived progenitor cells rapidly expand under the influence of interleukin-7 (IL-7), the receptor of which signals through the common γ chain, which is encoded on the X chromosome and is shared by several other cytokine receptors (IL-2, IL-4, IL-9, IL-15, and IL-21). This early thymocyte expansion is accompanied by induction of transcription

factors including *Notch*, which commits precursors to the T cell lineage and induces the expression of genes essential in TCR assembly (314). The expanded progenitor then differentiates in an antigen-independent process in which a coordinated series of genomic rearrangements lead to the creation of functional genes encoding the α and β or γ and δ chains of the TCR. Thus, the configuration of TCR loci contains arrays of the genes encoding V, D, and J segments. Although all the TCR loci have the V and J, only the β and δ loci have the D segment. One V, one D (for β and δ), and one J segment are randomly spliced together in a spatially and sequentially ordered process mediated by an enzymatic complex known as the V(D)J recombinase. The V(D)J recombinase comprises 2 proteins encoded by the recombinase-activating genes 1 and 2 (RAG1 and RAG2). Each assembled V-D-J cassette represents one of a vast number of possible permutations of recombinations of component V, D, and J segments. The resulting structure dictates the amino acid sequence and binding specificity of the TCR referred to as combinatorial diversity (315). Additional diversity, known as junctional diversity, develops through some inherent imprecision in the DNA-joining reactions involved in the ligation of double-strand DNA breaks, resulting in some addition or removal of bases. More significant variability is produced by the template-independent addition of several (generally 1-5) nucleotides at the joints that encode the third complementarity determining region of the antigen-binding pocket of the TCR. The enzyme terminal deoxyribonucleotidyl transferase catalyzes this. The transition from a pre-T to double positive T cells expressing CD4 and CD8 occurs through sequential rearrangements of 2 TCR genes, leading to surface expression of an $\alpha\beta$ or $\gamma\delta$ TCR. The TCR chains are assembled at the cell surface as a complex with the proteins constituting CD3, including the γ , δ , ϵ and ζ chains (316).

The resting state of the T lymphocyte is actively maintained (317,318). Upon ligation of TCR, T cells may become activated, resulting in expansion and cytokine expression (319). However, sometimes TCR ligation of antigen is insufficient to induce a T cell response and results in T cell anergy (320). However, T cell anergy can be prevented by co-stimulatory signals provided by accessory molecules or the interleukin 2 receptor (IL-2R) (321).

The quiescent state is characterized by low metabolic rates, low transcription levels limited to basic housekeeping genes, small cell size, and very long periods of survival (318). Although HIV can

infect quiescent CD4⁺ T cells, viral replication is inefficient in this cell phenotype, making it difficult for the virus to establish a productive infection (322). However, infection of quiescent CD4⁺ T cells may result in latent infection, which may be reactivated upon activation of the CD4⁺ cells (323,324). Thus, for HIV to establish a productive infection, it requires activated CD4⁺ T cells. Cytokines such as IL-4, IL-7, and IL-15 can render quiescent CD4⁺ T cells permissive without being fully activated (325).

T cells can be classified based on how fast they respond to an immune challenge or the type of antigen they detect as conventional or unconventional T cells. Conventional T cells recognize peptide antigens presented by MHC-I or MHC-II molecules. In contrast, unconventional T cells recognize nonpeptide antigens, bound and presented by diverse nonpolymorphic antigen-presenting molecules. Although unconventional T cells have some adaptive immune response characteristics, they are often referred to as innate T cells. This is because their immune response is faster and occurs within hours, as opposed to that of conventional T cells, which takes several days to develop. T cells can also be classified based on TCR expression into either $\alpha\beta$ or $\gamma\delta$ T cells. The majority of $\alpha\beta$ T cells are conventional T cells restricted to recognizing peptides bound to MHC molecules. However, some $\alpha\beta$ T cells, including mucosal-associated T cells (MAIT) and natural killer T (NKT) cells, recognize nonpeptide antigens and are restricted by MR1 and CD1d, respectively. In contrast, $\gamma\delta$ T cells do not require MHC antigen presentation to recognize nonpeptide antigens (326). Unconventional T cells may be involved in linking the innate and adaptive immune responses through differentiation and maturation of MDDCs and T cell priming (73,75,327).

1.2.2.2.1 Chemokine receptors involved in T-cell trafficking

There are 23 human chemokine receptors, classified depending on their biological functions as constitutive or inflammatory receptors depending on whether they are mostly involved in development and homeostasis, or in host response to inflammation and infection (328). Unnecessary movement of cells can result in immune activation and increased target cells thus leading to increased risk of HIV infection. The ligands for CCR6 are CCL20, also known as macrophage infiltrating factor protein-3 α (MIP-3 α), and liver activation regulated chemokine (LARC) (329). The interaction between CCR6 and CCL20 has been shown to be involved in

several autoimmune and inflammatory processes such as rheumatoid arthritis, (329) multiple sclerosis (330,331), psoriasis (332), and inflammatory bowel disease (333). Naïve T cells expressing high CCR7 continuously circulate between blood and secondary lymphoid organs in search of their cognate antigen whereas the CCR7 ligands CCL19 and CCL21 are homeostatically expressed. On activation by both antigen and innate stimuli, such as type I interferons, T cells alter their expression of chemokine receptors (334) so that some receptors (such as CCR7) are downregulated while inflammatory chemokine receptors, such as CXCR3, CXCR6, and CCR5 are upregulated (335). In humans, CXCR6 is expressed by a subset of CD4⁺ and CD8⁺ T cells and is upregulated after stimulation. CXCR6 may be used as a co-receptor by HIV and SIV to enter target cells. The ligand for CXCR6 is CXCL16. Thus, CXCR6 plays an important role in homing of polarized Th1 cells to inflamed tissues (336–338). High CXCR6 expression has been associated with severe pulmonary *Mycobacteria tuberculosis* infections, influenza virus infections (339), and symptomatic cytomegalovirus infection (CMVI) in lung tissue transplant recipients (340). CCR5 is a major HIV co-receptor (341) and is expressed on immature (Th0) and memory/primed Th1 cells, monocytes, macrophages, and immature DCs; on neurons, astrocytes, and microglia; on epithelium, endothelium, vascular smooth muscle, and fibroblasts. The ligands for CCR5 include macrophage inflammatory protein MIP-1 α (CCL3) and RANTES, also known as CCL5, CCL4 (MIP-1 β) (342), CCL2 (monocyte chemoattractant protein -1) (MCP-1), CCL7 (MCP-3), CCL8 (MCP-2), CCL11 (eotaxin1), and CCL13 (MCP-4) (343,344). The level of CCR5 expression on human cells varies, with some expressing high and others low levels of CCR5 (345). Chemokine binding to CCR5 activates cells expressing this receptors and has been shown to lead to its internalization, with the participation of clathrin-coated pits and caveolae, followed by recycling to the cell surface via recycling endosomes (346,347). Stimulation of $\gamma\delta$ T cells with heat-killed extracts of *Mycobacterium tuberculosis* down-modulated cell surface expression of CCR5 on $\gamma\delta$ T cells in a macrophage-dependent manner, while synthetic phosphoantigen isopentenyl pyrophosphate and CCR5 ligands directly triggered CCR5 down-modulation on $\gamma\delta$ T cells (348). CCR6 has been shown to be expressed by T helper 17 (Th17) and T regulatory (Treg) and mediate migration of these cells to inflamed tissues (331). CCR6 has also been shown to promote migration of IL-17-producing $\gamma\delta$ T cells to injured liver (349). MAIT cells have been shown to have an effector memory phenotype and to express high CCR5 and CCR6, indicating preferential homing to tissues and particularly the intestine and the liver (350,351). CXCR3 is an inflammatory

chemokine expressed on CD4⁺ T cells, CD8⁺ T cells (352), NK cells, NKT cells (353) pDCs (354) and subsets of B cells (355) where it may play a role in the migration of these cells to inflamed tissues. CXCR3 binds to monokine induced by gamma-interferon (MIG) (also known as CXCL9), interferon-induced protein of 10 kDa (IP-10) (also known as CXCL10), and interferon-inducible T cell alpha chemoattractant (I-TAC) (also known as CXCL11), to induce migration of activated T cells in vitro and in vivo (356–359). CCR3 is highly expressed in effector T cells and has been shown to be important in the recruitment of effector CD8⁺ T cells to allografts and sites of viral infection within the central nervous system (CNS) and genital tract, where its ligands, CXCL9 and CXCL10, are induced by IFN- γ (360). CXCR4 binds to CXCL12 also known as stromal cell-derived factor-1 (SDF-1) leading to several physiological and pathological processes including cell localization, chemotaxis, activation, migration, proliferation and differentiation (361–363). CXCR4 can also be used as a co-receptor by HIV to infect cells (364). CD161⁺CD8⁺ cells have been shown to express high levels of tissue-homing markers including CCR6, CCR5, CXCR6 and CXCR4 (365,366). Also, functional studies have reported migration of $\gamma\delta$ T cells in response to MCP-1 (367), RANTES, MIP-1 α or CCL3), and MIP-1 β (CCL4), but not in response to CXC chemokines IL-8 (CXCL8) or IP-10 or CXCL10) (368). However, in this study, the corresponding chemokine expression was not investigated. A study comparing the chemokine receptor expression of $\gamma\delta$ and $\alpha\beta$ T cells revealed higher CCR5 expression on $\gamma\delta$ T cells compared to the $\alpha\beta$ T cells (348). MAIT cells and $\gamma\delta$ T cells have an effector memory phenotype that enable them to respond quickly following stimulation leading to expression of cytokines (369,370).

1.2.2.2.2 CD4⁺ T cells

The CD4⁺ T cells are major MHC class II (HLA-DR, HLA-DQ, and HLA-DP) restricted cells that mediate adaptive immune responses. The MHC class II molecules are present on APCs and are inducible by innate immune stimuli, including ligands for TLRs. Activation of naïve T cells leads to differentiation into different subsets depending on the cytokine microenvironment. Subsets of CD4⁺ T cells include naïve T cells (Th0), T helper 1 (Th1), Th2, Th17, T regulatory (Treg), follicular Th (Tfh), and Th9 cells, each with a characteristic functions and cytokine profile (371).

1.2.2.2.1 CD4+ T cells in HIV infection

Not all subsets of CD4+ T cells are infected during the early stages of HIV transmission. It was demonstrated in a SIV infection model that during the early stage of viral infection, HIV preferentially infects CD4+CCR6+, ROR γ T+ Th17 cells (372). In one study, HIV-positive female sex workers in Kenya were found to have depleted Th17 cells in the cervix while uninfected individuals maintained high Th17 cell levels in the cervix, suggesting that HIV preferentially replicates within Th17 cells (169). The ectocervix also has more intraepithelial CD4+ T cells and macrophages than the endocervix and vaginal area, suggesting that most transmission could be occurring in the ectocervix. Susceptibility of CD4+ T cells also depends on the activation status of the CD4+ T cells. Although HIV can infect quiescent CD4+ T cells (373), it preferentially replicates in activated CD4+ T cells leading to HIV dissemination (374).

1.2.2.2.2 Immune quiescence and HIV risk

Immune quiescence is characterized by CD4+ T cells expressing low activation markers, including CD69 and low basal gene transcription (375). Vatakis et al. (376) demonstrated the reduced ability of HIV to infect quiescent CD4+ T cells in vitro. HIV relies on cellular resources to replicate, which are only present in replicating cells, thus it cannot efficiently infect quiescent CD4+ T cells due to their low metabolic rate and transcription (376). Multiple studies have linked low immune activation with natural resistance against HIV infection in HESN individuals (375,377–381), suggesting the importance of understanding how immune modulation may result in immune activation to lower the risk of HIV infection. Reduced activation in CD4+ T cell subsets and higher levels of Treg cells in HESN CSW were associated with resistance to HIV infection (382,383). Another study reported CD4+ and CD8+ T cells expressing low levels of activation markers HLA-DR, CD38, CD70, and Ki67 in a cohort of HESN MSM (88). A similar study found low expression of the activation markers CD38, HLA-DR, and CCR5 on CD4+ T cells on uninfected partners of serodiscordant couples (384,385), suggesting the need to maintain immune system quiescence to protect against HIV infection. Epithelial and cervical mucosal cells in HESN have been shown to have reduced expression of PRRs that recognize HIV proteins and nucleic acids, including RIG-1, TLR2, TLR4, TLR7, and TLR8 (378). However, in this study, it was also reported that TLR stimulation of CMC resulted in a robust antiviral response (378). Recognition of PAMPs by TLRs

leads to proinflammatory cytokines, which may modulate the immune system, resulting in immune activation (386). Inflammatory cytokines, TNF- α and IL-1, were shown to influence HIV replication by activating the NF- κ B transcription factor, which binds to the HIV promoter region (387). Furthermore, HESN CSWs have been found to have low levels of proinflammatory cytokines, including IL-1 β and IFN- γ -regulated chemokines MIG and IP-10. HIV-specific CD4+ cells that express a high level of IL-2 have been demonstrated in HESN subjects (388). Low CD4+ T cell gene expression has also been demonstrated in PBMCS and in whole blood from HESN CSWs (51).

CD4 is the primary receptor for HIV while the CCR5 and CXCR4 receptors act as HIV coreceptors. Human T lymphocytes can remain quiescent cells (in the G₀ phase of the cell cycle) and only proliferate upon activation. Activated CD4+ T cells can be infected by HIV, leading to their depletion and immune dysfunction (288). T cells that are susceptible to activation and depletion include effector memory CD4+ T cells, Th17 cells, and MAIT cells. Depletion of CD4+ T cells in gut lamina propria occurs early and is associated with increased microbial translocation across the gut wall and immune activation due to microbial products in the blood. Antiretroviral therapy does not restore CD4+ T cells in the gut mucosa (389,390).

Some individuals who have reduced progression to HIV disease have been reported to express CD4+ T cells that are polyfunctional following Gag stimulation (391). Higher HIV-specific Th17 cells expressing lower checkpoint inhibitors such as CTLA-4, PD-1 and Tim3 have also been reported in LTNPs compared to HIV progressors (392,393). Additionally those with reduced HIV disease progression have been reported to express higher numbers of the CD4+ Treg subset than progressors and CD4+ T cells express lower level of IL-10 in response to p24 stimulation in non-progressors compared to progressors (393). Taken together this shows that CD4+ T cells are important in the control of HIV progression.

1.2.2.2.3 CD8+ T cells

CD8+ T cells are immune cells that play an essential role in the adaptive immune response against pathogenic microorganisms and malignancies (394). Activation of naïve CD8+ T cells requires three signals, including TCR recognition of peptide antigens presented by MHC class I antigen,

binding of the CD28 receptor on CD8 T cells to the co-stimulatory receptors on APCs including CD80 and CD86, and cytokines expressed by innate cells in response to PAMPs, for example, IL-12 and type I IFN (395,396). Activated CD8⁺ T cells undergo clonal expansion, producing a large pool of effector cells that perform effector functions, such as the expression of cytokines, cytotoxic molecules, and a high capacity for degranulation (397–400). After undergoing clonal expansion, CD8⁺ T cells undergo apoptosis, and the remaining antigen specific CD8⁺ T cells become memory cells. Although HIV-specific T-cell responses have been identified in several HESN individuals from multiple cohorts, there have been controversial results in quantitative and qualitative differences in the T-cell response (384,401–404). Ritchie et al. (405) reported a higher magnitude of specific CD4⁺ T cell responses in HESN than HIV unexposed seronegative controls. However, in this study, even unexposed HIV individuals responded to the pool of HIV peptides, raising questions with respect to specificity of the experimental method in identifying HIV-specific T cell responses (405). Less proliferation and expression of IFN- γ has been observed in CD4⁺ T cells stimulated with p24 in HESN compared to HIV-seropositive patients (406). The blood and genital tract of HESN women have increased Tregs (407,408), lower CD4 T cell expression of the activation markers, CD69 (407) HLA-DR (384,409) and CD38, and reduced expression of the proinflammatory cytokines IL-17, IL-22, IL-1 β , IL-6, and TNF- α (410,411). In HESN individuals, HIV-specific CD4⁺ T cells have also been shown to express high IL-2 and CC-chemokines, including RANTES and MIP1- β (412). HIV-specific T-cell responses in HESNs may be markers for previous exposure to HIV rather than playing a role in preventing HIV infection.

1.2.2.2.3.1 CD8⁺ T cells in HIV infection

HIV infection has been shown to result in a robust CD8⁺ T cell response in most individuals, including those who fail to control the infection (413–415). Although, antigen-specific IFN- γ expressed by CD8⁺ T cells exposed to HIV antigens is widely used as a marker for CD8-specific T responses, it is not associated with HIV control (415–417). Although HIV-specific CD8⁺ T cells do not protect against HIV infection, there is considerable evidence to suggest that they are essential in suppressing HIV replication, which leads to slower diseases progression (418). In a rhesus macaques model immunized with virulent attenuated SHIV, the CTL response at the mucosal site of viral transmission was shown to be protective against mucosal challenge with

pathogenic SIVmac (419). Prior MHC class I tetramer-based studies demonstrated that the frequency of HIV-specific CD8⁺ T cells was inversely correlated with viral load (420). However, subsequent studies looking at the frequency of functional HIV-specific CD8⁺ T cells and HIV viral load have been inconclusive (414,415,421).

The number of epitopes recognized by HIV-specific CD8⁺ T cells does not correlate with control of viral replication or protection from disease progression (417). Also, HIV-specific CD8⁺ T cells that secrete IFN- γ were reported to be different from those that kill infected target cells (422). However, polyfunctional HIV-specific CD8⁺ T cells that secrete cytokines and effector molecules are more abundant in those that progress more slowly to HIV disease (423,424). HIV-specific CD8⁺ T cells have been associated with a lower viral load, smaller viral reservoirs, and the least culturable virus (425,426). Upon in vitro antigenic stimulation, HIV-specific CD8⁺ T cells from those progressing more slowly to HIV disease demonstrated a greater capacity to proliferate and develop cytolytic potential compared to progressors (427,428). Also, HIV-specific CD8 responses against Gag were shown to be polyfunctional, expressing more than one cytokine. Ex vivo CD8⁺ T cells from these individuals showed an ability to target and eliminate activated and non-activated CD4⁺ T cells infected with HIV (429).

HIV-specific CTL mediated by CD8⁺ T cells have also been demonstrated in HESN individuals (388). MHC Class I-restricted CTL to HIV-1 has also been reported in HIV-negative children of HIV-1-positive mothers (430,431). HIV-specific CD8 T cells have been described in HIV-resistant partners of HIV patients (432,433) and in HESN women from the Pumwani CSW cohort (434,435), who can be epidemiologically defined as resistant to HIV infection. However, HIV-specific CD8⁺ T cells in the peripheral blood and genital tract do not correlate with protection and resistance to HIV infection (432,433).

1.2.2.2.4 Unconventional T cells

Unlike conventional T cells that recognize peptide antigens presented by polymorphic MHC class I or class II molecules and require clonal expansion when they encounter an antigen, unconventional T cells recognize nonpeptide antigens presented by nonpolymorphic MHC-like molecules. Immune responses mediated by unconventional T cells are rapid since they do not

require clonal expansion. Therefore, these cells are sometimes referred to as innate T cells. Unconventional T cells can be classified as either alpha beta ($\alpha\beta$) or gamma delta ($\gamma\delta$) T cells (436).

1.2.2.2.4.1 Mucosal-associated invariant T cells

MAIT cells are unconventional T cells that express an invariant TCR consisting of an $\alpha\beta$ chain and recognize nonpeptide antigens presented by the MHC class I related protein (MR1) (437,438). MAIT cells are abundant in humans making up to 10% of peripheral blood and 45% of liver T cells (439–441). Human MAIT cells express a unique invariant TCR α chain consisting of TRAV1-2 joined to TRAJ33 with a constrained TCR β -chain repertoire (TRBV6 and TRBV20) (442). MAIT cells are restricted by the monomorphic MR1 (443), a β 2-microglobulin-associated antigen-presenting molecule (444). In humans, MR1 mRNA has been detected in the placenta, lung, liver, kidney, spleen, thymus, prostate, testis, ovary, small intestine, colon, and peripheral blood leucocytes (445). However, it is difficult to tell which cell types within these tissues express MR1, nor whether the expression is restricted to hematopoietic cells. Although surface expression of MR1 has been reported in different cell lines transfected with MR1, it has been challenging to detect MR1 on primary isolated human cells by flow cytometry. Thus, surface expression of MR1 was not detected on primary peripheral blood leucocytes, MDM, or DCs using conformation-dependent monoclonal antibodies, 12.2 and 26.5, or a rabbit polyclonal serum, RAMRN-2 (446). However, some studies have reported detecting small amounts of MR1 at the surface of DC and B cells by flow cytometry (447,448). In one study, human airway epithelial cells and DCs were infected with *Mycobacterium tuberculosis* and compared the ability of infected epithelial cells and DCs to activate CD8⁺ T cells. This study showed that airway epithelial cells activated MAIT cells via MR1 presentation of antigens. They also showed that airway epithelial cells expressed more MR1 on the cell surface than DCs did (447). In another study on the origin, location, and surface expression of MR1, cell surface proteins were biotinylated and then precipitated for MR1-specific immunoblot analysis. The authors suggested that MR1 was found in the endoplasmic reticulum, but surface expression required recognition of its vitamin B2 metabolite ligands.

MAIT cells can be activated in a TCR-dependent or TCR-independent manner (**Figure 3**). B cells were the first identified as APCs for MAIT cells. B cells are necessary to select and expand MAIT cells as they express beta 2 microglobulin (β 2m)-dependent, transporter associated with antigen

processing (TAP)- and invariant chain (Ii)-independent MHC class Ib that selects MAIT cells (449). Different B cell subsets express different TLRs, resulting in differences in antigen presentation, antibody, and cytokine production by different B cell subsets (450,451). For example, TLR9 stimulation has been shown to increase MR1 surface expression on B cells, exclusively, but not other APCs like monocytes DCs (452). Lung epithelial cells and DCs have also been shown to express MR1 (447,448). MAIT cells respond to many bacteria and yeast, but they fail to respond either to some bacterial strains that lack a vitamin B metabolite pathway or to viruses (439). MR1 binds vitamin B metabolites, including 6-formyl pterin (6-FP) and intermediate of vitamin B2 biosynthesis, presenting them to MAIT cells (**Figure 3**). Activation of MAIT cells leads to the expression of proinflammatory cytokines and cytolytic molecules (**Figure 3**) (188). The most potent intermediates of vitamin B biosynthesis recognized by MAIT cells are 5-(2-oxopropylideneamino)-6-D-ribityl amino uracil (5-OP-RU) (188).

TCR-independent activation of MAIT cells is mediated by cytokines, including IL-12 and IL-18 produced by APCs following stimulation through TLRs or viral infections (**Figure 3**) (189). MAIT cells express several cytokine receptors, including IL-1R, IL-7R, IL-12R, IL-15R, IL-18R, and IL-23R, which bind their respective cytokine leading to stimulation of MAIT cells. However, stimulation requires at least two cytokines; for example, IL-12 and IL-18 increase IFN- γ , TNF- α , and GrzB production (**Figure 3**). IL-15 activates MAIT cells only in the presence of monocytes that produce IL-18, and this leads to the production of IFN- γ , TNF- α , GrzB, and perforin (453). Activated MAIT cells have been shown to express cytokines, including IFN- γ , TNF- α , IL-17, and granulocyte colony stimulating factor (GM-CSF) (454).

In early studies, MAIT cells were defined as cells that were CD3⁺, TRAV1-2⁺, and CD161⁺⁺ (455,456). However, these surrogate markers to define MAIT cells were inaccurate because immature MAIT cells lack CD161 (457). Also, CD161 may be downregulated on MAIT cells following activation (458–460). Some conventional $\alpha\beta$ T cells also express TRAV1-2 (461). The creation of an MR1 tetramer (MR1AgTet) loaded with 5-OP-RU led to improved MAIT cell identification. Thus, MAIT cells can be defined as cells that express CD3, TRAV1-2, and CD161 and stain positively with MR1AgTet loaded with 5-OP-RU. MAIT cells can now be classified into five subsets based on the expression of CD4 and CD8 receptors: CD4⁺CD8⁻, CD4⁺CD8⁺, CD4⁻

CD8⁻, CD4⁻ CD8 $\alpha\alpha$ ⁺ and CD4⁻ CD8 $\alpha\beta$ ⁺ (440). The CD8⁺ and double negative (DN) MAIT cells differ in their transcriptional programs and functional characteristics. CD8⁺ MAIT cells respond more to activating factors by producing more IFN- γ , TNF- α , and GrzB consistent with their higher basal expression of IL-12R, IL-18R, coactivating receptors, cytotoxic molecules, and the transcription factors Eomes and T-bet. The DN MAIT cells produce more IL-17 upon stimulation, consistent with their higher ROR γ t expression (462). The CD4⁺ subset make up to 2-11% of MAIT cells but their function is not well known.

In humans, MAIT cell development begins in the thymus, and it involves three stages. Stage 1 thymic cells can be identified as CD3⁺, MR1AgTet⁺ CD27⁻ CD161⁻. Stage 2 cells are CD3⁺, MR1AgTet⁺ CD27⁺ CD161⁻ and mostly found in the thymus. However, a small population is also found in the blood. The transition of MAIT cells from stage 2 to 3 involves increased expression of promyelocytic leukemia zinc finger protein (PLZF) and IL-18R and acquisition of functionality. Stage 3 MAIT cells reside primarily outside the thymus and are CD3⁺, MR1-tet⁺ CD27⁺ CD161⁺ IL18R⁺(456). MAIT cells continue to expand after leaving the thymus until their numbers in the circulation peak (making up to 10% of T lymphocytes at 20–29 years of age) before starting to decline gradually thereafter, with individuals 70 years or older having less than 1% MAIT cells in the blood. As MAIT cells mature in the blood, they transition from CD8 $\alpha\beta$ ⁺ low IL-18R and PLZF expression to CD8 $\alpha\alpha$ ⁺, high IL-18R, and PLZF associated with a marked increase in cytokine producing potential (457,463). MAIT cells have been shown to respond rapidly to infections caused by bacteria or viruses, including *Francisella tularensis* (464), *Klebsiella pneumoniae* (465), *Legionella* spp. (466), and influenza (467,468), thus their classification as innate T cells (469).

1.2.2.2.4.1.1 MAIT cells and HIV infection

During HIV infection, MAIT cells play an essential role in immunity against *Mycobacterium tuberculosis* infections (470,471) and other opportunistic infections (472), making the study of the impact of HIV infection on the MAIT cell population a subject of significant interest. Several studies have demonstrated that both acute and chronic HIV infections lead to peripheral MAIT cell depletion that is not fully reversed upon highly active ART (473–476). Although the mechanism that leads to MAIT cell depletion is unknown, some studies have reported activation and exhaustion of these cell populations (458,477,478). During chronic HIV infection, bacterial

product translocation is increased due to gut barrier dysfunction (458,479). These could be the leading cause of activation, exhaustion, and loss of function of MAIT cells. Thus, the depletion and loss of MAIT cell function during HIV infection may contribute to an elevated risk of acquiring tuberculosis and other bacterial infections (469,472).

MAIT cells express high levels of chemokine receptors that enable them to migrate to the site of inflammation (480). In humans, MAIT cells have been shown to express high tissue-homing chemokine receptors, including CCR5, CCR6, CXCR6, as well as $\alpha 4\beta 7$ (481)(454). During viral infections, MAIT cell activation via APC's cytokines led to IFN- γ and cytotoxic factors expression by MAIT cells (468). Expression of IFN- γ has been associated with immune protection against HIV infection in HESN individuals (482). Cytotoxic factors expressed by CTLs have been implicated in eliminating HIV-infected CD4⁺ cells, thus preventing HIV acquisition and dissemination (429). However, activated MAIT cells have been shown to express high levels of proinflammatory cytokines, including IFN- γ , TNF- α , IL-17, and GM-CSF (454). Proinflammatory cytokines, including IFN- γ , TNF- α , and GM-CSF expression by MAIT cells, may modulate the immune system by increasing maturation of the DCs and priming of CD4⁺ T cells. Also, stimulation of MAIT cells may lead to upregulation of CD40L, leading to priming of CD4⁺ T cells and rendering them susceptible to HIV infection (73,327). Thus, this Thesis focused on investigating the nature of MAIT cell responses to TLR7 and TLR8 stimulation, to understand how innate recognition in immune activation relates to further susceptibility to HIV infection. This information might help understand how MAIT cells modulate immune activation and therefore HIV acquisition.

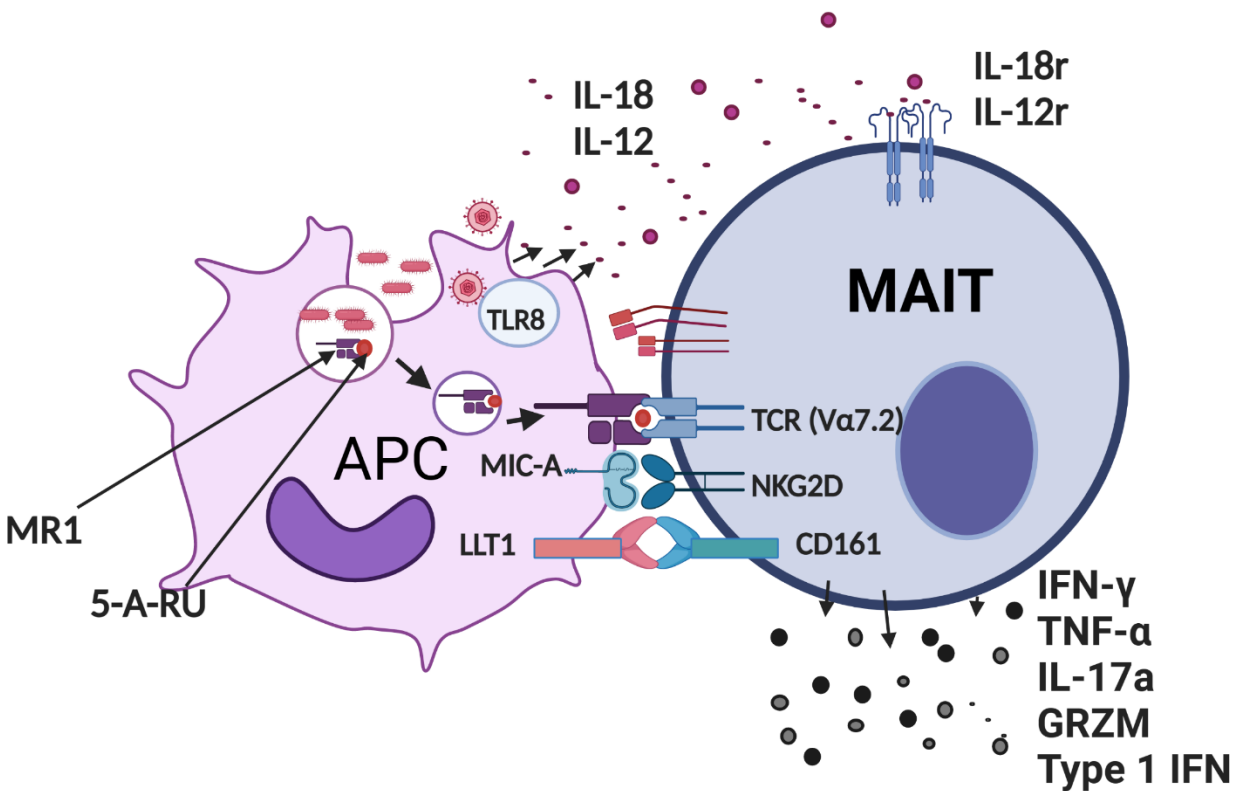


Figure 3. TCR-dependent and -independent activation of MAIT cells. TCR (Va7.2) recognizes bacterial vitamin B metabolites (5-A-RU) presented by MHC related protein 1 (MR1) leading to TCR-dependent activation of MAIT cells. Additionally, either independently, or in concert with TCR signalling, cytokines including IL-12 and IL-18 expressed by antigen-presenting cells can also activate MAIT cells. Other costimulatory molecules include lectin-like transcript 1 (LLT1) that recognize CD161 and natural killer group 2D (NKG2D) that sense MHC class I chain-related proteins (MIC-A). Activated MAIT cells express IFN- γ , TNF- α , IL-17a and type I IFN. Further, MAIT cells mediate cytotoxicity of infected cells by expressing cytotoxic molecules including granzyme.(Adapted from (189)).

1.2.2.2.4.2 Gamma delta T cells

Gamma delta ($\gamma\delta$) T cells are an evolutionarily conserved subset of lymphocytes found among almost all jawed vertebrates, indicating their importance in the immune system (483). Discovered 35 years ago after isolation of the TCR γ chain gene (484), $\gamma\delta$ T cells represent the subgroup of T cells that have γ and δ -glycoprotein chains linked by disulfide bonds. The function of $\gamma\delta$ T cells varies depending on the species, tissue, and immunological milieu (483,485–487). They can recognize, expand, and develop effector responses against infections by *Mycobacteria*, (488) *Plasmodium*, (489,490) *Cytomegalovirus* (CMV) (491,492) and HIV (493). Additionally, $\gamma\delta$ T

cells were shown to be effective in inducing antitumor responses (360,494). Unlike $\alpha\beta$ T cells, $\gamma\delta$ T cells do not require MHC presentation of antigens; they can develop naturally as shown in $\beta 2$ -microglobulin knockout mice. The $\gamma\delta$ TCR consists of two chains, which are generated by the recombination of the variable (V), diversity (D, only in δ -chain), and joining (J) fragments. Development of $\gamma\delta$ T cells occurs in the thymus from CD4⁻ CD8⁻ DN progenitor cells. Although CD4⁻ and CD8⁻ DN may also result in the generation of $\alpha\beta$ T cells, the cell lineage depends on the type of V(D)J rearrangements and the pre-TCR signal strength. Strong signals result in the development of $\gamma\delta$ T cells and a weak signal results in $\alpha\beta$ T cells (495,496). In humans, $\gamma\delta$ T cells have a smaller repertoire of V δ and V γ genes compared to that for $\alpha\beta$ T cells (497). The most frequently used V δ gene segments include V δ 1, V δ 2, and V δ 3 chains paired with one of the several functional V γ gene segments: V γ 2, V γ 3, V γ 4, V γ 5, V γ 8, V γ 9, or V γ 11. Although some combinations are more likely than others, the two major $\gamma\delta$ T cell subsets are V δ 2 and V δ 1, with V γ 9V δ 2⁺ constituting the majority of $\gamma\delta$ T cells in the peripheral blood of healthy donors. However, V γ 9V δ 2⁺ T cells are a minority in the gut, liver and other epithelial tissues, whereas V δ 1⁺ $\gamma\delta$ cells are present at higher frequencies at these sites (498). Although $\gamma\delta$ T cells express CD3 (a complex forming part of the TCR), they are mostly CD4⁻ CD8⁻ (DN), however, they may express variably CD4 or CD8 (499,500). In humans, $\gamma\delta$ T cells are involved in immunosurveillance (501) and immune response to viruses, intracellular bacteria, and parasitic protozoa (502–506) and the pathogenesis of autoimmune diseases (507). In addition, $\gamma\delta$ T cells are being explored in cell-based immunotherapy (508,509). Thus, in the peripheral tissues like liver, V δ 1 T cells are essential in maintaining epithelial tissue integrity via receptors that recognize the stress-inducible ligands MHC class I chain-related proteins (MIC) A and MICB expressed by virus-infected and transformed cells, and self-glycolipids presented by CD1c/d molecules (510). The V δ 2 subset is also found in other species, e.g., in non-human primates (511,512) and alpacas but not rodents (513). Although there are six subsets in total of $\gamma\delta$ T cells in humans, the 2 main subsets of $\gamma\delta$ T cells in humans are classified by their V δ chain rearrangement. The V δ 1 cells are predominantly found in the gut and other peripheral tissues (such as lung, kidney, and spleen), whereas the V δ 2 cells represent the major fraction of circulating $\gamma\delta$ T cells in blood (514). Some $\gamma\delta$ T cells express CD161, a C-type lectin, and such cells have been found to be involved in the pathogenesis of inflammatory disease such as multiple sclerosis (515).

The V γ 9V δ 2⁺ TCRs detect small non-protein phosphorylated molecules termed phosphoantigens (p-Ags) independent of MHC presentation (516). Although V δ 2 recognizes p-Ag, including isopentenyl pyrophosphate (IPP) and dimethylallyl pyrophosphate (DMAPP) present in both prokaryotes and eukaryotes, the most potent p-Ag is (E)-4-hydroxy-3-methyl-but-2-enyl pyrophosphate (HMBPP), an intermediate of the prokaryotic non-mevalonate pathway of isoprenoid biosynthesis. During stress situations like infection or malignant transformation, IPP and DMAPP can accumulate inside eukaryotic cells, whereas HMBPP is produced directly by pathogens such as Gram-positive bacteria, *Plasmodium*, or *Toxoplasma gondii* (517). Butyrophilin 3 A1 (BTN3A1), a protein that belongs to the B7 receptor family-like proteins, is essential for $\gamma\delta$ TCR-mediated p-Ag-recognition (518,519). BTN3A1 consists of two extracellular Ig-like domains, transmembrane and juxta membrane domains, and an intracellular B30.2 domain (520). The majority of $\gamma\delta$ T cells in the peripheral blood of healthy individuals are V γ 9V δ 2⁺. This is because V δ 2 but not V δ 1 express a memory phenotype CD45RO as early as one month after birth; therefore, early exposure to bacteria leads to the expansion and proliferation of the $\gamma\delta$ T cell subset, V δ 2 (521). Human $\gamma\delta$ T cells have been shown to have the ability to recognize a wide variety of antigens in an MHC-independent manner, leading to cytolysis of infected cells, or modulation of the immune system, thus bridging the gap between the innate and adaptive immune systems (522). Human $\gamma\delta$ T cells have also been shown to express TLR and can be activated directly through TLRs 7 and 8, recognizing their ligands (523,524) or by cytokines that are expressed by APC following TLR7 and TLR8 stimulation including IL-18 and IL-12 (525).

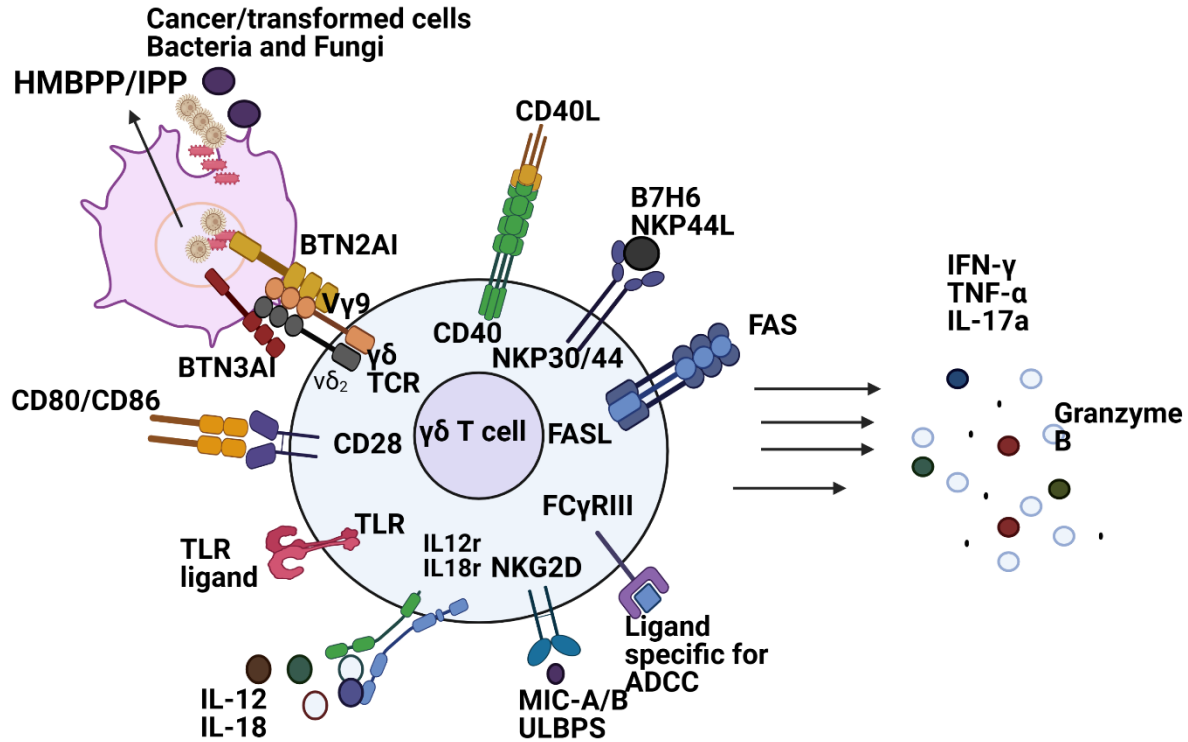


Figure 4. Expression of a wide range of receptors by $\gamma\delta$ T cells. TCR dependent and independent activation of gamma delta ($\gamma\delta$) T cell. TCR- dependent recognition of (E)-4-hydroxy-3-methyl-but-2-enyl pyrophosphate (HMBPP) or isopentenyl pyrophosphate (IPP) via butyrophilin subfamily 3 members A1 (BTN3A1) and BTN2A1 antigen presentation. TCR independent recognition of CD80/CD86 by CD28, TLR ligands by TLR, cytokines by cytokine receptors including IL-12 receptor (IL-12r), IL-18 receptor (IL-18r) that recognize IL-2, IL-8, natural killer group 2D (NKG2D) that sense MHC class I chain-related proteins (MIC-A/B or ULBPS), FC gamma receptor II (FC γ RII) that bind to ligand specific for ADCC, FAS ligand (FASL), natural cytotoxicity receptor (NKP30/44) that bind to FAS, D7H6 NKP44L and CD40 that bind to CD40L. Adapted from (526).

Table 1 Subsets of gamma delta T cells

Subset	V γ V δ pairing	Tissue distribution	Functions	References
Human				
V δ 1	Undefined	Blood, epithelia, dermis, spleen, and liver	Recognize CD1c lipid antigen-presenting cells expressed on APCs Infiltrate tumors of epithelial origin Reactive against MHC class I chain-related (MICA/MICB) stressed induced proteins antigens expressed on epithelial cells Lyse tumor cells expressing MICA/MICB ligands for NKG2D Produce TH1 cytokines	(527–533)
V δ 2	V γ 9V δ 2	Blood	TCR-dependent recognition of microbe- and host-derived phosphorylated prenyl metabolites (phosphoantigens)	(511,512,518,519,534–536)
V δ 3	Undefined	0.2% peripheral blood T cells Enriched in Liver and Gut epithelia	Recognize CD1d kill CD1d+ target cells released Th1, Th2, and Th17 cytokines Induce DC maturation of monocyte-derived dendritic cells	(537)
Mouse				
V γ 1	V γ 1V δ 6.3	Blood, spleen, Liver and lymphoid tissue	Produce IL-4. Promote Treg cells' function	(538)
V γ 2	Not defined	Very rare		
V γ 4		Lymphoid tissue, lungs, liver, CNS and inflamed dermis	Produce IL-17 and express IL-23R Promote virus-induced encephalitis	(538–543)
V γ 5	V γ 5V δ 1	Epidermis	Regulate skin inflammation by maintaining epidermal homeostasis	(544,545)
V γ 6	V γ 6V δ 1	Mucosal tissues, reproductive tract lungs, tongue, liver, placenta and kidney	Produce IL-17, IL22, IFN- γ and express IL-23R	(541)
V γ 7	V γ 7V δ 4 V γ 7V δ 5 V γ 7V δ 6	Intraepithelial lymphocytes and intestinal mucosa	Prevent colitis by protecting the intestinal barrier	(546–548)

1.2.2.2.4.2.1 Gamma delta T cells and immune activation

Although $\gamma\delta$ T cells have a less diverse range of TCR compared to $\alpha\beta$ T cells, they recognize a wide range of molecules, including nonpeptide metabolites of isoprenoid biosynthesis, stress molecules (MICA and MICB), heat shock proteins, and IL-12 together with IL-18 cytokines. Human $\gamma\delta$ T cells have also been shown to express TLR1, TLR2, TLR3, TLR4, TLR5, TLR6, TLR7, and TLR8 (549). Activation of $\gamma\delta$ T cells may lead to the expression of proinflammatory cytokines, including TNF- α , IFN- γ , IL-4, IL-6, and cytotoxic molecules, which may increase immune activation. Gamma delta T cells have also been shown to be crucial in linking the innate and adaptive immunity by encouraging MDDC maturation, differentiation of B cells into APCs, and therefore priming of $\alpha\beta$ T cells (75,550). The CD1c-restricted V δ 1 $\gamma\delta$ T cell subsets, in direct contact with CD1c+ myeloid DC cells (mDCs) can induce the maturation of MDDC in vitro (551), suggesting that similar interactions may also occur at mucosal sites in vivo. V δ 1 $\gamma\delta$ T cell subsets-induced maturation of CD1+ mDC is not directly dependent on a foreign antigen but is mediated by TNF- α activation of the V δ 1 $\gamma\delta$ T cell subsets (552–554). Gut-tropic $\gamma\delta$ T cells can promote Th1/Th17 differentiation of CD4+ T cells in vivo, and this has been associated with exacerbated colitis in murine models (555,556). The V δ 2 $\gamma\delta$ T cell subsets expressing the PD1 isoform Δ 42 may promote DC maturation during gut inflammation in humanized mice (557). Most of the V δ 2 $\gamma\delta$ T cell subsets tissue tropic cells express homing receptors for the mucosal barrier, including the skin cutaneous lymphocyte-associated antigen (CLA) (558) and intestine integrin α 4 β 7 and CCR9 (557,559); these play a role in epithelial barrier protection against pathogenic bacteria and epithelial barrier integrity. The V δ 2 $\gamma\delta$ T cell subsets express high levels of IL-22, which is involved in maintaining epithelial barrier integrity (559).

1.2.2.2.4.2.2 Gamma delta T cells and HIV infection

HIV infection results in an altered distribution of $\gamma\delta$ T cell subsets within the blood of an infected individual that results in more V δ 1 cells than V δ 2 $\gamma\delta$ T cell subsets (560). This may be due to the observation that unlike V δ 1 $\gamma\delta$ T cell subsets, the V γ 9V δ 2 $\gamma\delta$ T cell subsets are more susceptible to activation-induced cell death. In contrast, V δ 1 $\gamma\delta$ T cell subsets can persist in the circulation for many years, although they have an activated phenotype as evidenced by their expression of HLA-DR (560–562). The inverted ratio of V δ 2/V δ 1 $\gamma\delta$ T cell subsets may also be due to V δ 1 $\gamma\delta$ T cell

subsets expansion as observed during early HIV infection (505,563). It is suggested that the expanded V δ 1 $\gamma\delta$ T cell subsets contribute to the control of HIV replication at mucosal sites of entry (564).

Peripheral blood V γ 9V δ 2 $\gamma\delta$ T cell subsets isolated from uninfected rhesus monkeys (naïve to viral antigens) were directly cytotoxic for SIV-infected target cells (564), suggesting a role for V γ 9V δ 2 $\gamma\delta$ T cell subsets in protection against HIV infection. Furthermore, healthy V γ 9V δ 2 $\gamma\delta$ T cell subsets have been reported to produce large amounts of IFN- γ , TNF- α , and the chemokines RANTES or MIP-1 β , which are associated with antiviral immunity (565). RANTES, MIP-1 β , and MIP-1 α have also been shown to block HIV entry by competing for the CCR5 on CD4+ cells. Peripheral blood V γ 9V δ 2 $\gamma\delta$ T cell subsets can also produce proinflammatory IFN- γ and TNF- α or regulatory cytokines that modulate the innate and acquired immunity (566).

1.2.2.2.4.3 Effect of MAIT and $\gamma\delta$ T cells activation on T cells during HIV infection

MAIT cells rapidly respond against bacterial as well as viral infections in an innate-like manner. In bacterial infection, MR1 presents small molecule ligands from the riboflavin biosynthesis pathway to MAIT cells, activating them and leading to effector functions. Viruses lack metabolic pathways to activate MAIT cells through MR1. However, during viral infections, the activation of MAIT cells is mediated by cytokines expressed by APCs following TLR stimulation (567). MAIT cells can be activated by cytokines, including IL-7, IL-12, IL-15, IL-18, and type I IFNs (477,567–569). IL-12, together with IL-18, produced from APCs in response to TLR ligands, stimulates MAIT cells to produce IFN- γ and potentiate MR1-dependent bacterial MAIT cell activation.

Although T cells express TLRs, their levels of TLR are lower compared to expression in NK cells, B cells, and APCs (570–572). TLRs signalling can also indirectly modulate T cell functions through activation of pDCs and mDCs, facilitating the presentation of HIV antigens and cytokines priming of T cells, potentially leading to HIV-specific T cell responses (573). The $\gamma\delta$ T cells express low levels of TLRs and receptors for cytokines including IFN- α , IL-12, and IL-18 (523,574–576). Thus, TLRs can activate $\gamma\delta$ T cells directly or indirectly via cytokines expressed by APCs, leading to modulation of the immune system (523). Activation of the V δ 2 subset of $\gamma\delta$ T cells by TLRs agonist has been shown to promote early IFN- γ expression.

In response to different cytokines, $\gamma\delta$ T cells have been shown to differentiate resulting in a highly polarized phenotype of $\gamma\delta$ T cells. For example, in the presence of IL-12 and IL-18, human adult V γ 9V δ 2 T cells differentiate into Th1-like T cells producing IFN- γ and TNF- α . In the presence of IL-4, V γ 9V δ 2+ cells differentiate to Th2-like cells expressing transcription factor GATA binding protein 3 (GATA-3) that produce IL-4, and in the presence IL-15 and TGF- α , V γ 9V δ 2 differentiates to Treg-like Foxp3 producing IL-10 and IL-4 (577,578). This characteristic is referred to as plasticity (579). Thus, differentiation of $\gamma\delta$ T cells can result in regulatory $\gamma\delta$ T cells that suppress the immune system reducing immune activation, and this may be important in preventing HIV infection. In the female genital mucosa, $\gamma\delta$ T cells makeup 20% of T cells. Although $\gamma\delta$ T cells are FOXP3 and CD25 negative, they have been reported to express high levels of IL-4, IL-10, and TGF- β , which will inhibit T cell proliferation, thus developing a regulatory profile that may play a role in suppressing the immune system (580).

Although the role of MAIT cells and $\gamma\delta$ T cells during HIV acquisition is not known, activated MAIT cells and $\gamma\delta$ T cells express granzyme that may kill infected cells, thus preventing further spreading of HIV to uninfected cells. MAIT cells and $\gamma\delta$ T cells activation may lead to GM-CSF expression that promotes monocyte differentiation into MDDC which may promote early priming of naïve CD4+ T cells, thus increasing HIV target cells and promoting HIV infection. Activation of MAIT and $\gamma\delta$ T cells also leads to IFN- γ , TNF- α , and CD40L expression, which enable the maturation of immature MDDC. This will increase T cell priming, thus increasing HIV target cells and promoting HIV infection (73,327,581). TNF- α may also increase HIV target cells by triggering vascular endothelial cells expression of leukocyte adhesion molecules that stimulate immune cell infiltration. TNF- α has been shown to play a role in the early response against viral infection by enhancing the infiltration of lymphocytes to the site of infection. In HIV, this is a disadvantage because it leads to an increase in HIV target cells. Thus, this thesis focuses on understanding how TLR7 and TLR8 stimulation of PBMCs may lead to activation of MAIT and $\gamma\delta$ T cells and their expression of cytokines, modulating the immune system and increasing immune activation.

Chapter 2: Rationale, Hypothesis, and Objectives

Prevention of HIV transmission remains a global priority. Therefore, it is crucial to understand the correlates of protection against HIV infection. Susceptibility to HIV has been clearly shown to depend on inflammation (60,375). Several recent studies have shown that CD161⁺⁺ CD8⁺ T cells and MAIT cell subset are located at the mucosal epithelia – in particular in the lamina propria, a potential site of HIV entry (449,582,583). MAIT and $\gamma\delta$ T cells express high levels of chemokine receptors, including CCR5 and CCR6, that enable the MAIT and $\gamma\delta$ T cells to be rapidly trafficked to the mucosal site during infection or inflammation. Activated MAIT and $\gamma\delta$ T cells have also been shown to express high levels of proinflammatory cytokines including IFN- γ and other proinflammatory cytokines and chemokines, which modulate the immune system leading to increased immune activation. This facilitates HIV infection by recruiting and activating HIV target cells, reducing epithelial barrier integrity, and promoting HIV replication through NF- κ B activation. Although MAIT and $\gamma\delta$ T cells are not preferentially infected by HIV, they play an important immunomodulatory role.

Previously, it was shown by Were et al. (unpublished data) that HIV-resistant women had differential cytokine responses to TLR7 and TLR8 stimulation. This suggests a link between TLR signalling and altered susceptibility to HIV. However, little is known about the effects of TLR7 and TLR8 stimulation of PBMCs on MAIT and $\gamma\delta$ T cell activation and cytokine expression. This study seeks further understanding of the regulatory role that MAIT and $\gamma\delta$ T cells stimulated by TLR7 and TLR8 ligands may play towards enhancing or reducing HIV infection of CD4⁺ T cells *in vitro*.

2.1 Hypothesis

TLR7 or TLR8 stimulation in PBMCs will lead to MAIT and $\gamma\delta$ T cell activation and expression of proinflammatory cytokines. Furthermore, TLR7 or TLR8 stimulation will lead to increased MR1 expression on APCs and/or IL-12 and IL-18 expression, and TLR7 or TLR8 stimulation will alter functional characteristics of MAIT and $\gamma\delta$ T cells.

2.1.1 Sub-hypotheses

TLR7 and TLR8 stimulation in PBMCs will lead to MAIT and $\gamma\delta$ T cells activation and expression of proinflammatory cytokines including IFN- γ , TNF- α , GM-CSF, and IL-17a.

TLR7 and TLR8 stimulation in PBMC will stimulate MAIT and $\gamma\delta$ T cells leading to increased proinflammatory cytokines, and this contributes to immune activation and advanced HIV infection.

MDDCs matured after TLR7 and TLR8 stimulation express high levels of interleukin (IL)-12 and IL-18 and surface MR1 molecules.

TLR7 or TLR8 stimulation will alter functional characteristics of MDCC's, MAIT and $\gamma\delta$ T cells including cytokine receptor expression.

MAIT cell stimulation with IL-12 and IL-18 increases HIV infection of CD4+ T cells.

2.2 Objectives

- To assess the effect of TLR7 and TLR8 stimulation of *in vitro* PBMCs on MAIT and $\gamma\delta$ T cell activation and cytokine and chemokine expression
- To assess the effect of media supplementation with recombinant IL-12 (rIL-12) and rIL-2 on MAIT and $\gamma\delta$ T cell cytokine expression following stimulation of *in vitro* PBMCs with TLR7 and TLR8
- To quantify IL-12 and IL-18 cytokine responses and MR1 surface expression in MDDCs following *in vitro* TLR7 and TLR8 stimulations
- To assess the effect on HIV infectivity of *in vitro* stimulation of purified MAIT cells with rIL-12 and rIL-18

Chapter 3: Materials and Methods

3.1 Study participants

The study participants in this study are local donors from Winnipeg, Manitoba, Canada.

Blood samples for all experiments were obtained from a healthy local donor cohort consisting of students and employees of the Public Health Agency of Canada, Winnipeg.

3.2 Ethics statement

Informed consent was obtained from each study participant prior to sample collection, and the study was performed according to Helsinki declaration and guidelines for conducting of research involving human subjects. Ethical approval for this study was obtained from the Public Health Agency of Canada, Winnipeg.

3.3 General reagents

3.3.1 TLR agonists and other stimulants

TLR ligands used in the study were imiquimod (TLR7 agonist) and ssRNA40/LyoVec (TLR8 agonist) (all from Invivogen, San Diego, CA).

Positive controls: A combination of phorbol 12-myristate 13-acetate (PMA) and ionomycin (ION) (all from Sigma-Aldrich, St Louis, MO), or paraformaldehyde (PFA) fixed *E. coli* (Invitrogen, San Francisco, CA) were variously used as positive controls for TLR stimulations.

***E. coli* culture inoculation**

Lysogeny broth (LB)-Miller (Sigma-Aldrich,) was aseptically transferred to a 500 mL sterile Erlenmeyer flask (Millipore Sigma, Burlington MA). A vial of One Shot® TOP10 *E. coli* (Invitrogen, San Francisco, CA) was inoculated into the LB-Miller media and incubated at 4°C overnight while shaking at 150 revolutions per minute (rpm). Optical density was measured using a Synergy H1 microplate reader (Bio Tek, Santa Clara, CA) by transferring 200 µL of culture to

each well in a flat-bottom 96 well plate (Thermofisher, San Francisco, CA) Also, a dilution of 2^{-1} was made and measurements were done in triplicates. The concentration of the bacteria was calculated using the following formula: $OD_{600}=8 \times 10^8$ cells/mL. The *E. coli* was stored at -80°C .

Paraformaldehyde fixation (PFA) of *E. coli*

Fixing *E.coli* with PFA was done according to reference (475). Frozen *E. coli* was thawed and 6.25 μL of 16% PFA (Sigma-Aldrich, St Louis, CA) was added to a 100 μL aliquot of the *E. coli*. The mixture was vortexed and incubated at room temperature for 5 min before washing with 400 μL phosphate-buffered saline (PBS) at pH 7.4 (Gibco-Invitrogen Thermo Fisher Scientific, Waltham, MA) twice. The *E. coli* was resuspended in 100 μL RPMI media supplemented with 10% fetal calf serum (FCS) (R10 media).

Recombinant human interleukin 18 (rIL-18) (IL-1F4) and rIL-12 (both obtained from R&D Systems, Minneapolis, MN)) were combined and used in the study to stimulate MAIT cells. rIL-4 (InvivoGen) and recombinant granulocyte monocyte colony stimulating factor (rGM-CSF) (from Miltenyi Biotech, San Diego, CA) were used for the experiment in monocyte differentiation to MDDCs.

3.3.2 Culture media and tissue processing reagents

Roswell Park Memorial Institute (RPMI) 1640 medium with 10% fetal bovine serum (R10) culture media was made from RPMI 1640 complemented with 10% fetal bovine serum (FBS) (heat inactivated at 56°C for 1 h) and 2% of 100x antibiotic-antimycotic solution (all from Gibco-Life Technologies-Thermo Scientific, ON, Canada).

Freezing media was made from 90% FBS (heat inactivated at 56°C for 1 h) (Gibco-Life Technologies-Thermo Scientific, ON, Canada) and 10% dimethyl sulphoxide (DMSO) (Sigma-Aldrich). This was used to freeze PBMCs for storage.

3.3.3 Flow cytometry reagents

Antibodies. Fluorochrome conjugated antibodies to the following markers were used for phenotyping and intracellular staining:

BV421-CD161 (clone HP-3G10), PerCP-Cyanine 5.5-V α 7.2 TCR (clone 3C10), BV605-CD4 (clone RM4-5), BV650-CD8 (clone SK1), and Alexa Flour 700-CCR5 (clone J418F1) (all from Biolegend San Diego, CA), TCR PAN GAMMA/DELTA-PC5 (clone IMMU510) (from Beckman, Indianapolis, IN), APC-H7-CD3 (clone SK7), PE-CyTM7-CD56 (clone B159), V500-IFN- γ (clone B27), Alexa Flour700-TNF- α (clone MAB11), PE-CF594-GM-CSF (clone BVD2-21C11), BV786-IL-17a (clone N49-653), APC-CCR6 (clone 11A9), BV786-CD69 (clone FN50), BUV395-IFN- γ (clone B27), FITC-CD80 (clone BB1), PE-CyTM7-CD19 (clone SJ25C1), BUV395-CD14 (clone M5E2), BB515-CD56 (clone B159), PE-Cy5-CD11C (B-Ly6), BV605-HLA-DR (clone G46-6), BV786-HLA-DR (clone Tu39), BV711-CD83 (clone HB15e), (all from BD Bioscience, San Jose, CA), APC-MR1 Tetramer (National Institute of Health (NIH) Tetramer Core Facility, Atlanta, GA) and Live/Dead Aqua (Life Technologies, NY) (see **Table 2**).

FACS Wash, used to wash cells before and after extracellular staining, was prepared from PBS (PH 7.4) (Gibco-Invitrogen Thermo Fisher Scientific, Waltham, MA), 2% FBS (heat inactivated at 56°C for 1 h) and 2 mM ethylenediaminetetraacetic acid (EDTA) (both from Sigma-Aldrich).

Perm/WashTM Buffer (BD Bioscience, San Jose, CA) is commercially available as 10X stock solution. The working solution of Perm/Wash used for washing flow cytometry samples was prepared by diluting the 10X perm/wash with double distilled water in a ratio of 1:10.

Cytofix/cytopermTM Solution (BD Bioscience) is commercially available at working concentration.

3.3.4 Monocyte isolation kit

EasysepTM Human monocyte isolation kit (StemCell, Vancouver, BC, Canada) was used to isolate CD14+CD16- cells from fresh PBMCs sample. The kit contains isolation cocktail, Platelet removal cocktail, and magnetic beads.

EasySep™ Magnet (StemCell™ Technologies) used to separate monocyte.

Easysep™ Isolation media used was made from PBS (Gibco-Invitrogen Thermo Fisher Scientific), 2% FBS heat inactivated at 56° C for 1 h and 1 mM EDTA (both from Sigma-Aldrich).

3.3.5 HIV p24 Enzyme Linked Immunosorbent Assay (ELISA) reagents Kit (Cat# 5447, Advanced Bioscience Laboratories (ABL), Rockville, MD)

HIV p24 was quantified by using p24 antigen capture ELISA as previously described (584), in accordance with manufacturers instructions (ABL, Rockville, MD). The HIV p24 Kit included the following reagents: Micro Elisa Plate precoated with murine monoclonal antibodies to HIV-1 p24, disruption buffer consisting of Triton® X-100 detergent and phosphate buffer, conjugate solution consisting of horseradish peroxidase labeled with, immunoaffinity purified, human antibodies to HIV-1 p24, and peroxidase substrate consisting of hydrogen peroxide and tetramethylbenzidine in acidic buffer. The kit also contained Wash buffer (20X) consisting of phosphate buffered saline and Tween 20® concentrates. The wash buffer working concentration was prepared by diluting 25ml of wash buffer in 475ml distilled water. Stop solution was also included in the kit at a working concentration of sulfuric Acid. A standard was included in the kit as purified native HIV-1 IIIB p24 at 1ng/ml. Working concentration of the standard was prepared by diluting 50µl of 1ng/ml HIV-1 p24 in 450 µl R-10 media and further diluting into final concentration of 100 pg/mL, 50 pg/mL, 25 pg/mL, and 12.5 pg/mL.

Protocol: To a micro-ELISA plate disruption buffer was added to each well followed by addition of 100 µL of each diluted HIV-1 p24 standard in duplicate, 100 µL of R10 media to 4 wells (to serve as a negative control) and 100 µL of prepared test sample to appropriate wells. The side of the plate was gently tapped to mix contents, the plate covered with a plate sealer and incubated at 37°C for 60 min. The plate was washed by aspirating the well content into a waste tray then filling the well with wash buffer (PBS/Tween 20® concentrate; working concentration prepared by diluting 25 mL of wash buffer in 475 mL distilled water). The plate was left to soak for 15 s before aspirating into the waste tray. This washing step was repeated four times. The plate was tapped firmly on absorbent paper.

To each well of micro-ELISA plate, 100 μ L of conjugate solution (working concentration of horseradish peroxidase-labelled, immunoaffinity purified, human antibodies to HIV-1 p24) was added, the plate covered and incubated at 37°C for 60 min. The washing step described above was repeated and 100 μ L of peroxidase substrate (working concentration of hydrogen peroxide and tetramethylbenzidine in acidic buffer) was added to each well. The plate was incubated uncovered for 30 min at room temperature (19–23°C). In the same manner that peroxidase substrate was added, 100 μ L of stop solution (working concentration of sulfuric acid) was added to each well and the plate read at 450 nm in a micro-ELISA plate reader (Synergy Hi multi-reader machine, BioTek) within 20 min.

3.3.6 Human IL-18 duo set ELISA kit (R&D Systems Cat# DV318, Minneapolis, MN)

IL-18 levels in culture supernatants were determined by ELISA following the manufacturer's instructions (IL-18 Duo-Set ELISA kit, R&D Systems Cat# DV318). A flat-bottom 96-well Nunc MaxiSorp™ flat-bottom microplate (Cat# 12565136, Gibco-Invitrogen Thermo Fisher Scientific) was precoated by adding 100 μ L of capture antibody diluted to the working concentration in PBS pH 7.4 (Gibco-Invitrogen Thermo Fisher Scientific), without carrier protein, and incubating overnight at room temperature. After washing the plate four times with PBS containing 0.05% Tween®20 (Sigma-Aldrich) the plate remaining binding sites were removed by adding 300 μ L of reagent diluent (75 μ L of 7.5% BSA, (Sigma-Aldrich), in PBS pH 7.2–7.4, (Gibco-Invitrogen Thermo Fisher Scientific) to each well and incubating at room temperature for 30 min. The standard was provided in the kit as human recombinant IL-18. Each vial was reconstituted with 0.5 mL of reagent diluent. A seven-point standard curve using 2-fold serial dilutions in reagent diluent was prepared. After washing four times with PBS containing 0.05% Tween®20, 100 μ L of samples of MDDC culture supernatant or standards in reagent diluent was added in duplicate. The plate was covered with an adhesive strip and incubated for 2 h at room temperature. The plate was then washed four times with PBS containing 0.05% Tween®20, and 100 μ L of the biotinylated mouse anti-human IL-18 detection antibody reconstituted with reagent diluent to 500 ng/mL working solution and added to each well. The plate was covered with a new adhesive strip and incubated for 2 h at room temperature. After washing four times with 100 μ L PBS containing 0.05% Tween®20, a working dilution of streptavidin conjugated to horseradish peroxidase (HRP) was added. The plate was covered and incubated for 20 min at room temperature in the dark. The

substrate solution was provided in the kit as colour reagent A (H_2O_2) and colour reagent B (tetramethylbenzidine) (R&D Biosystems, Cat# DY999). A working solution of the substrate solution was prepared by adding reagent A to reagent B at a ratio of 1:1. The plate was washed four times with PBS containing 0.05% Tween®20, 100 μL of substrate solution added, and the plate was incubated for 20 min at room temperature in the dark. The reaction was stopped by the addition of 50 μL of Stop Solution (provided in the kit as 2N H_2SO_4 (R&D Systems, Cat# DY994) to each well. The plate was gently tapped to ensure thorough mixing, and the optical density of each well was determined immediately using a microplate reader (Synergy Hi multi-reader machine, BioTek) set to 450 nm and a wavelength correction set to 570 nm.

3.3.7 IL-12(p70) reagents and kit

IL-12(p70) levels in culture supernatants were determined by ELISA following the manufacturer's instructions (ABCAM, Cat# ab213791, Waltham, MA). IL-12p70 standard was prepared not more than 2 h prior to the experiment by adding 1 mL sample diluent buffer to 10 ng to create 10,000 pg/mL of human IL-12(p70) stock solution. The tube was kept at room temperature for 10 min and then mixed thoroughly. Standard concentration of 500 pg/mL IL-12(p70) solution was prepared by adding 50 μL of the 10,000 pg/mL IL-12(p70) stock solution into a tube with 950 μL sample diluent buffer. Six dilutions were prepared: 250 pg/mL, 125 pg/mL, 62.5 pg/mL, 31.25 pg/mL, 15.625 pg/mL and 7.8125 pg/mL. A 96-well microtiter plate precoated with anti-human IL-12(p70) was rinsed with sample diluent buffer followed by addition of 100 μL of each standard and 100 μL of sample of MDDC culture supernatant to the appropriate wells in duplicate. After preparing working solution of biotinylated anti-human IL-12(p70) by diluting biotinylated anti-human IL-12(p70) antibody in diluent buffer in 1:100, 50 μL of biotinylated anti-IL-12(p70) was added to all wells and the plate covered and incubated for 3 h at room temperature. The plate was washed four times by aspirating the liquid from each well and adding 300 μL of 1x wash buffer into each well before adding 100 μL of streptavidin-HRP solution into all wells. The plate was covered and incubated at room temperature for 30 min. After washing the plate, 100 μL of Chromogen TMB substrate solution was added into each well and incubation in the dark for 12 to 15 min at room temperature. Stop reagent (100 μL) was added into each well and the results taken immediately after. The absorbance of each well was read on a spectrophotometer using 450 nm as the primary wavelength and a reference wavelength of 620 nm.

3.4 Routine procedures

3.4.1 Specimen preparation

Blood samples were collected from study participants of a Winnipeg cohort of healthy laboratory staff. Blood was drawn using sterile needles with syringes and collected in heparinized BD Vacutainer tubes (BD, Zelienople, PA, USA), and later used in isolation of PBMCs (section 3.3.1.2).

3.4.2 PBMC isolation

Whole blood was centrifuged at 1200 rpm for 7 min with brakes to remove plasma and diluted 1:1 with sterile PBS containing 2% FCS (both Gibco-Invitrogen Thermo Fisher Scientific, Waltham, MA). The diluted blood was layered onto Lymphoprep (Ficoll-Histopaque) (Stem Cell Technologies) and centrifuged at 1400 rpm for 25 min without braking. The white cell layer of PBMCs was collected into 6 mL R10 in a 50 mL tube and diluted to 40 mL with sterile PBS followed by centrifugation at 1400 rpm for 10 min with braking. The supernatant was poured off from the cell pellet and the cells gently resuspended. The viability testing of isolated PBMCs was done using the Trypan Blue (Sigma-Aldrich) exclusion method (378). Three tubes of blood (10 mL each) collected per study participant yielded 40–60×10⁶ PBMCs. Most experiments were performed using fresh samples.

PBMC freezing. After PBMC isolation, the PBMCs that were used primarily for optimization experiments were counted using a haemocytometer (from Sigma-Aldrich St Louis, MO) using the Trypan Blue exclusion method. After counting, 10×10⁶ PBMCs were suspended in 1 mL of freezing media containing 90% FBS and 10% dimethylsulfoxide (DMSO) solution (all from Gibco-Life Technologies, Thermo Scientific, ON, Canada) and stored in sterile 2 mL vials. The cells were gradually frozen to -80°C in Mr Frosty™ containers (Gibco-Invitrogen Thermo Fisher Scientific) filled with isopropanol (Gibco-Invitrogen Thermo Fisher Scientific).

3.4.3 TLR stimulation and cell culture

Freshly isolated PBMCs were cultured in R10 culture media under seven conditions: (1) a negative or unstimulated control; (2) PFA-fixed *E. coli* (at ratio of bacteria to PBMCs 5:1); (3&4) 1 µg/mL or 5 µg/mL imiquimod-TLR7 (Cat No. Hkb-htrlr7, Invitrogen); (5&6) 2.5 µg/mL or 5 µg/mL ssRNA40/LyoVec-TLR8 (Cat. No tlr1-lrna40, Invitrogen); and (7) PMA (Cat No. P8139, Sigma-Aldrich) with 0.01 µg/mL ION (Cat. No I3909, Sigma-Aldrich). The incubation occurred at 37°C in a humidified 5% CO₂ incubator for 24 h (or different durations for kinetic experiments). Where appropriate, combination cytokine release blockers 1.0 µL of 1 µg/mL brefeldin A (Golgiplug™) and 1.0 µL of 1 µg/mL monensin (Golgistop™) (both from BD Biosciences), were added to 1 mL of (10⁶) PBMCs 2 h after PMA/ION stimulation or 6 h in unstimulated control, PFA-fixed *E. coli*. For TLR7 and TLR8 stimulations, four time points (2, 6, 14, or 24 h) were selected for kinetic experiments. PBMC culture supernatants (without protein transport inhibition) were harvested and frozen at -80°C for later use in cytokines and chemokines assays.

3.4.5 Flow cytometry

3.4.5.1. Flow cytometry panels

The monoclonal antibodies listed in 3.3.3 above were used in phenotyping of different populations of T cells, monocytes and DCs. The antibodies were combined into flow panels as indicated in the tables below:

Table 2. Flow cytometry antibody panel

Table 2.1 T cell activation and chemokine receptor panel

	Phenotyping marker	Vendor	Clone	Cat#
CD3 APC-H7	T cells	BD Bioscience	SK7	560176
CD8 BV650	T cells	Biolegend, San Diego, CA	SK1	301042
CD4 BV605	T cells	Biolegend	RM4-5	300556
Vα7.2 TCR PerCP/Cyanine5.5	MAIT cells	Biolegend	3C10	351710
CD161 BV421	T cells	Biolegend	HP-3G10	339914
Γδ TCR PE-Cy5	Γδ T cells	Beckman, Indianapolis, IN	IMMU510	IM2662U
CD56 PE-Cy7	T cells	BD Bioscience	B159	56)0916

CD69 BV786	T cells activation	BD Bioscience, San Jose, CA	FN50	563834
CCR5 Alexa Flour 700	Chemokine receptor	Biologend	J418F1	359116
CCR6 APC	Chemokine receptor	BD Bioscience	11A9	560619
Live/dead aqua	Live or dead cells	ThermoFisher, Live technologies, Grand Island, NY		L34957

Table 2.2. ICS cytokine panel

	Phenotyping marker	Vendor	Clone	Cat#
CD3 APC-H7	T cells	BD Bioscience	SK7	560176
CD8 BV650	T cells	Biologend	SK1	301042
CD4 BV605	T cells	Biologend	RM4-5	300556
V α 7.2 TCR PerCP/Cyanine5.5	MAIT cells	Biologend	3C10	351710
CD161 BV421	T cells	Biologend	HP-3G10	339914
MR1 Tetramer(5-OP-RU) APC	MAIT cells	NIH Tetramer Core facilities Atlanta GA		
$\Gamma\delta$ TCR PE Cy5	$\Gamma\delta$ T cells	Beckman, Indianapolis, IN	IMMU510	IM2662U
CD56 PE Cy7	T cells	BD Bioscience	B159	560916
V500 IFN- γ	IFN- γ cytokine	BD Bioscience	B27	561980
IL-17a BV786	IL-17 cytokine	BD Bioscience	N49-653	563745
TNF- α Alexa Flour 700	TNF- α cytokine	BD Bioscience	MAB11	557996
GM-CSF PE-CF594	GM-CSF cytokine	BD Bioscience	BVD2-21C11	562857
Green Live/Dead	Live or dead cells	ThermoFisher, Live technologies		L23101

Table 2.3. Chemokine receptor surface staining panel

	Phenotyping marker	Vendor	Clone	Cat#
CD3 APC-H7	T cells	BD Bioscience	SK7	560176
CD8 BV650	T cells	Biologend	SK1	301042
CD4 BV605	T cells	Biologend	RM4-5	300556
V α 7.2 TCR PerCP-/Cyanine5.5	MAIT cells	Biologend	3C10	351710
CD161 BV421	T cells	Biologend	HP-3G10	339914
CXCR6 APC	Chemokine receptor	Biologend		356006
$\gamma\delta$ TCR PE Cy5	$\gamma\delta$ T cells	Beckman,	IMMU510	IM2662U
CCR4 PE Cy7	Chemokine receptor	BD Bioscience	B159	561034
CCR6 BV786	Chemokine receptor	BD Bioscience	11A9	563704
	Chemokine receptor	Biologend	J418F1	359116

CXCR3 PE-CF594	Chemokine receptor	BD Bioscience	1C6/CXC R3	562451
Green live/dead	Live or dead cells	ThermoFisher, Live technologies,		L23101

Table 2.4. MAIT cell and CD4+ T cells sorting panel

	Phenotyping Marker	Vendor	Clone	Cat#
CD3 APC-H7	T cells	BD Bioscience	SK7	560176
CD4 BV605	T cells	Biologend	RM4-5	300556
V α 7.2 TCR PerCP/Cyanine 5.5	MAIT cells	Biologend	3C10	351710
CD161 BV421	T cells	Biologend	HP-3G10	339914
MR1 tet (5-OP-RU) APC	MAIT cells	NIH Tetramer core facilities		
Live/dead aqua	Live or dead cells	ThermoFisher, Live technologies		L34957

Table 2.5. Monocyte purity panel

	Phenotyping marker	Vendor	Clone	Cat#
CD3 APC-H7	T cells	BD Bioscience	SK7 B159	560176
CD19 PE-Cy TM 7	T cells	BD Bioscience	SJ25C1	34113
CD56 BB515	NK cells	BD Bioscience	B159	564489
CD14 BUV395	Monocytes	BD Bioscience	M5E2	563561
Live/Dead Aqua	Live or dead cells	ThermoFisher, Live technologies		L34957

Table 2.6. Monocyte-derived dendritic cell (MDDC) maturation panel

	Phenotyping marker	Vendor	Clone	Cat#
CD11C PE-Cy5	MDDC	BD Bioscience	B-Ly6	551077
CD80 FITC	MDDC maturation	BD Bioscience	BB1	555683
HLA-DR BV786	MDDC	BD Bioscience	Tu39	740983
CD14 BUV395	Monocyte	BD Bioscience	M5E2	563561
CD83 BV711	MDDC maturation	BD Bioscience	HB15e	740802
MR1 APC	MDDC	Biologend,	8F2F9	396104
Live/dead Aqua	Live or dead cells	ThermoFisher, Live technologies		L34957

3.4.5.2. Surface staining

Freshly isolated or TLR-stimulated PBMCs were transferred from culture plates (or centrifuge tubes) into appropriately labelled polypropylene tubes (BD Bioscience, San Jose, CA), and washed

once with 2 mL FACS wash at 1500 rpm for 5 min. This was followed by the addition of a cocktail of monoclonal antibodies for phenotyping surface markers on T cells, monocytes or MDSCs (see Table 2). The cells were stained for 30 min at 4°C in the dark, and subsequently washed to remove excess antibodies using 1 mL of FACS wash and centrifugation at 1500 rpm for 5 min. The stained cells were then fixed using 300 µL of 1% paraformaldehyde (PFA) solution (Sigma-Aldrich) prior to flow analysis.

3.4.5.3 Intracellular cytokine staining (ICS)

The PBMCs stimulated with TLR were cultured with protein transport inhibitors. The PBMCs were first stained for surface markers (using the method in section 3.4.2 above); then permeabilized using 150 µL of cytoperm/cytofix mixture (BD Bioscience) for 20 min, washed once using 2 mL of Perm wash and centrifuged at 1500 rpm for 5 min. ICS followed with the addition of specific cocktails of antibodies for intracellular markers (see Table 2.2), and incubation in the dark for 1 h. Excess antibody was removed after staining using a single wash with perm wash (BD Bioscience) prior to flow analysis. Flow data acquisition was done using FACS DIVA version 6.0 (BD Bioscience), and flow data analyzed using FlowJo version 10.6.5TM (BD Bioscience).

3.4.5.4 Gating strategy for MAIT and $\gamma\delta$ T cells

Fluorescence minus one (FMO) experiments were used to optimize the gating strategy for MAIT cells and $\gamma\delta$ T cells. PBMCs from a healthy donor were stained with all antibodies on table 2.1 except for one of the following fluorochrome conjugated antibodies: TCR PAN GAMMA/DELTA-PC5- $\gamma\delta$ -TCR (IMMU510), BV650-CD8 (SKI), BV605-CD4 (RM4-5), BV421CD161 (HP-3G10), PerCP/Cyanine 5.5-V α 7.2TCR (3C10). To optimize for gating of MAIT and $\gamma\delta$ T cells, gates were set in the following order: Singlets gate on forward scatter (FSC)-height and FSC-area (FSC-A), live cells that were negative for live dead aqua stain, CD3⁺, $\gamma\delta$ TCR⁻ and CD3⁺, $\gamma\delta$ TCR⁺ off live cells, CD8⁺ off CD3⁺, $\gamma\delta$ TCR⁻, CD4⁺ T cells off CD3⁺, $\gamma\delta$ TCR⁻, V α 7.2 TCR off CD3⁺, CD8⁺, CD4-CD8⁻ (DN), CD161 off CD3⁺, CD8⁺, CD4-CD8⁻ (DN), CD8⁺ and CD4⁺ of CD161⁺⁺V α 7.2-TCR. A representative flow cytometry plotting showing how gates were established is shown in **Figure 5**. CD3⁺, $\gamma\delta$ TCR⁺ were classified as $\gamma\delta$ T cells (**Figure 5**). The gating strategy was used for subsequent experiments.

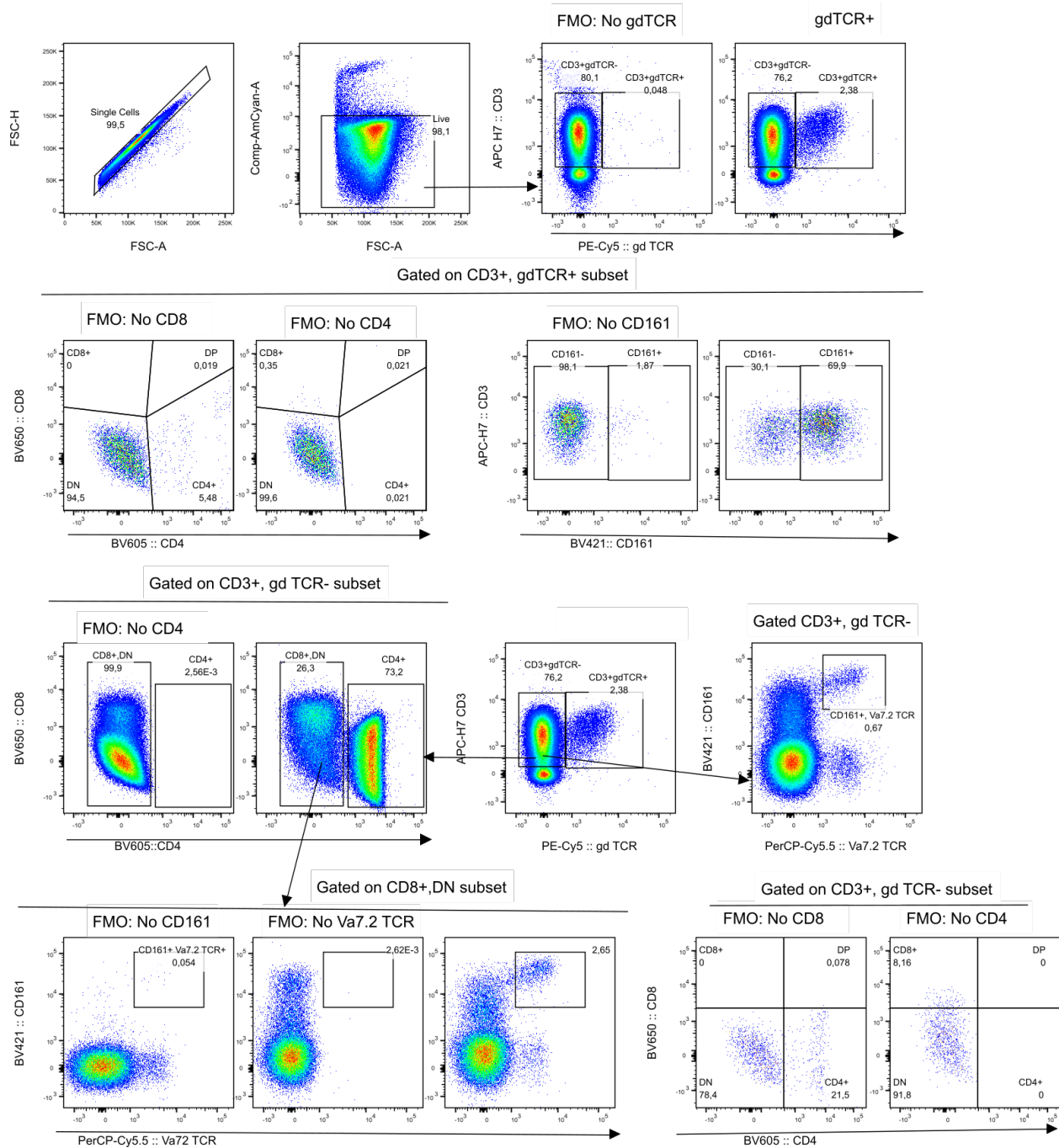


Figure 5. Fluorescence minus one (FMO) gating for: $\gamma \delta$ TCR PE Cy5, BV650 CD8, BV605 CD4, BV421 CD161, and PerCP-/Cyanine5.5 Va7.2TCR. Representative flow cytometry plot of one healthy blood donor showing how gates for $\gamma \delta$ TCR PE Cy5, BV650 CD8, BV605 CD4, BV421 CD161, and PerCP-/Cyanine5.5 Va7.2TCR were established. MAIT cells were gated as CD3+, $\gamma \delta$ TCR-, CD161+, Va7.2TCR+ cells or as CD3+, $\gamma \delta$ TCR-, CD8+, CD4/CD8 DN, CD161+, Va7.2TCR+ cells. Cells that were CD3+, $\gamma \delta$ TCR+ were classified as $\gamma \delta$ T cells. Forward scatter-height (FSC-H) and FSC-A gating for singlets to isolate singlets from doublets. Live cells were

selected by gating on live/dead aqua stain negative off singlets' gate. $\gamma\delta$ TCR FMO was used to gate for CD3+ $\gamma\delta$ -T cells off live cells. CD8 FMO was used to gate for CD8+ T cells off the CD3+ $\gamma\delta$ TCR- gate. CD4 FMO was used to gate for CD4+ cell off the CD3+ $\gamma\delta$ TCR- gate. CD8+CD4-CD8-(DN) and CD4 was gated off CD3+ $\gamma\delta$ TCR- gate CD3+ $\gamma\delta$ TCR- gate was gated off the live cells gate. CD161++ V α 7.2TCR gate was gated off the CD3+ $\gamma\delta$ TCR-. CD161 FMO was used to establish CD161 gate on CD8+ CD4-CD8- (DN) cells. V α 7.2TCR FMO was used to establish V α 7.2TCR gate on CD8+CD4-CD8-(DN) cells. CD161++ V α 7.2TCR+ was gated on CD8+CD4-CD8-(DN) cells, lastly, CD8 FMO was used to gate for CD8+ MAIT cells on CD161++ V α 7.2TCR and CD4 FMO was used to gate for CD4+ MAIT cells on CD161++ V α 7.2TCR gate

To optimize gating for MAIT cells and $\gamma\delta$ for chemokine expression, PBMCs from a healthy donor were stained with all antibodies in table 2.3 except for one of the following antibodies: Alexa flour 700-CCR5 (J418F1), PE-Cy7-CCR4 (B159), BV786-CCR6 (11A9) and PE-CF594-CXCR3 (IC6/CXCR3) and APC-CXCR6. FMO was used to set gates for CCR5+ $\gamma\delta$ T cells, CCR4+ $\gamma\delta$ T cells, CCR6+ $\gamma\delta$ T cells, CXCR3+ $\gamma\delta$ T cells, and CXCR6+ $\gamma\delta$ T cells off CD3+, $\gamma\delta$ TCR+ gate and CCR5+, CCR4+ s, CCR6+, CXCR3+, and CCXR6+ MAIT cells off CD161+V α 7.2-TCR gate (**Figure 6**).

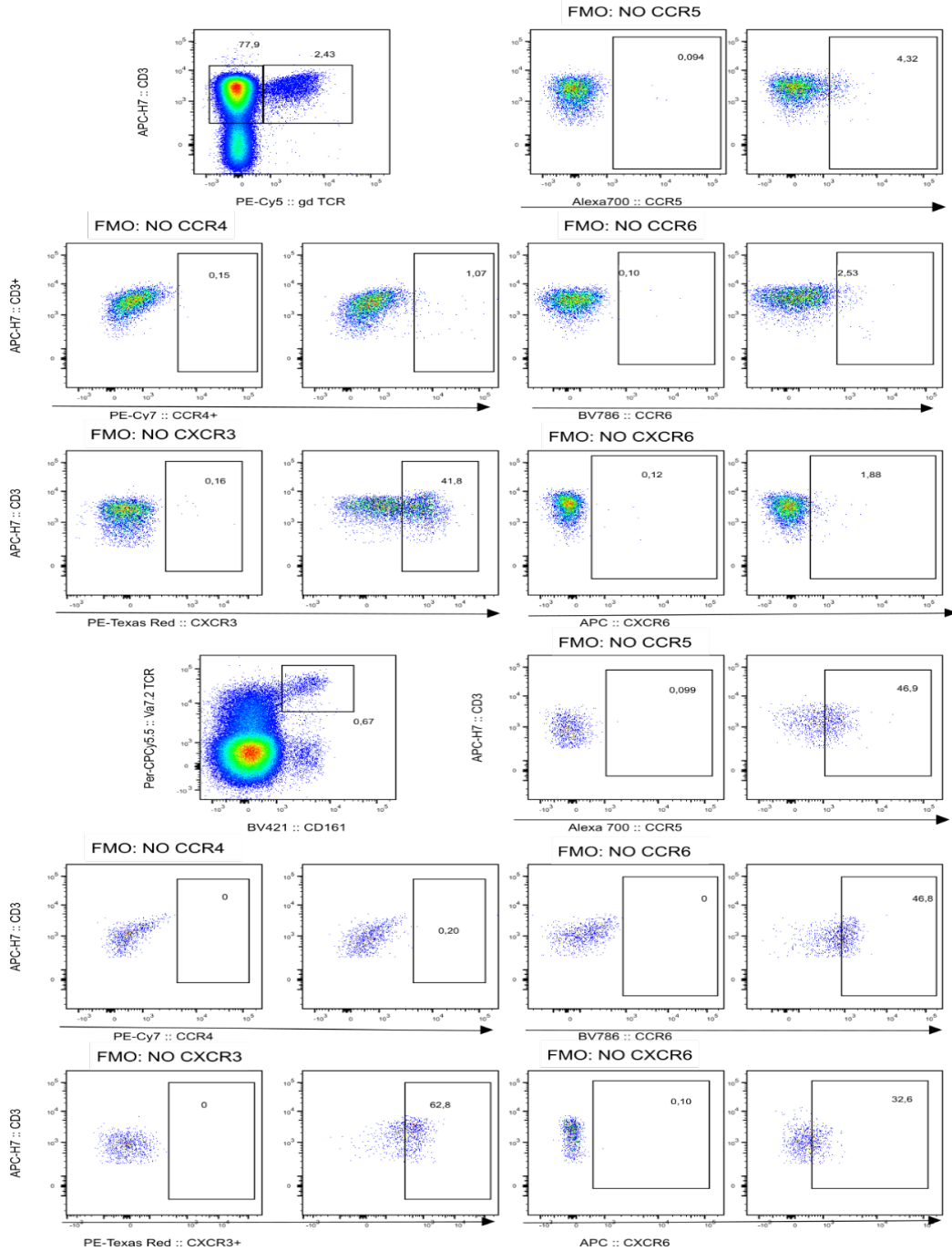


Figure 6: Fluorescence minus one (FMO) gating for CCR5+, CCR4+, CCR6+, CXCR3+ and CXCR6+ -MAIT cells and - $\gamma\delta$ T cells. Representative flow cytometry plotting showing how CCR5+, CCR4+, CCR6+, CXCR3+ and CXCR6+ $\gamma\delta$ T cells, and CCR5+, CCR4+, CCR6+, CXCR3+ and CXCR6+ MAIT cells gates were established. From top left to right: CD3+ $\gamma\delta$ TCR+ and CD3+ $\gamma\delta$ TCR- were gated off the live cells, CCR5 FMO was used to gate for CCR5+ $\gamma\delta$ T cells off the CD3+ $\gamma\delta$ TCR+ gate. CCR4 FMO was used to gate for CCR4+ $\gamma\delta$ T cells off the CD3+ $\gamma\delta$ TCR+ gate. CCR6 FMO was used to gate for CCR6+ $\gamma\delta$ T cells off the CD3+ $\gamma\delta$ TCR+ gate.

CXCR3 FMO was used to gate for CXCR3+ $\gamma\delta$ T cells off the CD3+ $\gamma\delta$ TCR+ gate and finally CXCR6 FMO was used to gate for CXCR6+ $\gamma\delta$ T cells off the CD3+ $\gamma\delta$ TCR+ gate. CD161+V α 7.2TCR+ cells were gated off the CD3+, CD3+ $\gamma\delta$ TCR- cells. CCR5 FMO was used to gate for CCR5+ MAIT cells off the CD161+V α 7.2TCR+ gate. CCR4 FMO was used to gate for CCR4+ MAIT cells off the CD161+V α 7.2TCR+ gate. CCR6 FMO was used to gate for CCR6+ MAIT cells off the CD161+V α 7.2TCR+ gate. CXCR3 FMO was used to gate for CXCR3+ MAIT cells off the CD161+V α 7.2TCR+ gate. and finally, CXCR6 FMO was used to gate for CXCR6 MAIT cells off the CD161+V α 7.2TCR+ gate.

To optimize gating for MAIT cells and $\gamma\delta$ for activation, PBMCs from a healthy donor were stimulated overnight with PMA/ION and stained with all antibodies on table 2.1 except for one the following antibodies: TCR PAN GAMMA/DELTA-PC5- $\gamma\delta$ -TCR (IMMU510), BV650-CD8 (SKI), BV605-CD4 (RM4-5), BV421-CD161 (HP-3G10), PerCP/Cyaninine 5.5-V α 7.2TCR (3C10), BV786-CD69, APC-CCR6 (11A9), Alexa Flour 700-CCR5 (J418F1). FMO was used to set gates for CD69+ MAIT cells, CCR6+ MAIT cells, and CCR5+ MAIT cells off CD161++ V α 7.2TCR and CD69+ $\gamma\delta$ T cells, CCR6+ $\gamma\delta$ T cells, and CCR5+ $\gamma\delta$ T cells off CD3+ $\gamma\delta$ TCR gate (**Figure 7**).

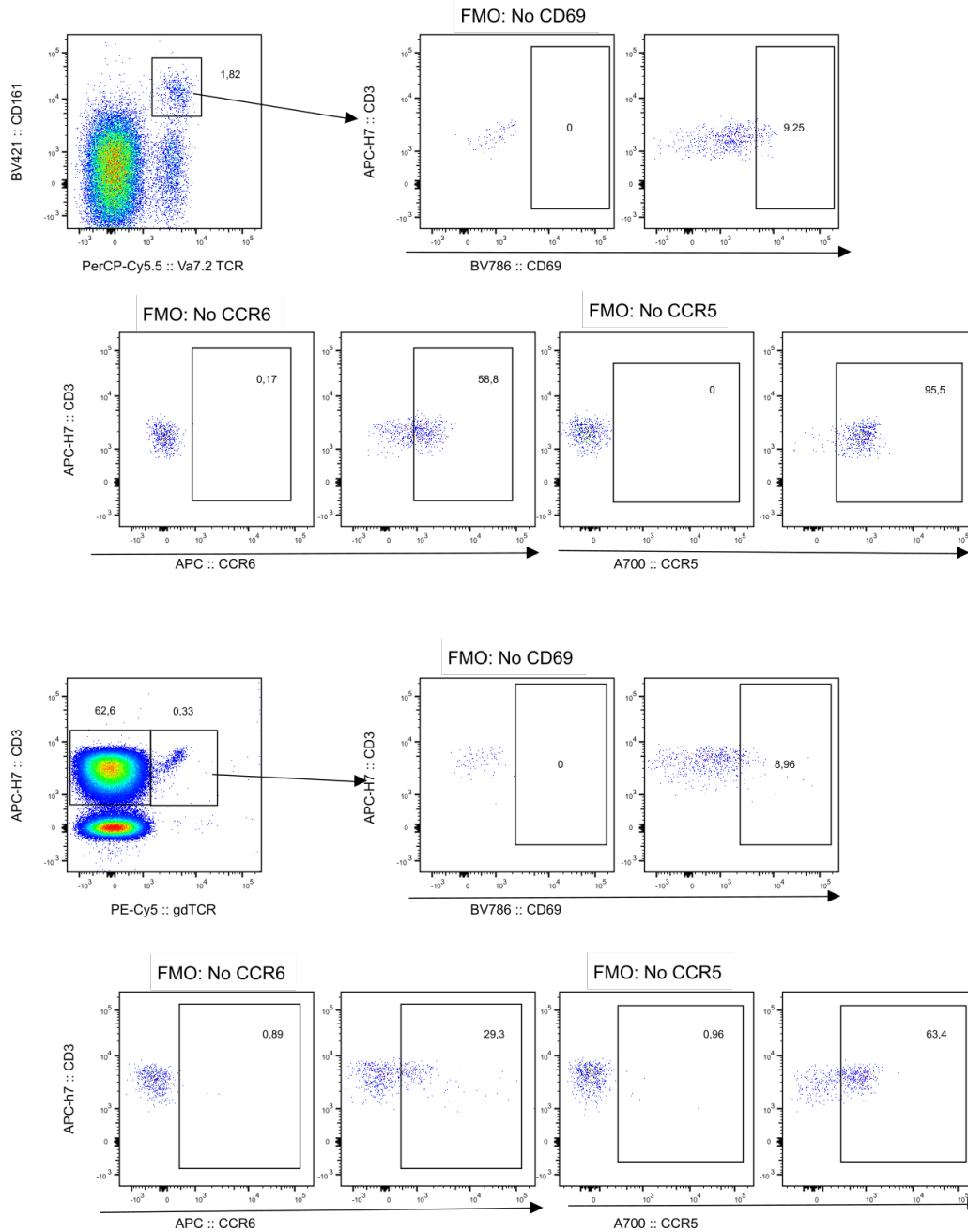


Figure 7: Fluorescence minus one (FMO) gating for CD69+, CCR5+ and CCR6+ MAIT cells and CD69+, CCR5+ and CCR6+ $\gamma\delta$ T cells. Representative flow cytometry of one healthy blood donor showing how gates for CD69+, CCR5+ and CCR6+ MAIT cells and CD69+, CCR5+ and CCR6+ $\gamma\delta$ T cells were established. From top left to right: CD161+Va7.2TCR+ cells were gated off the CD3+ $\gamma\delta$ TCR- cells. CD69 FMO was used to gate for CD69+ MAIT cells off the CD161+Va7.2TCR+ gate. CCR6 FMO was used to gate for CCR6+ MAIT cells off the CD161+Va7.2TCR+ gate. CCR5 FMO was used to gate for CCR5+ MAIT cells off the CD161+Va7.2TCR+ gate. CD3+ $\gamma\delta$ TCR+ and CD3+ $\gamma\delta$ TCR- were gated off the live cells. CD69 FMO was used to gate for CD69+ $\gamma\delta$ T cells off the CD3+ $\gamma\delta$ TCR+ gate. CCR6 FMO was used to gate for CCR6+ $\gamma\delta$ T cells off the CD3+ $\gamma\delta$ TCR+ gate. and CCR5 FMO was used to gate CCR5+ $\gamma\delta$ T cells off the CD3+ $\gamma\delta$ TCR+ gate.

To optimize the gating strategy for MAIT and CD4⁺ T cells sorting, PBMCs from a healthy donor were stained with all antibodies in table 2.4 except for one of the following antibodies: APC-H7-CD3 (SK7), PerCP/Cyanine 5.5-V α 7.2 TCR (3C10), APC-MR1AgTet (5-OP-RU), BV421-CD161 (HP-3G10), BV605-CD4⁺ (RM4-5). FMO was used to set gates for CD3⁺ cells, CD161⁺ MR1AgTet⁺ T cells, CD161⁺ acetyl-6-formylpterin (AC-6FP⁺), CD4⁺ T cells (**Figure 8**).

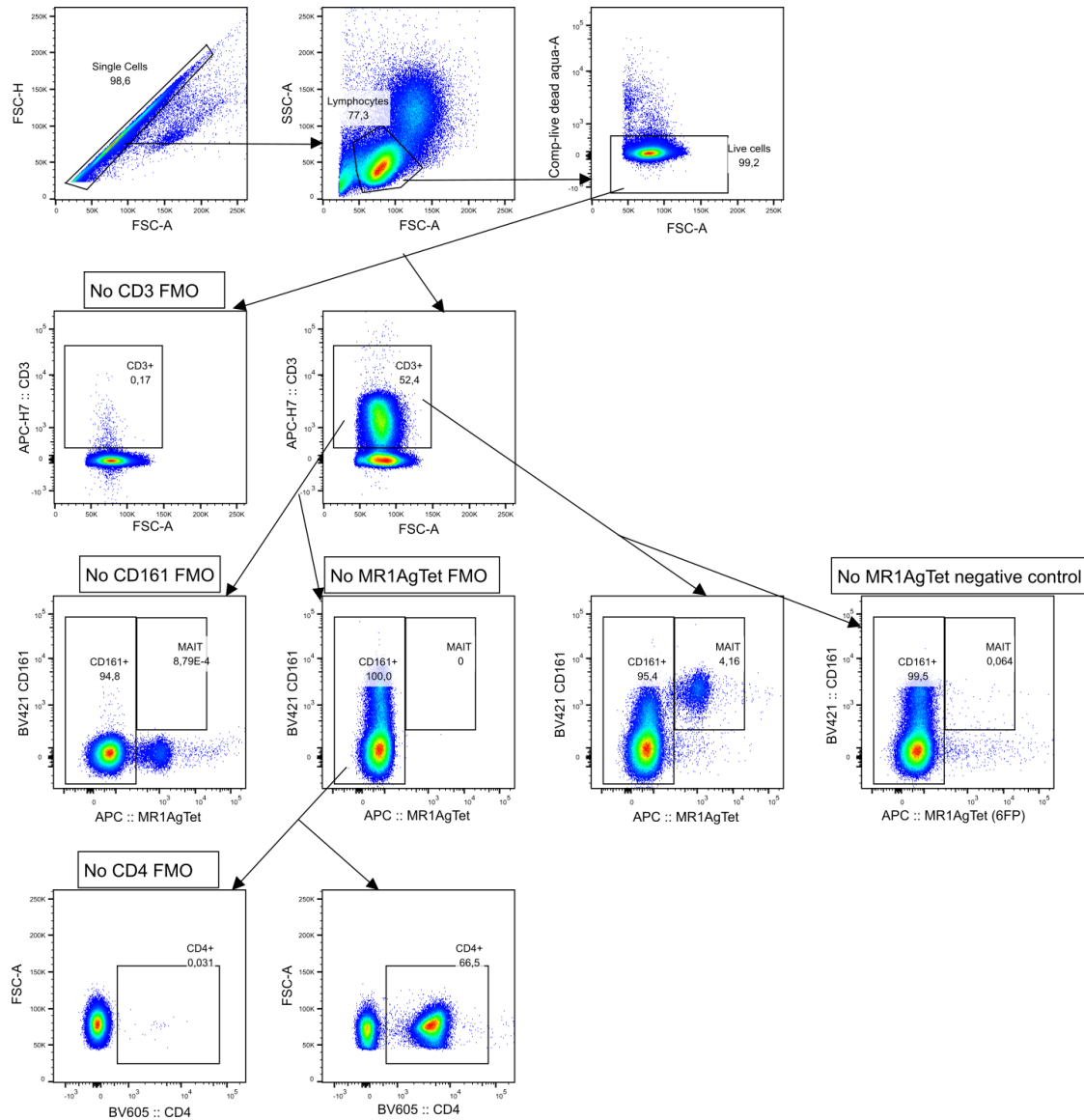


Figure 8. Fluorescence minus one (FMO) gating for MAIT and CD4+ T cells. Representative flow cytometry of one healthy blood donor showing how gates for MAIT and CD4+ T cells were established. MAIT cells were gated as CD3+, CD161+, MR1AgTet+ cells and CD4+ T cells were gated as CD3+CD4+ T cell. Cells were gated on singlets by FSC-H/FSC-A then on lymphocytes by FSC/SSC and live cells. CD3 FMO was used to gate for CD3+ cells off live cells. CD161 FMO was used to gate for CD161+ cells off the CD3+ gate. MR1AgTet FMO was used to gate MR1AgTet off the CD3+ gate. MR1AgTet negative control FMO was used to gate MR1AgTet negative control off the CD3+ gate. CD4 FMO was used to gate for CD4+ cell off the CD3+MR1AgTet- gate.

FMO was used to optimize the gating strategy for MDDC. Monocytes were cultured in media supplemented with GM-CSF and IL-4 clear flat bottom polystyrene round clear wells plate (ThermoFisher Scientific) for 7 days. Fresh media supplemented with GM-CSF and IL-4 was added to the culture every 2 days. On day 5 of the culture, PFA-fixed *E. coli* was added and cultured for 2 days. Semi-adherent cells were resuspended by adding cold PBS for 5 min before gently scraping them off the polystyrene plate using a rubber cell scraper. Cells were stained with antibodies in table 2.6 except for one of the following antibodies: PE-Cy5-CD11C (B-Ly6), BV786-HLA-DR (Tu39), FITC-CD80 (BB1), BV711-CD83 (HB15e), and APC-MR1 (8F2F9) and analyzed by flow cytometry. FMO was used to set gates for CD11C+, HLA-DR+, CD80+, CD83+, and MR1+ cells.

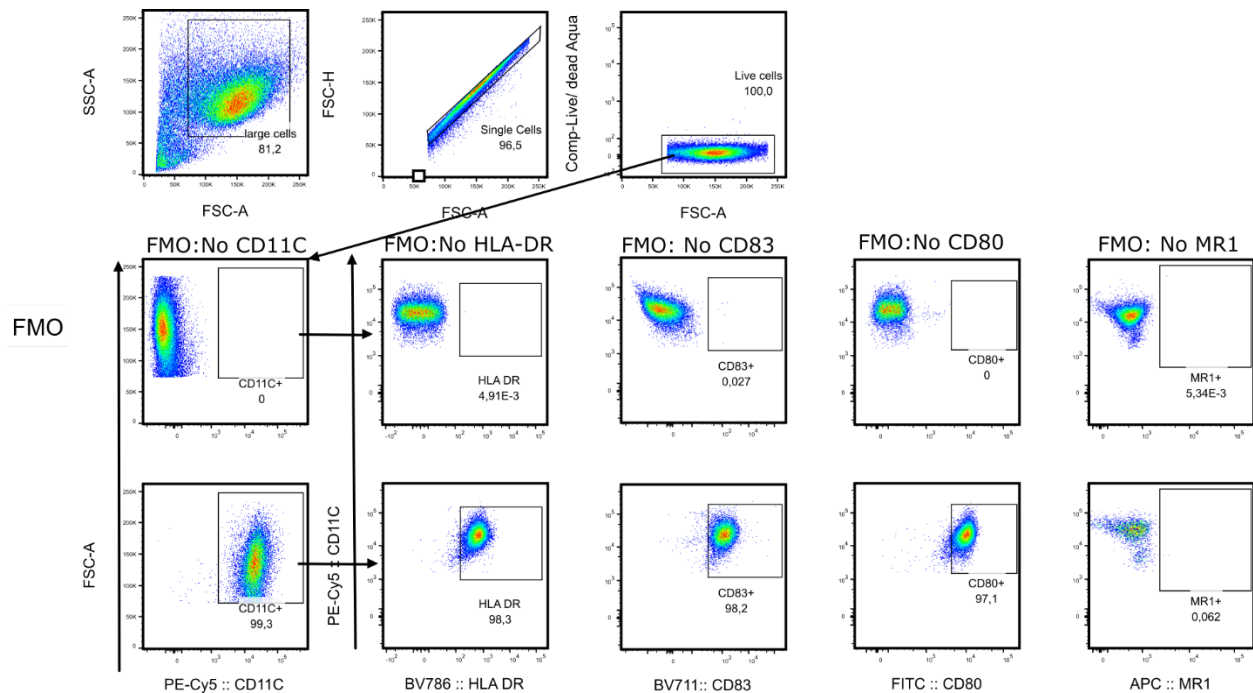


Figure 9. Fluorescence minus one (FMO) gating strategy for MDDCs. Representative flow cytometry plot of FMO showing how CD11C+, HLA-DR+, CD83+, CD80+, and MR1+ cells were gated on. Gates were set by SSC-A and FSC-A to show size and granularity, FSC-H by FSC-A to gate for singlets, Live/Dead Aqua stain vs. FSC-A to gate for live cells. CD11C+ FMO was used to gate on 11C+ cells off the live cells gate, HLA-DR+ FMO was used to gate on HLA-DR+ cells off the CD11C+ cells. CD80+ FMO was used to gate on CD80+ cells off the CD11C+ gate. CD83+ FMO was used to gate on CD83+ cells off the CD11C+ gate, and MR1 FMO was used to gate on MR1+ cells off the CD11C+ gate.

3.4.6. Monocyte enrichment

Monocytes were enriched by negative sorting using EasySep™ (Cat# 19359, StemCell). Freshly isolated PBMCs were suspended in isolation buffer to 5×10^7 cells/mL and transferred to a polystyrene round-bottom tube. For the enrichment cocktail media, 50 μ L/mL of sample was added, followed by a platelet removal cocktail at 50 μ L/mL of sample, mixed, and then incubated for 5 min at room temperature. The magnetic beads were vortexed for 30 seconds to ensure even distribution followed by addition of 50 μ L/mL of sample then mixed and incubated at room temperature for 5 min. Isolation media was added to top up sample to 2.5 mL. The tube was placed without a lid into the magnet (Cat# 18000, StemCell) and incubated at room temperature for 2.5 min. Magnet and tube were picked up together and in one continuous motion the enriched cell suspension was poured into a new sterile tube.

3.4.6.1. Monocyte differentiation

Enriched monocytes were counted and cultured in RPMI media supplemented with 10% FCS, 1% L-glutamin, 1% penicillin and streptomycin, 75 ng/mL of GM-CSF and 100 ng/mL of IL-4 at 37°C for 7 days. Media was changed every 2 days by removing 500 μ L culture supernatant and adding 500 μ L fresh RPMI media containing 10% FCS, 1% L-glutamine, 1% penicillin and streptomycin, 75 ng/mL of GM-CSF and 100 ng/mL of IL-4. On day 4, immature MDDCs were stimulated with TLR8-ligand (ssRNA40), TLR7-ligand (imiquimod), and *E. coli*. On day 7, the culture supernatant was removed and stored at -80°C. MDDC were harvested by adding cold PBS and incubating at room temperature for 5 min. The PBS was removed into the flow tubes. Rubber scrapers were used lift the semi-attached cells off the plate. The cells were centrifuged and stained.

3.4.7. HIV assays

3.4.7.1. Viral stock preparation

Viral stock provided to us by a former student in the lab, HIV-1_{Bal} 1 strain (3 vials of HIV-GFP ML4.3) was prepared by propagating and expanding in phytohemagglutinin-stimulated, IL-2-treated PBMCs. PBMCs from HIV-seronegative blood donors were isolated by Ficoll-Hypaque

density gradient centrifugation of heparin-treated venous blood. Prior to HIV-1 infection, the cells were stimulated with 2 µg/mL of phytohemagglutinin (Gibco-BRL) for 3 to 4 days and maintained in R10 media (Cellgro, Fisher Scientific, Ottawa, ON, Canada), supplemented with 10 mM HEPES buffer (Cellgro, Fisher Scientific), 1 ng/mL of interleukin (IL)-2 (Gibco, ThermoFisher Scientific, Ottawa, ON, Canada), 100 U/mL of penicillin, and 100 ng/mL of streptomycin (both from Cellgro, Fisher Scientific, Ottawa, ON, Canada). After infecting the cells, feeder cells (mainly PBMCs) were pretreated with 2 µg/mL PHA in R10 media supplemented with 10 mM HEPES buffer and 1 ng/mL IL-2 was added every 3 days before harvesting the virus on day 15.

3.4.7.2. Calculation of T_{CID50}.

Serial dilutions of 5⁻¹, 5⁻², etc. were applied. For each dilution, I indicated the number of replicates which were infected (out of 4), identified the dilutions that contained both infected and uninfected wells and the nearest dilutions that contain either all infected wells or all uninfected wells.

Table 3 P24 ELISA

Row on plate	1	2	4	5	6	7	8	9	10	11	12
Dilution	5 ⁻¹	5 ⁻²	5 ⁻³	5 ⁻⁴	5 ⁻⁵	5 ⁻⁶	5 ⁻⁷	5 ⁻⁸	5 ⁻⁹	5 ⁻¹⁰	5 ⁻¹¹
Number of positive wells	4	4	4	4	4	4	3	0	2	1	0

The values were carried out to **Table 4** below.

Table 4 Cell Mortality ratio calculation

Dilution	P24+	P24-	Infected	Uninfected	Mortality	
					Ratio	%
5 ⁻⁷	4	0	10	0	10/10	100
5 ⁻⁸	3	1	6	1	6/7	85.7142
5 ⁻⁹	0	4	3	5	3/8	37.5
5 ⁻¹⁰	2	3	3	8	2/11	18.18
5 ⁻¹¹	1	0	1	9	1/10	10
5 ⁻¹²	0	0	0	9	0/9	0

The infected wells were calculated by adding the total number of p24+ wells starting from the bottom and adding towards the top and the uninfected wells by adding the total number of p24-

wells starting from the top and adding towards the bottom. The ratio of infected to uninfected wells at each dilution was calculated and converted to %.

The range of dilutions containing the 50% endpoint dilution was used to calculate the TCID50, in this case, 50% lies between 5^{-7} and 5^{-8}

The extrapolated 50% endpoint dilution equals

$$X = \frac{(\% \text{ mortality next above } 50\%) \text{ minus } 50\%}{(\% \text{ mortality at dilution next above } 50\% \text{ minus } (\% \text{ mortality at dilution next to } 50))}$$

$$X = \frac{85.7142 - 50}{85.7142 - 37.5}$$

$$X = 35.7142/48.0442$$

$$X = 0.7432$$

The interpolated value determines the precise number within the range determined above.

$X = 0.7432$ means that in the range 5^{-7} and 5^{-8} .

The 50% endpoint dilution equals $X=5^{-7.7432}$.

Dilution of 1/5 were used, so I multiplied the endpoint dilution by log 5

$$X = (-7.7432) (\log 5)$$

$$X = -5.4123$$

The 50% endpoint dilution is estimated at $10^{5.4123}$. To calculate TCID50/mL the dilution was accounted for.

Since 100 μL was carried across the plate

$$\frac{10^{5.4123} \text{TCID50}}{0.01} = 25840445.69 = 2.584 \times 10^7 \text{ per mL}$$

Taken together, the results show that there were 2.584×10^7 virus per mL. Based on the TCID50, for $\text{MOI}=3$

$$\frac{9 \times 10^5}{2.584 \times 10^7} = 39 \mu\text{L/well was needed for infection.}$$

3.4.7.3. p24 ELISA

Tissue culture supernatant from infected and noninfected unstimulated CD4⁺ T cells, unstimulated CD4⁺ T cells co-cultured with unstimulated MAIT cells, unstimulated CD4⁺ T cells co-cultured with stimulated MAIT cells, stimulated CD4⁺ T cells co-cultured with unstimulated MAIT cells, stimulated CD4⁺ T cells co-cultured with stimulated MAIT cells, and stimulated CD4⁺ T cells were centrifuged at 1500 rpm for 15 min to remove cells and debris and 25 μ L of disruption buffer was added to each well of microELISA plate used in the assay. To appropriate wells of microELISA plate, 100 μ L of diluted HIV-1 p24 standard was added in duplicate and 100 μ L complete tissue culture media containing 10% FBS served as a negative control. This was followed by adding 100 μ L of test samples in duplicate to appropriate wells containing disruption buffer. The plate was gently tapped on the side, covered, and incubated at 37°C for 60 min. The plate was washed by aspirating the well contents into a waste tray then filling the well with wash buffer, leaving it to soak for 15 s before aspirating into the waste tray. This washing step was repeated four times. After the last wash, the plate was inverted and tapped firmly on absorbent paper. 100 μ L of conjugate solution was added to each well, the plate was covered and incubated at 37°C for 60 min. The washing step was repeated and 100 μ L of peroxidase substrate added to each well. The plate was incubated uncovered for 30 min at room temperature (19-23°C). In the same order peroxidase substrate was added, 100 μ L of stop solution was added to each well and the plate read at 450 nm in a micro-ELISA plate reader (Synergy Hi multi-reader machine, BioTek) within 20 min.

3.4.7.4. MAIT and CD4⁺ T cells sorting

MAIT cells were isolated for cell sorting by centrifuging 20 mL blood at 1500 rpm for 7 min and removing plasma. The blood was diluted with PBS to approximately 2x the starting volume. In 50 mL tubes, 10 mL lymphoprep™ (Cat# 07851, Stem cell Technologies) was added (for up to 20 mL diluted blood) and diluted blood was carefully layered over the lymphoprep™. The tubes were centrifuged with the brake turned off (deceleration at 0) at 1400 rpm for 25 min. The white cell layer was carefully collected into R10 in 50 mL tube and sterile PBS added. The tubes were gently swirled to mix before spinning. The supernatant was poured off and the cells pellets gently

resuspended in 40 μ L of buffer per 10^7 total cells. T cells were enriched by negative selection using MACS separator (Cat # 130-096-535, MACS Miltenyi, Friedrich-Ebert-Straße BG, Germany). Per 10^7 total cells, 10 μ L of Pan T Cell Biotin-antibody cocktail containing monoclonal antibodies against CD14, CD15, CD16, CD19, CD34, CD36, CD56, CD123, and CD235a (GlycophorinA) was added. After mixing well and incubating for 5 minutes in the refrigerator (2–8 °C), 30 μ L of buffer per 10^7 total cells was added. 20 μ L of Pan T Cell microbead cocktail per 10^7 total cells was added, mixed well, and incubated for 10 minutes in the refrigerator (2–8 °C), LS Column was placed in the magnetic field of MACS separator. The column was rinsed with 3 mL of buffer and cell suspension applied onto the column. Flow-through containing unlabeled cells, representing the enriched T cells was collected. Enriched T cells were stained with antibodies in table 2.4 before sorting the cells on BD FACSAria™ Fusion sorter as per manufacturer's recommendations.

3.4.7.5. HIV infection assay

Enriched MAIT cells were stimulated with 50 ng/mL of rIL-18 and 50 ng/mL of rIL-12 and cultured for 18 hrs at 37°C in a humidified, 5% CO₂ incubator. CD4⁺ T cells were stimulated by culturing in 96-well plate coated with 4 μ L anti-CD3 and 4 μ L anti-CD28 antibodies in 200ul sterile PBS. The CD4⁺ T cells were washed to remove unbound anti-CD3/CD8 beads, and the MAIT cells washed to remove IL-18 and IL-12. CD4⁺ T cells were co-cultured with MAIT cells and infected with HIV-1 virus for 7 days.

3.4.7.6 p24 staining

Seven days after infection, Golgi plug, and Golgi stop were added and incubated for 18h at 37°C in in a humidified, 5% CO₂ incubator. Cells were collected in 5 mL tubes and centrifuged at 1800 rpm for 3 min. Supernatant was collected into 10% Triton X media and stored at -30°C. The cells were resuspended, and live/dead aqua stain added. The cells were incubated for 20-30 min at 4°C. Cells were washed with 800 mL FACs wash buffer, and stained for cells surface markers for 20–30 min at 4°C. The cells were fixed with FoxP3 permfix buffer for 20 min at 4°C, washed with FOXp3 perm wash then stained with p24 and incubated for 45 min at 4°C. Cells were washed resuspended in PBS and analyzed by flow cytometry.

3.5 Data and statistical analysis

Values are expressed as median, and range were analysed using PRISM program (GraphPad Software Inc, CA, USA). Comparison between two paired groups (stimulated versus unstimulated) was done using Wilcoxon signed rank tests while two unpaired groups were compared using Mann–Whitney U tests. More than two groups were analysed by Friedman’s tests. All P values <0.05 were reported as statistically significant.

3.5.1 tSNE analysis

To perform t-distributed stochastic neighbour embedding (tSNE) analysis, the data events were standardized by down sampling on the FlowJo platform. A column was created on FlowJo for merging the samples depending on experimental condition, A value was assigned to separate the samples depending on whether they were stimulated or unstimulated. The samples were concatenated and used to derive tSNE plots.

Chapter 4 Results

4.1 Defining MAIT cells by surrogate markers

Rationale. Human MAIT cells are unconventional T cells that express a semi-invariant TCR made up of an invariant V α 7.2 coupled with restricted J α segments (J α 33, J α 12, or J α 20) and limited V β repertoires. MAIT cells comprise about 10% of circulating CD3⁺ T lymphocytes (585,586). MAIT cells express high level of C-type lectin receptor CD161 (456), IL-18R (439) and CD26 (366). To define MAIT cells, *ex vivo* cells from healthy donors were stained with an antibody panel (**Table 2.1**) and analyzed by high-dimensional flow cytometry. Live/dead aqua stain was used to distinguish between live and dead cells. CD3% was defined as the percent of the physical lymphocyte gate. CD4% and CD8% are presented as percentages of CD3⁺ $\gamma\delta$ TCR⁻ cells. MAIT cells defined by surrogate markers such as V α 7.2-TCR⁺, CD161⁺⁺ cells were presented as a subset of CD8⁺, CD4-CD8⁻ (DN) cells. A representative flow cytometry plot for one healthy donor showing the gating strategy for defining MAIT cells using antibodies specific for CD161, CD8 and V α 7.2TCR is shown in **Figure 10**.

Of the CD3⁺, $\gamma\delta$ TCR⁻ cells, 0.6% were MAIT cells as defined by being CD161⁺⁺, V α 7.2TCR⁺. Of the CD8⁺, CD4-CD8⁻ T cells, 2.7% could be identified as positive for the MAIT markers CD161⁺⁺, V α 7.2TCR⁺. Further, the 2.7% positive cells are in line with other studies using these markers(587,588). Of the CD8⁺ T cells, 2.1% were MAIT cells while of the CD4⁺ T cells only 0.04% were MAIT cells as defined by being CD161⁺⁺V α 7.2⁺ (**Figure 10**). Of CD4⁻, CD8⁻ T cells, 4.8% were MAIT cells, whereas of CD4⁺, CD8⁺ T cells, only 0.04% were MAIT cells as defined by being CD161⁺⁺, V α 7.2-TCR⁺.

These findings are consistent with what was previously reported (455,457,461).

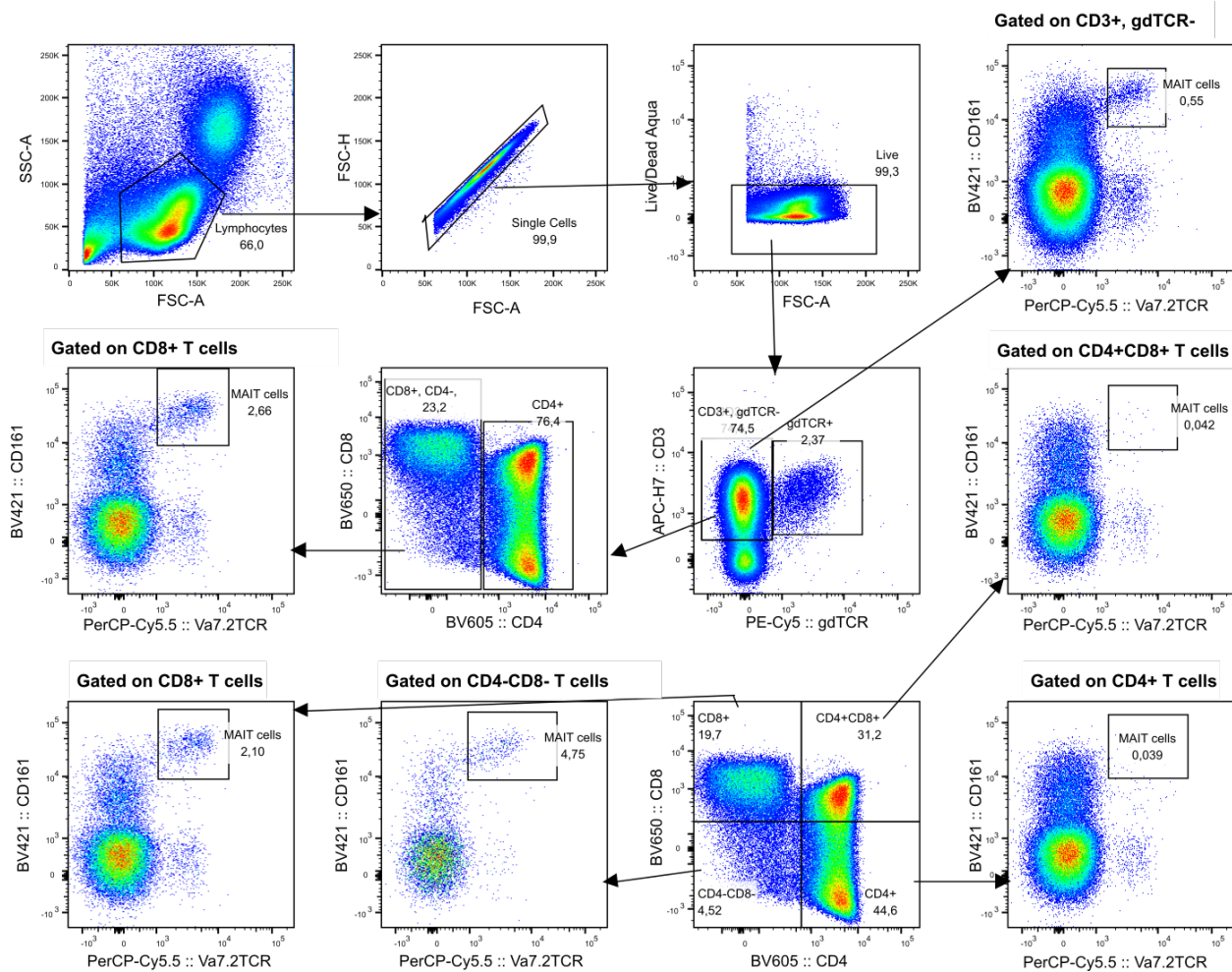


Figure 10. MAIT cells defined by surrogate markers. Representative flow cytometry plot of one healthy blood donor showing gating for MAIT cells. MAIT cells were defined as CD4-CD161⁺⁺, Va7.2-TCR⁺ T cells. Cells were gated on lymphocytes by FSC/SSC, then on singlets by FSC-H/FSC-A and live cells. CD161⁺⁺Va7.2⁺ T cells were gated off the CD3+ $\gamma\delta$ - T cells gate, CD161⁺⁺Va7.2⁺ T cells were gated off the CD4- T cells gate, CD8+ CD4-CD8- T cells and CD4+ T cells were gated off the CD3+ $\gamma\delta$ - T cells gate, CD3+ $\gamma\delta$ - T cells and CD3+ $\gamma\delta$ + T cells were gated off the live cells gate, CD161⁺⁺Va7.2⁺ T cells were gated off the CD4+CD8+ T cells gate, CD161⁺⁺Va7.2⁺ T cells were gated off the CD8+ T cells gate, CD161⁺⁺Va7.2⁺ T cells were gated off the CD4-CD8- gate, CD4-CD8-T cells, CD4+CD8+, CD4+ and CD4-CD8- T cells were gated off the CD3+ $\gamma\delta$ - T cells gate and CD161⁺⁺Va7.2⁺ T cells were gated off CD4+ T cells.

4.1.1 Use of MR1 tetramers to confirm gating strategy for MAIT cells

MAIT TCRs are specific for small molecule metabolites produced by microbes, presented by the nonpolymorphic MHC class I-like molecule MR1 (436). The most potent MR1 ligand is 5-OP-RU, a derivative of intermediates produced during bacterial riboflavin biosynthesis (449,589). Since the majority of MAIT cell studies were carried out before the MR1 tetramer became available, studying MAIT cells relied on a combination of antibodies for cell surface markers, referred to as surrogate markers, including CD161, CD26, and V α 7.2-TCR. Although CD161⁺⁺, CD26⁺ V α 7.2⁺ showed enrichment for MAIT cells, not all cells identified by these surrogate markers may be positively identified as MAIT cells by MR1 tetramer staining, because the V α 7.2 classification relies on reactivity with an anti-V α 7.2 mAb. However, V α 7.2 usage is not limited to MAIT cells, as other T cells also express V α 7.2 including public MHC-restricted T cells, as well as CD1b-restricted germline-encoded mycolyl lipid reactive (GEM) T cells (590–592). Furthermore, not all MAIT cells are captured by these surrogate markers (440) as some such as CD161 are absent from immature MAIT cells (457) and may be downregulated on MAIT cells following activation (458–460). For example, in HIV-infected patients, a loss of CD161⁺⁺V α 7.2⁺ cells was interpreted as a loss of MAIT cells associated with HIV infection (475); however, it was later shown that although many MAIT cells persisted, CD161 downregulation rendered them undetectable using the CD161⁺⁺ V α 7.2⁺ surrogate phenotype (476). Therefore, use of these surrogate markers may lead to misclassification of MAIT cells in disease states. Recently, an MR1-antigen loaded tetramer (MR1AgTet⁺) has been developed for specific identification of MAIT cells (585,589). Therefore, when using surrogate markers to define a MAIT cell population, it is important to confirm with MR1 tetramer reactivity.

To confirm the MAIT cell subset, PBMCs from healthy donors (n=8) were stained with human MR1Ag tetramers, and the results were compared with MAIT cell-staining protocol using anti-CD3, CD161, CD8, CD4, and V α 7.2 markers. Live/dead aqua stain was used to distinguish between live and dead cells. CD3% was defined as the percent of CD3⁺ cells in the physical lymphocyte gate, and CD4% and CD8% are presented as the percentage of CD3⁺ γ δ - cells. MAIT cells defined by surrogate markers as V α 7.2-TCR⁺, CD161⁺⁺ cells were presented as a subset of

CD4⁻ cells. MAIT cells were also defined by MR1Ag tetramer staining as CD3⁺, CD161⁺⁺, MR1AgTet⁺ cells as a subset of CD8⁺, CD4⁻CD8⁺-T cells. A representative flow cytometry plot for one healthy donor showing the gating strategy for defining MAIT cells using surrogate markers CD161, CD8 and V α 7.2-TCR and MR1 tetramer loaded with 5-OP-RU is shown in **Figure 11a**.

Of the CD8⁺DN T cells, 9.1% and 6.6% could be identified as positive for the MAIT markers CD161, V α 7.2-TCR and CD161⁺⁺, MR1AgTet⁺, respectively (**Figure 11a**). Of the CD8⁺ T cells, 6.9% were MR1AgTet⁺, while of the CD4⁺ T cells only 0.01% were MR1AgTet⁺ (**Figure 11a**). Of the double positive (DP) (CD4⁺ and CD8⁺) T cells, 0.5% were MR1AgTet⁺, while of the double negative (DN) (CD4⁻ and CD8⁻) T cells 2.2% were MR1AgTet⁺ (**Figure 11a**). The Wilcoxon test was used to compare MAIT cell frequencies as defined by surrogate markers CD161⁺⁺, V α 7.2 vs. CD161⁺⁺, MR1AgTet⁺. In the CD3⁺CD8⁺, and. DN T cells, the frequency of CD161⁺⁺, V α 7.2⁺ cells was significantly higher than that of CD161⁺⁺, MR1AgTet⁺ (median, range, 5%, 31% vs. 3.5%, 18.2%, p=0.002) (**Figure 11b**). Even though the differences appeared to be driven by the two subject data points with higher frequencies than the other 9%, after eliminating the outliers a between-group significance was maintained (median, range, 4.5%, 7% vs. 2.6%, 6%, p=0.002).

Taken together, these results show that in healthy individuals the frequency of MAIT cells identified as CD161⁺⁺MR1AgTet⁺ was 4% lower than that of MAIT cells identified as CD161⁺⁺, V α 7.2. This may be due to the detection of other T cells that express surrogate markers CD161 and V α 7.2 that are not classified as MAIT cells. Also, MR1AgTet cells were mainly CD161⁺⁺ and CD4⁻. This is consistent with previous studies that reported TRAV1-2 usage by non-MAIT cells (366,456,585). Reantragoon et al. (585) reported that V α 7.2 detected 10-24% more MAIT cells than the MR1 tetramer.

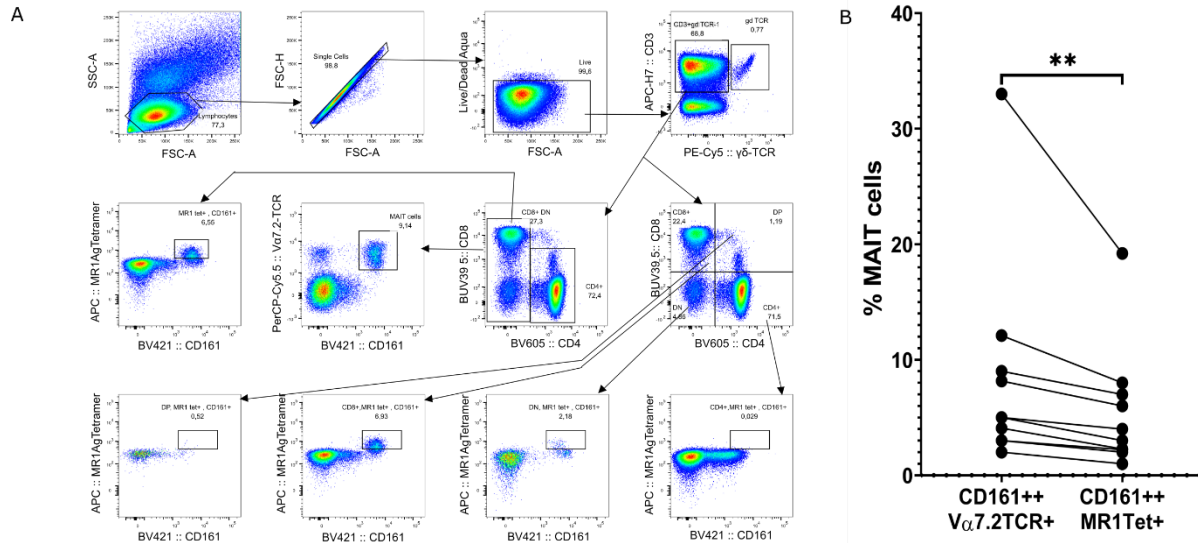


Figure 11. Ag-specific identification of MAIT cells. (A) Representative staining of PBMC of one healthy donor blood sample. Cells were gated on lymphocytes by FSC/SSC, then on singlets by FSC-H/FSC-A and live cells which were negative for the live/dead aqua discriminant dye. CD3+ $\gamma\delta$ - T cells and CD3+ $\gamma\delta$ + T cells were gated off the live cells gate, MAIT cells were gated as CD161⁺⁺, MR1AgTet⁺ off the CD8⁺, CD4-CD8- (DN) T cells gate, CD161⁺⁺V α 7.2+ T cells were gated off the CD8⁺ CD4-CD8- (DN) T cells gate, CD8⁺ CD4-CD8- (DN) T cells and CD4⁺ T cells were gated off the CD3+ $\gamma\delta$ - T cells gate, CD8⁺, CD4+CD8+ (DP), CD4⁺, and CD4-CD8- (DN) T cells were gated off the CD3+ $\gamma\delta$ - T cells gate, MAIT cells were gated as CD161⁺⁺, MR1AgTet⁺ off the CD4+CD8+ (DP) T cells gate, off the CD8⁺ T cells gate, off the CD4-CD8- (DN) gate and off the CD4⁺ T cells gate. (B) MAIT cell frequency for each participant as defined by surrogate markers CD161⁺⁺V α 7.2TCR⁺ or CD161⁺⁺MR1AgTet⁺. Analysis was done using a Wilcoxon test. ** $p < 0.01$

4.1.2 MAIT cell subsets

In humans, MAIT cell development occurs in the thymus in three stages through positive selection. In the circulation of healthy human adults, MAIT cells are predominantly CD8⁺ with a smaller DN subset (456,457,586). MAIT cells are classified into different subsets depending on CD4 and CD8 co-receptor expression and have been shown to be phenotypically and functionally distinct in response to bacterial and fungal infection. Majority of peripheral blood CD8⁺ and DN CD161^{hi}V α 7.2⁺ MAIT cells are MR1-restricted compared to CD4⁺ MAIT cells. Additionally, CD8⁺ MAIT cells express higher levels of coactivating receptors including CD101, CD2 and CD9 and cytolytic effector molecules than DN MAIT cells (593). Here, CD4 and CD8 co-receptor expression by MAIT cells defined by MR1-5-OP-RU tetramer and CD161⁺⁺V α 7.2 staining was examined.

To assess MAIT cell co-receptor expression, PBMCs from healthy donors were stained for human MR1AgTet and anti-CD3, CD161, CD8, CD4, and V α 7.2 markers. Live/dead aqua stain was used to distinguish between live and dead cells. CD3% was defined as the percent of the CD3⁺ cells within the physical lymphocyte gate. MAIT cells defined by surrogate markers V α 7.2TCR⁺, CD161⁺⁺ cells or antigen-specific markers CD161⁺⁺MR1AgTet⁺ were presented as a percentage of CD3⁺ γ δ TCR⁻ cells. CD4% and CD8% were presented as a percentage of V α 7.2TCR⁺, CD161⁺⁺ or CD161⁺⁺MR1AgTet⁺ cells. A representative flow cytometry plot for one healthy donor showing the gating strategy for defining MAIT cells using surrogate markers CD161, CD8 and V α 7.2-TCR and MR1 tetramer loaded with 5-OP-RU is shown in **Figure 12a**.

In one representative donor, of the CD161⁺⁺V α 7.2⁺ cells, 82.6% were CD8⁺, 1.4% were CD4⁺, 1.7% were DP and 14.3% were DN. Out of the CD161⁺⁺MR1AgTet⁺ cells, 78.9% were CD8⁺, 1.7% were CD4⁺, 3% were DP and 16.4% were DN. (**Figure 12a**). The significant difference in CD4 and CD8 co-receptor expression between CD161⁺⁺V α 7.2⁺ cells and CD161⁺⁺MR1AgTet⁺ cell was assessed using a Wilcoxon test (**Figure 12b**). There was no significant difference between the frequency of CD8⁺ (84.7%, 89.6% vs. 71.9%, 82.2%, p=0.7209), CD4⁺ (0.1%, 5.8 vs. 1.2%, 3%, p=0.4418), DP (0.4% \pm 34% vs. 0.9%, 4.4%, p=0.7718) and DN (14.5%, 50.26% vs. 23.3%, 75.9%, p=0.6454) CD161⁺⁺V α 7.2⁺ cells and CD161⁺⁺MR1AgTet⁺ cells (**Figure 12b**).

Consistent with what has been reported before, MAIT cells are predominantly CD8+ and CD4-CD8-(DN) and a very small subset were CD4+ (588,593).

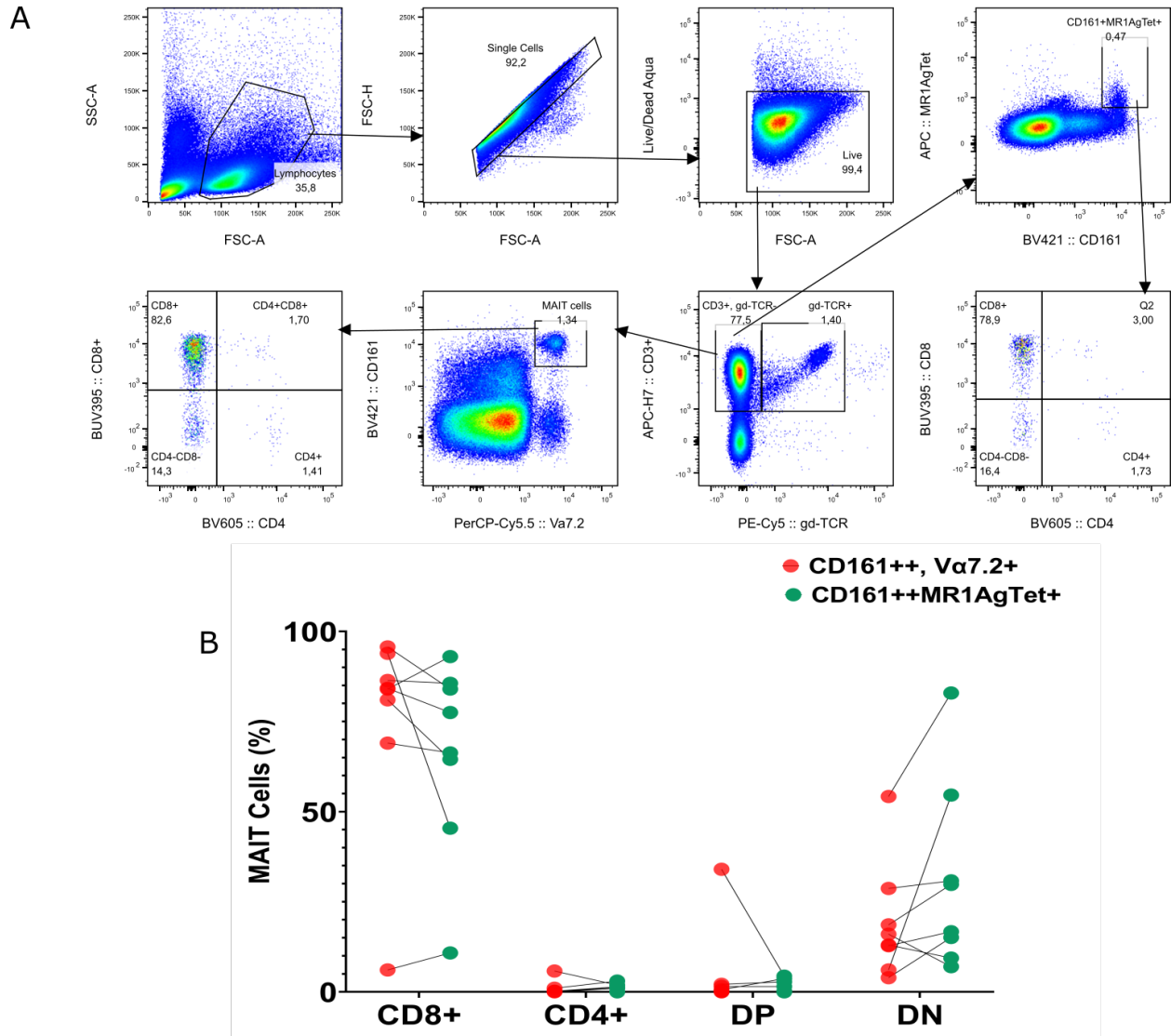


Figure 12. MAIT cells are predominantly CD8⁺ and CD4-CD8⁻(DN). A Representative staining of PBMC of one healthy donor blood sample. Cells were gated on lymphocytes by FSC/SSC, then on singlets by FSC-H/FSC-A and live cells which were negative for the live dead aqua discriminant dye. MAIT cells were gated as CD161⁺⁺, MR1AgTet⁺ off the CD3⁺γδ⁻ T cells gate, CD8⁺, CD4+CD8⁺ (DP), CD4⁺ and CD4-CD8⁻ (DN) T cells were gated off the CD161⁺⁺Va7.2⁺ T cells gate, CD161⁺⁺Va7.2⁺ T cells were gated off the CD3⁺γδ⁻ T cells gate, CD3⁺γδ⁻ T cells and CD3⁺γδ⁺ T cells were gated off the live cells gate, and CD8⁺, CD4+CD8⁺ (DP), CD4⁺ and CD4-CD8⁻ (DN) T cells were gated off the CD161⁺⁺, MR1AgTet⁺ gate. B Scatter diagram comparing frequency of CD8⁺, CD4+CD8⁺ (DP), CD4-CD8⁻ (DN) MAIT cells as defined by surrogate markers CD161⁺⁺Va7.2⁺ (green) or CD161⁺⁺MR1AgTet⁺ (red) for 8 participants each represented by a single dot. Analysis was done using Wilcoxon tests.

4.1.3 Gamma delta T cells were gated as CD3+ $\gamma\delta$ TCR+ cell

T cells can be classified as $\alpha\beta$ or $\gamma\delta$ based on their antigen receptors. The $\gamma\delta$ T cells make up approximately 0.5–10% of all peripheral blood lymphocytes (594). Cells expressing CD161 have been shown to have tissue-homing markers and characteristics, in addition to expressing high proinflammatory cytokines and high IL-17 (583,595,596) To define $\gamma\delta$ T cells *ex vivo*, cells from healthy donors were stained with the antibody panel shown in **Table 2.1** and analyzed by high-dimensional flow cytometry. The $\gamma\delta$ T cells were defined as CD3+ $\gamma\delta$ TCR+ cells. A representative flow cytometry plot for one healthy donor showing the gating strategy for defining $\gamma\delta$ T cells is shown in (**Figure 13A**).

Live/dead aqua stain was used to distinguish between live and dead cells. CD3% was defined as the percent of the physical lymphocyte gate. To confirm what has been previously observed, two subsets of $\gamma\delta$ T cells were defined by CD3+ $\gamma\delta$ TCR+: the CD3+ $\gamma\delta$ TCR^{high} population made up of 4.54% while the CD3+ $\gamma\delta$ TCR^{low} populations made up 1.4% of the live cells. Of the CD3+ $\gamma\delta$ TCR^{high} cells, 36% were CD161+, 10.5% were CD8+, 0.4% were CD4+, 0% were DP for CD4 and CD8, and 89.2% were DN for CD4 and CD8. However, for the CD3+ $\gamma\delta$ TCR^{low} cells, 3.1% were CD161+, 25.5% were CD8+, 1.7% were CD4+, 0% were DP, and 70% were DN (**Figure 13A**). These results align with other studies that have reported two phenotypically different subsets of $\gamma\delta$ T cells classified by the intensity of $\gamma\delta$ TC on CD3+ $\gamma\delta$ TCR (597).

CD161 and co-receptor CD4, and CD8 expression on CD3+ $\gamma\delta$ TCR^{low} and CD3+ $\gamma\delta$ TCR^{high} cells were compared by Wilcoxon tests (high vs. low) (**Figure 13b**). The frequency of CD161+ CD3+ $\gamma\delta$ TCR^{high} cells was significantly higher compared to the frequency of CD161+ CD3+ $\gamma\delta$ TCR^{low} (median, range frequency: 52.1%, 73.2% vs. 14.5%, 39.4%, $p < 0.0001$) T cells. However, the frequency of CD8+ CD3+ $\gamma\delta$ TCR^{high} cells was significantly lower than the frequency of CD8+ CD3+ $\gamma\delta$ TCR^{low} cells (2.7%, 26% vs. 5.3%, 71.1%, $p = 0.0035$). The frequency of CD4+ CD3+ $\gamma\delta$ TCR^{high} cells was also significantly lower than the frequency of CD4+ CD3+ $\gamma\delta$ TCR^{low} cells (1.1%, 77.2% vs. 12.7%, 33.9%, $p < 0.0092$). No significant difference in frequency of DP CD3+ $\gamma\delta$ TCR^{high} T cells and DP CD3+ $\gamma\delta$ TCR^{low} T cells was observed (0%, 3.5% vs. 0.4%, 3.2%, $p = 0.1099$). The frequency of DN CD3+ $\gamma\delta$ TCR^{high} cells was significantly higher compared to the

frequency of DN CD3+ $\gamma\delta$ TCR^{low} T cells (93.5%, 81.9% vs. 75.8%, 62.7%, p=0.0062) (**Figure 13b**).

Taken together, these results show that there were two subsets of $\gamma\delta$ T cells, that is, $\gamma\delta$ TCR^{high} and $\gamma\delta$ TCR^{low}. Majority of the $\gamma\delta$ TCR^{high} subset was also CD161+ and DN for CD4 and CD8. The frequency of CD4+ and CD8+ cells was higher in CD3+ $\gamma\delta$ TCR^{low} compared to CD3+ $\gamma\delta$ TCR^{high} cells.

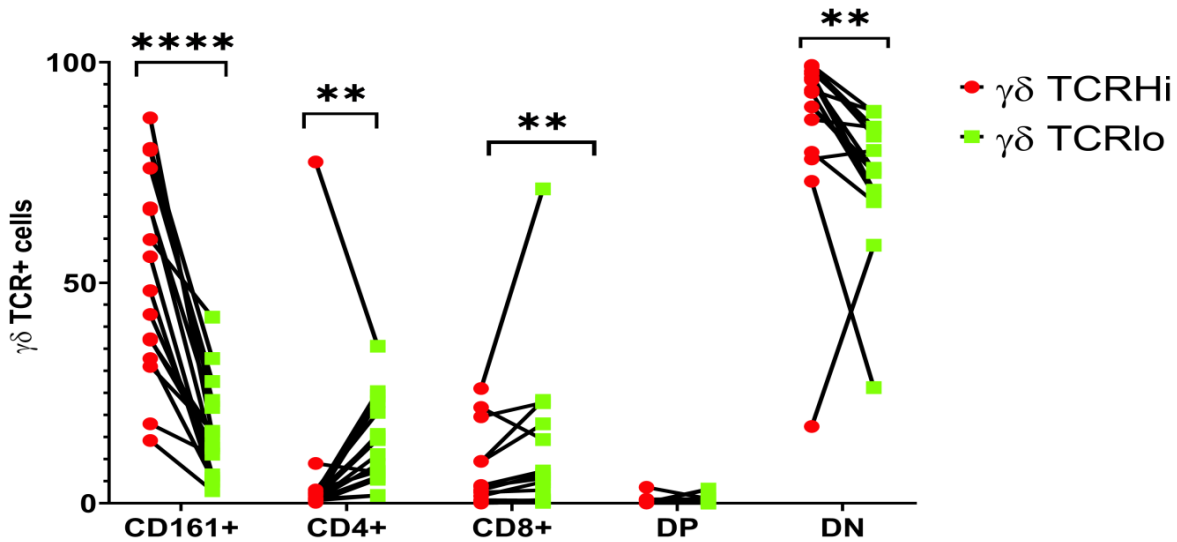
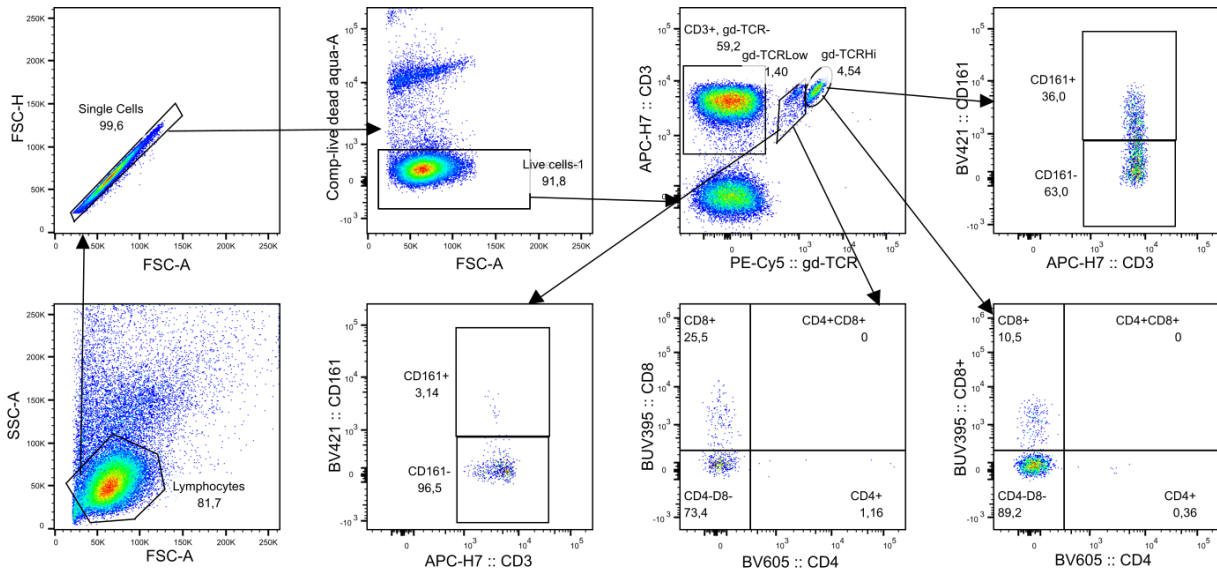


Figure 13. Two subsets of $\gamma\delta$ T cells defined by $\gamma\delta$ TCR as $\gamma\delta$ TCR^{high} and $\gamma\delta$ TCR^{low}. Top: Representative staining of PBMC of one healthy donor blood sample. Cells were gated on lymphocytes by FSC/SSC, then on singlets by FSC-H/FSC-A and live cells, which were negative for the live dead aqua discriminant dye. Two subsets of $\gamma\delta$ T cells were defined as CD3+ $\gamma\delta$ TCR^{high} and CD3+ $\gamma\delta$ TCR^{low} off the live cells gate. CD161+ $\gamma\delta$ T cells and CD161- $\gamma\delta$ T cells were gated off the CD3+ $\gamma\delta$ TCR^{high} gate. CD161+ $\gamma\delta$ T cells and CD161- $\gamma\delta$ T cells were gated off CD3+ $\gamma\delta$ TCR^{low} gate, CD8+, CD4+CD8+ (DP), CD4+ and CD4-CD8- (DN) T cells were gated off the CD3+ $\gamma\delta$ TCR^{high} gate and finally CD4+CD8 (DP), CD4+ and CD4-CD8- (DN) T cells were gated off the CD3+ $\gamma\delta$ TCR^{low} gate. Bottom: Frequency of $\gamma\delta$ T cell subsets in 16 individuals each represented by a single dot. Wilcoxon tests were used to compare frequency of CD161+, CD4+, CD8+ CD4+ CD8+ (DP), CD4-CD8- (DN) between $\gamma\delta$ TCR^{high} (red dots) and $\gamma\delta$ TCR^{low} (green dots) of $\gamma\delta$ T cells. ** $p \leq 0.01$, **** $p \leq 0.0001$

4.1.4 Frequency of MAIT cells in healthy donors

MAIT cells have been found in low numbers in human umbilical cord blood. Their frequency increases gradually in the human bloodstream until around 20 years of age (585,595,598). The frequency of MAIT cells in the blood has been shown to increase gradually, peaking during reproductive age before declining to become 10 times lower by the of age 80 and beyond. In this same study, it was reported that the frequency of MAIT cells varied in different individuals with women of reproductive age having more MAIT cells than men of the same age (599). To assess the frequency of MAIT cells in the peripheral blood of n=16 healthy donors, *ex vivo* PBMCs were stained with antibodies and analyzed by high-dimensional flow cytometry.

MAIT cells were classified by the surrogate markers CD3+, CD161++, DN (CD4- CD8-), CD8+, V α 7.2-TCR+. Each dot in **Figure 14** represents a healthy blood donor. The median frequency of MAIT cells was 6.1% with a minimum of 1.1% and a maximum of 13%.

Variability in MAIT cells frequency was confirmed, with some individuals expressing high levels while others had very low levels of MAIT cells (599).

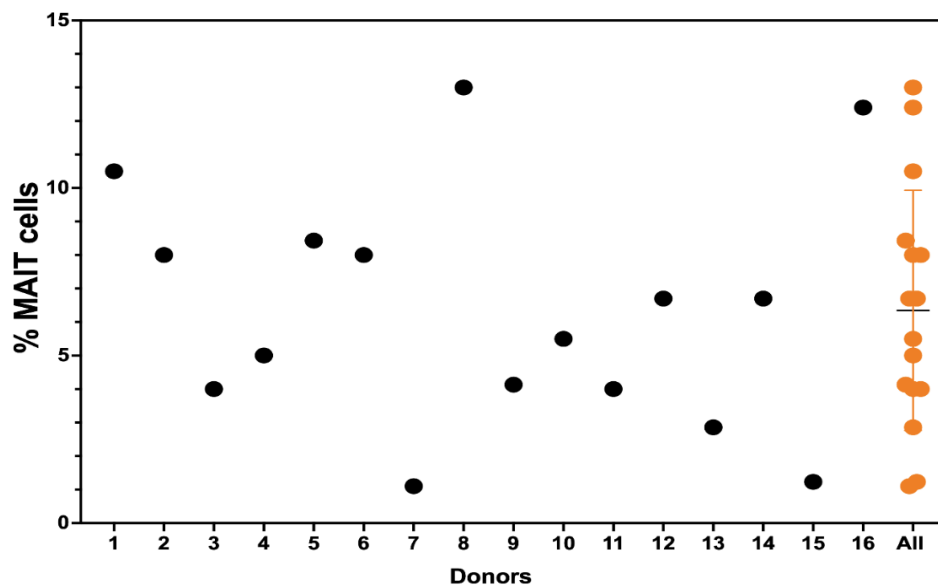


Figure 14. Variability in peripheral blood mucosal-associated invariant T (MAIT) cells frequency in healthy blood donors. Frequency of circulating MAIT cells in healthy blood donors expressed as a percentage of CD3+, $\gamma\delta$ -TCR-, CD4-, CD161++, V α 7.2-TCR+ cells in 16 healthy donors. Each dot represents the frequency of MAIT cells in one participant. The last column with orange dots represents a summary of the frequency of MAIT cells in all healthy blood donors. The horizontal black line represents the median for the data set. The orange vertical line represents 95% confidence interval.

4.1.5 Frequency of $\gamma\delta$ T cells in the peripheral blood of healthy adults

In humans, the pool of peripheral blood $\gamma\delta$ T cells is small at birth, and it expands during the first decade of life, from less than 2% of cord blood T cells to around 5% of PB T cell in adults (600). To assess the frequency of $\gamma\delta$ T cells in the peripheral blood of healthy donors, *ex vivo* PBMCs were stained with antibodies and analyzed by high-dimensional flow cytometry. The $\gamma\delta$ T cells were classified as CD3+, $\gamma\delta$ -TCR+ cells (**Figure 15**).

Variability in $\gamma\delta$ T cells frequency was confirmed, with some individuals expressing high levels of $\gamma\delta$ T cells while others had very low levels of $\gamma\delta$ T cells (599). Although in previous studies $\gamma\delta$ T cells have been reported to comprise of 1-10% of peripheral blood T lymphocytes, in some study participants a higher frequency of $\gamma\delta$ T cells was observed (median 5% and range 0.55% to 15.90% of the T lymphocytes).

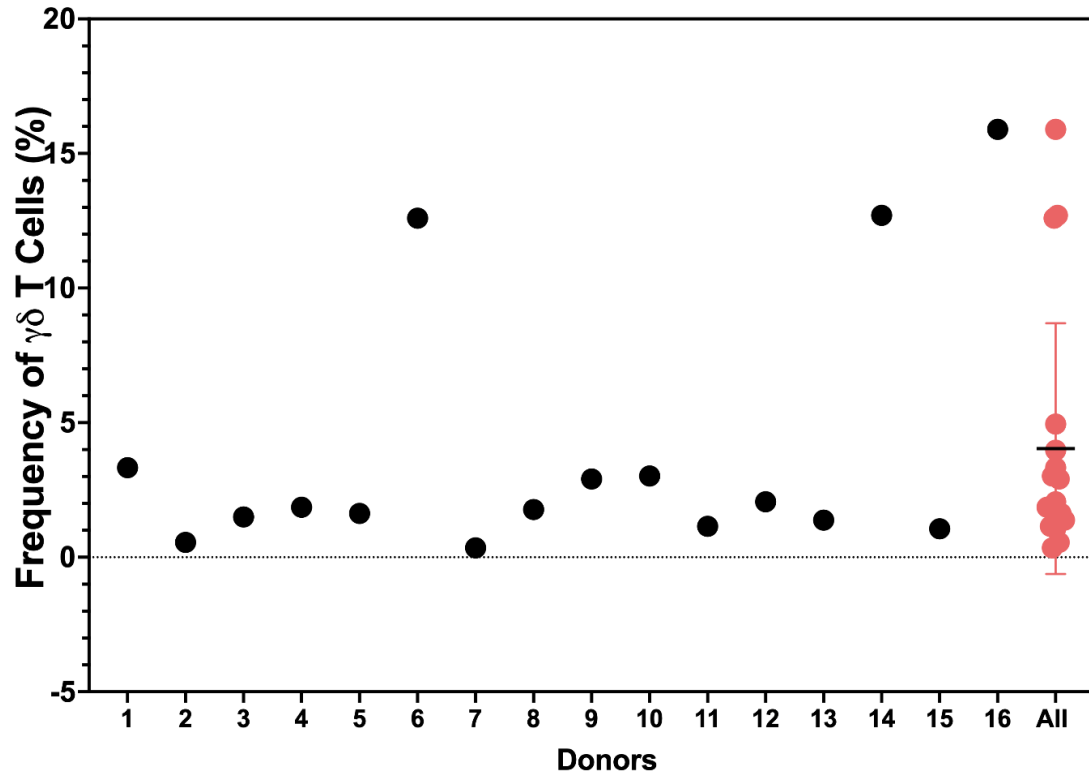


Figure 15. Variability in $\gamma\delta$ T cells frequency in peripheral blood. Frequency of circulating $\gamma\delta$ T cells in healthy blood donors expressed as a percentage of CD3+, $\gamma\delta$ TCR+ in 16 healthy donors. Each dot represents the frequency of $\gamma\delta$ T cells in one participant, with the orange dots representing a summary of the frequency of $\gamma\delta$ T cells in all healthy blood donors. The horizontal black line represents the median and the vertical orange line represents the 95% confidence interval for the frequency of $\gamma\delta$ T cells.

4.2. Differential response of MAIT and $\gamma\delta$ T cells in bulk PBMC culture to TLR7 and TLR8 stimulation

4.2.1. Rationale

TLR recognition of its ligand has been shown to lead to intracellular signalling resulting in expression of cytokines, chemokines, and antimicrobial peptides. MAIT cells and $\gamma\delta$ T cells can also respond to proinflammatory cytokines including IL-12 and IL-18 that are expressed by APCs, following microbial infections leading to their activation and cytokine expression (436,601). I sought to understand how TLR7/TLR8 stimulation of bulk PBMCs may result in MAIT cell and $\gamma\delta$ T cell stimulation and proinflammatory cytokine expression.

4.2.2. Hypothesis

Stimulation of PBMCs with TLR7-ligand (imiquimod) or TLR8 ligand (ssRNA40) will lead to MAIT and $\gamma\delta$ T cell activation and expression of proinflammatory cytokines including IFN- γ , TNF- α , GM-CSF and IL-17a.

To simplify data presentation, MAIT cell data is presented first, followed by $\gamma\delta$ T cell responses.

4.2.3. Time course and establishing MAIT cell culture conditions

To establish culture conditions for the TLR stimulation experiments, PBMCs from healthy donors (n=5) were cultured in the presence of TLR7 ligand, TLR8 ligand, PFA-fixed *E. coli*, and PMA/ION for 2, 6, 14, and 24 h, then stained with antibodies followed by flow cytometry analysis. Friedman tests were used to compare within individual differences in a CD69+MAIT cells at different time points after stimulation. The median and range for these values were reported

After stimulation of PBMCs with TLR7-ligand, the frequency of CD69+MAIT cells increased with time for up to 24 h (p=0.0025). The frequency of these cells was significantly higher at 14 h (p=0.0004) and 24 h (p<0.0001) compared to 0 h. (**Figure 16A**). After stimulation of PBMCs with TLR8-ligand, the frequency of CD69+MAIT cells increased with time for up to 24 h (p=0.0017). The frequency of these cells was significantly higher at 6 h (p=0.0024), 14 h (p<0.0001) and 24 h (p<0.0001) compared to 0 h. (**Figure 16B**). After stimulation of PBMCs with *E. coli*, the frequency

of CD69+MAIT cells increased with time for up to 24 h ($p=0.0025$). The frequency of these cells was significantly higher at 6 h (<0.0001), 14 h ($p<0.0001$) and 24 h ($p<0.0001$) compared to 0 h. **(Figure 16C)**.

Taken together, these results show that although MAIT cells were activated following TLR7, TLR8 and *E coli* stimulation as seen by the significant increase in the frequency of CD69+ MAIT cells. The frequency of CD69+MAIT cells remains stable between 14 and 24 h post stimulation indicating that MAIT cells activation can be analysed even after 24 h of stimulation.

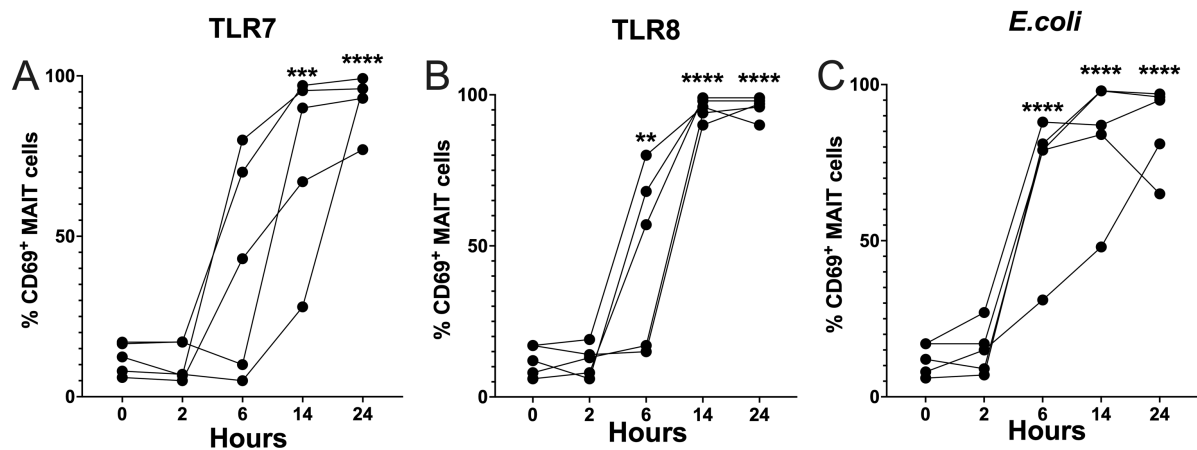


Figure 16. Increasing CD69+ MAIT cells with time over the course of a 24 h stimulation. Frequency of CD69 expression on MAIT cells at 2, 6, 14, and 24 h following TLR7 (A), TLR8 (B), and *E. coli* (C) stimulation. Each dot represents the frequency of CD69+ MAIT cells in a single donor. Analysis was done using Friedman tests. ** $p \leq 0.01$. Dunn's post-tests were used to indicate what time points were significantly different from baseline.

4.2.4. MAIT cells are highly activated following TLR 7/8 stimulation

Based upon the previous results, a 24 h stimulation was used for these next experiments (n=16). Analyses were performed using FlowJo V10 and gates were based on FMO and the presence of a clear positive population, as shown in **Figure 17A**. In one representative donor, TLR7 stimulation of PBMC led to an 11-fold increase in the frequency of CD69+ MAIT cells while TLR8 stimulation led to a 14-fold increase in the frequency of CD69+ MAIT cells (**Figure 17A**).

The Wilcoxon test was used to compare CD69+ MAIT cells between unstimulated vs. stimulated PBMCs from the 16 subjects. The median, and range between minimum and maximum frequency of CD69+ MAIT cells were reported. As observed in the time course experiments (**Figure 17**), stimulation of PBMCs with TLR7 ligand (8.6%, 20.6% vs. 80.7%, 89.6%, $p < 0.0001$), TLR8 ligand (8.6%, 20.6% vs. 71%, 87%, $p < 0.0001$) and *E. coli* (8.6%, 20.6% vs. 83.5, 37.6%, $p < 0.0001$) led to significant increase in median and range frequency of CD69+ MAIT cells (**Figure 17B**). The mean fluorescence intensity (MFI) of CD69 expression on MAIT cells was compared in unstimulated vs. stimulated PBMCs. Stimulation with TLR7 ligand (2362, 4752 vs. 11402, 44416, $p < 0.0001$), TLR8 ligand (2362, 4752 vs. 31885, 106095, $p < 0.0001$), *E. coli* (2362, 4752 vs. 66811, 120640, $p < 0.0001$) and PMA/Ion (2362, 4752, vs. 31180, 207120, $p < 0.0001$) led to significant increase in median and range of CD69 MFI (**Figure 17C**). To determine if CD69 expression is a characteristic of MAIT cells, CD69 + conventional CD4+ and CD8+ T cells was compared in PBMC cultured in the presence of TLR7 ligand, TLR8 ligand, or PFA-fixed *E. coli* for 24 h and PMA/ION for 14 h. The median and range frequency of CD69+CD4+ and CD69+ CD8+ T cells in (unstimulated vs stimulated) cells are shown. As observed previously by Were et al. (unpublished data), TLR7 stimulation led to a significant increase in CD69+CD4+ (1%, 3% vs. 2.5%, 16.7% $p = 0.0021$) and CD69+CD8+ T cells (1%, 14% vs. 4%, 15.2% $p < 0.0001$) (**Figure 17, D and E**). There was no significant change in frequency of CD69 + CD4+ T cells following TLR8 stimulation (1%, 3% vs. 1.5%, 14.9%, $p = 0.0723$). However, TLR8 stimulation led to a significant increase in the frequency of CD69+ CD8+ T cells (1%, 14% vs. 2%, 33% $p < 0.0001$) (**Figure 17, D and E**). The MFI of CD69 expression on CD4+ and CD8+ T cells was compared in unstimulated vs. stimulated PBMCs. Stimulation with TLR7 ligand (554, 1050 vs. 874, 3039 $p = 0.0052$), TLR8 ligand (554, 1050 vs. 1204, 3748 $p < 0.0013$), *E. coli* (554, 1050 vs. 1804, 2806 $p = 0.0156$) and PMA/ION (554, 1050 vs. 15149, 1541141 $p = 0.0034$) led to significant increase in CD69 MFI in

CD4⁺ T cells (**Figure 17E**). Stimulation with TLR7 ligand (476.5, 888 vs. 911.5, 2733 p=0.0002), TLR8 ligand (476.5, 888 vs. 1110, 2857 p<0.0001), *E. coli* (476.5, 888 vs. 1262, 1607 p=0.0156) and PMA/ION (476.5, 888 vs. 23172, 217507 p=0.0004) led to a significant increase in CD69 MFI in CD8⁺ T cells (**Figure 17F**).

Taken together, these results show that TLR7 and TLR8 stimulation of MAIT cells led to increased immune activation as measured by increase in frequency of CD69⁺ MAIT cells and MFI of CD69 expression by MAIT cells. MAIT cells were highly activated compared to baseline level on unstimulated cells but detectable increases in activation levels were also seen for both CD4⁺ and CD8⁺ T cells.

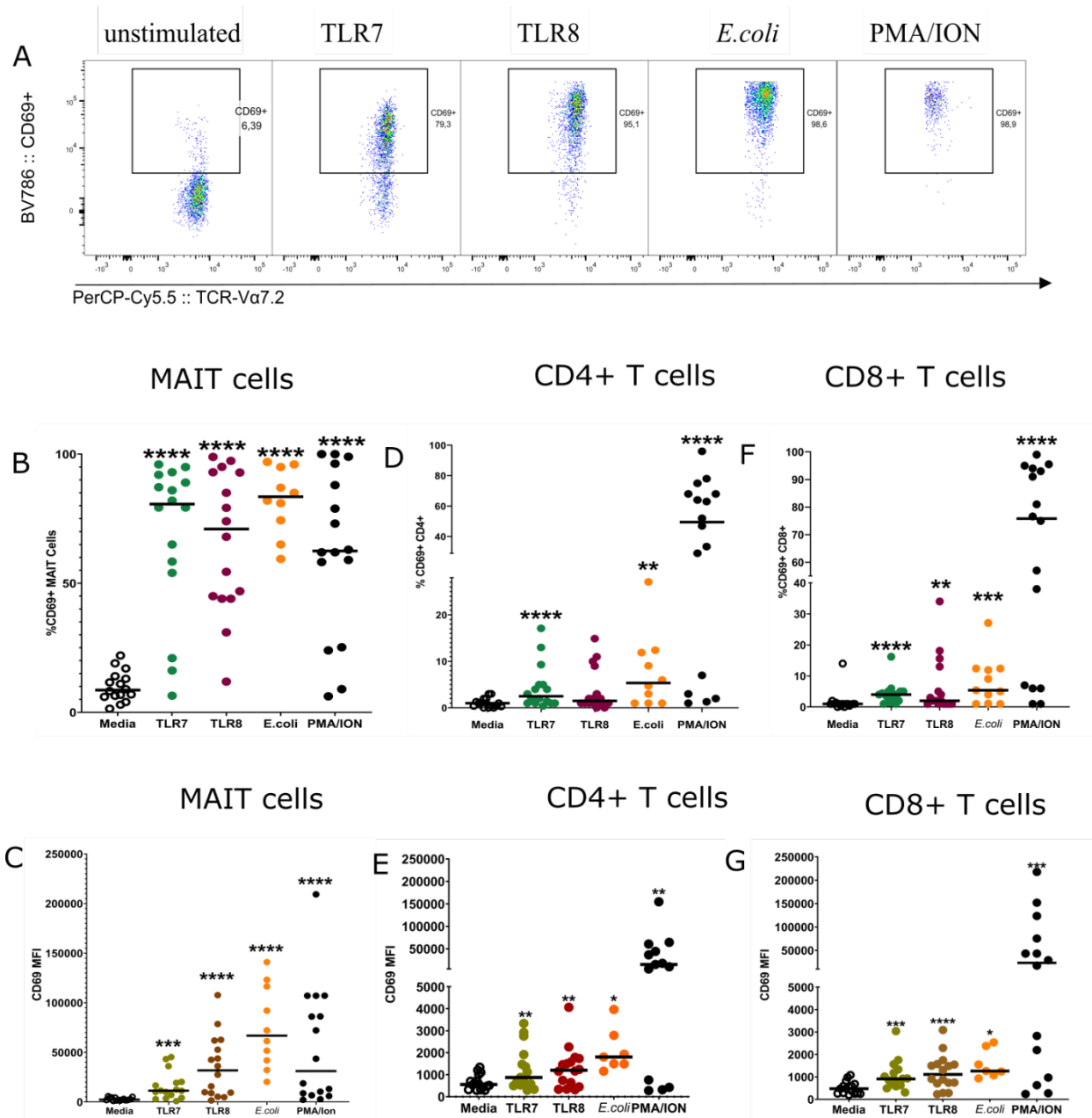


Figure 17. MAIT cells are highly activated following stimulation compared to CD4 and CD8 cells. (A) Representative flow cytometry plotting showing the frequency of CD69+ MAIT cells in unstimulated cells and after stimulation with TLR7-ligand, TLR8-ligand, *E. coli* and PMA/ION. (B) Frequency of CD69+ MAIT cells. (C) Mean fluorescent intensity (MFI) of CD69 expression on MAIT cells. (D) Frequency of CD69+ CD4+ T cells. (E) MFI of CD69 expression on CD4+ T cells. (F) Frequency of CD69+ CD8+ T cells. (G). MFI of CD69 expression on CD8+ T cells. Each dot represents the frequency of CD69+ cells in a single donor. Horizontal lines represent the median frequency or MFI. Analysis was done using Wilcoxon test, n=16. ** $p \leq 0.01$, *** $p \leq 0.001$, **** $p \leq 0.0001$.

4.2.5 Heterogeneity of MAIT cell activation as revealed by tSNE, UMAP and TriMap analysis

T-distributed stochastic neighbor embedding (tSNE) is an unsupervised nonlinear dimensional reduction algorithm that enables visualization of high-dimensional flow cytometry data in a dimension-reduced data set. Furthermore, tSNE is based on stochastic neighbour embedding (SNE) originally developed by Sam Roweis and Geoffrey Hinton (602) and it is a tool used to visualize high-dimensional data by giving each datapoint a location in a two- or three-dimensional map (603). Proposed by Laurens van der Maaten (603), tSNE can be used independently visualize an entire data file in an exploratory manner, as a preprocessing step in anticipation of clustering, or in other related workflows (603,604). The optimization of tSNE-generated parameters is in such a way that data points that were close to one another in the raw high-dimensional data are close in the reduced data space. As an unsupervised learning method, tSNE is commonly used to visualize high-dimensional data and provide crucial intuition in settings where ground truth is unknown. Uniform manifold approximation and projection (UMAP) is a manifold learning technique for dimension reduction constructed from a theoretical framework based in Riemannian geometry and algebraic topology. The outcome of UMAP is a scalable algorithm that applies to the real world. Although both tSNE and UMAP are dimension reduction algorithms, UMAP results in a better visualization quality, as it preserves a more global structure and has a shorter run time. Also, UMAP has no computational restrictions on the embedding dimension, making it viable as a general-purpose dimension reduction technique for machine learning (605). TriMap is a large-scale dimensionality reduction technique using triplets. Unlike tSNE and UMAP, TriMap preserves the global accuracy of the data. TriMap also has a shorter run time compared to tSNE and UMAP (606).

Expression of CD69 by MAIT cells was explored using t-SNE analysis and the quality of tSNE images compared with UMAP and TriMap images. Five independent experiments had either 3 or 4 participants each. PBMCs from each participant were cultured in the presence of TLR7 ligand, TLR8 ligand, PFA-fixed *E. coli*, and PMA/Iono. Expression of CD69 by MAIT cells was analyzed first by cell surface staining, then by flow cytometry.

To compare tSNE analysis in MAIT cells only, with MAIT cells as a subset of all live lymphocytes, analysis was done starting from the MAIT cell population. MAIT cells were concatenated depending on experimental conditions. Three healthy donor PBMC samples were merged to create a single t-SNE map. t-SNE analysis was performed using 1,000 iterations, a perplexity of 30, a trade-off θ of 0.5, and all phenotypic markers listed on table 2.1. Immune cell subsets were identified and manually gated in t-SNE space based on the signal intensity of the phenotypic markers. Although analysis was run on bulk PBMCs, MAIT cells were gated out and CD69 expression on MAIT cells compared between different stimulation conditions. The concatenated events were also used to generate UMAP and TriMap plots as indicated in **Figure 18**. The colour scale was used to compare MFI of CD69 marker. Cells with high MFI for CD69 marker expressed high CD69 and appeared deep orange and moderate to low CD69 appeared green. Cell that did not express CD69 appeared blue on the colour scale.

Among the stimulated cells, MAIT cells appeared to be highly activated upon TLR7 and TLR8 stimulation (cells appeared yellow, orange). Stimulation with *E. coli* led to higher activation as the cells appeared deep red. This observation is similar to a previous observation of high percentage of CD69+MAIT cells and a high expression of CD69 MFI after stimulation. The images obtained by tSNE, UMAP, and TriMap were similar.

Taken together, visually these results confirm that MAIT cells may be highly activated following TLR7 and TLR8 stimulation compared to conventional CD4+ and CD8+ T cells.

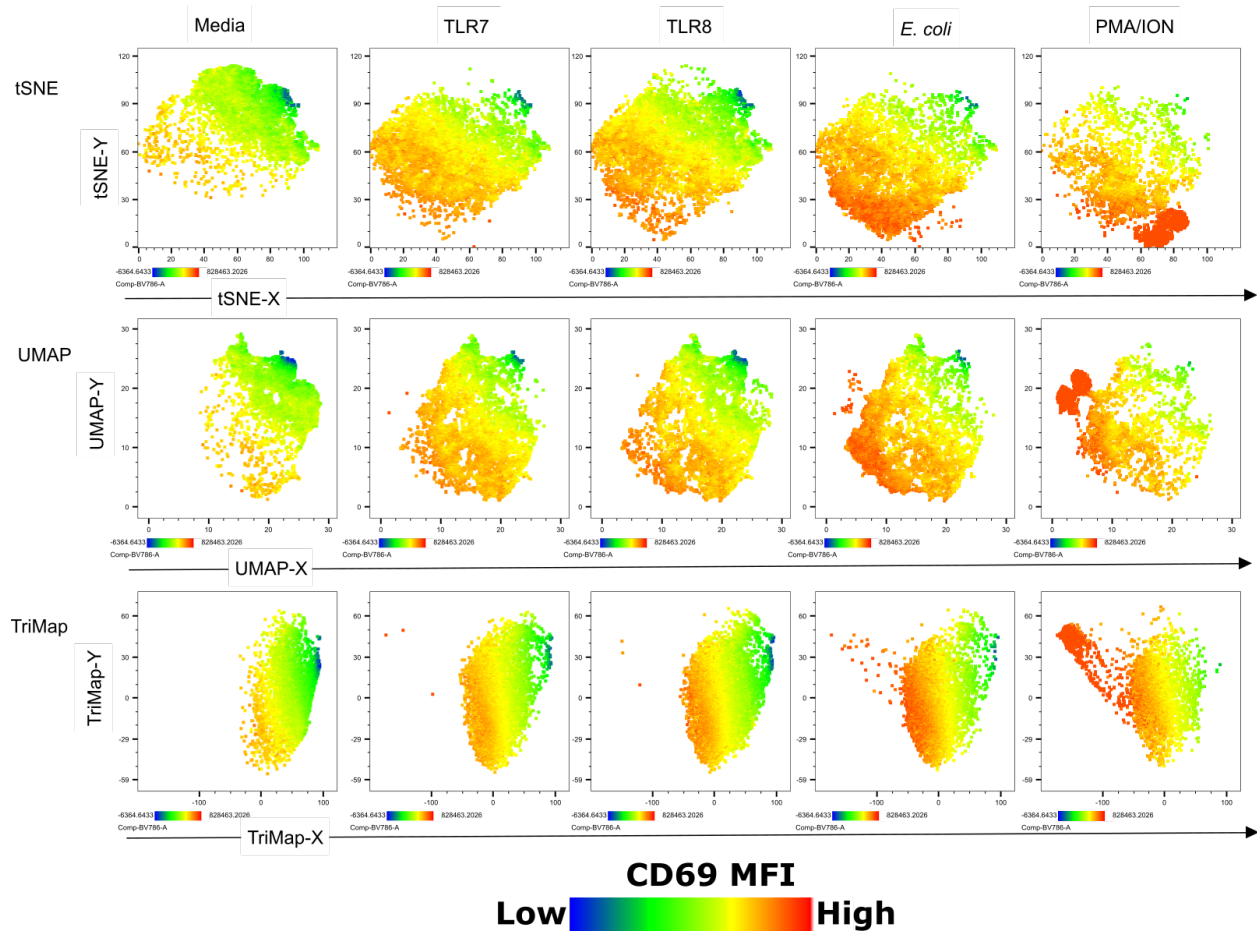


Figure 18. Heterogeneity in MAIT cell activation. Heatmap of MAIT cell expression of CD69 after stimulation represented by t-SNE, UMAP, and TriMap. (A) Top row: MAIT cells manually selected by gating showing heatmap of MAIT cells CD69 expression generated by tSNE. Middle row: UMAP plots showing the heatmap clustering of MAIT cells by CD69 expression. Bottom row: TriMap plots showing the heatmap clustering of MAIT cells by CD69 expression. From left to right columns correspond to TLR7, TLR8, *E. coli* and PMA/ION stimulation. Colour scale indicating low (blue) to high (red) MFI is shown.

4.2.6. MAIT cells express IFN- γ following TLR8 stimulation

MAIT cells express cytokines and other proinflammatory proteins after MR1 binding, direct TLR ligation and/or costimulation. MAIT cells also express receptors for cytokines including IL-12 and IL-18. TLR stimulation may lead to indirect stimulation of MAIT cells via cytokines expressed by APCs. TLR stimulation has also been shown to increase the amount of MR1 at the surface of THP1 but not B cell lines (452), suggesting differential regulation in different cell types. I next sought to understand whether TLR7 and TLR8 stimulation of PBMC led to expression of proinflammatory cytokines by MAIT cells directly, or indirectly.

To assess the effect of TLR7 and TLR8 stimulation on IFN- γ , TNF- α , IL-17a and GM-CSF expression, PBMCs from 16 donors were cultured in R-10 media in the presence of TLR7 ligand (imiquimod), TLR8 ligand (ssRNA40), or PFA-fixed *E. coli* for 24 h or PMA/ION for 14 h. Golgi plug and Golgi stop were added 6 h post TLR7, TLR8, and PFA-fixed *E. coli* stimulation and 2 h post PMA/ION stimulation. Cytokine expression by MAIT cells was assessed by first doing cell surface staining, then permeabilizing the cells and ICS staining with antibodies for IFN- γ , TNF- α , IL-17a and GM-CSF. Stained cells were analyzed by high-dimensional flow cytometry. A comparison of cytokine expression between stimulated and unstimulated PBMCs was analyzed by Wilcoxon sign rank tests.

There was no significant increase in the frequency of IFN- γ ⁺ MAIT cells after TLR7 stimulation with either 1 μ g/mL or 5 μ g/mL of imiquimod ($p > 0.05$). There was also no significant increase in the frequency of IFN- γ ⁺ MAIT cells after TLR8 stimulation with 2.5 μ g/mL of ssRNA40. However, there was a significant increase in the frequency of IFN- γ ⁺ MAIT cells after TLR8 stimulation with 5 μ g/mL of ssRNA40 ($p < 0.0001$). There also was no significant increase in the frequency of IFN- γ ⁺ MAIT cells after stimulation of PBMCs with *E. coli* ($p = 0.7230$). However, there was a significant increase in the frequency of IFN- γ ⁺ MAIT cells after PBMCs stimulation with PMA/Ion ($p < 0.0001$) (**Figure 19a**).

There was no significant increase in the frequency of TNF- α ⁺ MAIT cells after TLR7 stimulation with either 1 μ g/mL or 5 μ g/mL of imiquimod ($p > 0.05$). There was also no significant increase in the frequency of TNF- α ⁺ MAIT cells after TLR8 stimulation with either 2.5 μ g/mL or 5 μ g/mL

of ssRNA40. No significant increase in the frequency of TNF- α + MAIT cells was observed after stimulation of PBMCs with *E. coli* ($p>0.999$). However, there was a significant increase in the frequency of TNF- α + MAIT cells after PBMC stimulation with PMA/ION ($p<0.0001$) (**Figure 19b**).

There was no significant increase in the frequency of IL-17a+ MAIT cells after TLR7 stimulation with either 1 $\mu\text{g/mL}$ or 5 $\mu\text{g/mL}$ of imiquimod, or TLR8 stimulation with either 2.5 $\mu\text{g/mL}$ or 5 $\mu\text{g/mL}$ of ssRNA40 ($p<0.05$). There also was no significant increase in the frequency of IL-17a+ MAIT cells after stimulation of PBMC with *E. coli* ($p=0.2863$). However, there was a significant increase in the frequency of IL-17a+ MAIT cells after PBMC stimulation with PMA/ION ($p=0.0059$) (**Figure 19C**).

There was no significant increase in the frequency of GM-CSF+ MAIT cells after TLR7 stimulation with either 1 $\mu\text{g/mL}$ or 5 $\mu\text{g/mL}$ of imiquimod or TLR8 stimulation with 2.5 $\mu\text{g/mL}$ of ssRNA40 ($p>0.05$). However, there was a significant increase in the frequency of GM-CSF+ MAIT cells after TLR8 stimulation with 5 $\mu\text{g/mL}$ of ssRNA40 ($p<0.0175$). There was no significant increase in the frequency of GM-CSF+ MAIT cells after stimulation of PBMCs with *E. coli* ($p>0.999$). However, there was a significant increase in the frequency of GM-CSF+MAIT cells after PBMCs stimulation with PMA/ION ($p<0.0002$) (**Figure 19D**).

Taken together, these results show that TLR7 stimulation did not lead to increase in the frequency of IFN- γ +, TNF- α +, IL-17a+, or GM-CSF+ MAIT cells within PBMCs. However, TLR8 stimulation led to an increase in frequency of IFN- γ + and GM-CSF+ MAIT cells at the highest concentration tested.

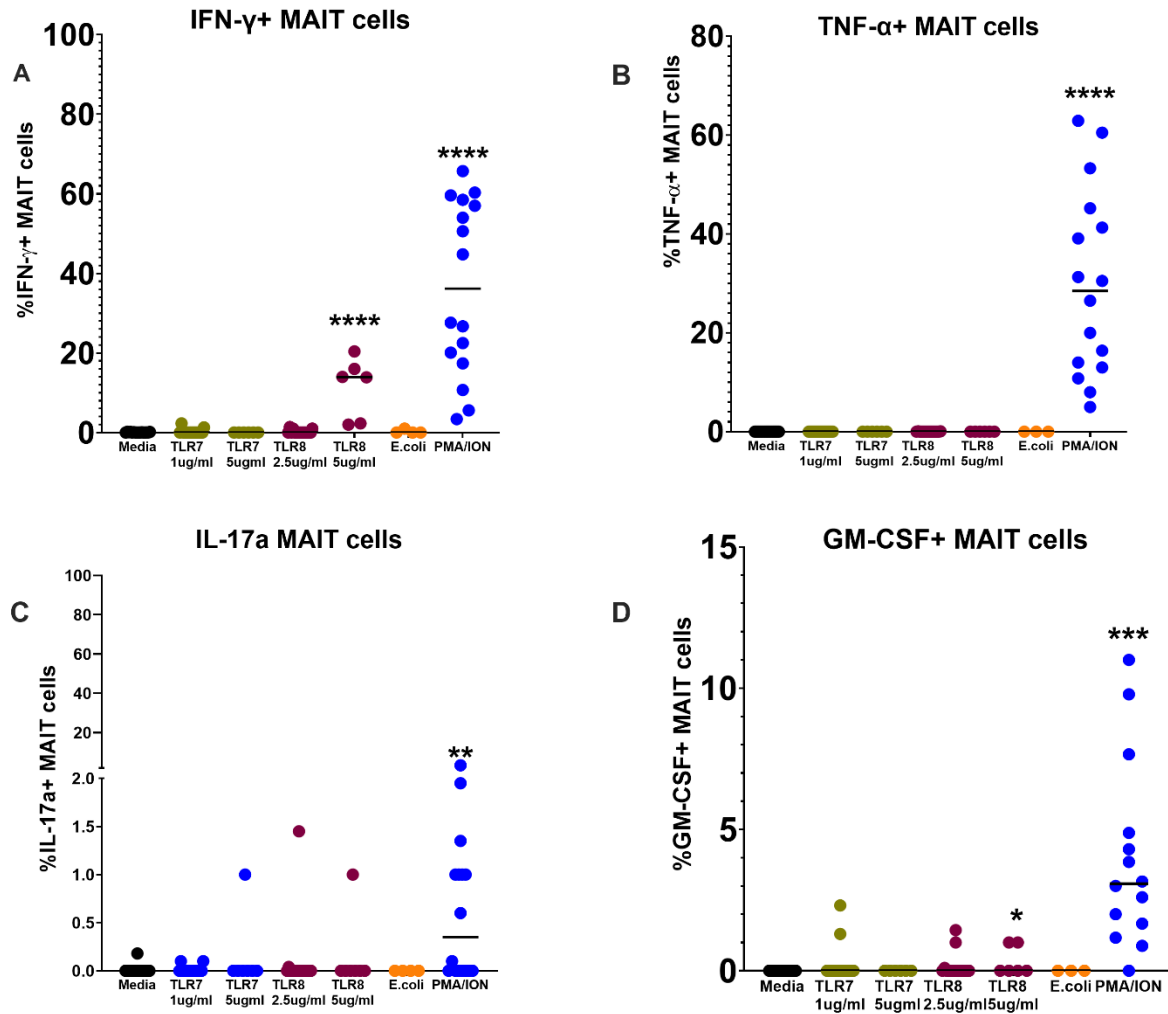


Figure 19. Expression of cytokines by circulating MAIT cells in PBMC after stimulation. Frequency of IFN- γ + (A), TNF- α + (B), IL-17a+ (C), and GM-CSF+ (D) MAIT cells was detected by high-dimensional flow cytometry (gated on CD161++V α 7.2TCR+) 24 h post stimulation by TLR7-ligand, TLR8-ligand, and *E. coli* and 14 h post stimulation with PMA/ION. Each dot represents a single individual. Median are represented by the horizontal bars through the data sets. Analysis was done using Wilcoxon sign rank tests n=16 individuals. For *E. coli* stimulation n=7 individuals **p \leq 0.01, ***p \leq 0.001, ****p \leq 0.0001

4.2.7 Analysis of cytokine expression on MAIT cells by tSNE

Analysis by tSNE enables identification of subsets of cells that are not obvious, making it highly suitable for visually examining complex data. As described, we used tSNE to visualize high-dimensional flow cytometry data, and it revealed heterogeneity in MAIT cell activation after stimulation. In this experiment, tSNE analysis was used to visualize cytokine data by examining the response of MAIT cell cytokine expression to TLR7 and TLR8 stimulation.

Five independent experiments had either 3 or 4 participants each. PBMCs from each participant were cultured in the presence of TLR7 ligand, TLR8 ligand, PFA-fixed *E. coli*, and PMA/ION. Golgi plug, and Golgi stop were added 6 h post TLR7, TLR8, and PFA-fixed *E. coli* stimulation and 2 h post PMA/ION stimulation. Cytokine expression by MAIT cells was assessed by first doing cell surface staining, permeabilizing the cells, and ICS using antibodies for IFN- γ , TNF- α , IL-17a and GM-CSF. Stained cells were analyzed by high-dimensional flow cytometry.

Analysis by tSNE began with the concatenated file of MAIT cells to produce a common dimensionally reduced data space. The tSNE analysis classified cells according to prevalence of cells expressing high or low cytokines. Therefore, events were classified according to mean MFI according to a colour scale, with cells expressing high cytokines appearing deep orange, and low cytokines appearing green. Cells that didn't express any cytokine appeared blue on the colour scale.

From **Figure 20**, it is apparent that TLR7 stimulation and TLR8 stimulation with 2.5 $\mu\text{g}/\text{mL}$ of ssRNA40 did not induce cytokine expression. However, a very small population of orange cells was observed expressing high IFN-levels after TLR8 stimulation with 5 $\mu\text{g}/\text{mL}$ of ssRNA40 (circled in **Figure 20**). This is in line with previous observations. Stimulation with *E. coli* did not appear to lead to expression of IFN- γ , TNF- α , and GM-CSF, but a small population expressed IL-17a (circled in **Figure 20**). PMA/ION stimulation appeared to lead to expression IFN- γ and TNF- α (circled in **Figure 20**). The shape of the heatmap revealed heterogeneity in MAIT cells, as cells with similar characteristics tend to be classified together.

Taken together, these results show that TLR8 stimulation of PBMC with highest dose of ssRNA40 used resulted in a small subset of MAIT cell expressing IFN- γ . A small population of MAIT cells in the PMA/Ion-stimulated PBMCs expressed IFN- γ and TNF- α .

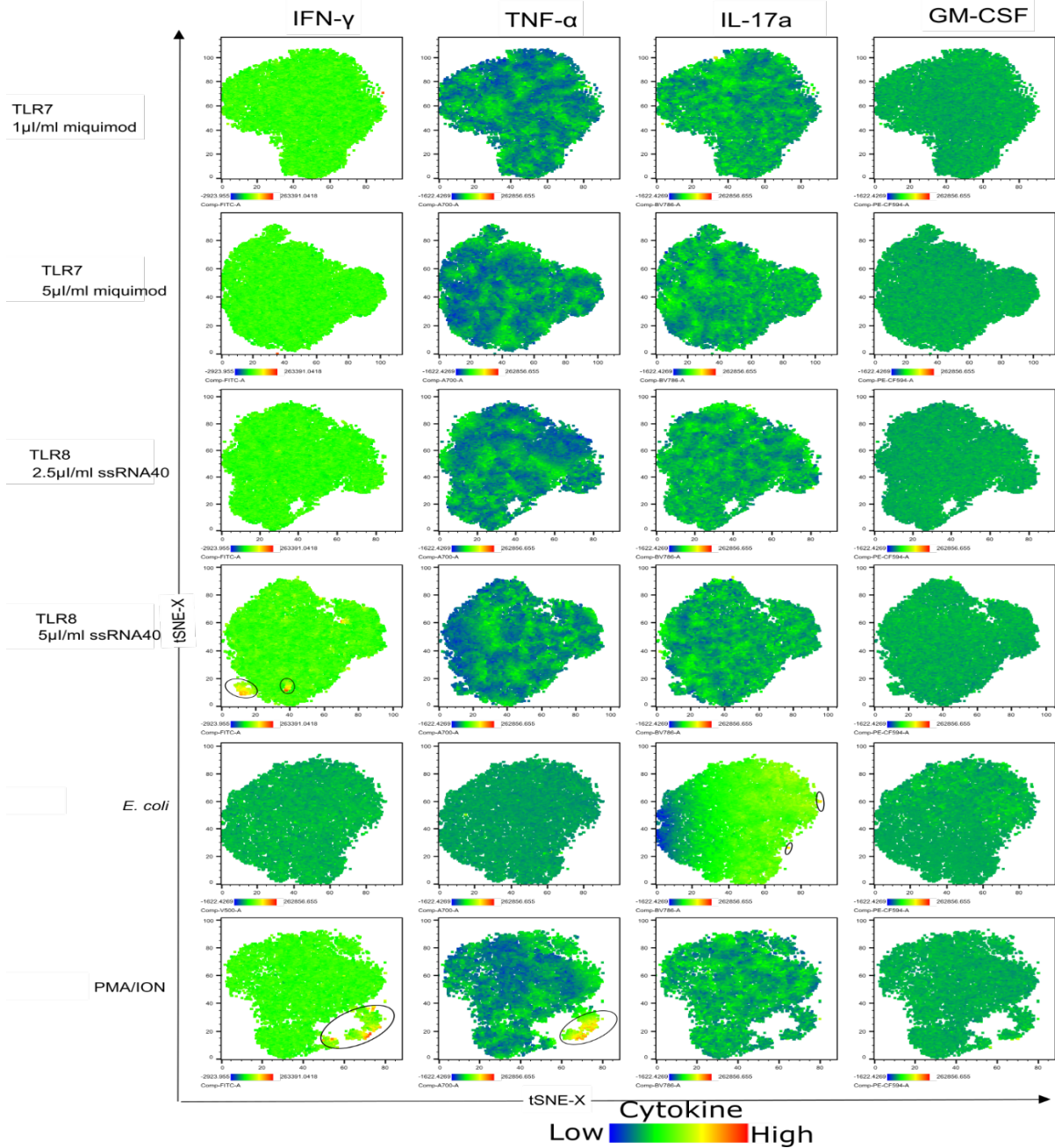


Figure 20. TLR8 stimulation of PBMC with the highest dose of ssRNA40 used resulted in a small subset of MAIT cell expressing IFN- γ . Healthy donor PBMC samples were merged to create a single t-SNE map (n=3). Heatmap of MAIT cells expression of IFN- γ , TNF- α , IL-17a, and GM-CSF. Rows correspond to TLR7-ligand, TLR8-ligand, *E. coli*, and PMA/ION stimulated PBMCs. From left to right, columns show clustering of MAIT cells by IFN- γ , TNF- α , GM-CSF, and IL-17a expression. Circled are a population of cells that appeared to express cytokines: IFN- γ , TNF- α , and IL-17a.

4.3 Time course and establishment of $\gamma\delta$ T cell culture conditions

To establish culture conditions for the TLR stimulation experiments, PBMCs from healthy donors (n=5) were cultured in the presence of imiquimod, ssRNA40, PFA-fixed *E. coli*, and PMA/ION for 2, 6, 14, and 24 h, then stained with antibodies followed by flow cytometry analysis. Differences in the frequency of CD69+ $\gamma\delta$ T cells at different time intervals post stimulation was assessed by Friedman test.

After stimulation of PBMCs with TLR7-ligand, there was no increase in frequency of CD69+ $\gamma\delta$ T cells (p=0.0708). However, the frequency of these cells was significantly higher at 14 h (p=0.0488) compared to 0 h. **(Figure 21A)**. After stimulation of PBMCs with TLR8-ligand, the frequency of CD69+ $\gamma\delta$ T cells increased with time for up to 24 h (p=0.0024). The frequency of these cells was significantly higher at 14 h (p<0.0071) and 24 h (p=0.0055) compared to 0 h. **(Figure 21B)**. After stimulation of PBMCs with *E. coli*, the frequency of CD69+ $\gamma\delta$ T cells increased with time for up to 24 h (p=0.0032). The frequency of these cells was significantly higher at 14 h (p=0.0078) and 24 h (p=0.0052) compared to 0 h. **(Figure 21C)**.

Taken together, these results show that although $\gamma\delta$ T cells were activated following TLR8, and *E. coli* stimulation as seen by the significant increase in the frequency of CD69+ $\gamma\delta$ T cells. The frequency of CD69+ $\gamma\delta$ T cells remains stable between 14 and 24 h post stimulation indicating that $\gamma\delta$ T cells activation can be analysed after 14 h of stimulation.

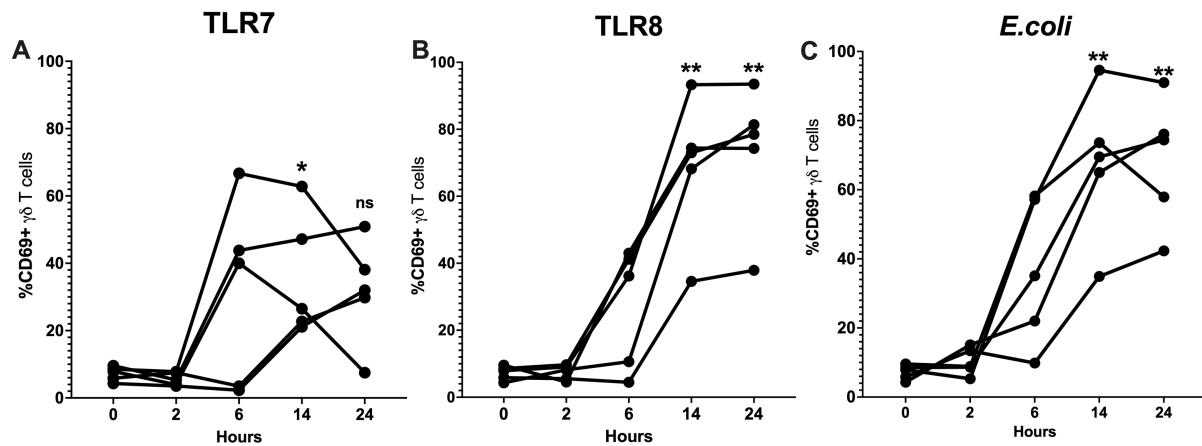


Figure 21. High frequency of CD69+ $\gamma\delta$ T cells after a 14 h stimulation. Frequency of CD69+ $\gamma\delta$ T cells at 2, 6, 14, and 24 h following TLR7 (A), TLR8 (B), and *E. coli* (C) stimulation. Each dot represents frequency of CD69+ $\gamma\delta$ T cells in a single individual. Analysis was done using Friedman tests, Dunn's post-tests were used to indicate what time points were significantly different from baseline. n=5 *p \leq 0.05, **p \leq 0.01

4.3.1. TLR7 and TLR8 lead to activation of $\gamma\delta$ T cells

Based upon the previous experiment, 14 h seemed to be optimal for TLR stimulation. However, I was based in a government lab that required special clearance for foreign-born workers and was therefore only able to reliably access my experiments on Monday to Friday between 8 am and 5 pm. I was also required to have a host to sign me into the lab, escort me and sign me out of the lab. The pandemic made it hard to get an escort due to social distancing and with many people working from home. Furthermore, designing experiments off site was not practical due to the logistics involved in moving the sample. Due to the challenges with lab access and security requirements, it was decided that I should combine MAIT and $\gamma\delta$ T cell culture and analysis with 24 h stimulation for TLR7, TLR8, and *E. coli*, and overnight stimulation for PMA/ION as this would enable me to combine experiments.

In one representative donor, TLR7 stimulation increased the frequency of CD69+ $\gamma\delta$ T cell from a baseline of 1.8% to 19.5%. TLR8 stimulation led to an increase in CD69+ $\gamma\delta$ T cells from 1.8% to 16.6%. Stimulation of PBMC with *E. coli* and PMA/ION increased the frequency of CD69+ $\gamma\delta$ T cells from 1.8% to 57.3% and 87% respectively (**Figure 22A**).

The Wilcoxon signed rank test was used to compare CD69 expression on $\gamma\delta$ T cells between unstimulated vs. stimulated PBMCs in 16 subjects. The median and range frequency of CD69+ $\gamma\delta$ T cells is shown. Stimulation of PBMCs with TLR7 ligand (2%, 11% vs. 23%, 57% $p < 0.0001$), TLR8 ligand (2%, 11%, vs. 20%, 89% $p < 0.0001$), *E. coli* (2%, 11% vs. 62%, 78.9% $p < 0.0001$) and PMA/ION (2%, 11% vs. 84%, 97% $p < 0.0001$) led to a significant increase in CD69+ $\gamma\delta$ T cell frequency (**Figure 22B**). The Wilcoxon test was further used to compare CD69+ MFI between unstimulated vs. stimulated PBMCs in 16 subjects. Stimulation of PBMCs with TLR7 ligand (791, 2102 vs. 2998, 9370 $p < 0.002$), TLR8 ligand (791, 2102 vs. 4675, 30088 $p < 0.0001$), *E. coli* (791, 2102 vs. 17346, 20712 $p < 0.0078$) and PMA/ION (791, 2102 vs. 25220, 145285 $p < 0.0001$) led to a significant increase in CD69 expression by $\gamma\delta$ T cells (**Figure 22C**).

To assess whether high CD69 expression after stimulation was a characteristic of $\gamma\delta$ cells, the frequency of CD69+ conventional CD4+ and CD8+ T cells was compared in PBMC cultured in the presence of TLR7 ligand, TLR8 ligand, or PFA-fixed *E. coli* for 24 h and PMA/ION for 14 h.

As observed previously by Were et al. (unpublished data), TLR7 stimulation led to significant increases in the frequency of CD69+ CD4+ (1%, 3% vs. 2.5%, 16.7% p=0.0021) and CD69+CD8+ T (1%, 14% vs. 4%, 10.2 p<0.0001) cells (**Figure 22D and F**). There was no significant change in the frequency of CD69+ CD4+ T cells following TLR8 stimulation (1%, 3% vs. 1.5%, 14.9 p=0.0723). However, TLR8 stimulation led to a significant increase in the frequency of CD69+ CD8+ T cells (1%, 14% vs. 2%, 33% p<0.0001). The MFI of CD69 expression on CD4+ and CD8+ T cells was compared between unstimulated vs. stimulated PBMCs. Stimulation with TLR7 ligand (554, 1050 vs. 874, 3039 p=0.0052), TLR8 ligand (554, 1050 vs. 1204, 3748 p<0.0013), *E. coli* (554, 1050 vs. 1804, 2806 p=0.0156) and PMA/ION (554, 1050 vs. 15149, 1541141 p=0.0034) led to significant increases in the expression of CD69 on CD4+ T cells (**Figure 22E**). Stimulation with TLR7 ligand (476.5, 888 vs. 911.5, 2733 p=0.0002), TLR8 ligand (476.5, 888 vs. 1110, 2857 p<0.0001), *E. coli* (476.5, 888 vs. 1262, 1607 p=0.0156) and PMA/ION (476.5, 888 vs. 23172, 217507 p=0.0004) led to a significant increase in expression of CD69 on CD8+ T cells (**Figure 22G**).

Taken together, these results show that TLR 7 stimulation of PBMCs led to higher activation of $\gamma\delta$ T cells as determined by the frequency of $\gamma\delta$ T cells that became CD69+ (compared to the minimal activation of CD4+ and CD8+ T cells). TLR8 stimulation also led to high activation of $\gamma\delta$ T cells and minimal activation of CD8+ T cells. Compared to MAIT cells, which were previously reported to have high CD69 MFI after 24 h TLR7 and TLR8 stimulation, $\gamma\delta$ T cells had low CD69 MFI. Stimulation with *E. coli* led to high CD69 MFI compared to stimulation with TLR7-ligand or TLR8-ligand.

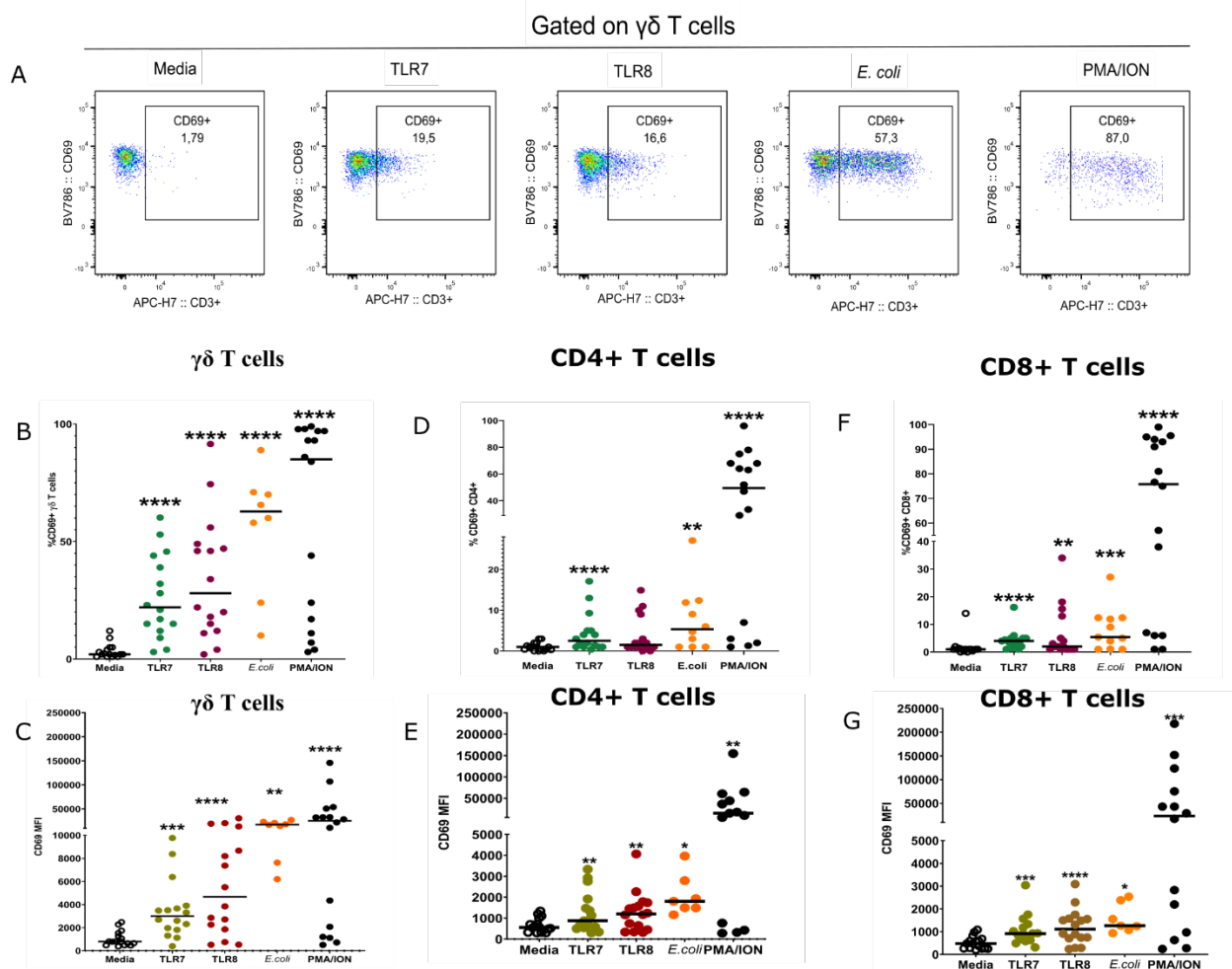


Figure 22. Highly activated $\gamma\delta$ T cells following stimulation compared to CD4 and CD8 cells. (A) Representative flow cytometry plotting showing CD69+ $\gamma\delta$ T cells in unstimulated and after stimulation with TLR7, TLR8, *E. coli* and PMA/ION. (B) Frequency of CD69+ $\gamma\delta$ T cells (C) CD69 expression on $\gamma\delta$ T cells. (D) Frequency of CD69+ CD4+ T cells. (E) CD69 expression on CD4+ T cells. (F) Frequency of CD69+ CD8+ T cells. (G). CD69 expression on CD8+ T cells. Each dot represents a single individual. Horizontal line represents the median. Analysis was done using Wilcoxon tests, n=16 donors. **p \leq 0.01, ***p \leq 0.001, ****p \leq 0.0001.

4.3.2. Analysis of $\gamma\delta$ T cell CD69 expression after stimulation by tSNE

Three healthy donor PBMC samples were merged to create a single t-SNE map. t-SNE analysis was performed using 1,000 iterations, a perplexity of 30, a trade-off θ of 0.5, and all phenotypic markers listed on table 2.1. Immune cell subsets were identified and manually gated in t-SNE space based on the signal intensity of the phenotypic markers. Although analysis was run on bulk PBMCs, $\gamma\delta$ T cells were gated out and CD69 expression on $\gamma\delta$ T cells compared between different stimulation conditions. The concatenated events were also used to generate UMAP and TriMap plots as indicated in **Figure 18**.

The tSNE analysis classified cells according to prevalence of cells expressing high or low CD69. Therefore, in the tSNE analysis, events were classified according to MFI using a colour scale, with cells expressing high CD69 appearing deep orange to yellow on the scale, and low CD69 appearing green. Cells that did not express any CD69 appeared blue (**Figure 23**). The tSNE analysis revealed heterogeneity in $\gamma\delta$ T cell activation after TLR7 and TLR8 stimulation, with some cells expressing high CD69 and others low CD69. There was a population of cells that appeared blue, meaning they were not activated.

Taken together, these results revealed three phenotypically different $\gamma\delta$ T cells: those that expressed high levels, low levels or no CD69. The shape of the graph revealed heterogeneity of $\gamma\delta$ T cells with cells that are phenotypically identical being placed closer together in a 2-dimensional graph.

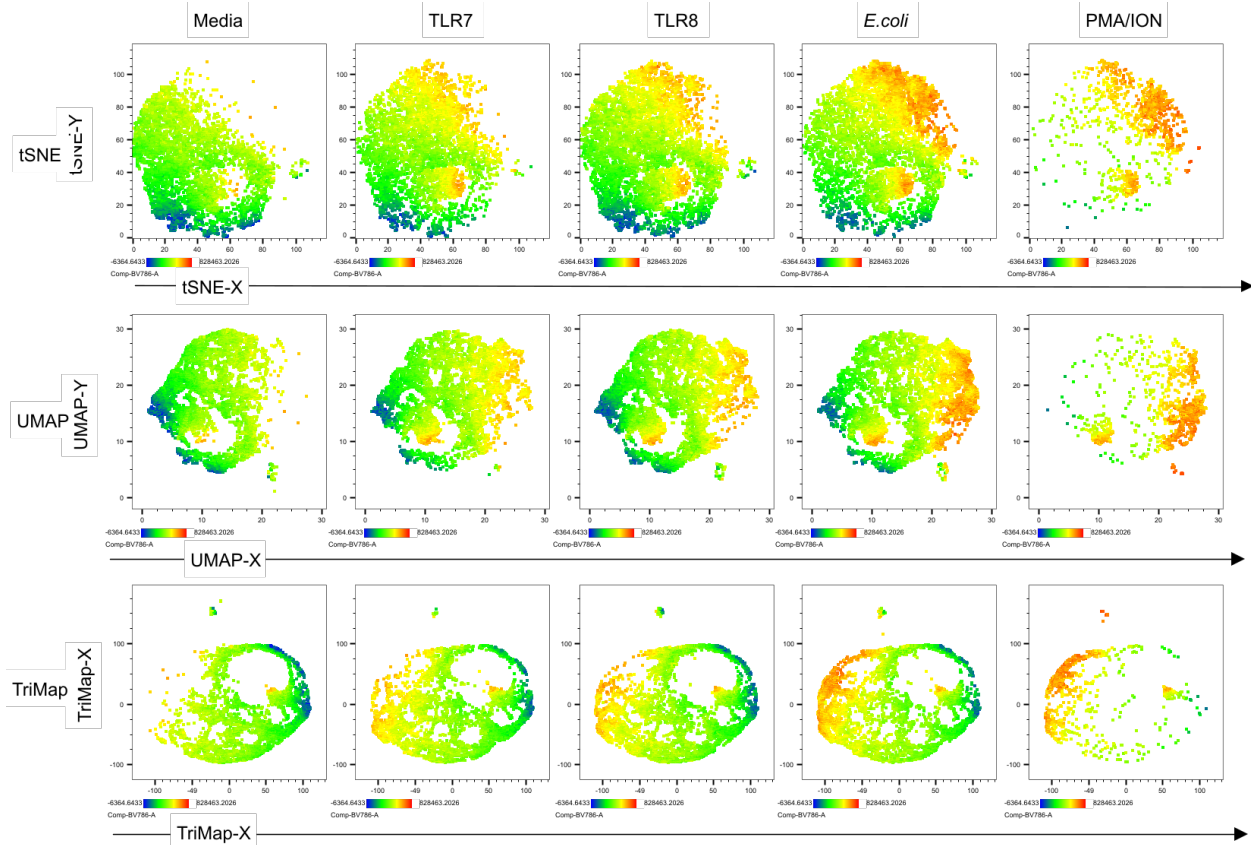


Figure 23. Heterogeneity in $\gamma\delta$ T cells activation. Heatmap of CD69 expression by $\gamma\delta$ T cells after TLR7, TLR8, *E. coli* and PMA/ION stimulation. Selection of $\gamma\delta$ T cells was done manually by gating. Top row heatmap of $\gamma\delta$ T cells CD69 expression generated by tSNE in PBMC cultured in media, or after TLR7, TLR8, *E. coli* and PMA/ION stimulation. Middle row UMAP plots showing the heatmap clustering of $\gamma\delta$ T cells CD69 expression. Bottom row TriMap plots showing the heatmap clustering of $\gamma\delta$ T cells by CD69 expression. Colour scale indicating no (blue) low (green) to high (red) expression of CD69 by $\gamma\delta$ T cells.

4.3.3. TLR8 but not TLR7 stimulates IFN- γ expression by $\gamma\delta$ T cells

In a healthy human peripheral blood, the major subset of $\gamma\delta$ T cells is V γ 9V δ 2, which recognize pyrophosphate intermediates of the eukaryotic and prokaryotic pathways of cholesterol synthesis, collectively termed phosphoantigens (pAg), in a TCR-dependent manner (607,608). Although $\gamma\delta$ T cells have been shown to be involved in the immune response to viruses, intracellular bacteria, and parasitic protozoa (502–506), viruses do not have the non-mevalonate (or Rohmer's) pathway of cholesterol synthesis. Therefore, the $\gamma\delta$ T cell immune response to virus may depend on TLR stimulation directly or indirectly. Activation of $\gamma\delta$ T cells may lead to the expression of proinflammatory cytokines, including TNF- α , IFN- γ , IL-4, IL-6, and cytotoxic molecules, which may increase immune activation. Purified $\gamma\delta$ T cells have been shown to express IFN- γ following TLR8 stimulation. (609).

To assess the effect of TLR7 and TLR8 stimulation on IFN- γ , TNF- α , IL-17a and GM-CSF expression, PBMCs from healthy donors (n=16) were cultured in R-10 media in the presence of TLR7 ligand, TLR8 ligand, PFA-fixed *E. coli* for 24 h and PMA/Iono for 14 h. Golgi plug and Golgi stop were added 6 h post TLR7, TLR8, and *E.coli* stimulation and 2 h post PMA/Iono stimulation. Cytokine expression by $\gamma\delta$ T cells was assessed by first doing cell surface staining, then permeabilizing the cells and ICS with antibodies for IFN- γ , TNF- α , IL-17a and GM-CSF. Stained cells were analyzed by high-dimensional flow cytometry. Cytokine expression between stimulated and unstimulated PBMC was compared by Wilcoxon sign rank tests.

There was no significant increase in frequency of IFN- γ + $\gamma\delta$ T cells following TLR7 stimulation with 1 μ g/mL or 5 μ g/mL of imiquimod and TLR8 stimulation with 2.5 μ g/mL of ssRNA40 ($p>0.05$). However, there was a significant increase in the frequency of IFN- γ + $\gamma\delta$ T cells following TLR8 ($p=0.0009$) stimulation with 5 μ g/mL of ssRNA40. Stimulation of PBMCs with *E. coli* ($p=0.0286$) and PMA/ION ($p<0.0001$) also led to a significant increase in the frequency of IFN- γ + $\gamma\delta$ T cells (**Figure 24A**).

There was no significant increase in the frequency of TNF- α + $\gamma\delta$ T cells following either TLR7 stimulation with 1 μ g/mL or 5 μ g/mL of imiquimod or TLR8 stimulation with 2.5 μ g/mL or

5µg/mL of ssRNA40 ($p > 0.05$). However, stimulation of PBMCs with *E. coli* ($p < 0.0001$) and PMA/ION ($p < 0.0039$) led to significant increase in the frequency of TNF- α + $\gamma\delta$ T cells (**Figure 24B**).

There was no significant increase in the frequency of IL-17a+ $\gamma\delta$ T cells following either TLR7 stimulation with 1µg/mL or 5µg/mL of imiquimod or TLR8 stimulation with 2.5 µg/mL or 5µg/mL ssRNA40 ($p > 0.05$). There was also no significant increase in the frequency of IL-17a+ $\gamma\delta$ T cells following stimulation of PBMCs with *E. coli* ($p = 0.1818$). However, stimulation of PBMCs with PMA/ION ($p < 0.0039$) led to significant increase in the frequency of IL-17a+ $\gamma\delta$ T cells (**Figure 24C**).

There was no significant increase in the frequency of GM-CSF+ $\gamma\delta$ T cells following either TLR7 stimulation with 1µg/mL or 5µg/mL imiquimod or TLR8 stimulation with 2.5 µg/mL or 5µg/mL ssRNA40 ($p > 0.05$). Neither did stimulation of PBMCs with *E. coli* led to significant increase in the frequency of GM-CSF+ $\gamma\delta$ T cells ($p = 0.3860$). However, PMA/ION ($p < 0.0001$) led to a significant increase in the frequency of GM-CSF+ $\gamma\delta$ T cells (**Figure 24D**).

Taken together, these results show that TLR7 stimulation led to activation of $\gamma\delta$ T cells but did not result in cytokine expression. TLR8 stimulation led to activation of $\gamma\delta$ T cells and an increase in frequency of IFN- γ + $\gamma\delta$ T cells.

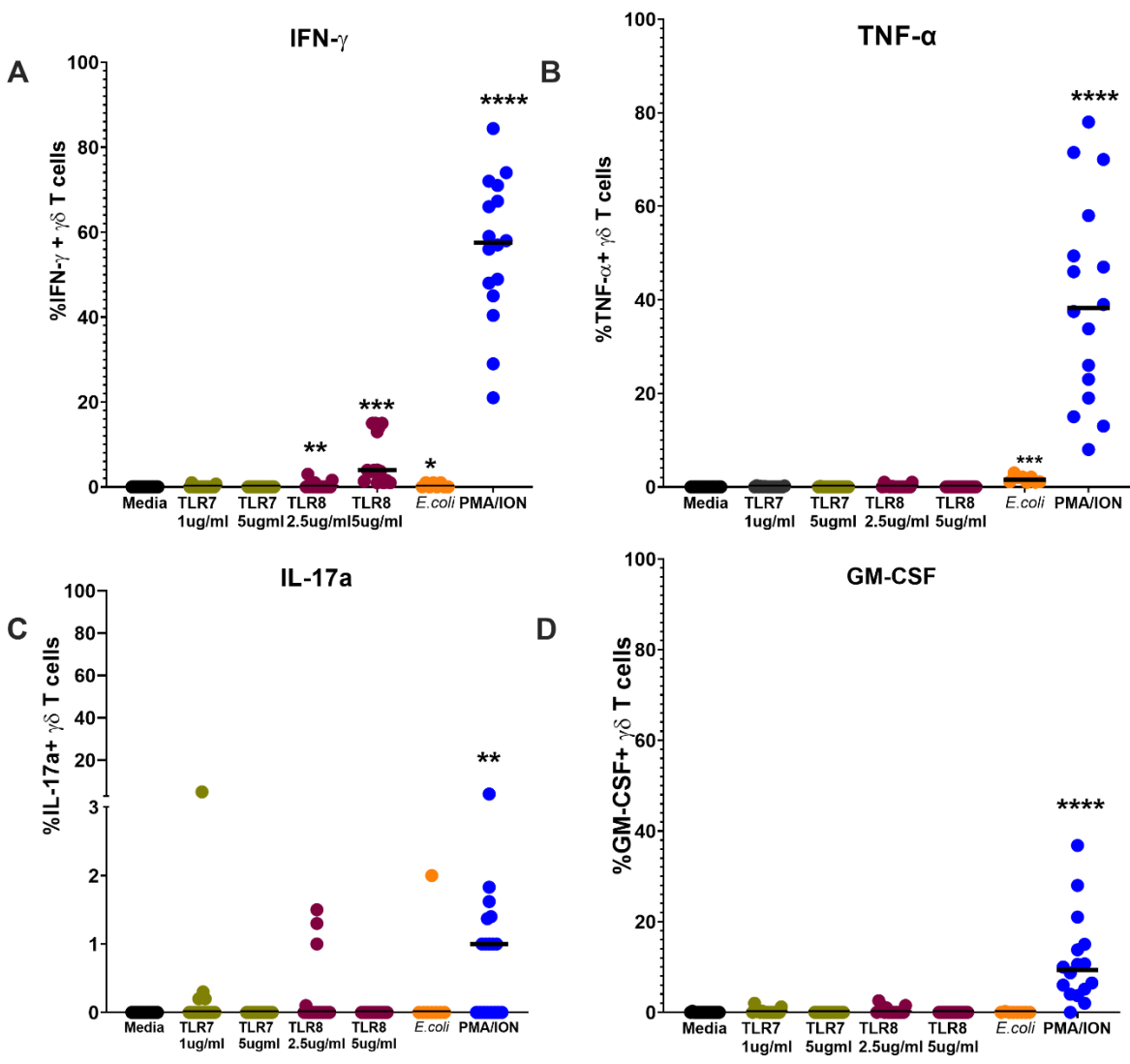


Figure 24. Frequency of $\gamma\delta$ T cells expressing cytokines following stimulation with TLR7-ligand, TLR8-ligand, *E. coli* and PMA/ION. Frequency of IFN- γ + (A), TNF- α + (B), IL-17a+ (C) and GM-CSF+ (D) $\gamma\delta$ T cells after 24 h of TLR7, TLR8, *E. coli* stimulation and after 14 h stimulation with PMA/ION. Each dot represents a single individual. Analysis was done by Wilcoxon signed rank tests, n=16 donor, * $p \leq 0.01$, ** $p \leq 0.001$, *** $p \leq 0.0001$

4.3.4 Analysis of $\gamma\delta$ T cell cytokine expression after stimulation by tSNE

In previous experiments, tSNE was used to visualize high-dimensional flow cytometry data, which revealed activation of $\gamma\delta$ T cells after TLR7/8 stimulation. Here, again tSNE analysis was used to visualize the cytokine data.

The expression of cytokines by $\gamma\delta$ T cells, following stimulation was examined by culturing PBMCs in the presence of TLR7 ligand, TLR8 ligand, PFA-fixed *E. coli* and PMA/ION. Golgi plug and Golgi stop were added 6 h post TLR7, TLR8, and PFA-fixed *E. coli* stimulation and 2 h post PMA/ION stimulation, thereafter, cultured 14 h. Cytokine expression by $\gamma\delta$ T cells was assessed first by cell surface staining and then by ICS after permeabilizing the cells and staining with antibodies for IFN- γ , TNF- α , IL-17a and GM-CSF. Stained cells were analyzed by high-dimensional flow cytometry.

Analysis by tSNE began with all $\gamma\delta$ T cells events. A keyword and code were assigned to each experimental condition. The $\gamma\delta$ T cell population from the study participants was concatenated depending on the experimental condition. The concatenated file was loaded into existing space and tSNE analysis performed on the concatenated file to produce a common dimensionally reduced data space. Gating was used to pull apart the concatenated file into stimulated and unstimulated data and compare how each sample is represented in the dimensionally reduced data space. A heatmap plot for a single experiment (n=4) showing $\gamma\delta$ T cell cytokine expression is shown in **Figure 25**.

From **Figure 25**, neither TLR7 stimulation nor TLR8 stimulation with 2.5 $\mu\text{g}/\text{mL}$ of ssRNA40 appear to have led to expression of IFN- γ , TNF- α , IL-17a or GM-CSF. The tSNE analysis revealed very small population of cells that expressed IFN- γ after TLR8 stimulation with 5 $\mu\text{g}/\text{mL}$ of ssRNA40 (**circled in Figure 25**). However, $\gamma\delta$ T cells did not appear to express TNF- α , IL-17a or GM-CSF after TLR8 stimulation with 5 $\mu\text{g}/\text{mL}$ of ssRNA40. Although IFN- γ and TNF- α expression was previously reported after stimulation with *E. coli*, no IFN- γ or TNF- α secreting cells were observed in this tSNE analysis. Similar to previous observations, a small population of $\gamma\delta$ T cells that expressed IFN- γ , TNF- α and GM-CSF after stimulation with PMA/ION was observed (**circled in Figure 25**).

Taken together, these results show that TLR8 stimulation of PBMC with a high dose of ssRNA40 resulted in a small subset of $\gamma\delta$ T cell expression of IFN- γ . Also, a very small subset of $\gamma\delta$ T cells stimulated with PMA/ION appeared to express IFN- γ , and TNF- α (**Figure 25**).

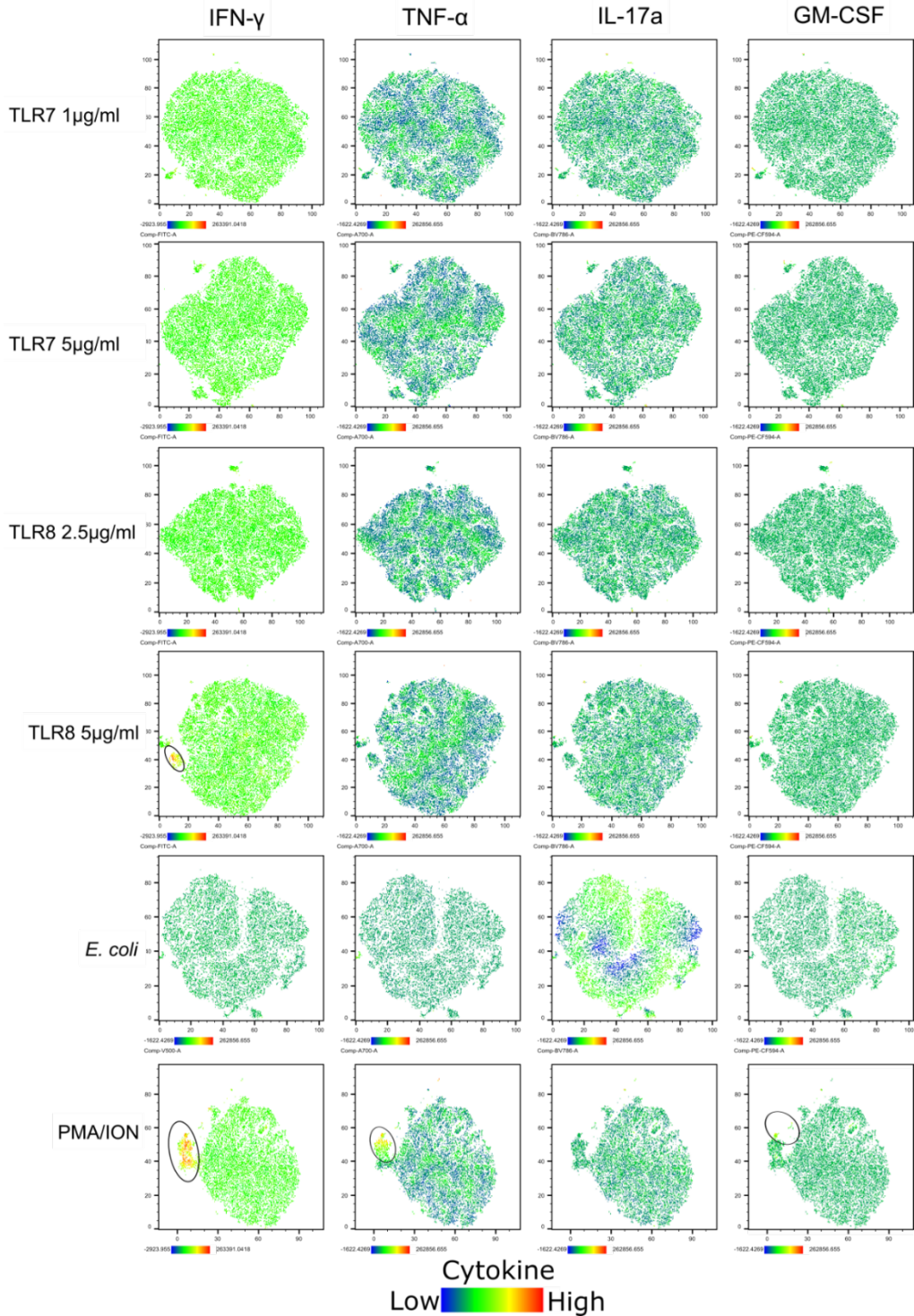


Figure 25. TLR8 stimulation of PBMC with highest dose of ssRNA40 used resulted in a small subset of $\gamma\delta$ T cells expressing IFN- γ . Heatmaps of $\gamma\delta$ T cells expression of IFN- γ , TNF- α , IL-17a, and GM-CSF in stimulated cells. Rows correspond to TLR7, TLR8, *E. coli*, and PMA/ION stimulated PBMCs. From left to right, columns show clustering of $\gamma\delta$ T cells by IFN- γ , TNF- α , GM-CSF, and IL-17a expression in stimulated cells. The colour scale corresponds to MFI. Circled are a population of cells that appeared to express cytokines: IFN- γ , TNF- α , and GM-CSF.

4.4 MAIT cells supplemented with IL-7 express high IFN- γ , TNF- α , IL-17a and GM-CSF after TLR8 stimulation

IL-7 is a cytokine that is mainly produced by epithelial and stromal cells, and it functions in regulating homeostasis, proliferation and survival of T cells (610,611). IL-7 signals through IL7R, a heterodimer composed of IL7R α (CD127) and the common cytokine receptor γ -chain (γ c) also known as CD132 (612). High expression of IL7R is linked to inflammatory diseases including rheumatoid arthritis (613), inflammatory bowel disease, type 1 diabetes (614,615) multiple sclerosis (616), colitis (617,618) systemic lupus erythematosus (619), and primary Sjögren's syndrome (620). Stimulation with IL-7 has been shown to restore the frequency of MAIT cells expressing cytolytic molecules like granzyme B and perforin (621,622). Use of IL-7 alongside antiretroviral therapy was also reported to increase the number and frequency of MAIT cells in the peripheral blood of patients chronically infected with HIV (623).

To assess cytokine expression by MAIT and $\gamma\delta$ T cells following TLR7 and TLR8 stimulation in media supplemented with IL-7, PBMCs from healthy donors (n=7) were cultured in the presence of TLR7-ligand, TLR8-ligand, PFA-fixed *E. coli*, and PMA/ION in R10 media supplemented with 20 IU of IL-2 and 10 ng/mL of IL-7. Golgi plug and Golgi stop were added 6 h post TLR7, TLR8, and *E. coli* stimulation and 2 h post PMA/ION stimulation, thereafter, cultured 14 h after golgi plug/stop. Cytokine expression by MAIT cells and $\gamma\delta$ T cells was assessed by first doing cell surface staining, then permeabilizing the cells and ICS staining with antibodies for IFN- γ , TNF- α , IL-17a, and GM-CSF. Stained cells were analyzed by flow cytometry. The Wilcoxon signed rank test was used to compare cytokine expression on MAIT cells between unstimulated vs. stimulated PBMCs in media supplemented with IL-7.

There was no significant increase in the frequency of IFN- γ +, TNF- α +, IL-17a+ or GM-CSF+ MAIT cells after TLR7 stimulation ($p > 0.05$ for all) (**Figure 26, A–D**). However, TLR8 stimulation led to significant increase in the frequency of IFN- γ + ($p = 0.0156$), TNF- α + ($p = 0.0210$), IL-17a+ ($p = 0.0312$), and GM-CSF+ ($p = 0.0156$) MAIT cells.

Taken together, these results show that IL-2 and IL-7 supplementation may increase frequency of IFN- γ +, TNF- α +, IL-17a+ and GM-CSF+ MAIT cells after TLR8 stimulation, but not after TLR7 stimulation.

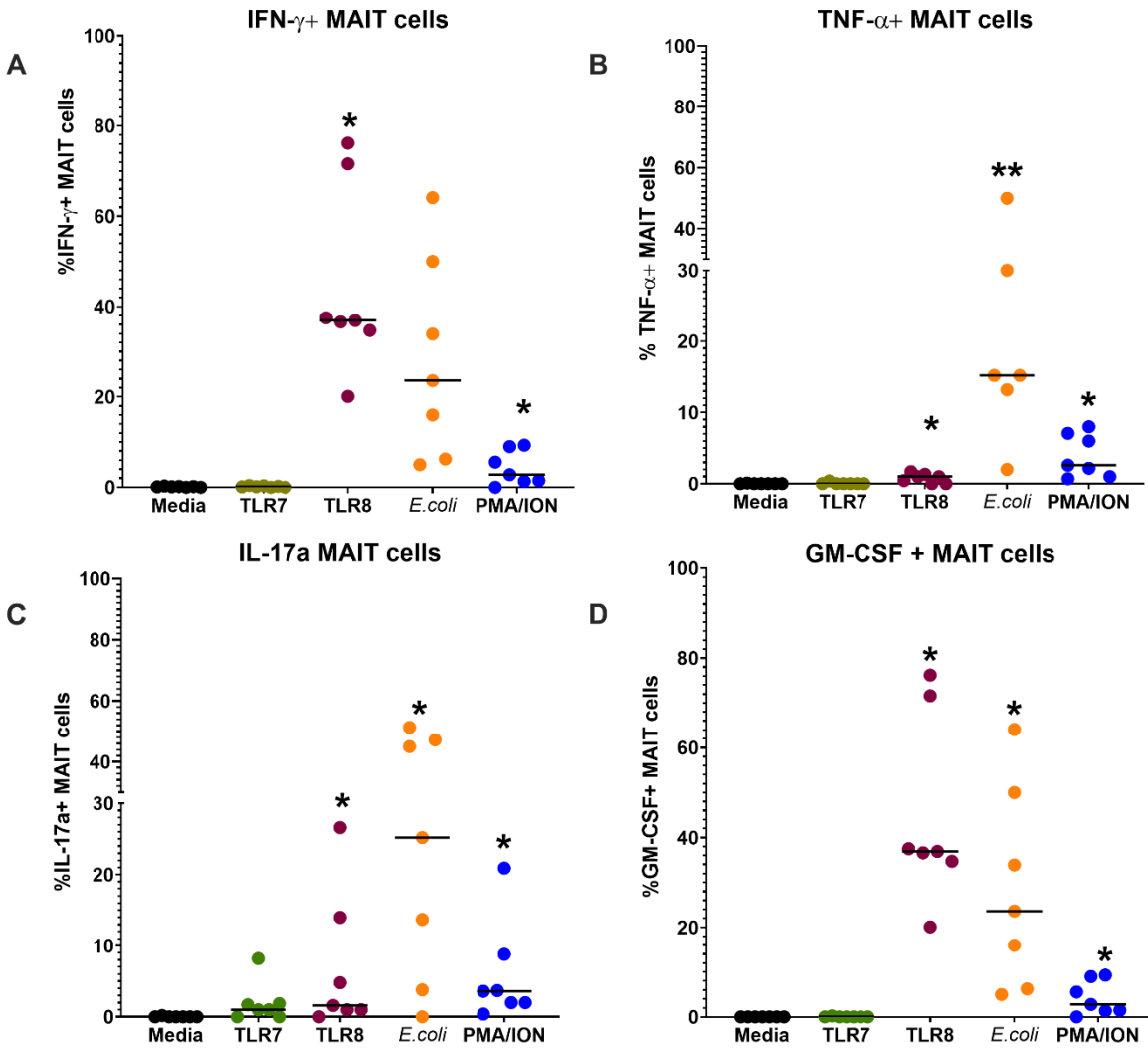


Figure 26. Increased frequency of IFN- γ + IL-17a, and GM-CSF+ MAIT cells after TLR8 stimulation. Frequency of IFN- γ + (A), TNF- α + (B), IL-17a+ (C) and GM-CSF+ (D) MAIT cells after a 24 h stimulation of TLR7, TLR8, and stimulation with *E. coli* and 14 h stimulation with PMA/ION. Each dot represents a single individual. Horizontal line represents median. Analysis was done using Wilcoxon sign rank test, n=7 *p \leq 0.05, **p \leq 0.01.

4.4.1 $\gamma\delta$ T cells in media supplemented with IL-7 express high IFN- γ , IL-17a, and GM-CSF after TLR8 stimulation

A significant increase in the frequency of IFN- γ ⁺, TNF α ⁺, IL-17a⁺ or GM-CSF⁺ $\gamma\delta$ T cells following TLR7 stimulation was not observed ($p > 0.0500$). There was also no significant increase in the frequency of TNF- α ⁺ $\gamma\delta$ T cells after TLR8 stimulation ($p = 0.0625$). However, TLR8 stimulation led to a significant increase in the frequency of IFN- γ ⁺ ($p = 0.0156$), IL-17a⁺ ($p = 0.0312$) and GM-CSF⁺ ($p = 0.0312$) $\gamma\delta$ T cells (**Figure 27**).

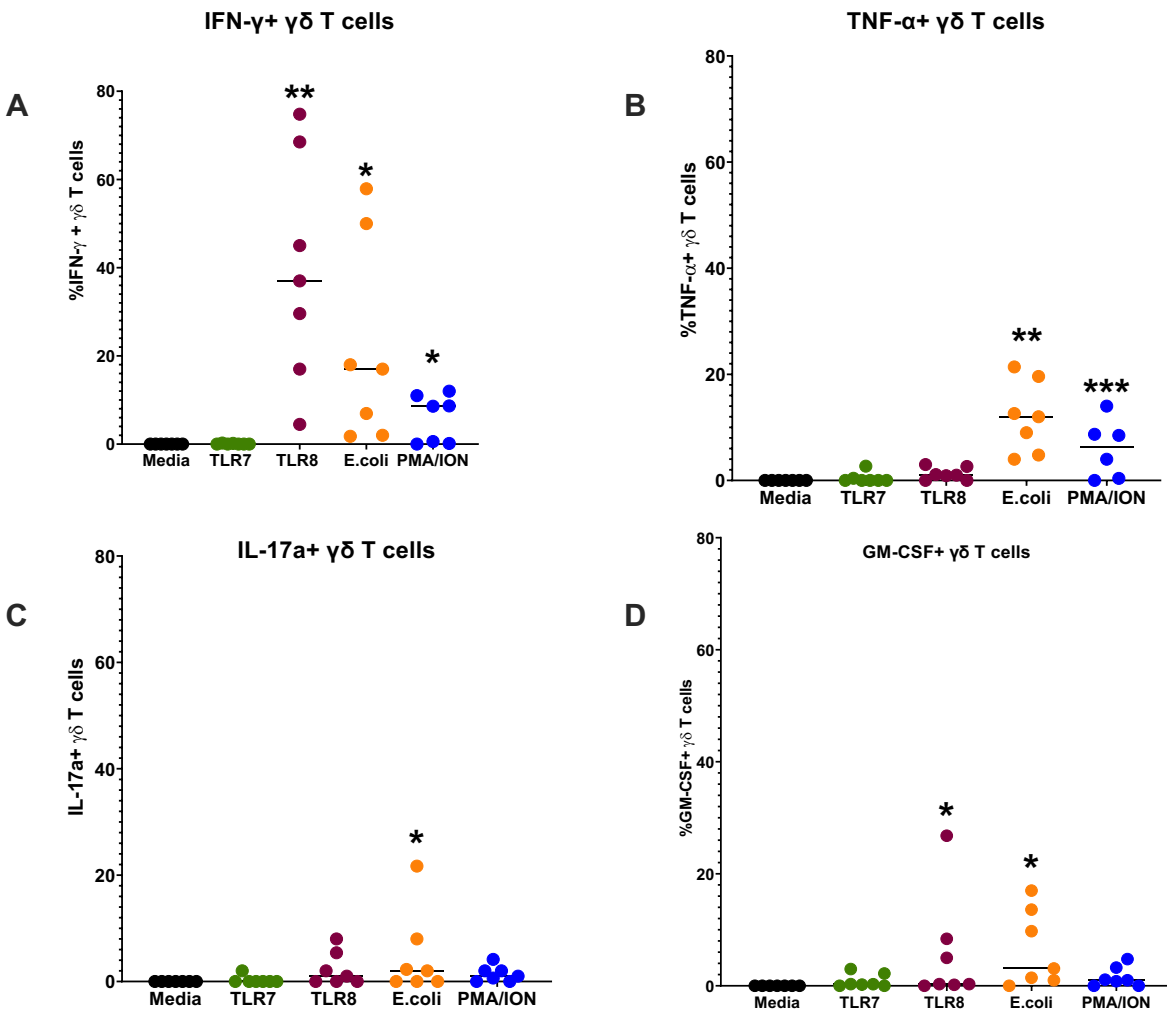


Figure 27. Increased frequency of IFN- γ and GM-CSF+ $\gamma\delta$ T cells following TLR8 stimulation. Frequency of IFN- γ + (A), TNF- α + (B), IL-17a+ (C) and GM-CSF+ (D) $\gamma\delta$ T cells after 24 h stimulation of TLR7, TLR8, and stimulation with *E. coli* and 14 h stimulation with PMA/ION. Each dot represents a single individual. Horizontal line represents medians through the data sets. Analysis was done using Wilcoxon sign rank tests on n=7 donors *p \leq 0.05, **p \leq 0.01, ***p \leq 0.001.

4.4.2 MAIT and $\gamma\delta$ T cells cultured in media supplemented with IL-7 express higher levels of IFN- γ , IL-17a, and GM-CSF after TLR8 stimulation compared to conventional CD4+ and CD8+ T cells

To determine if IL-7 supplementation increased the responsiveness of TLR7- and TLR8-induced cytokine responses, unsupplemented media alone and TLR7 and TLR8 stimulation in media supplemented with IL-7 were compared. Conventional CD4 and CD8 T cells cytokine response was also included in the analysis.

There was no significant increase in the frequency of IFN- γ +, TNF α +, or GM-CSF+ MAIT cells after TLR7 stimulation ($p > 0.05$ for all) (**Figure 28 A**). However, there was 150-fold higher frequency of IL-17a+ MAIT cells in PBMCs cultured in media supplemented with IL-7 than in PBMCs cultured in media alone following TLR7 ($p = 0.012$) stimulation. The frequency of IFN- γ + MAIT cells was 3-fold higher ($p \leq 0.0001$), TNF- α + MAIT cells 600-fold higher ($p = 0.0010$), IL-17a+ MAIT cells 69-fold higher, ($p = 0.0004$) and GM-CSF+ MAIT cells 264-fold higher ($p = 0.0010$) in PBMC supplemented with IL-7 compared to media alone after TLR8 stimulation. Also, stimulation of PBMCs with *E. coli* led to a higher frequency of IFN- γ + ($p = 0.0061$), TNF- α + ($p = 0.0119$), IL-17a+ ($p = 0.0273$), and GM-CSF+ ($p < 0.0001$) MAIT cells in media supplemented with IL-7 compared to media alone. However, the frequency of IFN- γ + MAIT cells was 6-fold lower ($p = 0.0002$) and TNF- α + MAIT cells 7-fold lower ($p < 0.0001$) in PBMCs supplemented with IL-7 compared to media alone after PMA/ION stimulation. The frequency of IL-17a+ MAIT cells was 7-fold higher in PBMCs supplemented with IL-7 compared to media alone after PMA/ION stimulation ($p = 0.0014$). However, there was no significant difference in the frequency of GM-CSF+ MAIT cells between with and without media supplementation after PMA/ION stimulation ($p = 0.9282$) (**Figure 28**)

No significant difference in the frequency of IFN- γ +, TNF- α +, IL-17a+, and GM-CSF+ $\gamma\delta$ T cells was observed between PBMCs cultured in media with or without IL-7 after TLR7 stimulation ($p > 0.05$). The frequency of IFN- γ + $\gamma\delta$ T cells was 5-fold higher ($p < 0.0001$), TNF- α + $\gamma\delta$ T cells 11-fold higher ($p = 0.0025$), IL-17a+ $\gamma\delta$ T cells 10-fold higher ($p > 0.0188$) and GM-CSF+ $\gamma\delta$ T cells 14-fold higher ($p = 0.0105$), with IL-7 supplementation compared to media alone, after TLR8 stimulation. Furthermore, the frequency of IFN- γ + $\gamma\delta$ T cells was 43-fold higher ($p = 0.0061$), TNF-

$\alpha+\gamma\delta$ T cells 7-fold higher ($p>0.0061$), and GM-CSF⁺ $\gamma\delta$ T cells 65-fold higher ($p>0.0273$) after stimulation with *E. coli* with IL-7 supplementation compared to media alone. However, there was no significant difference in the frequency of IL-17a⁺ $\gamma\delta$ T cells between PBMCs cultured in media with or without IL-7 after stimulation with *E. coli* ($p>0.4242$). The frequency of IFN- γ ⁺ $\gamma\delta$ T cells was 8-fold higher ($p<0.0001$), TNF- α ⁺ $\gamma\delta$ T cells 5-fold higher ($p>0.0034$) and GM-CSF⁺ $\gamma\delta$ T cells 6-fold higher in PBMCs cultured in media without IL-7 than in PBMCs cultured in media with IL-7 after stimulation with PMA/Iono. There was also no significant difference in the frequency of IL-17a⁺ $\gamma\delta$ T cells with or without IL-7 supplementation after stimulation with PMA/ION ($p>0.4692$) (**Figure 28**).

There was no significant increase in the frequency of IFN- γ ⁺, TNF α ⁺, IL-17⁺, or GM-CSF⁺ CD4⁺ T cells after TLR7 stimulation ($p>0.05$ for all) (**Figure 28**). The frequency of IFN- γ ⁺ CD4⁺ T cells was significantly higher within PBMC cultured in media supplemented with IL-7 than media alone after TLR8 stimulation ($p=0.011$). However, there was no significant increase in the frequency of TNF α ⁺, IL-17⁺, or GM-CSF⁺ CD4⁺ T cells after TLR8 stimulation ($p>0.05$ for all). There was no significant increase in the frequency of IFN- γ ⁺, TNF α ⁺, IL-17⁺, or GM-CSF⁺ CD4⁺ T cells after stimulation with *E. coli* ($p>0.05$ for all). The frequency of IFN- γ ⁺ CD4⁺ T cells was 10-fold higher ($p=0.0002$), TNF- α ⁺ CD4⁺ T cells 65-fold higher ($p>0.0004$), and GM-CSF⁺ CD4⁺ T cells was 22-fold higher ($p=0.0007$) *without* IL-7 supplementation than with IL-7 after stimulation with PMA/Iono. However, there was also no significant difference in the frequency of IL-17a⁺ CD4⁺ T cells between PBMCs cultured in media with or and PBMC cultured in media without IL7 after stimulation with PMA/ION ($p>0.1215$) (**Figure 28**).

There was no significant increase in the frequency of IFN- γ ⁺, TNF α ⁺, IL-17⁺, or GM-CSF⁺ CD8⁺ T cells after TLR7 stimulation ($p>0.05$ for all). The frequency of IFN- γ ⁺ CD8⁺ T cells was significantly higher with IL-7 supplementation than without after TLR8 stimulation ($p<0.0001$). However, there was no significant increase in the frequency of TNF α ⁺, IL-17⁺, or GM-CSF⁺ CD8⁺ T cells after TLR8 stimulation ($p>0.05$ for all). The frequency of IFN- γ ⁺ CD8⁺ T cells was significantly higher with IL-7 supplementation than without after stimulation with *E. coli* ($p=0.0242$). However, there was no significant increase in the frequency of TNF α ⁺, IL-17⁺, or GM-CSF⁺ CD8⁺ T cells after stimulation with *E. coli* ($p>0.05$ for all). The frequency of IFN- γ ⁺

CD8⁺T cells was 24-fold higher ($p=0.0002$), and TNF- α ⁺ CD8⁺ T cells 16-fold higher ($p>0.0001$) without IL-7 than with IL-7 after stimulation with PMA/Iono. However, there was also no significant difference in the frequency of GM-CSF⁺ CD8⁺ T and IL-17a⁺ CD8⁺ T cells with or without IL-7 supplementation after stimulation with PMA/ION ($p>0.05$ for all) (**Figure 28**).

Taken together, these results show greater increase in the frequency of IFN- γ ⁺, TNF- α ⁺, IL-17⁺ and GM-CSF⁺ MAIT cells and in the frequency of IFN- γ ⁺ $\gamma\delta$ T cells after stimulation compared to conventional T cells in IL-7 supplemented media.

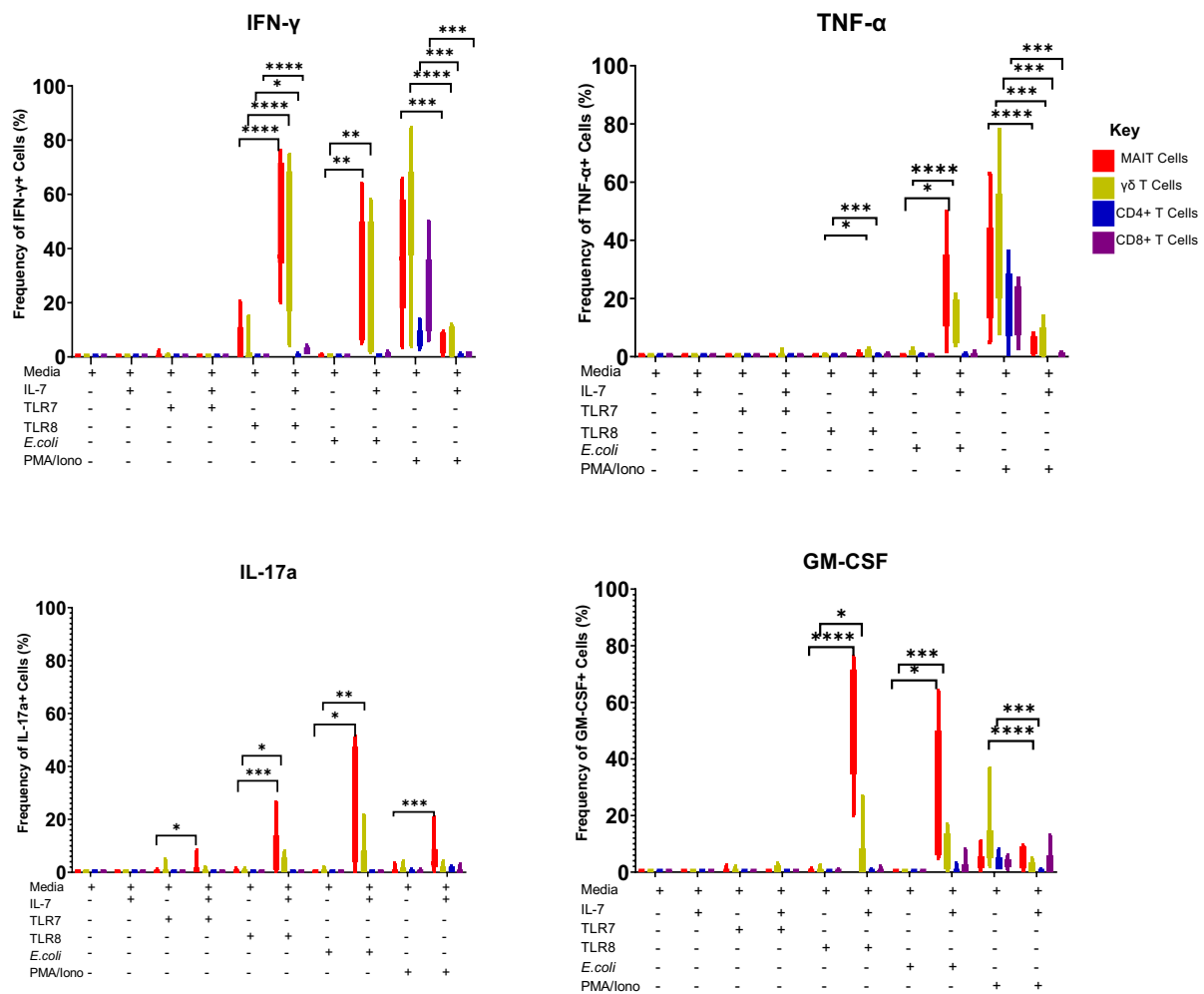


Figure 28. MAIT cells and $\gamma\delta$ T cells express higher IFN- γ , TNF- α , IL-17a and GM-CSF following stimulation compared to conventional T cells. Frequency of IFN- γ + (A), TNF- α +, (B) IL-17a (C), and GM-CSF+ (D) cells. Statistical analyses comparing frequency of cytokine secreting between cells cultured with or without IL-7 was performed using Mann–Whitney U tests, Bars represent interquartile ranges from 7 individual in media supplemented with IL-7 and 16 individuals in media alone. * $p \leq 0.05$, ** $p \leq 0.01$, *** $p \leq 0.001$ **** $p \leq 0.0001$

4.4.3. Analysis of cytokine expression by MAIT cells by tSNE

The response of MAIT cells and $\gamma\delta$ T cells, cytokine expression after TLR7 and TLR8 stimulation was examined by culturing PBMC in the presence of TLR7 ligand, TLR8 ligand, PFA-fixed *E. coli* and PMA/ION in media containing IL-7. Golgi plug and Golgi stop were added 6 h post TLR7, TLR8, and PFA-fixed *E. coli* stimulation and 2 h post PMA/ION stimulation, and thereafter cultured 14 h. Cytokine expression by MAIT cells was assessed first by cell surface staining, then by permeabilizing the cells and ICS with antibodies for IFN- γ , TNF- α , IL-17a, and GM-CSF. Stained cells were analyzed by high-dimensional flow cytometry.

MAIT and $\gamma\delta$ T cells were gated on after first gating on live cells, singlets and T cells. Beginning with MAIT cells, tSNE analysis was done by downsampling to standardize the number of events to be used and to normalize the number of events contributed from each file to the total concatenated file. A keyword was assigned and the experimental condition coded. The individual samples were concatenated into a single file depending on the experimental condition and loaded into existing space. tSNE analysis was performed on the concatenated file to produce a common dimensionally reduced data space. Gating was used to pull apart the concatenated file into individual samples and compare how each of those samples was represented in the dimensionally reduced data space.

This tSNE analysis classified cells according MAIT cells cytokine expression after stimulation. Therefore, events were classified according to MFI and using a colour scale, with cells expressing high cytokine appearing deep orange and low cytokines appearing green. Cells with no cytokine expression appeared blue. tSNE revealed heterogeneity in MAIT cells: cells that were phenotypically similar were close together while those that were phenotypically different were far apart. In media supplemented with IL-2 and IL-7. TLR7 stimulation did not to stimulate expression of cytokines by MAIT cells. However, a population of MAIT cells expressed IFN- γ after both TLR8 and *E. coli* stimulation. A very small subset of MAIT cells appeared to express TNF- α after stimulation with *E. coli*. Contrary to the increase in IFN- γ +, IL-17a+, and GM-CSF+ after TLR8 stimulation that was observed previously, tSNE analysis revealed only high IFN- γ expression after TLR8 stimulation.

Taken together, these results show that MAIT cells activated by TLR ligation appeared to be heterogeneous. TLR8 stimulation resulted in expression of IFN- γ by MAIT cells. MAIT cells from *E. coli* stimulated PBMCs expressed IFN- γ , TNF- α , and GM-CSF (**Figure 29**).

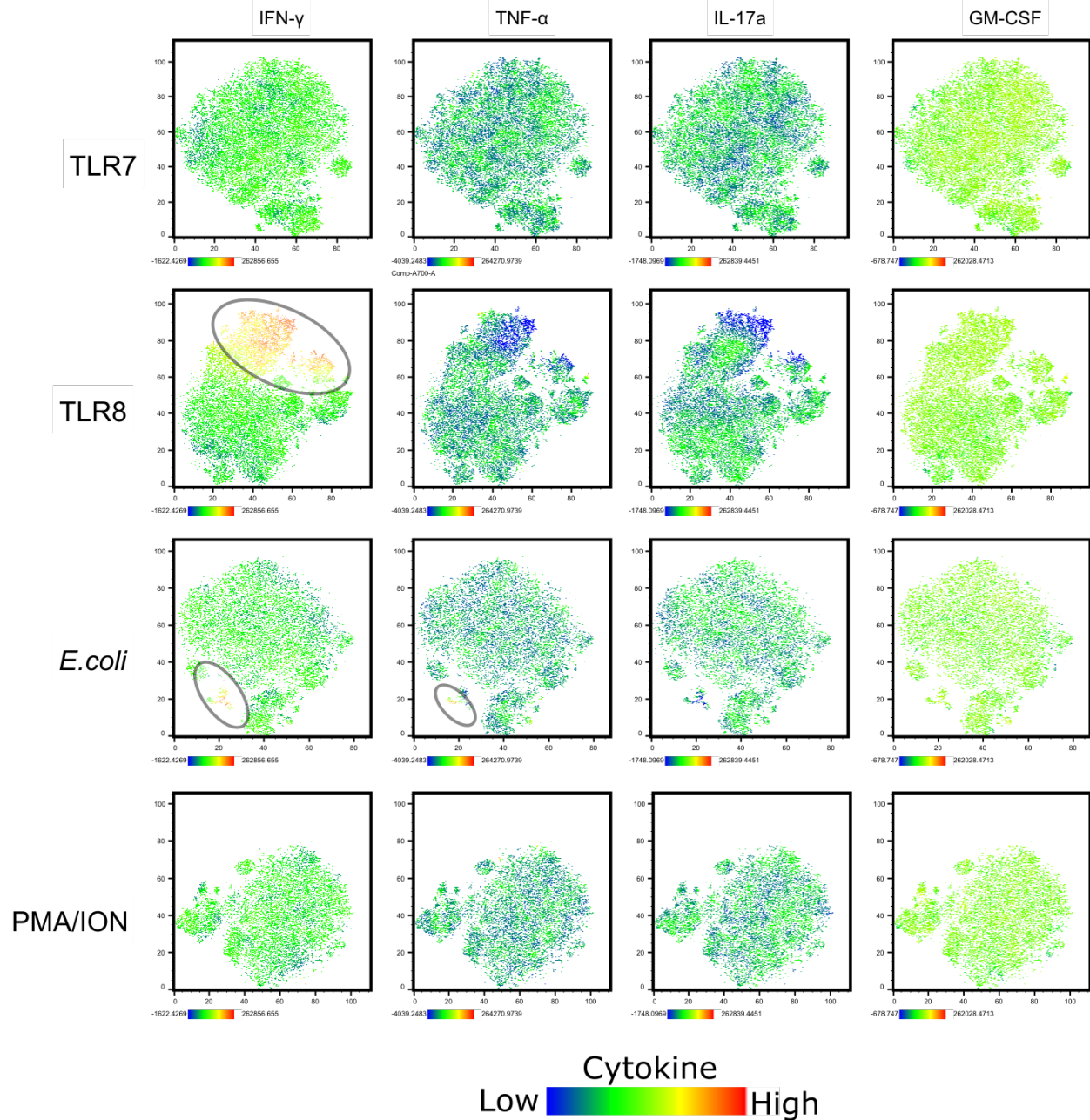


Figure 29. Heatmaps of tSNE analysis of MAIT cells cytokine expression after stimulation. Rows correspond to TLR7, TLR8, *E. coli*, and PMA/ION stimulated PBMCs. From left to right, columns show clustering of MAIT cells by IFN- γ , TNF- α , GM-CSF, and IL-17a expression in both stimulated and unstimulated cells. The colour scale corresponds to mean fluorescence intensity (MFI). Circled are a population of cells that appeared to express IFN- γ and TNF- α .

4.4.4 Analysis of $\gamma\delta$ T cells cytokine expression by tSNE

Next, tSNE analysis was done on $\gamma\delta$ T cells. Gating was used to pull apart the concatenated file into individual samples and compare how each of those samples are represented in the dimensionally reduced data space. The tSNE analysis classified the $\gamma\delta$ T cells according to phenotypic characteristics. A heatmap with colour scale was used to assess cytokine expression by the $\gamma\delta$ T cells, with cells expressing high cytokine appearing deep orange and low cytokines appearing green. Cells with no cytokine expression appeared blue.

Presented are heatmaps of tSNE analysis for one experiment (n=4). The shape of the tSNE heatmaps revealed heterogeneity in the $\gamma\delta$ T cell subset. Similar to previous observation, in media supplemented with IL-2 and IL-7, TLR7 stimulation did not lead to expression of cytokines. A population of $\gamma\delta$ T cells expressed IFN- γ after TLR8 stimulation and after stimulation with *E. coli* (**circled in Figure 30**). A small population of $\gamma\delta$ T cells expressed TNF- α after *E. coli* stimulation (**circled in Figure 30**) in the tSNE analysis.

Taken together, these results show that TLR8 stimulation resulted in IFN- γ expression by $\gamma\delta$ T cells (**Figure 30**).

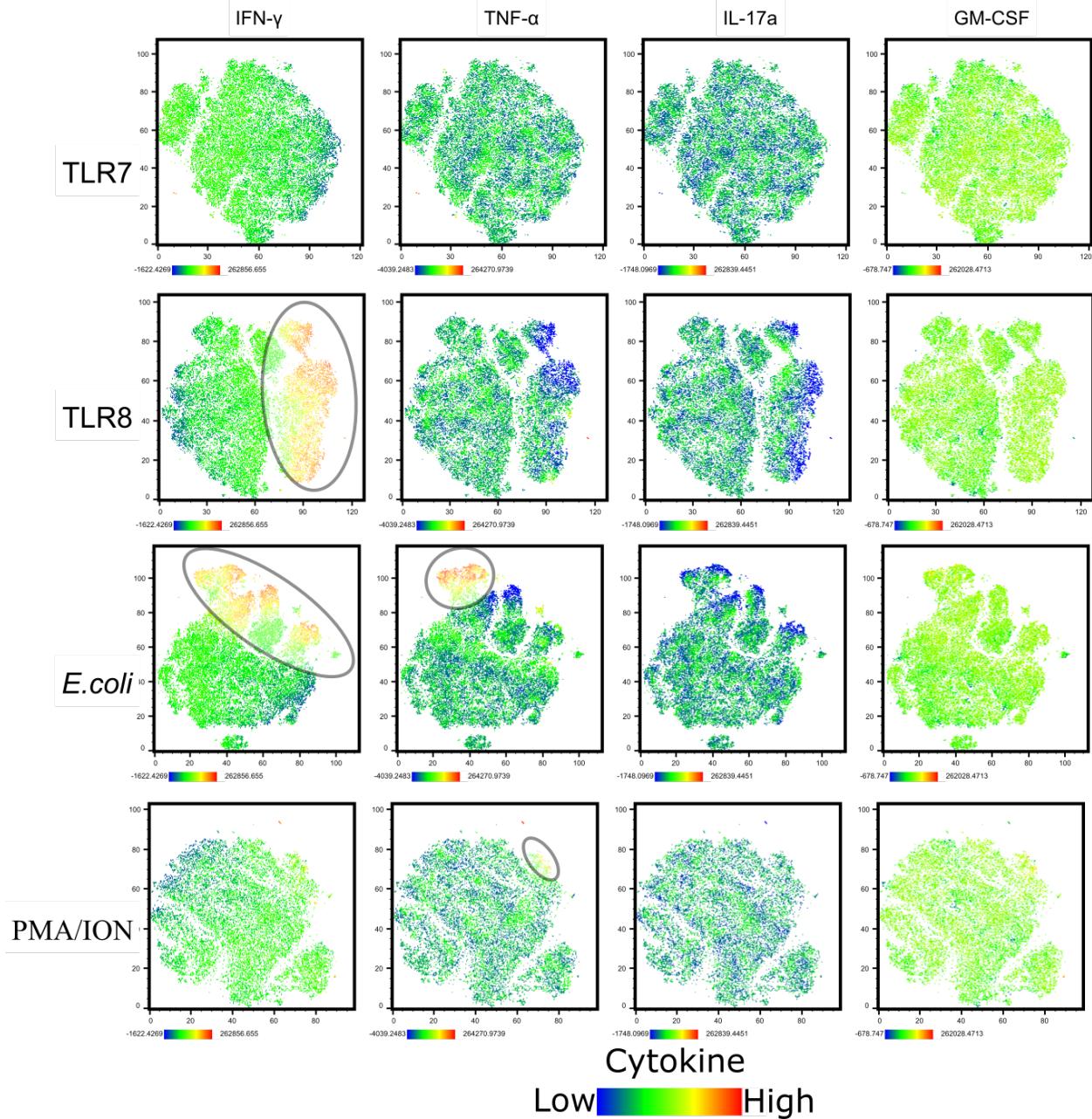


Figure 30. Heatmap of tSNE analyses of $\gamma\delta$ T cells cytokine expression after stimulation. The tSNE analyses show IFN- γ , TNF- α , GM-CSF, and IL-17a expression by $\gamma\delta$ T cells. Rows correspond to TLR7, TLR8, *E. coli*, and PMA/ION stimulated PBMCs. From left to right, columns show clustering of $\gamma\delta$ T cells by IFN- γ , TNF- α , GM-CSF, and IL-17a expression in both stimulated and unstimulated cells. The colour scale corresponds to MFI. Circled are a population of cells that expressed IFN- γ and TNF- α .

4.4.5 Frequency of IFN- γ +, TNF- α +, IL-17a+ and GM-CSF+ $\gamma\delta$ T cells by different subsets of $\gamma\delta$ T cells in IL-7 supplemented media

Expression of CD161 molecules has been observed in cells with a memory phenotype and tissue-homing characteristics and that express high IL-17 and other proinflammatory cytokines (624–626). Thus, cells expressing high CD161 may be important in the mucosal immune response and immune activation. Given our previous observation that IL-7 boosted cytokine expression by $\gamma\delta$ T cells, the frequency of IFN- γ +, TNF- α +, IL-17a+ and GM-CSF+ $\gamma\delta$ T cells by different subsets of $\gamma\delta$ T cells was assessed.

PBMCs from healthy donors (n=7) were cultured in R-10 media supplemented with IL-7, in the presence of TLR7-ligand, TLR8-ligand, PFA-fixed *E. coli*, and PMA/ION. Golgi plug and Golgi stop were added 6 h post TLR7, TLR8, PFA-fixed *E. coli* stimulation and 2 h post PMA/ION stimulation, and thereafter cultured 14 h. Cells were assessed by first doing cell surface staining, then permeabilizing the cells and ICS with antibodies for IFN- γ , TNF- α , IL-17a and GM-CSF. Stained cells were analyzed by high-dimensional flow cytometry. The frequency of IFN- γ +, TNF- α +, IL-17a+ and GM-CSF+ $\gamma\delta$ T cells by different subsets of $\gamma\delta$ T cells after stimulation of PBMC was analyzed by Mann–Whitney U tests.

There was no significant difference in IFN- γ +, TNF- α +, GM-CSF+ and IL-17a+ $\gamma\delta$ T cell between $\gamma\delta$ TCR^{high} and $\gamma\delta$ TCR^{low} $\gamma\delta$ T cells after TLR7 (p>0.05 for all) stimulation. Although the frequency of $\gamma\delta$ -TCR^{high} IFN- γ + cells showed a non-significant trend towards being higher compared to $\gamma\delta$ -TCR^{low} IFN- γ + after TLR8 stimulation (p=0.0583). There was no significant difference in the frequency of IFN- γ +, TNF- α +, GM-CSF+ and IL-17a+ $\gamma\delta$ T cells between $\gamma\delta$ -TCR^{high} and $\gamma\delta$ -TCR^{low} cells after stimulation with *E. coli* or PMA/ION (p>0.05 for all) (**Figure 31A**).

There was no significant difference in the frequency of IFN- γ +, TNF- α +, GM-CSF+ and IL-17a+ between CD161+ and CD161- $\gamma\delta$ T cells after TLR7, or TLR8 (p>0.05 for all) stimulation. There was no significant difference in the frequency IFN- γ +, TNF- α +, GM-CSF+ and IL-17a+ CD161+ and CD161- $\gamma\delta$ T cells after stimulation with *E. coli* or PMA/ION (p>0.05 for all) (**Figure 31B**).

Taken together, these results show that there is no significant difference between the frequency of IFN- γ +, TNF- α +, IL-17a+ and GM-CSF+ $\gamma\delta$ T cells in $\gamma\delta$ TCR^{high} and $\gamma\delta$ -TCR^{low} or in CD161+ and CD161- $\gamma\delta$ T cells.

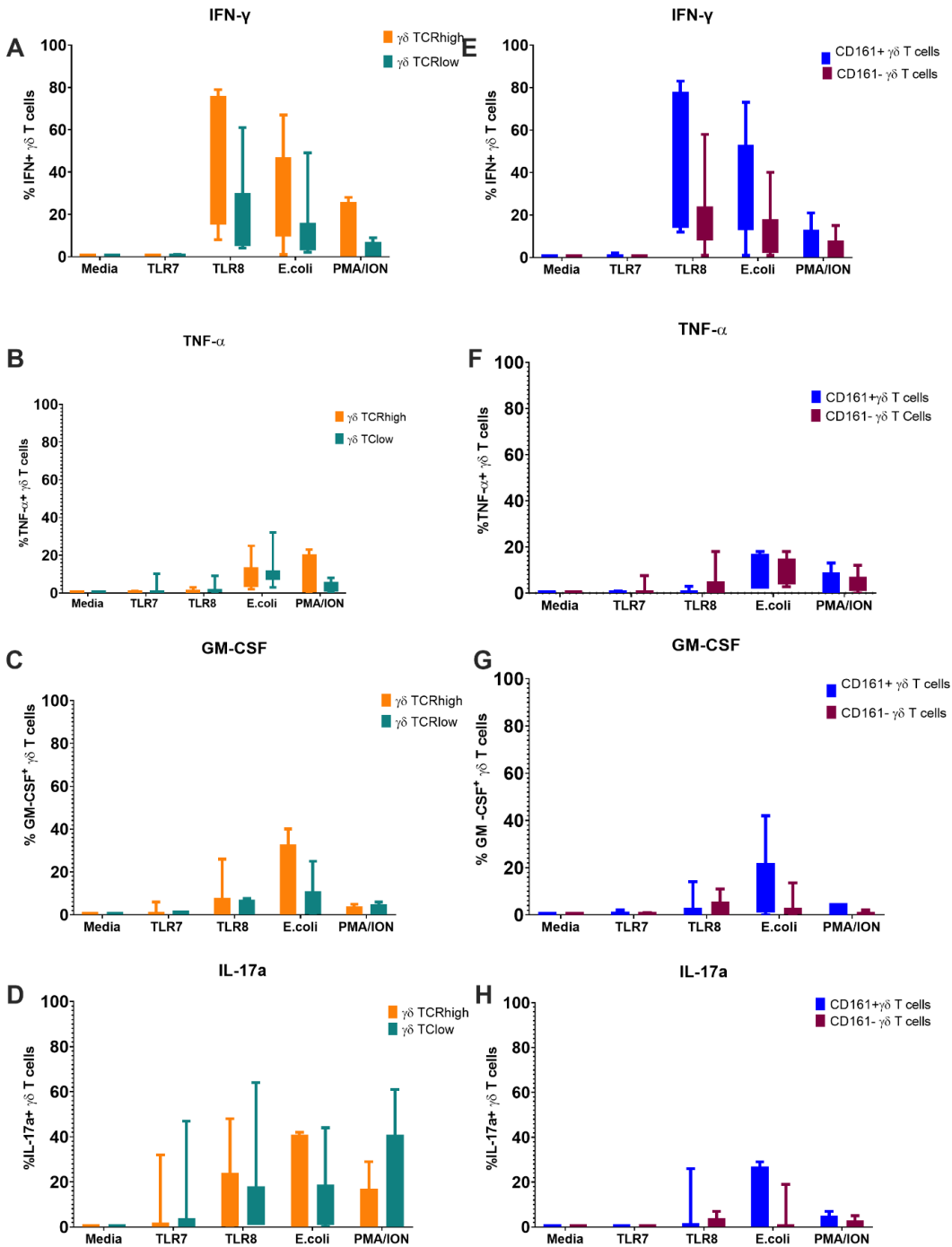


Figure 31 No significant increase in IFN- γ +, TNF- α +, IL-17a+ or GM-CSF+ $\gamma\delta$ TCR^{High}+, $\gamma\delta$ TCR^{low} or CD161+ and CD161- $\gamma\delta$ T after TLR8 stimulation. Frequency of (A) IFN- γ +, (B) TNF- α +, (C) IL-17a+, and (D) GM-CSF+ c vs. $\gamma\delta$ TCR^{low} T cells. Frequency of (E) IFN- γ +, (F) TNF- α +, (G) IL-17a+ and (H) GM-CSF+ CD161+ $\gamma\delta$ T cells vs. CD161- $\gamma\delta$ T cells. Bars represent interquartile range from 7 individuals, n=7. Analysis was performed using Mann-Whitney U test *P<0.05

4.4.6 Frequency of CD69+ $\gamma\delta$ T cells in different subsets of $\gamma\delta$ T cells

Previously, two subsets of $\gamma\delta$ T cells (i.e., $\gamma\delta$ TCR^{high} and $\gamma\delta$ TCR^{low} had been described (**Figure 16**). Furthermore, it had been shown that the majority $\gamma\delta$ TCR^{high} cells were CD161+ whereas this was not the case for $\gamma\delta$ TCR^{low} cells. Expression of CD161 on T cells has been associated with high activation and expression of proinflammatory cytokines (627). To assess the difference in activation of $\gamma\delta$ TCR^{high} and $\gamma\delta$ TCR^{low} or CD161+ $\gamma\delta$ T cells and CD161- $\gamma\delta$ T cells, the frequency of CD69+, $\gamma\delta$ TCR^{high}, CD69+ $\gamma\delta$ TCR^{low} and frequency of CD161+ or CD161- $\gamma\delta$ T cells subsets were compared by Mann–Whitney U tests. Median and IQR of frequency of D69+ $\gamma\delta$ T cells was reported.

No significant difference in the frequency of CD69+ $\gamma\delta$ T cells was observed between $\gamma\delta$ TCR^{low} and $\gamma\delta$ TCR^{high} in the media (2.5%, 12% vs. 3.5%, 26% p= 0.5532), after either TLR7 (10.5%, 58% vs. 11%, 63% p=0.2732), TLR8 (35%, 78.5% vs. 51.5%, 93% p=0.1119) *E. coli* (42%, 64% vs. 61.5%, 82% p=0.1683) or PMA/ION (64%, 87.7% vs. 39%, 88% p=0.3399) stimulation (**Figure 32A**).

However, there was a significant difference in frequency of CD69+ $\gamma\delta$ T cells between CD161+ and CD161- $\gamma\delta$ T cells in the media control (3%, 6% vs. 1%, 8% p= 0.0005), after either TLR7 (15%, 46% vs. 1%, 5% p<0.0001), TLR8 (35%, 85% vs. 1%, 16% p=0<0.0001), or PMA/ION (59%, 72% vs. 4.5%, 66% p=0.0002) stimulation (**Figure 32B**). No significant difference in the frequency of CD69+ $\gamma\delta$ T cells was observed between CD161+ $\gamma\delta$ TCR and CD161- $\gamma\delta$ TCR after *E. coli* stimulation (48%, 87% vs. 8%, 85% p=0.2213).

Taken together, these results show that there were no significant differences in activation between $\gamma\delta$ TCR^{high} and $\gamma\delta$ -TCR^{low} cells. However, CD161+ $\gamma\delta$ T cells are more highly activated compared to CD161- following TLR7 or TLR8 stimulation.

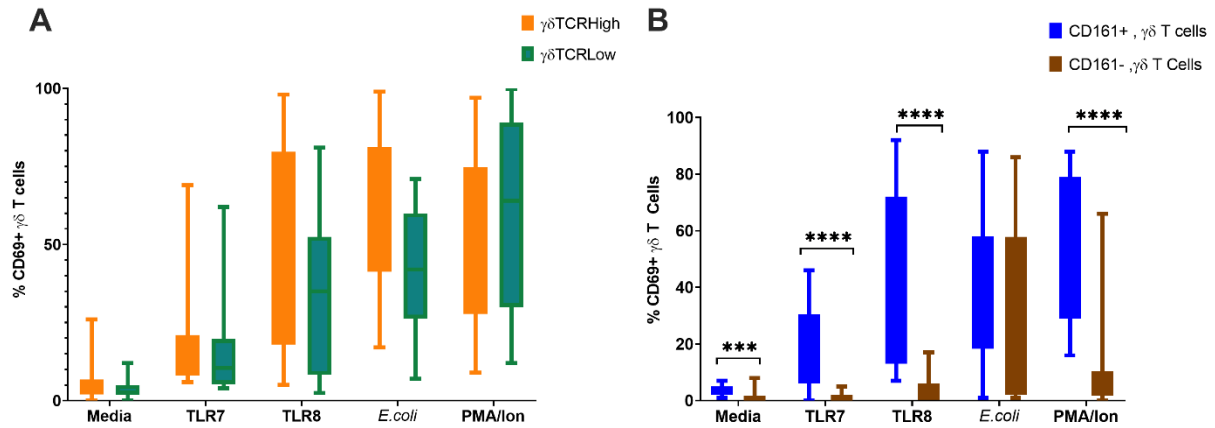


Figure 32. Higher frequency of CD69+ CD161+ $\gamma\delta$ T cells after stimulation. (A) Frequency of CD69+ $\gamma\delta$ T cells in $\gamma\delta$ TCR^{high} vs. $\gamma\delta$ TCR^{low} T cells. (B) Frequency of CD69+ $\gamma\delta$ T cells in CD161+ $\gamma\delta$ T cells vs. CD161- $\gamma\delta$ T Cells. Bars represent interquartile range from 7 individuals, Analysis by Mann-Whitney U tests * $p \leq 0.05$, *** $p \leq 0.001$, **** $p \leq 0.0001$

4.5 MAIT cells and $\gamma\delta$ T cells express high chemokine receptors

Chemokine receptors are G-proteins-coupled receptors (GPCRs) that are activated by chemoattractant cytokines known as chemokines. Chemokine receptors have been shown to play a role in the movement and controlled positioning of leukocytes by inducing directed cell movement towards the source of chemokine gradients (chemotaxis). I hypothesized that the frequency of CCR6+, CCR5+, CXCR6+, CXCR3+, and CCR4+ MAIT and $\gamma\delta$ T cells would be higher compared to the frequency of CD4+ and CD8+ T cells.

To confirm the previous observation by Dusseaux et al. (598), the frequency of CCR6+, CCR5+, CXCR6+, CXCR3+, and CCR4+ MAIT and $\gamma\delta$ T cells were assessed in blood from healthy donors and compared with the frequency of CCR6+, CCR5+, CXCR6+, CXCR3+, and CCR4+ CD4+ and CD8+ conventional T cells. Ex vivo cells were stained with antibodies and analyzed by flow cytometry. T cell expression of CCR6, CXCR6, CCR5, CCR4, and CXCR3 was assessed.

Figure 33A is a representative flow cytometry diagram for one donor, showing a higher frequency of CCR6+, CCR5+, and CXCR6+ MAIT cells. Friedmans tests was used to compare the frequency of chemokine receptor positive MAIT and $\gamma\delta$ T cells in blood from healthy donors with that of conventional T lymphocytes. The median and IQR values were reported.

There was a significant difference in the frequency of CCR5+ MAIT cells (48.4%, 42.1%), CCR5+ $\gamma\delta$ T cells (31.8%, 5.5), CCR5+ CD4+ T cells (1.3%, 1.4%), and CCR5+ CD8+ T cells (3.9%, 21.3%) ($p < 0.0001$). There was also a significant difference in the frequency of CCR6+ MAIT cells (51.4%, 40.8%), CCR6+ $\gamma\delta$ T cells (20%, 53%), CCR6+ CD4+ T cells (2.3%, 1.3%), and CCR5+ CD8+ T cells (1%, 1.8%) ($p = 0.0003$). There was a significant difference between frequency of CXCR3+ MAIT cells (54.3%, 40.8%), CXCR3+ $\gamma\delta$ T cells (43.2%, 35.3%), CXCR3+ CD4+ T cells (30.4%, 11.2%) and CXCR3+ CD8+ T cells (78%, 36.4%) ($p = 0.0001$). There was a significant difference in frequency of CXCR6+ MAIT cells (0.1%, 6.3%), CXCR6+ $\gamma\delta$ T cells (2.8%, 4.6%), CXCR6+ CD4+ T cells (0.2%, 0.1%) and CXCR6+ CD8+ T cells (2.3%, 1.7%) ($p = 0.0098$). The frequency of CCR4+ MAIT cells (25.3%, 36.4%), CCR4+ $\gamma\delta$ T cells (0.3%, 3.1%), CCR4+ CD4+ T cells (10.4%, 9.4%), and CCR4+ CD8+ T cells was significantly different (1.9%, 6.5%) ($p < 0.0001$).

Dunn's post-test was used to compare CCR6+, CXCR3+, CCR5+, CCR4+, and CXCR6+ MAIT cells and $\gamma\delta$ T cells and conventional CD4+ and CD8+ T cells. There was a significant difference between CCR5+ MAIT cells and $\gamma\delta$ T cells ($p=0.0062$), CD4+ ($p<0.0001$) and CD8+ T cells ($p<0.0001$). There was a significant difference between CCR6+ MAIT cells and $\gamma\delta$ T cells ($p=0.0009$), CD4+ ($p<0.0001$) and CD8+ T cells ($p<0.0001$). There was no significant difference between CXCR3+ MAIT cells and $\gamma\delta$ T cells ($p=0.5557$). However, there was a significant difference between CXCR3+ MAIT cells and CD4+ ($p=0.0001$) and CD8+ ($p=0.0041$) T cells. There was no significant difference between CXCR6+ MAIT and $\gamma\delta$ T cell, CD4+ and CD8+ T cells ($p>0.005$). There was a significant difference between CCR4+ MAIT cells and $\gamma\delta$ T cells ($p<0.0001$), CD4+ ($p=0.0295$) and CD8+ T cells ($p<0.0001$). There was a significant difference between CCR5+ $\gamma\delta$ T cells and CD4+ ($p<0.0001$) and CD8+ ($p<0.0001$) T cells. There was a significant difference between CCR6+ $\gamma\delta$ T cells and CD4+ ($p=0.0007$) and CD8+ ($p=0.0004$) T cells. There was no significant difference between CXCR3+ $\gamma\delta$ T cells and CD4+ ($p=0.0547$). However, there was a significant difference between CCR5+ $\gamma\delta$ T cells and CD8+ ($p<0.0001$) T cells. There was no significant difference between CCR6+ and CCR4+ $\gamma\delta$ T cells and CD4+ and CD8+ T cells ($p=0<0.05$).

Taken together, these results show that the frequency of CCR5+, CCR6+ and CCR4+ MAIT cells and CCR6+, CCR5+, and CCR4+ $\gamma\delta$ T cells was significantly higher than CCR6+, CCR5+, and CCR4+ CD4+ T cells and CCR6+, CCR5+, and CCR4+ CD8+ T cells. This suggests that MAIT cells and $\gamma\delta$ T cells are more responsive to trafficking to peripheral tissues including the gut, liver, oral mucosa, respiratory, intestinal, female genital tract, and skin.

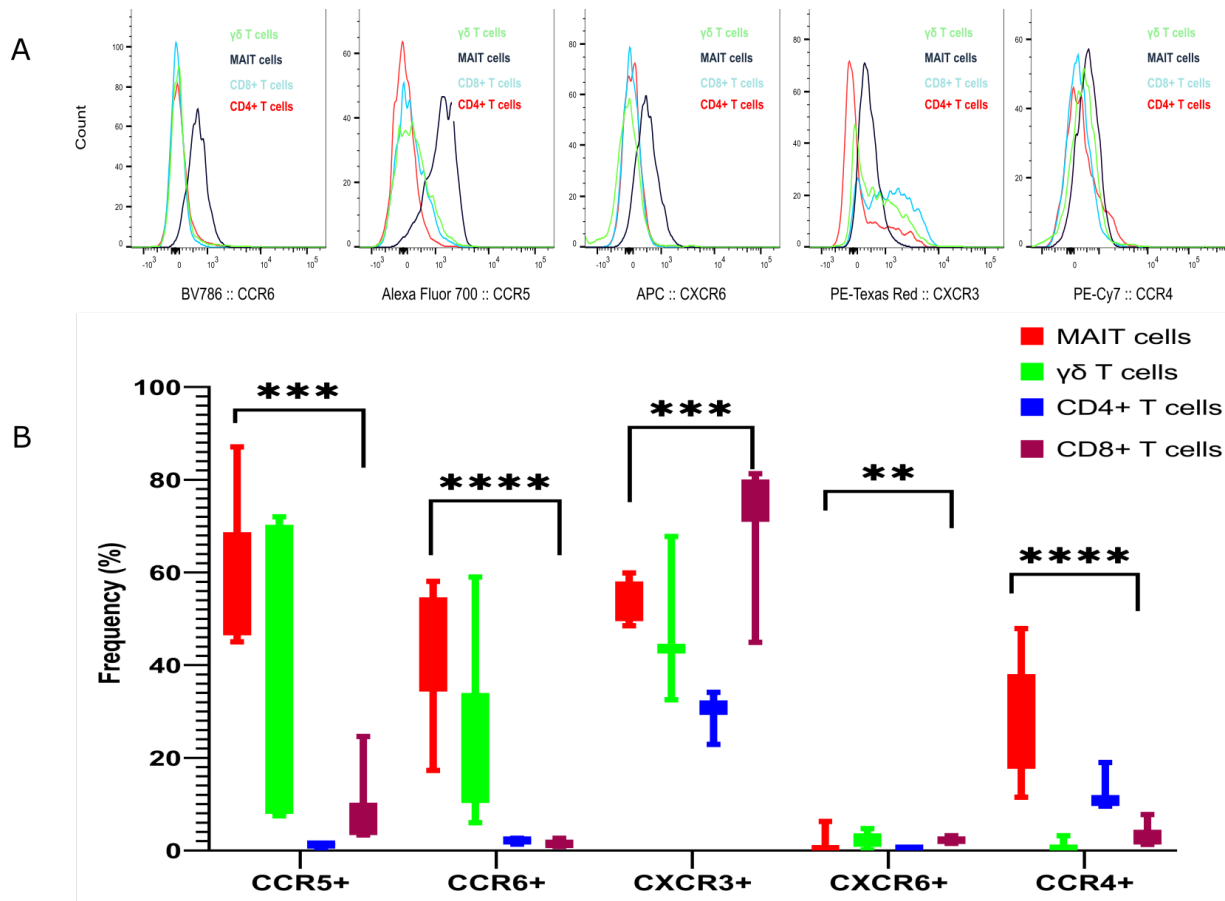


Figure 33. Frequency of chemokine expressing MAIT cells is high compared to conventional CD4 and CD8 T cells. (A) Flow cytometry plot showing chemokine receptor expression by T cells. (B) Frequency of chemokine receptors in T cells. Analysis was done by Friedman's test. Bars represent interquartile range from 8 individuals, $n=8$ ** $p\leq 0.01$, *** $p\leq 0.001$ and **** $p\leq 0.0001$

4.5.1. Downregulation of surface CCR5 on MAIT cells after TLR8 stimulation

In the previous experiment, the frequency of CCR5⁺ and CCR6⁺ MAIT and CCR5⁺ and CCR6⁺ $\gamma\delta$ T cells was significantly high. Although CCR5 binds several natural chemokines, it is also a co-receptor for entry of M tropic strains of HIV-1 into cells. CD4⁺ cells that express low CCR5 or completely lack CCR5 expression on the cell surface are resistant to mucosal HIV-1 infection (628). The levels of CCR5 on the cell surface are determined by several factors, including the rates of CCR5 internalization and recycling.

To determine if TLR ligation affected CCR5 expression on MAIT and $\gamma\delta$ T cells, PBMC from five healthy donors were cultured in the presence of TLR7 ligand, TLR8 ligand, and PFA-fixed *E. coli* and stained with antibodies followed by flow cytometry analysis. The frequency of CCR5⁺ and CCR6⁺ MAIT cells and CCR5⁺ and CCR6⁺ $\gamma\delta$ T cells 2, 6, 14, and 24 h after TLR7, TLR8, and *E. coli* stimulation was compared by Mann–Whitney U tests

There was no significant change in CCR5⁺ MAIT cell frequency after 2, 6, 14, and 24 h post TLR7 stimulation ($p>0.05$). There was also no significant change in percentage of CCR5⁺ MAIT cell 2 or 6 h after TLR8 stimulation ($p>0.05$). However, there was a significant decrease in CCR5⁺ MAIT cells 14 h ($p=0.0317$) and 24 h ($p=0.0435$) post TLR8 stimulation. No significant difference was observed in CCR5⁺ MAIT cells frequency after 2 h and 6 h stimulation with *E. coli* ($p>0.05$). However, a significant reduction in the percentage of CCR5⁺ MAIT cells was observed 14 h ($p=0.0079$) and 24 h ($p=0.0317$) post stimulation with *E. coli* (**Figure 34A**). No significant difference in the frequency of CCR5⁺ $\gamma\delta$ T cells was observed after 2, 6, 14, and 24 h stimulation with TLR7 or TLR8- ligand ($p>0.05$) s. (**Figure 34B**).

Taken together, this result show that CCR5 expression on MAIT cells is downregulated 14 h after TLR8 stimulation.

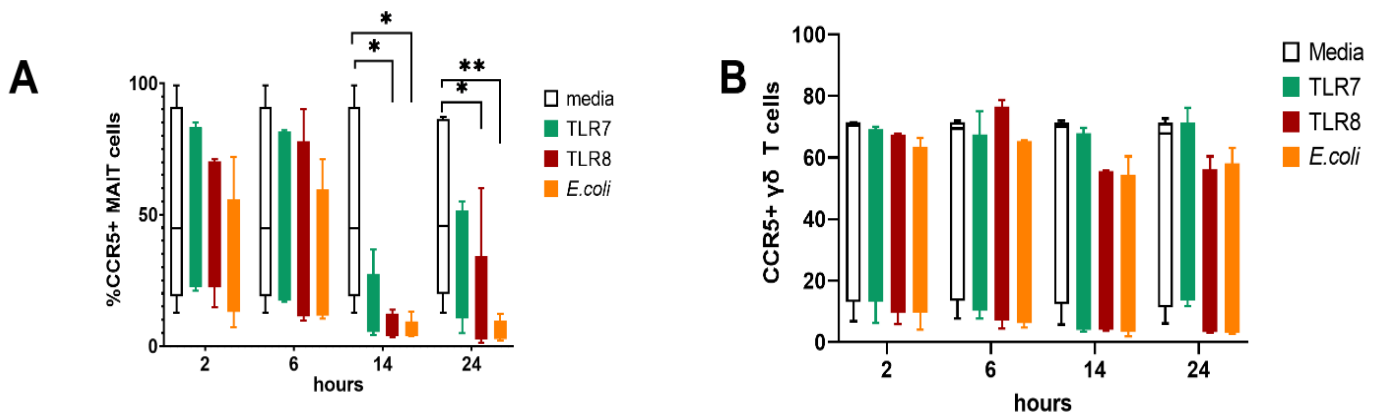


Figure 34. MAIT cell surface expression of CCR5 is significantly downregulated after 14h of TLR8 and *E. coli* stimulation. PBMCs from healthy donors were stimulated with TLR7, TLR8, PMA/ION (n=16 donors), and PFA-fixed *E. coli* (n=6), then stained and analyzed by flowcytometry. (A) Frequency of CCR5+MAIT cells in media, TLR7, TLR8, *E. coli* and PMA/Iono stimulated PBMCs. (B) Frequency of CCR5 + $\gamma\delta$ T cells at 2, 6, 14, and 24 h following TLR7, TLR8, and *E. coli* stimulation. Bars represent interquartile range from 5 individuals. Statistical analysis was performed using Mann–Whitney U tests, * $p \leq 0.05$ and ** $p \leq 0.01$.

4.5.2. CCR5 is downregulated on MAIT cells and CD4+ T cells after stimulation

To validate this apparent downregulation of CCR5 expression on the surface of MAIT cells, $\gamma\delta$ and conventional CD4+ T cells from 16 donors were compared before and after 24 h stimulation. PBMCs cultured in the presence of TLR7 ligand, TLR8 ligand, PFA-fixed *E. coli* and PMA/ION were stained with antibodies and analyzed by high-dimensional flow cytometry.

There was a non significant frequency of CCR5+ MAIT cells after TLR7 stimulation (86.2%, 79% vs. 47.1%, 97.5% p=0.0550). However, TLR8 (86.2%, 79% vs. 32%, 56.6% p=0.0098) *E. coli* (86.2%, 79% vs. 20.3%, 45.5% p=0.0012) and PMA/ION (86.2%, 79% vs. 25.3%, 80.9% p=0.0098) stimulation led to a significant reduction in CCR5+ MAIT cells (**Figure 35**). There was no significant change in CCR5+ $\gamma\delta$ T cells after either TLR7 (47.1%, 75.2% vs. 32.3%, 57.9% p=0.0796), TLR8 (47.1%, 75.2% vs. 34.4%, 86.9% p=0.2099), *E. coli* (47.1%, 75.2% vs. 27%, 46.1%, p=0.0887) or PMA/ION (47.1%, 75.2% vs. 47.7%, 44.7% p=0.0616) stimulation. No significant change in the frequency of CCR5+ CD4+ T cells after either TLR7 (4.6%, 26.2% vs. 3.7%, 27.7% p=0.2502), TLR8 (4.6%, 26.2% vs. 2.3%, 24.3% p=0.1804), or PMA/Iono (4.6%, 26.2% vs. 5.2%, 18.3% p=0.8376) stimulation. There was significant change in the frequency of CCR5+ CD4+ T cells after stimulation with *E. coli* (4.6%, 26.2% vs. 0.7%, 5% p=0.0127). There was no significant change in CCR5+ CD8+ T cells after either TLR7 (4.6%, 36.2% vs. 3.3%, 34.1% p=0.2502), TLR8 (4.6%, 36.2% vs. 2.5%, 31.1% p=0.1804), *E. coli* (4.6%, 36.2% vs. 2%, 15%, p=0.0523) or PMA/ION (4.6%, 36.2% vs. 4.8%, 25% p=0.7461) stimulation.

Taken together, this result show that the frequency of CCR5+MAIT cells is significantly reduced after TLR8 ligations.

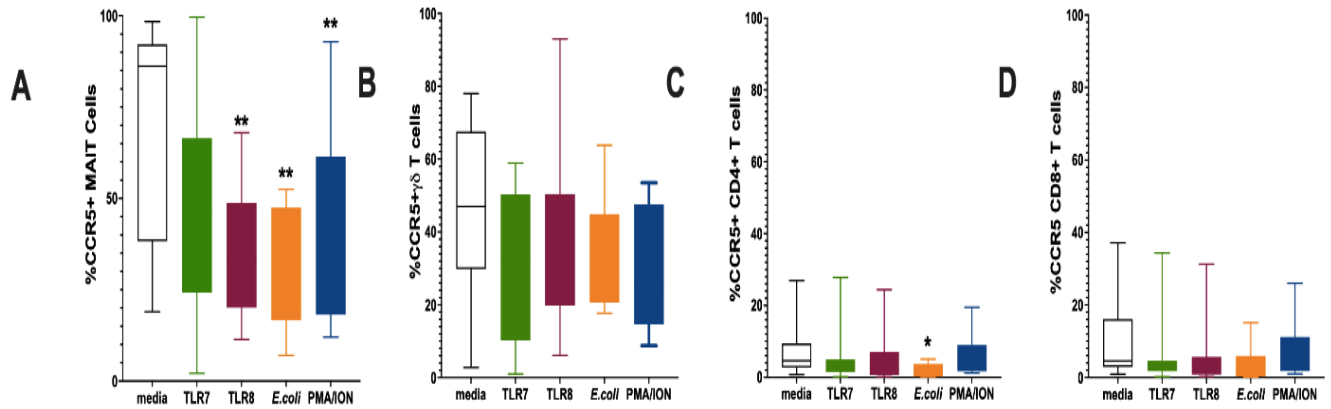


Figure 35. Frequency of CCR5+ MAIT cells downregulated following stimulation. PBMCs from healthy donors were stimulated with TLR7-ligand, TLR8-ligand, PMA/ION, (n=16) and PFA-fixed *E. coli* (n=6), then stained and analyzed by flow cytometry. (A) Frequency of CCR5+ MAIT cells. (B) Frequency CCR5+ $\gamma\delta$ T cells. (C). Frequency CCR5+ CD4+ T cells. (D) Frequency CCR5+ CD8+ T cells. Bars represent interquartile range from 16 individuals. Statistical analysis was performed using Mann–Whitney U test s* $p\leq 0.05$ and ** $p\leq 0.01$.

4.6 Summary

The number of MAIT cells identified as CD161⁺⁺MR1AgTet⁺ was 4% lower than the number of MAIT cells identified as CD161⁺⁺, V α 7.2. Two subsets of $\gamma\delta$ T cells (i.e., $\gamma\delta$ TCR^{high} and $\gamma\delta$ TCR^{low}) were identified. The majority of $\gamma\delta$ TCR^{high} were also CD161⁺. Although there appears to be little difference between $\gamma\delta$ TCR^{high} and $\gamma\delta$ -TCR^{low}, CD161⁺ $\gamma\delta$ T cells were highly activated compared to CD161⁻ following TLR7 and TLR8 stimulation. MAIT cells were found to be highly activated compared to $\gamma\delta$ T cells after TLR7 and TLR8 stimulation. Although TLR7 stimulation led to activation of MAIT and $\gamma\delta$ T cells, it did not lead to IFN- γ , TNF- α , IL-17a or GM-CSF expression by MAIT and $\gamma\delta$ T cells. However, TLR8 stimulation led to expression of IFN- γ and GM-CSF at the highest concentration tested. Media supplementation with rIL-7 and rIL-2 resulted in higher levels of IFN- γ , TNF- α , IL-17a and GM-CSF expression by MAIT cells and $\gamma\delta$ T cells after TLR8 but had no effect on cytokine expression by conventional CD4⁺ and CD8⁺ T cells.

Chapter 5: TLR8 Stimulation Results in Higher Maturation Markers on Monocyte-derived Dendritic Cells Compared to TLR7 Stimulation

5.1 Rationale

The TCR-mediated activation of MAIT cells requires antigen presentation of bacterial vitamin B2 metabolites by MHC class I-related protein (MR1). MR1 mRNA is widely expressed in various tissues (629) and cell lines (630). However, little is known about MR1 expression on the surface of primary cells. MAIT cells have been shown to be activated during viral infections. However, viruses do not express vitamin B2 metabolites that are required for TCR-mediated activation of MAIT cells. This suggests that activation of MAIT cells during viral infection occurs in a TCR-independent manner via cytokines expressed by TLR stimulation of APCs (468). MAIT cells have been shown to express high levels of receptors for IL-12 and IL-18 (189) and therefore may be activated by these cytokines leading to increased proinflammatory cytokine expression and immune activation.

5.2 Hypothesis

MDDCs mature in response to TLR7 and TLR8 stimulation, leading to expression of IL-12 and IL-18 and increased MR1 surface expression.

5.3 Objectives

- i. To quantify the changes in frequency and surface expression of activation and maturation markers HLA-DR, CD80, and CD83 on MDDCs following *in vitro* TLR7 and TLR8 stimulation
- ii. To quantify IL-12 and IL-18 cytokine levels and MR1 surface expression in MDDCs following *in vitro* TLR7 and TLR8 stimulation

5.4 Results

5.4.1 Monocyte enrichment

Monocytes are one of the components of mononuclear phagocytes systems, comprising up to 10% of circulating leukocytes (631). Monocytes were first described as circulating precursors for tissue macrophages, and later it was shown that they can be differentiated to DCs (632). Studying DCs is difficult due to their low concentration in the peripheral blood. Methods for *in vitro* generation of DC have therefore been developed (633); however, one of the most commonly used method involves magnetic beads to yield highly viable and pure monocytes (634). As described in Chapter 3, magnetic beads were used to sort CD14⁺ cells from PBMCs of healthy blood donors by negative selection according to the manufacturer's protocol (635). The purity of the monocyte population was evaluated by flow cytometry. To assess the viability and purity of the enriched monocytes, cells were stained with CD14, live/dead Aqua, CD19 and CD3 antibodies and analyzed by flow cytometry.

In one representative blood donor (**Figure 36A**), before enrichment, the PBMCs were 47% CD14⁺, 55% CD3⁺, 45% CD19⁺, and 19% CD56⁺ cells. After enrichment the proportions changed to 91% CD14⁺, 0.4% CD3⁺, 0.6% CD19⁺, and 0.1% CD56⁺ cells.

To assess the purity of the enriched monocytes, CD14⁺ cells in PBMC and CD14⁺ enriched cells were compared by Mann–Whitney U test. CD14⁺ cells in PBMC were significantly enriched after sorting with median and IQR of (24.5±17.7% vs. 84.2±3.5% respectively $p < 0.0001$) (**Figure 36B**).

This result shows that CD14⁺ T cells were isolated by negative selection using magnetic beads.

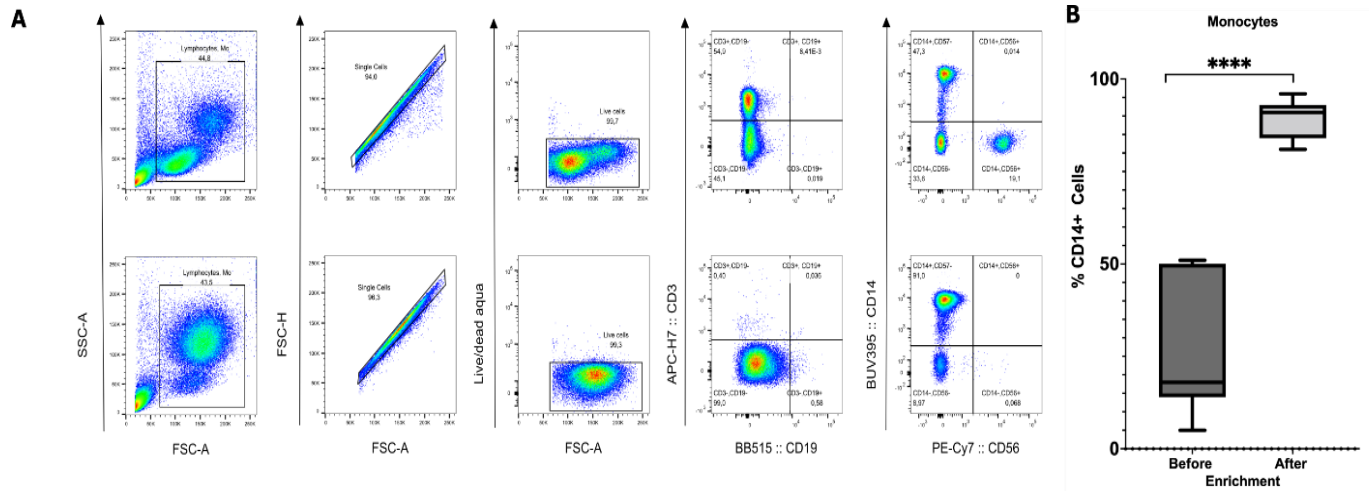


Figure 36. CD14⁺ staining of *ex vivo* PBMCs and enriched monocytes. (A) Representative flow cytometry showing CD14⁺ cells before and after enrichment. Gates were set by SSC-A and FSC-A to show size and granularity, FSC-H by FSC-A to gate for singlets, live/dead Aqua stain vs. FSC-A to gate for live cells. CD3⁺ cells and CD19⁺ cells were gated on live cells, CD14⁺ and CD56⁺ cells were gated on live cells (B) Frequency of CD14⁺ cells before and after enrichment. Bars represent interquartile range from 7 individuals, n=7. Analysis was performed by Mann Whitney U tests. ****p<0.0001.

5.4.2 Monocyte differentiation

The ability of blood monocytes to differentiate to DCs or macrophages was explored *in vitro* 25 years ago (636,637). Myeloid DCs can be generated *in vitro* from CD34+ progenitor cells present in cord blood (638,639) or from peripheral blood monocytes (640).

The primary goal of this section was to differentiate monocytes into MDDCs *in vitro*. Monocytes from PBMC of healthy donors were cultured in media supplemented with GM-CSF and IL-4 as previously described (634). Briefly, the monocytes were cultured in media supplemented with GM-CSF and IL-4 for 4 days. Fresh media supplemented with GM-CSF and IL-4 was added to the culture every 2 days.

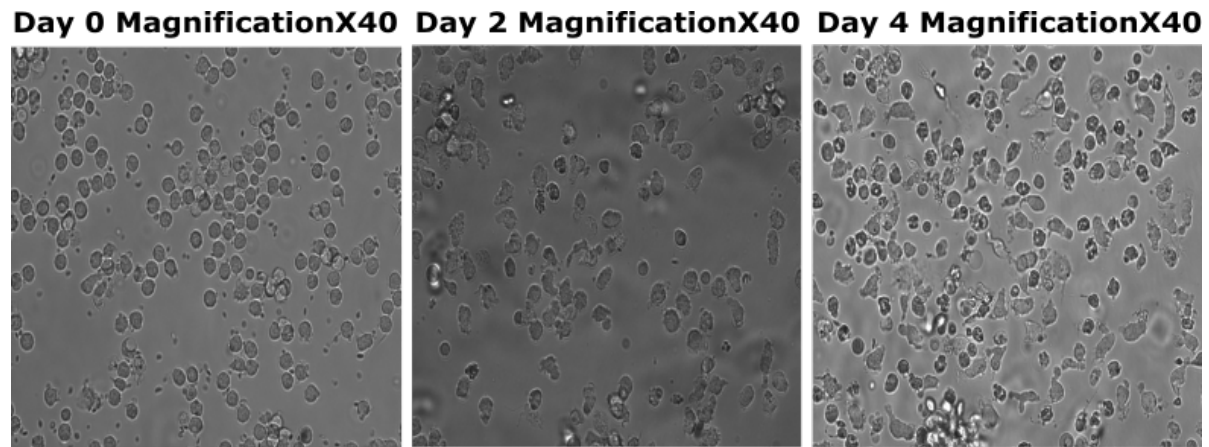


Figure 37. Light microscope images of monocyte differentiation day 0, day 2 and 4

5.4.3 Monocyte-derived maturation

DCs are professional APCs that act as sentinels of the immune system (641–643). Most DCs in human tissues are immature and can not stimulate T cells since they express low levels of stimulatory signals such as CD40, CD80, CD58, CD86, and CD54. However, these immature DCs are extremely well equipped to capture antigens, a very important event in the induction of immunity. Maturation and mobilization of DCs can be induced by antigens, cytokines or TLRs. Once immature DCs are cultured, there are phenotypic changes that occur within a day of culture and the cells undergo extensive transformation, their antigen-capturing function disappears, and

T-cell stimulatory functions increase. Maturation of MDDCs may lead to surface expression of MR1 (644).

To assess the effect of TLR7 and TLR8 on MDDC maturation and surface expression of MR1, monocytes were cultured in media supplemented with GM-CSF and IL-4 for 7 days. On day 5, TR7-ligand, TLR8 ligand, and PFA-fixed *E. coli* were added to appropriate wells and cultured for 2 days. The culture supernatant was harvested on day 7 and stored at -80°C until used in ELISAs. Semi-adherent cells were resuspended by adding cold PBS for 5 min before gently scraping them using a rubber cell scraper. Cells were stained with antibodies and analyzed by flow cytometry. The Mann–Whitney U test was used to assess the significance of differences in maturation between unstimulated vs. stimulated MDDCs in 7 subjects. However, in this assay MR1 was not detected, and repeated experiments to detect it with these reagents were unsuccessful.

No significant difference was observed in the frequency of CD11C+ (79.1%, 44.8% vs. 88%, 21.3% p=0.4015), HLA-DR+ (65.6%, 84.7% vs. 85.2%, 58.3% p=0.0973), CD80+ (11.3%, 77.6% vs. 39.5%, 84.2 p=0.3829), and CD83+ cells (8.4%, 48.8% vs. 9.4%, 50.6% p=0.5350) after TLR7 stimulation (**Figure 3**).

There was no difference in the frequency of CD11C+ (79.1%, 44.8% vs. 80.6%, 45.6% p=0.9015) and HLA-DR+ (65.6%, 84.7% vs. 92.2%, 26.9% p=0.0973) cells after TLR8 stimulation. However, there was a significant difference in the frequency of CD80+ (11.3%, 77.6% vs. 90.7%, 27.9% p=0.0251) and CD83+ (8.4%, 48.8% vs. 62%, 89.9% p=0.0175) cells after TLR8 stimulation (**Figure 38**).

There was no difference in the frequency of CD11C+ (79.1 %, 44.8% vs. 89.4%, 40% p=0.6177) and HLA-DR+ (65.6%, 84.7% vs. 91.6%, 43.8% p=0.7815) cells after stimulation with *E. coli*. However, there was a significant difference in the frequency of CD80+ (11.3%, 77.6% vs. 90.7%, 27.9% p=0.0041) and CD83+ cells (8.4%, 48.8% vs. 75.2%, 61.4% p=0.0082) after stimulation with *E. coli* (**Figure 38**).

Taken together, these results show that TLR7 stimulation had no effect on the maturation of MDDC. On the other hand, TLR8 stimulation led to maturation of MDDCs but did not increase

surface expression of MR1. These findings are similar to what was observed in a previous study (645).

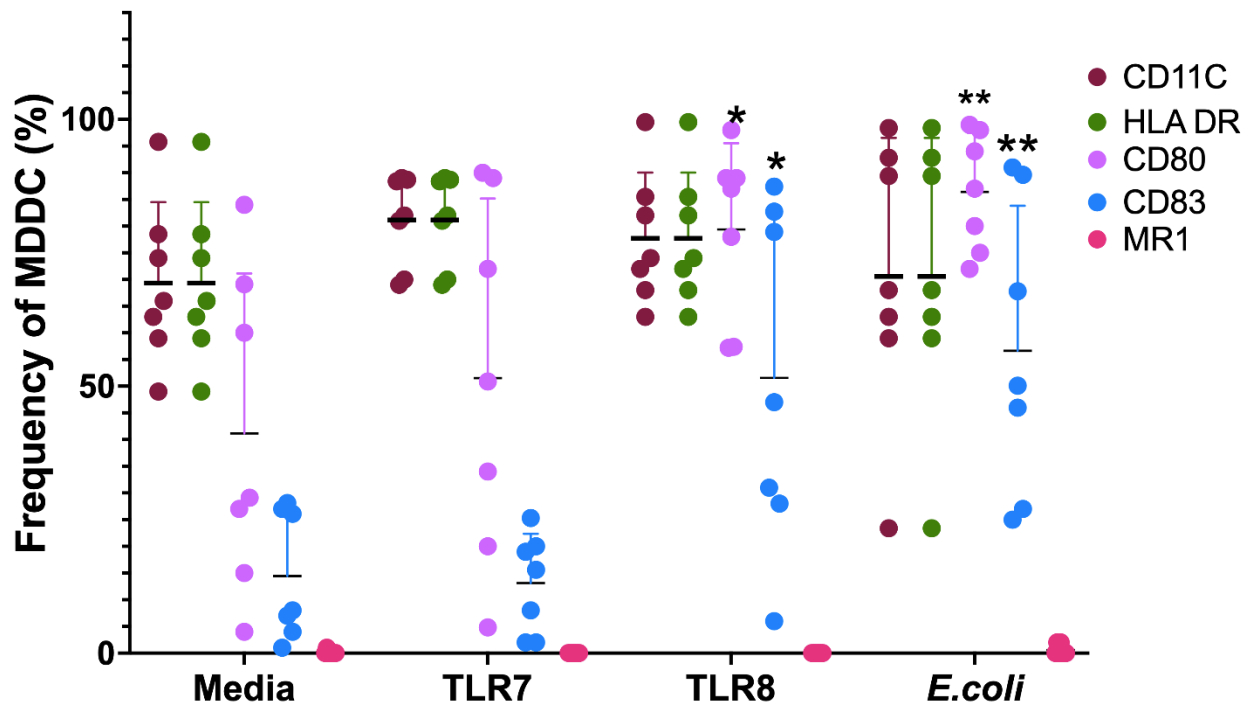


Figure 38. Increased expression of maturation markers on MDDCs after stimulation. Immature DCs were matured for 48 h with different maturation markers. CD11C, HLA-DR, D83, and CD80, and MR1 were evaluated by flow cytometry, and the frequency of each marker is plotted for unstimulated and TLR7, TLR8, and *E. coli*-matured MDDCs. Each dot represents a single individual of n=7. Lines and error bars through each data set medians and represent 95% confidence intervals. The significance of between-group differences was analyzed using Mann Whitney U tests * $p \leq 0.05$, ** $p \leq 0.01$

5.4.4 Analysis by tSNE

MDDC phenotypes were characterized by tSNE analysis (**Figure 39**). The MDDC events from two donors were concatenated, resulting in a total of 40,000 events. The concatenated events were used to generate tSNE plots as indicated in **Figure 39**.

The shape of the tSNE heatmaps revealed heterogeneity in the MDDC subset: Cells that were phenotypically similar were close together while those that were phenotypically different were placed far apart. From the heatmaps, a subset of cells appeared to express high CD11C after TLR7 and TLR8 stimulation, circled in figure 39. This is in line with what was previously reported. In contrast to what I had reported, what is shown in **Figure 38**, a subset of cells also appeared to HLA-DR, CD80 and CD83 after stimulation. In line with what was shown in **Figure 38**, TLR8 and *E. coli* stimulation induced low CD83 expression. A small subset of cells expressed MR1 in unstimulated and following TLR7, TLR8, and *E. coli* stimulation. This is contrary to what was reported before.

Taken together, these results show heterogeneity in the MDDC population as well as low levels of baseline MR1 expression in MDDCs (**Figure 39**).

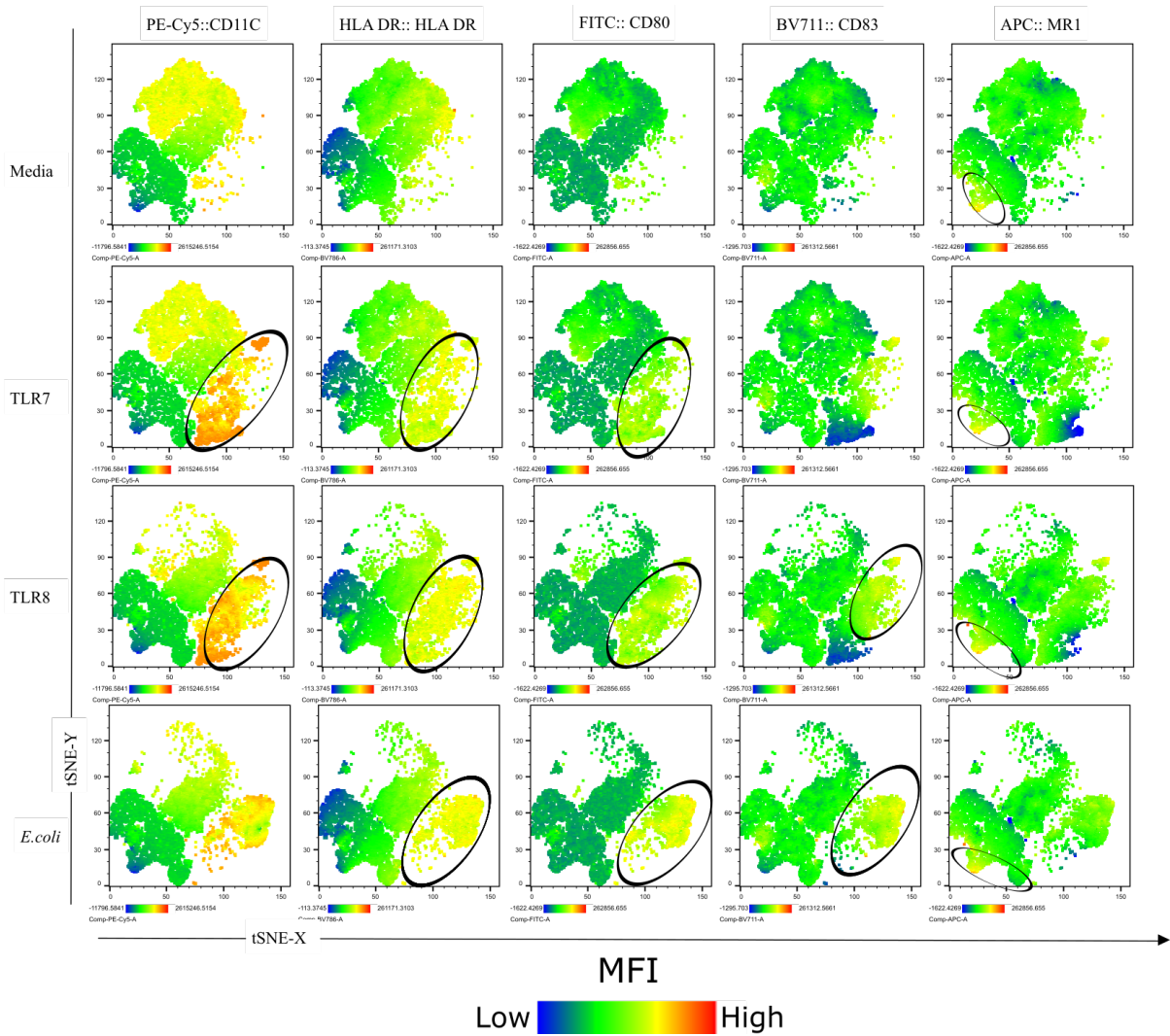


Figure 39. Heatmap of tSNE analysis of MDDCs. Analysis by tSNE of MDDCs from two donors demonstrates phenotypic differences based on maturation condition. Rows correspond to TLR7, TLR8, and *E. coli* stimulated MDDC. From left to right, columns show clustering of MDDC by CD11C, HLA-DR, CD80, CD83 and MR1 expression in both stimulated and unstimulated cells. The colour scale corresponds to MFI.

5.4.5 MDDCs matured by TLR8 stimulation secrete a higher amount of IL-12p70 than those matured by TLR7 stimulation

DCs link the innate and adaptive immune response by acting as APCs (646). DCs also regulate the innate immune response by secreting proinflammatory cytokines when they come in contact with microbes (646,647). To assess the effect of TLR7 and TLR8 on MDDC IL-12 and IL-18 expression, monocytes were cultured in media supplemented with GM-CSF and IL-4 for 7 days. Fresh media supplemented with GM-CSF and IL-4 was added to the culture every 2 days. On day 5 of the culture, TR7-ligand, TLR8-ligand and PFA-fixed *E. coli* were added to appropriate wells and cultured for 2 days. The culture supernatant was harvested on day 7 and stored at -80°C for ELISA.

IL-12p70 and IL-18 were measured using ELISA kits for human IL-12p70 (Cat# ab213791, abcam, Boston, MA) and IL-18 (Cat# DY318-05, R&D Systems, Minneapolis, MN), respectively, according to manufacturer's instruction as described in Chapter 3. Mann-Whitney U tests were used to compare levels of IL-12p70 in the supernatant of unstimulated (media) versus stimulated MDDC. There was no significant increase in IL-12p70 after TLR7 stimulation ($p>0.999$). However, a significant increase in IL-12p70 occurred after TLR8 stimulation ($p=0.0079$). A significant increase in IL-12p70 after stimulation of MDDC with *E. coli* ($p=0.005$) was also observed (**Figure 40A**). There was no significant increase in IL-18 after TLR7 or TLR8 stimulation ($p>0.05$). Furthermore, there was no significant increase in IL-18 after stimulation with *E. coli* ($p=0.1143$) (**Figure 40B**).

Taken together, these results show that IL-12p70 was detected after maturation of MDDCs with TLR8 ligand and *E. coli*. However, no significant change in MDDC IL-18 expression was observed.

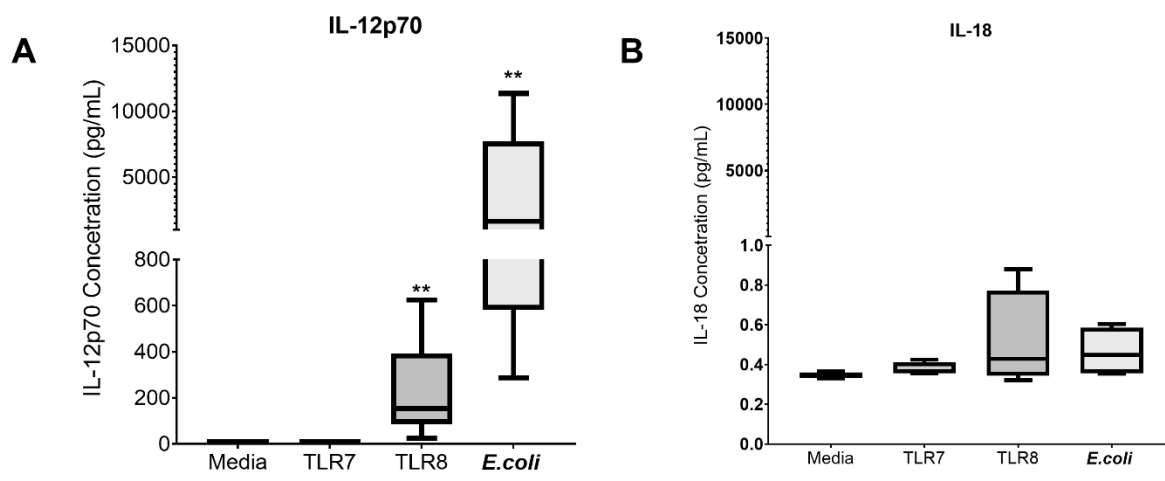


Figure 40. IL-12p70 expression after DC maturation with TLR8 compared to TLR7 stimulation. (A) Measurement of IL-12p70 after (B) Measurement of IL-18 after TLR7, TLR8 and *E. coli* stimulation of immature MDDCs. Lines and error bars on box a whisker represent medians interquartile ranges from 7 individuals, n=7. Analysis was performed with Mann–Whitney U tests **p≤0.01.

Chapter 6: HIV Infection Assay

6.1 Rationale

MAIT cells comprise 1–10% of T lymphocytes in the circulation but have a strong tissue-homing characteristic (441,456,648). In the lower and upper female genital mucosa, MR1⁺ APCs and MAIT cells have been identified (649). Since the majority of transmission of HIV occurs via sexual transmission, there is a need to understand the effect of MAIT cells on activation of CD4⁺ cells and HIV infection. Emerging evidence indicates that MAIT cells are activated during viral infections (25, 26). In addition, high expression levels of the receptors for IL-18 and IL-12 provides MAIT cells with the capacity to respond to these APC-derived cytokines (439).

I hypothesize that co-culture of CD4⁺ T cells with MAIT cells stimulated with rIL-18 and rIL-12 will lead to increased activation and increased HIV infection of the CD4⁺ T cells.

6.1.1 Pure MAIT and CD4⁺ cells sorted from the blood of healthy blood donors

To isolate pure populations of MAIT and CD4⁺ T cells, PBMCs were isolated from blood samples from 2 healthy donors and stained with the fluorochrome conjugated antibodies in **Table 2.4**. After staining, cells were washed, passed through a 40 mm cell strainer, and sorted on an BDFACs flow cytometer. Two groups of live cells were sorted (CD3⁺ CD161⁺MR1AgTet⁺ and CD3⁺CD4⁺) to a purity of 99%. In one representative donor, MAIT cells comprised 6.88% and CD4⁺ T cells 57.7% of T cells (**Figure 41**). With these conditions established, highly pure MAIT (>99%) and CD4⁺ (>99) T cell subsets were sorted out from 4 donor samples.

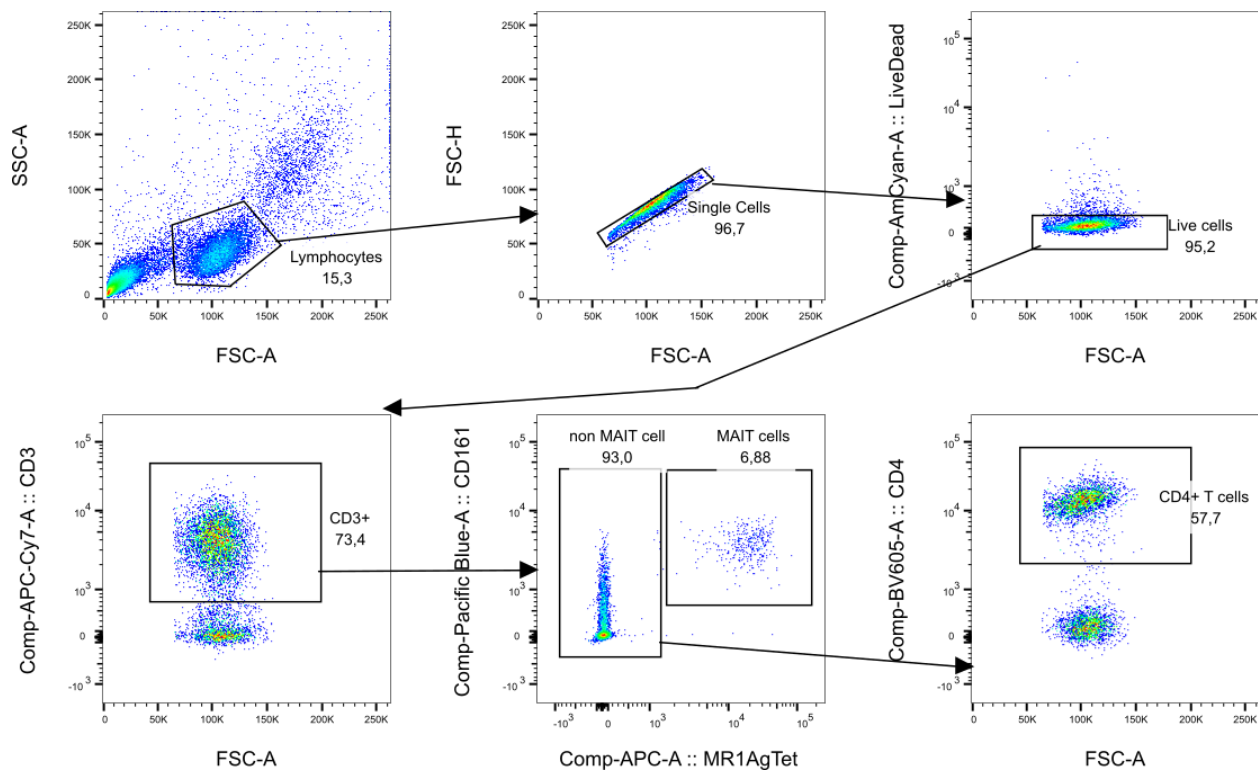


Figure 41. Gating strategy for sorting pure populations of MAIT cells and CD4+ T cells. Representative staining of PBMC of one healthy donor blood sample. Cells were gated on lymphocytes by FSC/SSC, then on singlets by FSC-H/FSC-A and live cells which were negative for the live dead aqua discriminant dye. CD3+ T cells were gated off the live cells, MAIT cells were gated on CD161+ MR1AgTet cells off the CD3+ T cells. CD4+ T cells were gated off the CD3+ MR1AgTet- cells.

6.2 MAIT cells induction alters HIV replication in vitro

MAIT cells express high levels of IL-12R and IL-18R (189). Stimulation of MAIT cells with IL-12 and IL-18 has been shown to lead to secretion of IFN- γ (189). During viral infections, TLR8 stimulation is proposed to lead to cytokine expression by APCs, which stimulate MAIT cells to express high levels of IFN- γ and cytotoxic molecules, resulting in protection against infection (650).

To assess the role of MAIT cells in HIV infection of CD4⁺ T cells, a 48 well plate was coated with anti-CD3 and anti-CD28 antibodies for 1h at 37°C. The solution was removed, and the plate washed with sterile PBS. Pure CD4⁺ T cells were added and incubated overnight. The CD4⁺ T cells were washed with sterile PBS to remove unbound anti-CD3/anti-CD28. In parallel MAIT cells were stimulated with IL-12 and IL-18 for 18 h. CD4⁺ T cells were co-cultured with MAIT cells and immediately infected with HIV (MOI=3) for seven days. On the seventh day cells were harvested, stained with surface markers BV605 CD4, APC-H7 CD3, PerCP/Cyanine5.5 V α 7.2 TCR, BV421 CD161, APC MR1Tet and thereafter ICS staining for FITC p24. Analyses was done by high dimensional flow cytometry. Since Vpu and Nef have been shown to remodel cell surface receptors, to assess the effect of MAIT cells stimulation on HIV infection, the frequency of CD4⁺ cells was compared between uninfected and infected unstimulated CD4⁺ T cells (unstim CD4⁺ cells), unstimulated CD4⁺ T cells cocultured with unstimulated MAIT cells (unstim CD4⁺ cells/unstim MAIT cells), unstim CD4⁺ cells/stim MAIT cells, stim CD4⁺ cells/stim MAIT cells, stim CD4⁺ cells/unstim MAIT cells, and stim CD4⁺ T cells by Wilcoxon test.

In one representative donor, HIV infection of unstimulated CD4⁺ T cells led to a 15-fold, unstimulated CD4⁺ T cells cocultured with unstimulated MAIT cells (unstim CD4⁺/unstim MAIT) 0.6-fold, unstim CD4⁺/stim MAIT 0.3-fold, stim CD4⁺/stim MAIT, 0.4-fold stim CD4⁺/unstim MAIT, 2.4-fold stim CD4⁺, 11.4-fold reduction in CD4⁺ receptor **Figure 42A**. There was a significant difference in frequency of CD4⁺ T cells between uninfected and infected (p=0.0046).

There was no significant difference in frequency of CD4⁺ T cells between uninfected and infected unstim CD4⁺ T cells, unstim CD4⁺ cells/unstim MAIT cells, stim CD4⁺ cells/stim MAIT cells,

and stim CD4⁺ cells/unstim MAIT cells ((**Figure 42A**). However, there was a significant difference in CD4⁺ cells frequency between uninfected and infected unstim CD4⁺ cells/stim MAIT cells and stim CD4⁺ T cell (**Figure 42B**).

Taken together, these result show that CD4 receptor was downmodulated following HIV infection in unstimulated CD4⁺ T cells cocultured with stimulated MAIT cells.

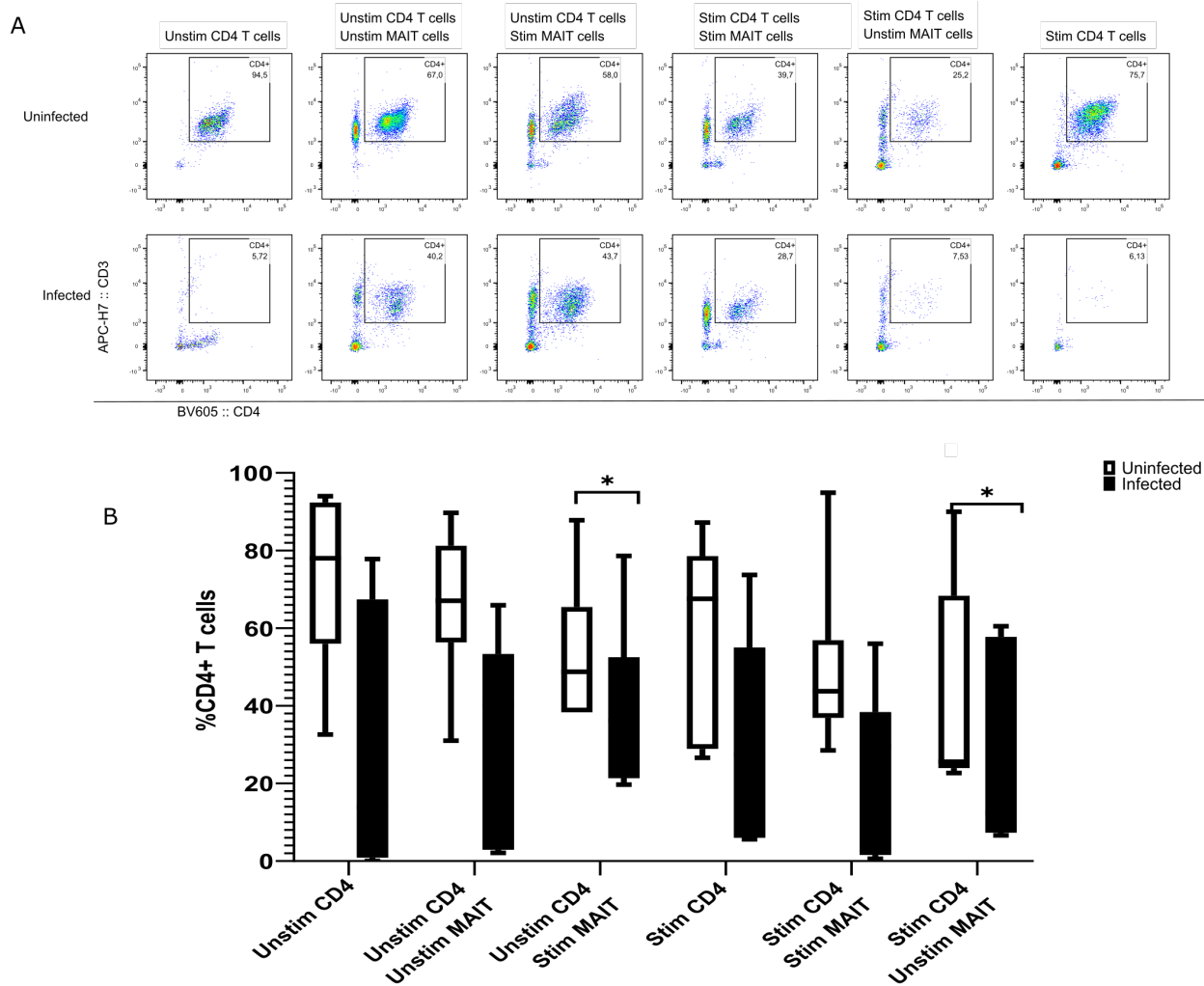


Figure 42. Downmodulation of CD4 receptor following HIV infection. A. Representative flow cytometry staining showing CD4⁺ T cells in uninfected and HIV infected cells. B Frequency of CD4⁺ T cells in uninfected (white bars) and (infected black bars) cells. Bars represent interquartile range from 4 individuals, n=4. Analysis was performed by Wilcoxon Test *p_≤0.05

6.2.1 No effect on HIV-1 infection in CD4+ T cells co-cultured with MAIT cells

To confirm the previous result, secreted p24 as a marker for HIV replication was measured by ELISA. As in the experiment above, on day 7 the culture supernatant was harvested for p24 ELISA. Analysis was performed using GainData® Origo ELISA calculator (**Appendix 4**). The Mann–Whitney U test was used to compare HIVp24 expression between the different culture conditions in HIV-infected CD4+ T cells (**Figure 43**). There was no significant difference in HIV-p24 expression between unstim CD4 vs. unstim CD4/unstim MAIT or unstim CD4 vs. unstim CD4/stim MAIT ($p>0.05$). There was also no significant difference in HIV-p24 expression between unstim CD4 vs. stim CD4, between stim CD4 vs. stim CD4/unstim MAIT or stim CD4+ vs. stim CD4/stim MAIT ($p>0.05$).

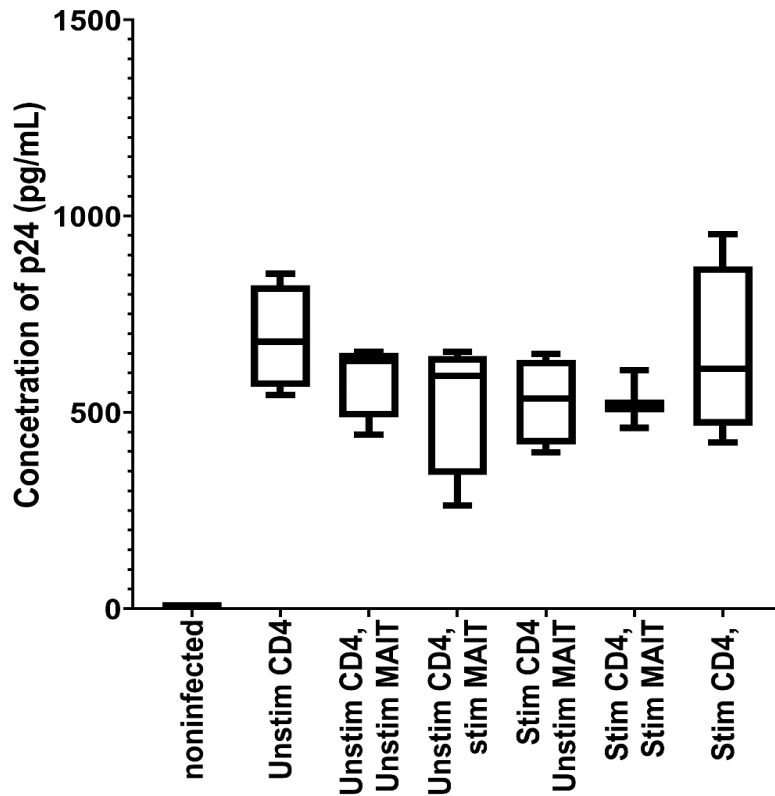


Figure 43. HIV-1 p24 expression by CD4⁺ T cells co-cultured with MAIT cells. Concentration of p24 in culture supernatant was measured by ELISA. Bars represent interquartile range from 4 individuals, n=4. Analysis was performed by Wilcoxon.

6.3 Summary

Although MAIT cells did not prevent HIV infection of CD4⁺ T cells, the effect of MAIT cells on HIV infection of CD4⁺ T cells can not effectively be assessed at this point due to low sample size. However, there was significant reduction in the frequency of CD4⁺ receptor between uninfected and infected unstimulated CD4⁺ T cells coculture with stimulated CD4⁺ T cells.

Chapter 7 General Discussion, Conclusion, Limitations, and Significance

7.1 Discussion

Not all HIV exposures lead to infection (651). Therefore, identifying the correlates of HIV protection will aid in the development of a vaccine that can protect against HIV infection. In this study, bulk PBMCs were used to study TLR stimulation of MAIT and $\gamma\delta$ T cells by flow cytometry. This study demonstrates functional responses of MAIT and $\gamma\delta$ T cells to TLR7 and TLR8 stimulation.

7.1.1 Use of surrogate markers to identify MAIT cells leads to overestimation of MAIT cells compared to use of MR1 Ag-loaded tetramers

MAIT cells are highly conserved unconventional T cells that are abundant in humans and express a semi-invariant TCR, comprising TRAV1-2-TRAJ33/12/20 α -chains paired with a limited array of TCR- β chains (typically TRBV6-1, TRBV6-4, or TRBV20). MAIT cells recognize vitamin B₁₂-based antigens presented by the nonpolymorphic MR1. Thus, human MAIT cells can be defined by co-staining with a panel of antibodies, mainly CD3, CD161, and TRAV1-2 (V α 7.2). Markers that specifically identify MAIT cells as MR1-riboflavin-Ag reactive cells have been developed.

I compared the use of MR1 tetramers and surrogate markers to examine all MAIT cell populations in healthy blood donors. Of the CD8⁺, CD8-CD4⁻(DN) T cells, 9.36% were positive for the MAIT markers CD161, V α 7.2-TCR CD161⁺⁺, while only 6.08% were MR1AgTet⁺. This is similar to what was reported by Reantragoon et al. (585), who reported V α 7.2 detecting 10-24% more cells than the MR1 tetramer.

One possible explanation for these observations is that V α 7.2 expression is not limited to MAIT cells; other T cells that express the V α 7.2 marker include public MHC-restricted T cells (189) as well as CD1b-restricted germline-encoded mycolyl-reactive (GEM) T cells (590–592).

We can speculate that although T cells from healthy individuals that expressed CD161, CD8 and TRAV1-2 showed considerable enrichment for MAIT cells, not all these cells were MAIT cells, as evidenced based on MR1 tetramer staining. Therefore, relying on surrogate markers to define MAIT cells may result in phenotypically different cells being classified generally as MAIT cells.

7.1.1.1 Variability in MAIT cell frequency

MAIT cells develop in the thymus and migrate into the periphery (652). However, the frequency of MAIT cells varies widely between human individuals, and the basis for this is unclear.

I evaluated the frequency of MAIT cells in ex vivo PBMC of healthy blood donors with the aim of getting the range of MAIT cells frequency in the study population. I confirmed variability in the frequency of MAIT cells in different individuals (599). It has recently been shown that MAIT cells downregulate CD161 upon infection with HIV-1 (585). One can speculate that the variability of MAIT cells observed in this study, using the combination of CD161 and Va7.2 mAbs, may be due to missing MAIT cells due to downregulation of CD161 because of lifetime exposure to infection. However, I obtained similar results on the variability of MAIT cells frequencies when I used antigen loaded MR1 tetramers to confirm our findings.

Although MAIT cells are involved in protective immunity against bacteria and fungal infection at barriers such as the skin and mucous membranes, MAIT cells also respond to HIV, even though it is a viral infection, via the production of cytokines including IL-18 and IL-12 and/or other cytokines (e.g., IL-15 and type I IFNs)(468,567,653). Its not clear whether MAIT cells responses during HIV may protect against infection or promote HIV infection via an increase in immune activation. Although women of reproductive age have been reported to have higher MAIT cells frequencies compared to men of the same age (599) they have also been shown to have a higher incidence of HIV infection compared to men (654). It is tempting to speculate that MAIT cells activation during HIV infection may contribute to increased immune activation and HIV infection.

Several studies have reported peripheral MAIT cell depletion in both acute and chronic HIV infections that is not fully reversed upon suppressive combination antiretroviral therapy (474–476,655). During chronic HIV infection there is also gut barrier dysfunction and translocation of bacterial products into the circulation (479,656), which is associated with activation and exhaustion of the remaining MAIT cell population (476). Thus, the loss and dysfunction of MAIT cells during HIV infection may contribute to an elevated risk of acquiring tuberculosis and other bacterial infections (469,472).

7.1.1.2 MAIT cells are highly activated and reveal a heterogeneous population following TLR7 and TLR8 stimulation

Although TLRs are predominantly expressed in innate immune cells, some TLRs are also functionally expressed in adaptive immune cells like B cells and T cells, and therefore certain TLR ligands can modulate T-cell activation either directly or indirectly via proinflammatory cytokines (657,658). TLR7 and TLR8 stimulation may model stimulation with HIV genetic material. During HIV, infection MAIT cells are found to be highly activated, exhausted, and then highly depleted as they lose functionality (476). CD69 is a membrane-bound, type II C lectin receptor used as an early marker of activation, mostly expressed on surface of activated lymphocytes (648). CD69 can be detected within 2-3 h of stimulation. However, CD69 expression is transient as it peaks 18–24 h after stimulation, then decreases (659).

The effect of TLR7 and TLR8 stimulation on MAIT cell CD69 expression was investigated with the aim of understanding whether MAIT cells are activated early during viral infections. In section 4.2.3 (**Figure 16**) TLR7 and TLR8 stimulation led to a significant increase in the frequency of CD69⁺ MAIT cells ($p < 0.0001$), and it remained high even after 24 h. Furthermore, tSNE analysis revealed apparent phenotypic differences in MAIT cells, with some appearing to be highly activated and others moderately activated after stimulation. Other MAIT cells appeared not to express CD69 at all. **Figure 17** also showed that MAIT cells expressed a higher CD69 MFI compared to conventional CD4⁺ and CD8⁺ T cells that express low CD69 MFI.

In similar studies, MAIT cells were shown to express cytokine receptors, and therefore during viral infection they can be activated via cytokines expressed by APCs following TLR7 and TLR8 stimulation, including IL-12 and IL-18 (525,660).

It is possible that some MAIT cells are more responsive to stimulation than others. MAIT cells express an invariant TCR α -chain paired with one of a select group of TCR β -chains (586,661). In humans, the TCR α -chain encoded by the TRAV1-2 gene combined with the segment encoded by the TRAJ33 gene segment, with limited non-nucleotide (N) additions/deletions at the TRAV1-2-TRAJ33 junction (585). Although the human MAIT TCR β -chain repertoire was considered to mainly be encoded by *TRBV20*, *TRBV6-1*, and *TRBV6-4* genes (586), MR1-tetramer-based studies have demonstrated that the MAIT TCR β -chain repertoire is more diverse (585,662,663). It may be that the diversity of MAIT cell compartments observed in this study is due to variability in the β -chain.

MAIT cells also display a transcriptional profile characterized by the expression of promyelocytic leukemia zinc finger (PLZF), also called zinc finger and BTB domain containing 16 (ZBTB16), and retinoid-related orphan receptor (ROR) γ t (456,598,664). They also express eomesodermin (Eomes) and T box transcription factor 21 (TBX21 or T-bet) (477,665), which are reciprocally expressed in effector and memory CD8⁺ T cells (665)), and Helios (or IKAROS family zinc finger 2, IKZF2) (477,649), which are involved in T-cell activation and proliferation (666). Therefore, MAIT cells may display receptor diversity, and the phenotypic differences of activated MAIT cells require further study using flow cytometry and single-cell transcriptomics. Furthermore, since surrogate markers were used to define the MAIT cell population, it is possible that some cell populations classified as MAIT cells were not, as defined by MR1AgTet (667). We can also speculate that high CD69 expression on MAIT cells following TLR7 and TLR8 stimulation is a characteristic of MAIT cells, because some MAIT cells are CD161⁺⁺ and some are CD161⁺ (625). CD161 is a C-type lectin-like receptor expressed on the majority of NK cells (668). CD161 was shown to define NK cells that have retained the ability to respond to IL-12 and IL-18 during differentiation, expressing the highest levels of IFN- γ and CD69 following stimulation compared to CD161⁻ T cells (596). MAIT cells have been shown to undergo degranulation following activation (453,669), and increased degranulation has been associated with increased HIV

infection (670). The observed increased activation of MAIT cells supports the hypothesis that activation of MAIT cells may result in immune activation and increased HIV infection.

7.1.1.3 TLR8 stimulation led to MAIT cell activation and expression of IFN- γ and GM-CSF while TLR7 stimulation activated MAIT cells but did not lead to cytokine expression

MAIT cells can be activated in a TCR-dependent or TCR-independent manner via cytokines expressed following TLR stimulation leading to expression of proinflammatory cytokines (189). Increased proinflammatory cytokines is associated with immune activation and increased susceptibility to HIV infection (671). Although most studies have looked at cytokine-mediated stimulation of MAIT cells (189,672–674), little is known about the effect of TLR7 and TLR8 stimulation on the activation of and cytokine expression by MAIT cells.

In section 4.2.6 (**Figure 19**), the effect of TLR7 and TLR8 stimulation on cytokine expression by MAIT cells was assessed with the aim of understanding whether MAIT cells express cytokines during viral infection. Although MAIT cells were activated after both TLR7 and TLR8 stimulation, TLR7 stimulation did not lead to IFN- γ , TNF- α , IL-17a or GM-CSF expression by MAIT cells ($p>0.05$). TLR8 stimulation did not lead to significant increase in TNF- γ and IL-17a, but it did lead to a significant increase in both IFN- γ ($p<0.0001$) and GM-CSF ($p=0.0175$) when exposed to the highest concentration of TLR8 ligand.

Similar to what has been reported in virus-mediated MAIT cell activation (468,675), cytokine-mediated MAIT cell activation primarily induces IFN- γ production in MAIT cells (189). IL-12 or IL-15 together with IL-18 can directly stimulate MAIT cells to produce IFN- γ (567,676,677) and release granzyme B and perforin (569). Type I IFNs significantly induce IFN- γ and granzyme B only when combined with IL-12 or IL-18 (567). Likewise, the gut-associated proinflammatory cytokine TNF-like protein 1A (TL1A/TNFSF15) activates MAIT cells in combination with IL-12 and IL-18 (678).

The results in **Figure 19** show that a higher dose of ssRNA40 (TLR8 ligand) is required to stimulate MAIT cell IFN- γ expression, and that TLR8 but not TLR7 stimulation led to IFN- γ expression. We can postulate that TLR7 and TLR8 activate different pathways and have a unique

pattern of cell type-specific expression that is thought to be responsible for the response to different pathogens. TLR7 mRNA was detected at high levels in pDCs and B cells; only low mRNA expression was detected in monocytes, macrophages, mDCs, and MDDCs; whereas TLR8 mRNA was found to be highly expressed in monocytes, mDCs, MDDCs, and macrophages (679). Since TLR8 is expressed in more cell types, this may imply that TLR8 stimulation leads to increased expression of more than one type of cytokine that stimulate MAIT cells to express IFN- γ . Cytokine-mediated induction of IFN- γ by T cells requires simultaneous stimulation by more than two cytokines (568,680). Although TLR7 stimulation led to increased frequencies of CD69+ MAIT cells, it did not lead to a significant increase in IFN- γ or any other cytokines tested by MAIT cells. TLR7 stimulation has been shown to contribute to IFN- α expression by pDC in both *in vitro* and *in vivo* experiments (567,673,681–686). Therefore, viral infections that induce mainly type I IFN expression did not result in any increase in IFN- γ or any other cytokine in MAIT cells (453).

Activation of MAIT cells results in increased proinflammatory cytokine expression (189,678). Proinflammatory cytokines in the lower reproductive tract have been associated with increased immune activation and high frequencies of neutrophils, T and B cells (687,688). Women with higher concentrations of proinflammatory cytokines, including MIP-1 α , MIP-1 β , and IP-10, in their genital tracts have been reported to be at higher risk of HIV acquisition (165). Since HIV replication depends on the presence of target cells and the level of immune cell activation and monocyte differentiation to macrophages or dendritic cells, and proinflammatory cytokines and chemokines are involved in activation, differentiation and recruitment of immune cells to the genital tract, this may increase HIV transmission (687,689). In rhesus macaques, vaginal SIV exposure led to proinflammatory cytokine production, which resulted in recruitment of CD4+ T cells required for establishment of SIV infection (690,691). Furthermore, the major role of inflammation in SIV infection was highlighted when topical application of the anti-inflammatory glycerol-monolaurate downregulated chemokine concentrations, inhibited inflammatory cell influx to the genital tract, and prevented SIV infection in macaques (690).

Since increased cytokine expression by MAIT cells after TLR7 stimulation was not observed (**Figure 19**), this may not support the hypothesis that TLR7 stimulation leads to MAIT cell cytokine expression and immune activation, which is associated with increased HIV infection.

However, our results may not reflect *in vivo* TLR7 stimulation under complex conditions. Furthermore, TLR7 stimulation may lead to expression of other factors that were not assessed in this experiment that may be involved in driving immune activation. TLR8 stimulation led to increase in frequency of IFN- γ + MAIT cells (**Figure 19**) which may increase immune activation that is associated with increased HIV susceptibility, therefore supporting my hypothesis.

7.1.1.4 TLR7 and TLR8 stimulation moderately increased CD69 expression by $\gamma\delta$ T cells

Human $\gamma\delta$ T cells express some TLRs and can be activated directly by corresponding ligands (523,524). In addition, $\gamma\delta$ T cells can be indirectly activated via cytokines after TLR stimulation of APCs (609).

In section 4.3, the effect of TLR7 and TLR8 stimulation on $\gamma\delta$ T cell CD69 expression was evaluated in order to understand whether $\gamma\delta$ T cells are activated early during viral infection. There was an increase in CD69 expression by $\gamma\delta$ T cells after TLR7 and TLR8 stimulation ($p < 0.0001$) (**Figure 22**). Moderately high levels of activation of $\gamma\delta$ T cells were observed, compared to the minimal activation of CD4⁺ and CD8⁺ T cells after TLR7 and TLR8 stimulation. Analysis of CD69 expression on $\gamma\delta$ T cells by tSNE revealed heterogeneity of the $\gamma\delta$ T cell population. Although there was no significant difference detected in the frequency of CD69⁺ cells between the $\gamma\delta$ TCR^{high} and $\gamma\delta$ TCR^{low} subpopulations of $\gamma\delta$ T cells, there was significantly higher frequency of CD69⁺ cells among CD161⁺ compared to CD161⁻ $\gamma\delta$ T cells ($p < 0.0001$) (**Figure 32**).

In a similar study, $\gamma\delta$ T cells were shown to express moderate CD69 after 24 h stimulation with rIL-12 alone, rIL-12 combined with α CD3/CD28, or rIL-12 combined with bromohydrin pyrophosphates (BrHPP) (692).

We can speculate that the moderate expression of CD69 occurs because compared to MAIT cells, only a subset of $\gamma\delta$ T cells (60%) express CD161. V γ 9V δ 2 $\gamma\delta$ T cells are the major population of CD161⁺ $\gamma\delta$ T cells, and the CD161⁺ subset has been shown to have enhanced innate-like phenotype and functionality (567,662). Cells expressing high CD161 may be highly activated compared to cells that do not express CD161. The observed heterogeneity in $\gamma\delta$ T cell activation may also be due to different subsets of $\gamma\delta$ T cell in the circulation. In human peripheral blood there

are two main subsets of $\gamma\delta$ T cells, V δ 1 and V δ 2, and the V γ 9V δ 2 subset constitutes the main circulating $\gamma\delta$ T cells (527,693,694). Since activated $\gamma\delta$ T cells have been shown to act as APCs leading to activation of $\alpha\beta$ T cells (695), it is possible that $\gamma\delta$ T cell activation may increase activation of other T lymphocytes, leading to immune activation and HIV infection.

7.1.1.5 TLR8 stimulation activated $\gamma\delta$ T cells and IFN- γ expression, while TLR7 stimulation activated $\gamma\delta$ T cells but did not lead to cytokine expression

Human $\gamma\delta$ T cells express some TLRs, and the corresponding ligands can directly modify $\gamma\delta$ T cell activation (657,696). In addition, some indirect effects of ligands for some TLR upon $\gamma\delta$ T cell activation, mediated via APC cells, have been reported (696).

Section 4.3.3 investigated the effect of TLR7 and TLR8 stimulation on IFN- γ , TNF- α , IL-17a, and GM-CSF expression by $\gamma\delta$ T cells to understand whether $\gamma\delta$ T cells express cytokines during viral infection. Although there was moderate activation of $\gamma\delta$ T cells after both TLR7 and TLR8 stimulation, TLR7 stimulation did not lead to IFN- γ , TNF- α , IL-17a and GM-CSF expression by $\gamma\delta$ T cells (**Figure 24**). TLR8 stimulation did not lead to a significant increase in TNF- γ and IL-17a expression by $\gamma\delta$ T cells. However, TLR8 stimulation led to a significant increase in of IFN- γ ($p < 0.0001$) and GM-CSF ($p = 0.0175$) expression by $\gamma\delta$ T at the highest concentration tested.

This result is similar to what was reported by Serrano et al (696). Also, in a similar study, TLR7 stimulation did not lead to IFN- γ expression, but TLR8 stimulation led to expression of IFN- γ by $\gamma\delta$ T cells (697). A third similar study also showed that stimulation of V γ 9V δ 2 T cells with IL-18 and IL-12 led to expression of IFN- γ (698).

It is possible that a higher ssRNA40 dose than was applied would be required to stimulate TLR8 enough to lead to cytokine expression. Although $\gamma\delta$ T cells are shown to be directly activated by TLR, it may be that they express low or no TLR7. Since increased cytokine expression by $\gamma\delta$ T cells after TLR7 was not observed in **Figure 24**, this may not support our hypothesis that TLR7 stimulation may lead to the $\gamma\delta$ T cell cytokine expression and immune activation that is associated with increased HIV infection. However, these results may not reflect *in vivo* TLR7 stimulation, where conditions are complex. Furthermore, TLR7 stimulation may lead to expression of other

factors were not assessed in this experiment that may be involved in driving immune activation. Nevertheless, in **Figure 24**, TLR8 stimulation led to IFN- γ expression by $\gamma\delta$ T cells, which may increase the immune activation associated with increased HIV susceptibility, therefore supporting my hypothesis.

7.1.1.6 Media supplementation with rIL-7 further increased IFN- γ , IL-17a, and GM-CSF expression by MAIT and $\gamma\delta$ T cells after TLR8 stimulation

MAIT cells have been shown to be highly activated and to lose functionality in patients with chronic HIV infections (458). IL-7 is expressed by non-hematopoietic stromal cells, with small amounts of the cytokine produced by DCs (699). IL-7 is used for immunotherapy to rescue T cells. Treatment of *ex vivo* MAIT cells isolated from HIV-1 infected patients with IL-7 was previously shown to restore their effector functions (477). Furthermore, subcutaneous injection of IL-7 could restore the levels of MAIT cells in these HIV-1 infected patients (700). IL-7 immunotherapy is currently being evaluated as a treatment to reverse lymphopenia in COVID-19 patients; it was shown to restore lymphocyte count in critically ill COVID-19 patients without worsening pulmonary injury and inflammation (701). Although human $\gamma\delta$ T cells represent a relatively small subset of T cells in peripheral blood, they are enriched in epithelial and mucosal tissues where they are thought to serve as the first line of defense against pathogenic challenge (702,703). IL-7 has been shown to stimulate expansion of Th17 $\gamma\delta$ T cells (704).

Section 4.4 describes the comparison of cytokine expression by MAIT, $\gamma\delta$, CD4⁺ and CD8⁺ T cells after TLR7 and TLR8 stimulation in media with or without IL-7 to understand the pattern of response of T cells to viral infections. Incubation with IL-7 made no significant difference in the frequency of IFN- γ ⁺, TNF α ⁺, or GM-CSF⁺ MAIT cells, $\gamma\delta$ T cells, or CD4⁺ or CD8⁺ T cells after TLR7 stimulation ($p > 0.05$ for all) (**Figure 26**). However, IL-7 supplementation resulted in a significantly higher frequency of IFN- γ ⁺, TNF- α ⁺, IL-17a⁺, and GM-CSF⁺ MAIT cells compared to media alone after TLR8 stimulation ($p < 0.05$). Also, stimulation of PBMCs with *E. coli* led to higher IFN- γ ⁺, TNF- α ⁺, IL-17a⁺, and GM-CSF⁺ MAIT cells in media supplemented with IL-7 compared to media alone. There was higher frequency of IFN- γ , TNF- α , IL-17a and GM-CSF by $\gamma\delta$ T cells in PBMCs cultured in media with IL-7 compared to PBMCs cultured in media without IL-7 after TLR8 stimulation ($p < 0.05$ for all). Although there was no significant increase in TNF-

α^+ , IL-17a⁺, and GM-CSF⁺, I observed significantly higher frequencies of IFN- γ^+ CD4⁺ and CD4⁺ CD8⁺ T cells within PBMCs supplemented with IL-7 than within PBMCs cultured in media alone after TLR8 stimulation ($p < 0.05$).

In a similar study, stimulation of MAIT cells with IL-12/IL-18 together with IL-7 led to high expression of IFN- γ and TNF- α (621).

Treatment of MAIT cells with IL-7 may increase cytokine expression and increase polyfunctionality of the MAIT cells and $\gamma\delta$ T cells. We can further speculate that although IL-7 immunotherapy increases T cells and improves the effector function of MAIT and $\gamma\delta$ T cells, thereby improving protection against bacterial infections, IL-7 may also increase proinflammatory cytokine expression, leading to immune activation and increased HIV susceptibility. CD161⁺⁺CD8⁺ T cells have been linked to several inflammatory conditions independent of bacterial infections. They have been detected in the brains of patients with multiple sclerosis, where they are thought to play a pathogenic role (705). They have also been found to be enriched in the liver of patients with liver diseases including chronic hepatitis C (HCV) infections, primary biliary cirrhosis, alcohol liver disease and non-steatohepatitis (626,706). MAIT cell activation has also been implicated in SARS-CoV-2 severity (707). Overall, there is overwhelming evidence implicating CD161⁺⁺CD8⁺ T cells including MAIT cells in inflammation [18–20].

7.1.2 MAIT cells and $\gamma\delta$ T cells express high levels of chemokine receptors

Chemokines and their corresponding receptors are involved in migration of leukocytes (708). Migration of leukocytes is essential for immune surveillance of the body's tissues, and for focusing immune cells to sites of antigenic challenge (709,710).

Section 4.5 describes the investigation of chemokine receptor expression by MAIT cells and $\gamma\delta$ T cells in *ex vivo* PBMCs isolated from the whole blood of healthy donors, compared with conventional CD4⁺ and CD8⁺ T cells. The aim was to determine whether major differences in expression patterns exist. A significantly higher frequency of MAIT cells expressed CCR5⁺, CCR6⁺ and CCR4⁺ cells than conventional CD4⁺ and CD8⁺ T cells ($p < 0.05$) (**Figure 33**). However, there was no significant difference in the frequency of CXCR3⁺ and CXCR6⁺ between

MAIT and conventional CD4⁺ and CD8⁺ T cells. There was a higher frequency of CCR5⁺ and CCR6⁺ $\gamma\delta$ T cells compared to CCR5⁺ CD4⁺ T cells and CCR5⁺ CD8⁺ T cells ($p < 0.002$). There was significantly a higher CXCR3⁺ CD8⁺ T cells compared to $\gamma\delta$ T cells ($p = 0.437$).

A similar study that compared chemokine expression in peripheral blood MAIT cells compared to lymph node MAIT cells revealed high expression of CCR6 in both blood and lymph MAIT cells, higher CCR4 expression in blood MAIT cells compared to lymph MAIT cells and higher expression of CXCR3 by lymph MAIT cells compared to blood MAIT cells (711). Furthermore, a study that evaluated chemokine expression in $\gamma\delta$ T cells vs. $\alpha\beta$ T cells in healthy blood donors reported higher CCR5 and CXCR3 on $\gamma\delta$ T cells (712). MAIT cells have been reported to preferentially home to tissues, especially the gut, liver and the lung, due to their high expression of multiple chemokine receptors and integrins such as $\alpha 4\beta 7$ (441). All CD8 α MAIT cells have shown co-expression of CCR6 with CD161 (713). CCR5 and CXCR3 have been shown to be expressed on activated T lymphocytes with a memory phenotype and to control the migration of activated T cells to the site of inflammation (352). Human adult blood MAIT cells have effector memory phenotype (CD45RO⁺, CD27⁺, CCR7⁻, CD44^{high}, CD62L^{low}) and express numerous integrin and tissue-homing chemokine receptors (CCR5^{high}, CCR6^{high}, CXCR6^{high}, CCR9^{int}) (366,714–716). Thus, MAIT cells have been shown to home to peripheral tissues at local inflammatory sites (717–719). The effector memory phenotype is also expressed in $\gamma\delta$ T cells (720,721).

Figure 33 shows intense CCR5 and CCR6 expression as a selective feature of *ex vivo*–analyzed peripheral blood MAIT and $\gamma\delta$ T cells, which distinguishes these cells from circulating conventional T lymphocytes. We can speculate that MAIT and $\gamma\delta$ T cells are poised to migrate promptly to local tissue during an antigenic challenge, where they express Th1 cytokines and GM-CSF, which increases differentiation and maturation of DCs and improves conventional T cell activation and recruitment. The collective result of this may be increased HIV target cells and immune activation, which may be associated with increased susceptibility to HIV infection.

7.1.2.1 CCR5 is downregulated on MAIT cells after stimulation

Chemokine receptor expression can be modulated (up- or downregulated) by T cells in response to cellular activation or ligand binding (722). There is evidence that CCR5 is internalized following stimulation with its ligand and later recycled back to cell surface (347).

Section 4.5.1 describes assessment of possible modulation of CCR5 on MAIT cells and $\gamma\delta$ T cells after TLR7 and TLR8 stimulation, with the aim of understanding the effect of MAIT cell and $\gamma\delta$ T cell activation on migration. There was no significant change in the frequency of MAIT cells expressing CCR5 2, 6, 14, or 24 h after TLR7 stimulation; nor was there a significant change in frequency of CCR5+ MAIT cell 2 or 6h after TLR8 stimulation (**Figure 34**). There was a significant downregulation of the frequency of CCR5+MAIT cells 14 h ($p=0.0317$) and 24 h ($p=0.0435$) post TLR8 stimulation. Although there was no significant difference in the frequency of CCR5+MAIT cells after a 2 and 6 h stimulation with *E. coli*, there was a significant reduction in frequency of CCR5+ MAIT cells 14 h ($p=0.0079$) and 24 h ($p=0.0317$) post stimulation with *E. coli*. There was no significant difference in the frequency of CCR5+ $\gamma\delta$ T cells after 2, 6, 14, or 24h post TLR7 or TLR8 stimulation. Neither was there any significant difference in the frequency of CCR5+ $\gamma\delta$ T cells after stimulation with *E. coli* at any time point. Although there was no significant change in CCR5 expression by CD4+ T cells after TLR7 or TLR8 stimulation, *E. coli* stimulation of PBMCs with led to a significant reduction in CCR5+ CD4+ T cells.

A similar study evaluating the effect of seminal plasma on CCR5 expression on T cells revealed that seminal plasma induced CCR5 ligand secretion, resulting in the downregulation of CCR5 on T cells. However, seminal plasma exposure *in vivo* failed to downregulate CCR5 and, in some cases, resulted in increased frequencies of CD4+ CCR5+ T cells at the vaginal mucosa (723).

It is possible that CCR5 may have been internalized in MAIT cells following ligation with its ligand. Thus, MAIT cell stimulation during exposure to HIV may lead to changes in MAIT cell migration patterns. However, since the *in vitro* experiment is a closed system, this result may not reflect *in vivo* conditions. Further investigation is required using *in vivo* experimental models to assess effect of TLR8 stimulation of MAIT cells alters CCR5 expression.

7.1.3 TLR8 stimulation results in higher MDDC maturation markers compared to TLR7 stimulation

DCs are the most potent APCs (184). Circulating monocytes differentiate into immature DCs, therefore continuously replenishing tissues with immature DCs. These capture antigens and migrate to germinal centers, where they present antigens as mature DCs (724,725). Pathogen recognition by pattern recognition receptors (PRR) causes maturation of immature DCs and their migration to lymphoid organs (726). DCs cell surface express MR1, a nonpolymorphic MHC class IB antigen-presenting molecule that is required for TCR-mediated activation of MAIT cells (727).

Section 5.4.3 examines the effect of TLR7 and TLR8 stimulation on the expression of CD83, CD80, HLA-DR, and CD11C by MDDCs, which were differentiated by culturing *ex vivo* monocytes, isolated from whole blood of healthy donors, in the presence of GM-CSF and IL-4 with the aim of understanding the effect of TLR7 and TLR8 stimulation of immature MDDCs on maturation (**Figure 38**). TLR7 stimulation did not lead to significant changes in the frequency of CD11C⁺, HLA-DR⁺, CD80⁺, or CD83⁺ MDDCs. Neither did TLR8 stimulation lead to significant changes in the frequency of CD11C⁺ or HLA-DR⁺ MDDCs; however, there was a significant difference in the frequency of CD80⁺ and CD83 (p<0.05) cells after TLR8 stimulation.

A similar study that investigated the involvement of MAPK, NF-KB, and JAK/STAT signalling pathways in the maturation of human MDDCs derived from CD34⁺ progenitors induced by TLR7 or TLR8 agonists showed that both TLR7 and TLR8 stimulation increased the maturation markers CD40, CD86, and CD83 on MDDCs (728). This difference from the present study can be explained by the MDDC source, which in this thesis is adult peripheral blood.

We can speculate that the poor induction of maturation markers observed after TLR7 stimulation may be due to either the low frequency of TLR7⁺ MDDCs or the low level of TLR7 MFI on MDDCs. Although TLR7 is expressed in plasmacytoid DCs (pDCs) (203,729), its expression in CD11C⁺ mDCs is still controversial (730,731). In some studies, TLR7 expression was not detected in human MDDCs (732). Other studies have reported low or no TLR7 and high levels of TLR8 expression in MDDCs (728). Still others have reported that although TLR8 is highly expressed on

MDDCs, TLR7 expression is donor dependent (732,733). However, recently, it was reported that MDDCs and Langerhans cell (LC)-like DCs derived from CD34+ hematopoietic progenitors expressed low levels of TLR7 (734), suggesting that the origin of the DCs, and the culture protocol used, may determine TLR7 expression. MDDC differentiation led to downregulation of CD14. In some studies, TLR7 expression was not detected in human MDDCs (732).

7.1.3.1 MDDCs matured by TLR8 stimulation secrete higher amounts of IL-12p70 compared to MDDC matured by TLR7 stimulation

DC maturation has also been shown to lead to expression of IL-12 and IL-18 (263). IL-12 and IL-18 are potent activators of MAIT cells via a TCR-independent mechanism (735).

Section 5.4.5 describes the effect of TLR7 and TLR8 stimulation on the production of IL-12p70 and IL-18 after culturing monocytes in media supplemented with GM-CSF and IL-4 for 7 days. On day 5, the TR7-ligand imiquimod, the TLR8 ligand ssRNA40, or *E. coli* was added to the culture. After 2 days of stimulation, the supernatant was harvested and IL-12p70 and IL-18 measured using ELISAs. Although there was no significant change in IL-12p70 production after TLR7 stimulation, I observed a significant increase in IL-12p70 by MDDCs after TLR8 stimulation ($p=0.0079$). There was no significant change in IL-18 after TLR7 or TLR8 stimulation.

A similar study that investigated the IL-12 production by MDDCs, derived from CD34+ progenitors, after TLR7 and TLR8 stimulation reported that TLR8 but not TLR7 stimulation led to production of IL-12 by MDDCs (728). Although little is known about IL-18 secretion by MDDCs after TLR7 and TLR8 stimulation, a study by Kolb-Mäurer et al. (263) revealed that infection of immature MDDCs with *Listeria monocytogenes* led to the secretion of both IL-12 and IL-18.

The observed lack of IL-12 and IL-18 secretion by MDDCs in this study after TLR7 stimulation may be a result of using GM-CSF and IL-4 in the differentiation of MDDCs. IL-4 has been shown to suppress DC responses to stimulation with TLR7 and TLR9 and to inhibit the expression and secretion of the classic proinflammatory cytokines IL-12, TNF- α , and IL-6 upon TLR7 and TLR9

stimulation (736,737). The lack of IL-18 secretion after TLR8 stimulation may also reflect a requirement for other stimulatory pathways to activate MDDCs and secrete IL-18.

7.1.4 MAIT cells induction alters HIV replication in vitro

TLR7 and TLR8 stimulation of MAIT cells occurs *in vivo* via cytokines expressed by APCs. Cytokine-mediated stimulation of MAIT cells has been shown to lead to expression of IFN- γ , CCR5 ligands, granzyme B, and perforin (189,455,678), which may interfere with HIV infection of CD4⁺ T cells. Section 6.2.1 assesses the effect of MAIT stimulation with rIL-18 and rIL-12 on HIV infection of CD4⁺ T cells. Lower HIV-p24 expression was observed in CD4⁺ T cells co-cultured with activated MAIT cells before infection. Furthermore, cell death occurred in co-cultures with activated MAIT cells.

A similar study reported an increase in HIV-1 restriction factors that reduced levels of infection in MAIT cells during early stages of HIV infection (738). In another study that evaluated MAIT cell phenotypes before infection and during acute and chronic HIV infection, MAIT cells were expanded during acute HIV infection but were highly activated and depleted during chronic HIV infection. The innateness of MAIT cells, which includes IL-18 receptor expression, was also increased (478).

The findings in section 6.2.1 suggest that activation of MAIT cells before exposure to HIV may not prevent HIV infection but may contribute to reduced HIV infection of CD4⁺ T cells. MAIT cells may also contribute to the death of activated CD4⁺ T cells during HIV infection via degranulation and expression of cytotoxic molecules. Thus, MAIT cells may increase immune activation via expression of Th1 cytokines and degranulation, releasing perforin and granzyme A/B that activate the immune system. High cytokine expression by MAIT cells may lead to reduced integrity of the mucosa and increase in mucosal HIV transmission. However, MAIT cells have also been shown to maintain mucosal homeostasis, and cytokines expressed by MAIT cells may contribute to tissue repair (739). It is possible that MAIT cells also contribute to the antiviral response by expressing MIP-1 α , MIP-1 β , RANTES, and MCP-1, 3 and 4, which compete with CCR5, therefore reducing infection.

Activated MAIT cells may express IFN- γ , which promotes antiviral immunity through its regulatory effects on the innate immune response and acts as a key link between the innate immune response and activation of the adaptive immune response (114). IL-12 and IL-18 stimulation of MAIT cells has been shown to lead to the expression of proinflammatory cytokines including IL-17A and IL-17F, which promote tissue inflammation (674). Lower IL-17 levels in blood and genital mucosa of highly exposed HIV-seronegative female sex workers was associated with reduced inflammation and HIV infection (411). The most common sites of HIV-1 transmission are mucosal. Cytokine assays from freshly acquired colorectal biopsy explants revealed lower proinflammatory cytokines and T cell density in HESN homosexual men (740). MAIT cells are positioned to respond early to infection (622). Activation of MAIT cells has been shown to lead to expression of proinflammatory cytokines (189).

7.1.4.1 Measuring p24 by antibody flow cytometry staining and ELISA

Although both assays measure p24 protein expression, p24 antibody staining (ICS) measures intracellular p24 in CD4⁺ cells as an infected percentage of total CD4⁺ cells, whereas p24 ELISA measures p24 protein secreted into the media (741). Both assays are used to assess HIV replication, and although ICS is convenient, fast, and cheaper than ELISA, ICS is less sensitive (742). The amount of p24 in the culture media is proportional to the amount of virus particles (743).

7.1.5 A proposed role for unconventional MAIT and $\gamma\delta$ T cell stimulation in immune activation and HIV infection

HIV infection thrives in activated rather than resting CD4⁺ T cells. It has been hypothesized that in HESN, a state of immune quiescence in which there is lowered immune activation is associated with reduced risk of HIV acquisition due to the lowered capacity of HIV to infect target cells and allowing anti-HIV adaptive responses to clear or limit virus establishment. Although various studies have demonstrated the development of HIV-specific responses, the mechanism involved is not well known. MAIT cells are strategically located in mucosal layers, and in the female genital tract they make up to 2% of T cells in the cervix and 6% of T cells in the endometrium (649). Based on the findings of this thesis, early exposure to HIV PAMPs such as ssRNA may result in early activation of MAIT and $\gamma\delta$ T lymphocytes, which express IFN- γ . HIV-specific IFN- γ has

been associated with a reduced risk of HIV infection in infants who remained HIV seronegative for one year even though they were breastfed by HIV+ mothers (744).

TLR8 stimulation was shown to lead to MAIT and $\gamma\delta$ T cells activation and GM-CSF expression. Activated $\gamma\delta$ T cells have been shown to affect CD4+ and CD8+ T cell responses, either directly by expressing cytokines that increase maturation of DCs or indirectly by adjuvant activity on professional APCs (74,745). MAIT cells and $\gamma\delta$ T cells may be driving increased activation of CD4+ T cells via three different mechanisms. First, MAIT cell activation has been shown to lead to increased expression of CD40L, which in turn leads to maturation of MDDCs (73,327). During HIV infection, this may increase antigen presentation to CD4+ T cells, increased immune activation and HIV infection. Since HIV replication depends on the presence of target cells, the level of immune cell activation, and monocyte differentiation to macrophages or dendritic cells, and since proinflammatory cytokines and chemokines are involved in activation, differentiation, and recruitment of immune cells to the genital tract, all of this may increase HIV transmission (687,689). These supports the hypothesis that MAIT and $\gamma\delta$ T cells activation may increase immune activation therefore increasing the risk of HIV acquisition.

Secondly, exposure of unconventional T cells to bacteria may result in activation and expression of proinflammatory cytokines including IFN- γ and TNF- α , which may interfere with mucosal integrity (746) and increase the risk of HIV infection. Activation of MAIT cells has been shown to lead to increased expression of proinflammatory cytokines (189,678). Women with higher concentrations of proinflammatory cytokines, including MIP-1 α , MIP-1 β , and IP-10, in their genital tracts have been reported to be at higher risk of HIV acquisition (165). Proinflammatory cytokines in the lower reproductive tract have been associated with increased immune activation and high frequencies of neutrophils, T and B cells (687,688). In rhesus macaques, vaginal SIV exposure led to proinflammatory cytokine production, which resulted in recruitment of CD4+ T cells needed for establishment of SIV infection (690,691). Furthermore, the major role of inflammation in SIV infection was highlighted when topical application of the anti-inflammatory glycerol-monolaurate downregulated chemokine concentrations, inhibited inflammatory cell influx to the genital tract, and prevented SIV infection in macaques (690).

I propose that TLR8 maturation of MDSCs leads to expression of IL-12p70, activating MAIT cells and leading to IFN- γ release. TLR7 stimulation increased CD69⁺ conventional CD4⁺ T cells, while TLR8 stimulation resulted in an HIV-specific immune response. Inflammation creates a favourable environment for HIV replication and establishment of a productive infection.

A third mechanism by which MAIT cells and $\gamma\delta$ T cells may be driving increased activation of CD4⁺ T cells is based on the evidence that MAIT cells and $\gamma\delta$ T cells undergo degranulation following activation (453,622,669,747). Increased degranulation has been associated with increased HIV infection (670). In this thesis, I showed that MAIT cells and $\gamma\delta$ T cells are highly activated following TLR7 and TLR8 stimulation. I propose that this may lead to increased degranulation of MAIT and $\gamma\delta$ T cells, resulting in increased activation of other cells of the immune system and therefore immune activation and HIV infection.

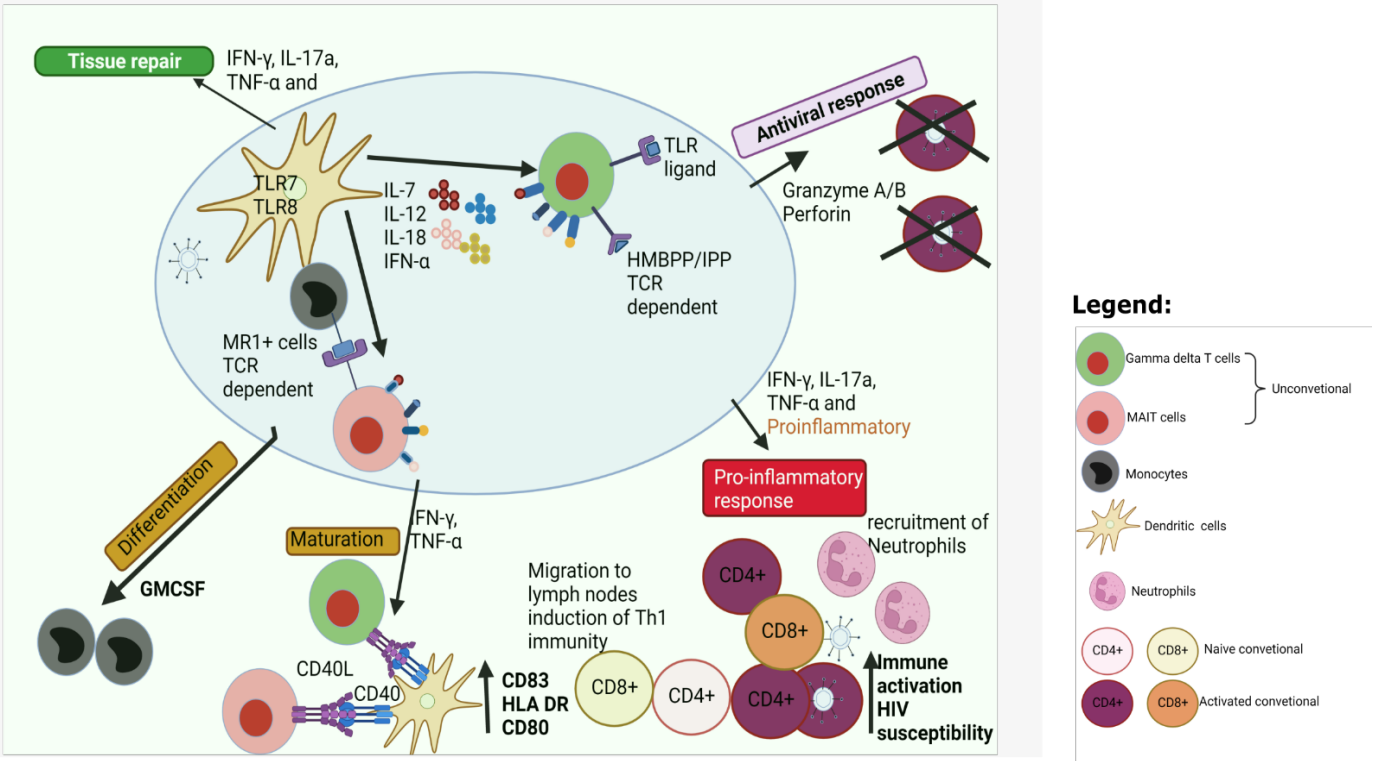


Figure 44. Proposed role for MAIT and $\gamma\delta$ T cell stimulation in immune activation and HIV susceptibility. MAIT cells respond to riboflavin metabolites presented by MR1, and $\gamma\delta$ T cells recognize HMBPP or phosphoantigens. TLR7 and TLR8 stimulation leads to expression of cytokines including IL-12, IL-18, IL-7, and IFN- α , which stimulate MAIT and $\gamma\delta$ T cells. Activated MAIT and $\gamma\delta$ T cells express proinflammatory cytokines, which increase immune activation; GM-CSF, which stimulates monocyte differentiation; and CD40L, TNF- α , and IFN- γ , which stimulate maturation of DCs. DCs migrate to lymphoid tissue where they induce Th1 immunity. Activated MAIT and $\gamma\delta$ T cells degranulate, expressing granzyme A/B and perforin, which lyse infected cells and may increase immune activation. Cytokines expressed by activated MAIT and $\gamma\delta$ T cells, including IL-17, TNF- α and IFN- γ , increase tissue repair.

7.2 Conclusion

In this Thesis I have evaluated the effect of TLR7 and TLR8 stimulation of PBMCs on innate T cell activation, cytokine expression, and modulation of CD4⁺ T cells, which may result in increased or reduced HIV infection. The results showed that MAIT and $\gamma\delta$ T cells are activated after TLR7 and TLR8 stimulation. TLR8 stimulation led to increased IFN- γ expression by MAIT and $\gamma\delta$ T cells, with the latter also expressing TNF- α . Therefore, pre-treatment of PBMCs with TLR8 ligand may make the CD4⁺ T cells more refractory to HIV infection. On the other hand, TLR7 stimulation led to an increase in activated CD4⁺ T cells and may be associated with increased HIV infection.

7.3 Limitations

All experiments were conducted *in vitro*. Considering the complex nature of innate T cell activation, modulation of the immune system, and HIV transmission, the findings of this study can only be used as postulations or as a rationale for trials, for example, of adoptive transfer of MAIT or $\gamma\delta$ T cells, or of TLR8 agonists as therapeutics, or of adjuvants to increase the effectiveness of HIV vaccines. The following are the limitations of this study:

- The study did not quantify TLR7 and TLR8 expression in MDDCs and innate T lymphocytes. This data would have been extremely useful in understanding the differences in responses to TLR7 and TLR8 stimulation. This limitation is due to a lack of sufficient sample, as healthy blood donors were scarce.
- Due to time constraints and the complications brought about by the COVID-19 pandemic, I was unable to assess the effect of MAIT and $\gamma\delta$ T cell activation by cytokines on degranulation.
- Due to lack of an MR1 ligand, I was not able to assess MR1 expression on MDDCs.

7.4 Significance

The search for a vaccine against HIV-1 has many hurdles to overcome. Ideally, the stimulation of both broadly neutralizing antibodies and cell-mediated immune responses remains the best option, but no candidate in clinical trials at present has elicited such antibodies, and efficacy trials have not demonstrated any benefit for vaccines designed to stimulate immune responses of CD8⁺ T cells. Modulation of the immune system through selective activation of TLR pathways are being evaluated as therapeutics for treating allergies and malignancies as well as infectious and autoimmune diseases. Unconventional T cells, including MAIT and $\gamma\delta$ T cells, have become evident as important immune mediators in both inflammatory and infectious diseases. While their role in immune activation and HIV infection and progression has not been fully elucidated, MAIT and $\gamma\delta$ T cells have been shown to be enriched in mucosal surfaces, and they play an important role as the first line of defense against pathogens and in modulation of the adaptive immune system. Therefore, understanding how MAIT and $\gamma\delta$ T cell activation modulates the immune system, leading to increase or prevention of immune activation and HIV infection, is important in developing HIV vaccines and/or a cure. TLR7 and TLR8 are being evaluated for use as a vaccine and/or adjuvants for different diseases, including cancer, hepatitis B, and HIV.

This Thesis demonstrates that simulating the recognition of HIV through TLR7 and TLR8 agonists such as ssRNA40 and imiquimod leads to activation of MAIT and $\gamma\delta$ T cells, but that only TLR8 stimulation results in cytokine expression. Knowledge of how the immune system works in the initial phase of HIV infection, such as the activity and properties of MAIT and $\gamma\delta$ T cells, can facilitate the finding of future interventions. This is the first study to show that *in vitro*, MAIT cells do not prevent infection, but they restrict HIV replication. MAIT cells are mainly CD8⁺ T cells, and stimulation of CD8⁺ T cells is being evaluated by others as an HIV vaccine with promising results. To realize this goal, there is a need for greater understanding of the nature of protective MAIT cell TLR7 or TLR8 responses, as a means to guide the selection of suitable TLR7 or TLR8 agonists or antagonists for microbicide development. Several studies have demonstrated the HIV inhibitory effect of TLR8 agonist ssRNA, and the HIV infection enhancing effects of TLR7-imiquimod treatments *in vitro* and *in vivo*. This study is the first to compare the effects of selectively activating TLR7 or TLR8 signalling pathways on MAIT and $\gamma\delta$ T cell stimulation. This

is also the first study to demonstrate differences in cytokine production profiles by T cells following TLR7 or TLR8 stimulation and their potential importance on HIV infectivity *in vitro*. Cytokine expression by MAIT and $\gamma\delta$ T cells described by others *in vitro* was also present in the healthy donors recruited for this Thesis. This study is also the first to compare cytokines in MAIT cells, $\gamma\delta$ T cells, and conventional CD4⁺ and CD8⁺ cells after TLR7 or TLR8 stimulation. It is the first to compare chemokine receptor expression on MAIT cells, $\gamma\delta$ T cells, and conventional CD4⁺ and CD8⁺ cells as well as the effect of TLR8 stimulation on CCR5 expression by MAIT and $\gamma\delta$ T cells. Finally, this study is also the first to assess MR1 expression on MDDCs and the effect of TLR stimulation of MAIT cells via IL-12 and IL-18 on HIV infectivity.

The major findings from this work are (i) the higher activation of antiviral functions in MAIT cells and $\gamma\delta$ T cells after TLR8 stimulation compared to TLR7 stimulation in healthy individuals and (ii) the potential of MAIT cells to limit HIV infectivity *in vitro*. Finally, this work represents the first reporting that differences in the profiles of MDDC activation have been linked MAIT cell activation and susceptibility to HIV *in vitro*. TLR8 but not TLR7 stimulation led to maturation of MDDCs and expression of IL-12 and IL-18. This demonstrates that the specific ligand, and the immune subset it activates, have consequences on HIV susceptibility.

7.5 Future directions

The main finding of this Thesis is the discovery of MAIT and $\gamma\delta$ T cell responses to TLR7 and TLR8 stimulation with respect to HIV infectivity *in vitro* in PBMCs of healthy blood donors. There are many questions arising from this, many which could not be exhaustively addressed within the scope of this Thesis. Therefore, I would like to propose some future directions which may be beneficial in advancing the findings of this study. The first is comparison of MAIT cell and $\gamma\delta$ T cell responses to TLR7 and TLR8 stimulation in HESN and HIV susceptible populations. Although there are many studies that have evaluated conventional T cells in HESN and susceptible populations (380,382,383,748–750), little is known about differences in MAIT cell and $\gamma\delta$ T cell phenotypes and cytokine responses to TLR7 and TLR8 in these groups. Such studies may reveal the role of innate T cells in HIV protection or susceptibility during HIV infection. Secondly, since HIV-specific cytotoxic T cells responses have been shown to be high in HESN, innate T cells which have been shown to be highly cytotoxic could be explored for immunotherapy and vaccine

development. In this thesis I have shown that activated MAIT cells co-cultured with infected CD4+ T cells led to cell death. However, the number of donors was small, and therefore there is need to perform more experiments with more blood donors to confirm the findings.

A third proposed future direction is a complete proteomic assessment and RNA sequencing of MAIT and $\gamma\delta$ T cell activation after TLR7 and TLR8 stimulation. My work revealed heterogeneity of MAIT cells and $\gamma\delta$ T cells after TLR7 and TLR8 stimulation. Although quantitative mass spectrometry has been used to quantify proteins that differentiate the MAIT cell TCR-dependent immune response from that of conventional CD8+ T cells (751), little is known about the proteins expressed by MAIT cells following TLR7 and TLR8 stimulation. Another study applied a multi-omics approach using global transcriptomic, proteomic and metabolomic profiling to define MAIT cell activation after stimulation with IL-12/IL-18, anti-CD3/CD28, or both. However, little is known about the profile of proteins expressed by MAIT cells after TLR7 and TLR8 stimulation. Comparing cytokine and chemokine expression, cytotoxic factors, and transcription factors by MAIT cells in PBMCs, colon, and genital tract following TLR7 and TLR8 stimulation would provide information on different phenotypes of MAIT cells and their activation. Furthermore, identifying genes that are upregulated in MAIT cells following TLR7 and TLR8 stimulation will provide useful information on activation of MAIT cells.

References

1. Friedland GH, Klein RS. Transmission of the Human Immunodeficiency Virus. *N Engl J Med* [Internet]. 1987;317(18):1125–35. Available from: <https://doi.org/10.1056/NEJM198710293171806>
2. Hymes KB, Cheung T, Greene JB, Prose NS, Marcus A, Ballard H, et al. Kaposi's sarcoma in homosexual men—a report of eight cases. *Lancet* (London, England). 1981 Sep;2(8247):598–600.
3. Gottlieb MS, Schroff R, Schanker HM, Weisman JD, Fan PT, Wolf RA, et al. *Pneumocystis carinii* pneumonia and mucosal candidiasis in previously healthy homosexual men: evidence of a new acquired cellular immunodeficiency. *N Engl J Med*. 1981 Dec;305(24):1425–31.
4. Durack DT. Opportunistic infections and Kaposi's sarcoma in homosexual men. Vol. 305, *The New England journal of medicine*. United States; 1981. p. 1465–7.
5. Centers for Disease Control (CDC). A cluster of Kaposi's sarcoma and *Pneumocystis carinii* pneumonia among homosexual male residents of Los Angeles and Orange Counties, California. [Internet]. Vol. 31, *MMWR. Morbidity and mortality weekly report*. 1982. p. 305–7. Available from: <http://www.ncbi.nlm.nih.gov/pubmed/6811844>
6. Masur H, Michelis MA, Greene JB, Onorato I, Stouwe RA, Holzman RS, et al. An outbreak of community-acquired *Pneumocystis carinii* pneumonia: initial manifestation of cellular immune dysfunction. *N Engl J Med*. 1981 Dec;305(24):1431–8.
7. Centers for Disease Control and Prevention. *Epidemiologic Notes and Reports* Immunodeficiency among Female Sexual Partners of Males with Acquired Immune Deficiency Syndrome (AIDS) -- New York [Internet]. Vol. 31, *Morbidity and Mortality Weekly Report*. 1983. p. 1981–3. Available from: <http://www.cdc.gov/mmwr/preview/mmwrhtml/00001221.htm>

8. Hahn BH, Shaw GM, De Cock KM, Sharp PM. AIDS as a zoonosis: Scientific and public health implications. *Science* (80-). 2000;287(5453):607–14.
9. Retroviruses H. HIV sequence database The Human Retroviruses and AIDS 1998 Compendium Introduction , Glossary , and Landmarks of the Genome PART I . HIV-1 / CPZ and HIV-2 / SIV Nucleotide Alignments of Complete Genomes PART II . Amino Acid Alignments. 2020;1–3.
10. Sharp PM, Hahn BH. The evolution of HIV-1 and the origin of AIDS. *Philos Trans R Soc B Biol Sci.* 2010;365(1552):2487–94.
11. Vallari A, Holzmayer V, Harris B, Yamaguchi J, Ngansop C, Makamche F, et al. Confirmation of putative HIV-1 group P in Cameroon. *J Virol.* 2011 Feb;85(3):1403–7.
12. HIV strains and types Strains and types Groups within HIV-1 Subtypes within HIV-1 group M Do differences in subtypes matter ? Averting HIV AIDs [Internet]. 2016;1:3–5. Available from: Avert.org
13. UNAIDS. Advancing towards the three zeros. In: UN AIDS Data [Internet]. 2020. Available from: file:///C:/Users/Owner/Desktop/thesis articles/2020_aids-data-book_en.pdf
14. UNAIDS. UNAIDS Data 2018. 2018;1–376.
15. UNAIDS. The cost of inaction: COVID-19-related service disruptions could cause hundreds of thousands of extra deaths from HIV [Internet]. UNAIDS Press Release. 2020. Available from: <https://www.who.int/news/item/11-05-2020-the-cost-of-inaction-covid-19-related-service-disruptions-could-cause-hundreds-of-thousands-of-extra-deaths-from-hiv> <https://www.unaids.org/en/resources/presscentre/pressreleaseandstatementarchive/2020/may/202005>
16. Gonda MA. Molecular genetics and structure of the human immunodeficiency virus. *J*

- Electron Microsc Tech. 1988 Jan;8(1):17–40.
17. Blumenthal R, Durell S, Viard M. HIV entry and envelope glycoprotein-mediated fusion. *J Biol Chem.* 2012;287(49):40841–9.
 18. Zwick MB, Saphire EO, Burton DR. OUR TENTH YEAR gp41 : HIV ' s shy protein. *Nat Med.* 2004;10(2):133–4.
 19. Fiorentini S, Marini E, Caracciolo S, Caruso A. Functions of the HIV-1 matrix protein p17. *New Microbiol.* 2006;29(1):1–10.
 20. Seitz R. Human Immunodeficiency Virus (HIV). *Transfus Med Hemotherapy.* 2016;43(3):203–22.
 21. Gelderblom HR. Fine structure of HIV and SIV. *Los Alamos Natl.* 1997;9 %6:%&.
 22. Giroud C, Chazal N, Briant L. Cellular kinases incorporated into HIV-1 particles: Passive or active passengers? *Retrovirology* [Internet]. 2011;8(1):71. Available from: <http://www.retrovirology.com/content/8/1/71>
 23. Sauter D, Unterweger D, Vogl M, Usmani SM, Heigele A, Kluge SF, et al. Human Tetherin Exerts Strong Selection Pressure on the HIV-1 Group N Vpu Protein. *PLoS Pathog.* 2012;8(12).
 24. Watts JM, Dang KK, Gorelick RJ, Leonard CW, Jr WB, Swanstrom R, et al. performed the statistical analyses; J.W.B. produced and purified HIV-1 virions. *Nature* [Internet]. 2009;460(7256):711–6. Available from: http://www.nature.com/authors/editorial_policies/license.html#terms
 25. Swanstrom R, Wills JW. Synthesis, Assembly, and Processing of Viral Proteins. In: Coffin JM, Hughes SH, Varmus HE, editors. *Cold Spring Harbor (NY)*; 1997.

26. Mattei S, Tan A, Glass B, Müller B, Kräusslich HG, Briggs JAG. High-resolution structures of HIV-1 Gag cleavage mutants determine structural switch for virus maturation. *Proc Natl Acad Sci U S A*. 2018;115(40):E9401–10.
27. Chen Y, Garcia R, Baralle FE. [HIV-1 env glycoprotein gp120 and gp160 expressed in vaccinia virus system and their antigenicity analysis]. *Zhongguo Yi Xue Ke Xue Yuan Xue Bao*. 1997 Apr;19(2):120–6.
28. Coffin JM, Hughes SH VH. *Retroviral Taxonomy, Protein Structures, Sequences, and Genetic Maps - Retroviruses* - NCBI Bookshelf [Internet]. C Retroviruses. Cold Spring Harbor (NY): Cold Spring Harbor Laboratory Press; editor. 1997. Available from: <https://www.ncbi.nlm.nih.gov/books/NBK19417/>
29. Rein A. RNA Packaging in HIV. *Trends Microbiol*. 2019;27(8):715–23.
30. Kleinpeter AB, Freed EO. HIV-1 maturation: Lessons learned from inhibitors. *Viruses*. 2020;12(9).
31. Hutson TH, Foster E, Moon LDF, Yáñez-Muñoz RJ. Lentiviral vector-mediated rna silencing in the central nervous system. *Hum Gene Ther Methods*. 2014;25(1):14–32.
32. Wu L, Gerard NP, Wyatt R, Choe H, Parolin C, Ruffing N, et al. CD4-induced interaction of primary HIV-1 gp120 glycoproteins with the chemokine receptor CCR-5. *Nature*. 1996 Nov;384(6605):179–83.
33. Antu DK, David KB, Per J, Klasse A, Moore JP. Specific amino acids in the N-terminus of the gp41 ectodomain contribute to the stabilization of a soluble, cleaved gp140 envelope glycoprotein from human immunodeficiency virus type 1. *Virology* [Internet]. 2007;360(1):199–208. Available from: <https://www.ncbi.nlm.nih.gov/pmc/articles/PMC1857345/pdf/nihms20217.pdf>
34. Didigu CA, Doms RW. Novel approaches to inhibit HIV entry. *Viruses*. 2012;4(2):309–

- 24.
35. Stein BS, Gowda SD, Lifson JD, Penhallow RC, Bensch KG, Engleman EG. pH-independent HIV entry into CD4-positive T cells via virus envelope fusion to the plasma membrane. *Cell*. 1987 Jun;49(5):659–68.
36. Abbondanzieri, Elio A (Department of Chemistry and Chemical Biology, Harvard University, Cambridge, MA 02138 U, Gregory, Bokinsky (Department of Chemistry and Chemical Biology, Harvard University, Cambridge, MA 02138 U, Rausch JW, Zhang, Jennifer X (Department of Chemistry and Chemical Biology, Harvard University, Cambridge, MA 02138 U, LeGrice SF. J, Zhuang X. Dynamic binding orientations direct activity of HIV reverse transcriptase. *Nature*. 2008;10(1):11–23.
37. Auewarakul P, Wacharapornin P, Srichatrapimuk S, Chutipongtanate S, Puthavathana P. Uncoating of HIV-1 requires cellular activation. *Virology*. 2005;337(1):93–101.
38. Arhel N. Revisiting HIV-1 uncoating. *Retrovirology* [Internet]. 2010;7(1):96. Available from: <http://www.retrovirology.com/content/7/1/96>
39. Levin JG, Mitra M, Mascarenhas A, Musier-Forsyth K. Role of HIV-1 nucleocapsid protein in HIV-1 reverse transcription. *RNA Biol*. 2010;7(6):754–74.
40. Roebuck KA, Saifuddin M. Regulation of HIV-1 transcription. *Gene Expr*. 1999;8(2):67–84.
41. Sandri-Goldin RM. Viral Regulation of mRNA Export. *J Virol*. 2004;78(9):4389–96.
42. Fischer U, Huber J, Boelens WC, Mattajt LW, Lührmann R. The HIV-1 Rev Activation Domain is a nuclear export signal that accesses an export pathway used by specific cellular RNAs. *Cell*. 1995;82(3):475–83.
43. Henderson BR, Percipalle P. Interactions between HIV Rev and nuclear import and export

- factors: The Rev nuclear localisation signal mediates specific binding to human importin- β . *J Mol Biol.* 1997;274(5):693–707.
44. Olson ED, Musier-Forsyth K. Retroviral Gag protein - RNA interactions: Implications for specific genomic RNA packaging and virion assembly. *Semin Cell Dev Biol* [Internet]. 2019;86:129–39. Available from: <https://www.ncbi.nlm.nih.gov/pmc/articles/PMC6167211/pdf/nihms957328.pdf>
 45. Briggs JAG, Grünewald K, Glass B, Förster F, Kräusslich HG, Fuller SD. The mechanism of HIV-1 core assembly: Insights from three-dimensional reconstructions of authentic virions. *Structure.* 2006;14(1):15–20.
 46. Vogt VM. Proteolytic processing and particle maturation. *Curr Top Microbiol Immunol.* 1996;214:95–131.
 47. Wieggers K, Rutter G, Kottler H, Tessmer U, Hohenberg H, Kräusslich H-G. Sequential Steps in Human Immunodeficiency Virus Particle Maturation Revealed by Alterations of Individual Gag Polyprotein Cleavage Sites. *J Virol.* 1998;72(4):2846–54.
 48. Langford SE, Ananworanich J, Cooper DA. Predictors of disease progression in HIV infection: A review. *AIDS Res Ther.* 2007;4:1–14.
 49. Gonzalo-Gil E, Ikediobi U, Sutton RE. Mechanisms of virologic control and clinical characteristics of HIV+ elite/viremic controllers. *Yale J Biol Med.* 2017;90(2):245–59.
 50. Kulkarni PS, Butera ST, Duerr AC. Resistance to HIV-1 infection: lessons learned from studies of highly exposed persistently seronegative (HEPS) individuals. *AIDS Rev.* 2003;5(2):87–103.
 51. McLaren PJ, Blake Ball T, Wachihi C, Jaoko W, Kelvin DJ, Danesh A, et al. HIV-exposed seronegative commercial sex workers show a quiescent phenotype in the CD4+ T cell compartment and reduced expression of HIV-dependent host factors. *J Infect Dis.*

- 2010;202(SUPP.3):339–44.
52. Makedonas G, Bruneau J, Lin H, Sékaly R-P, Lamothe F, Bernard NF. HIV-specific CD8 T-cell activity in uninfected injection drug users is associated with maintenance of seronegativity. *AIDS*. 2002 Aug;16(12):1595–602.
 53. Clerici M, Levin JM, Kessler HA, Harris A, Berzofsky JA, Landay AL, et al. HIV-specific T-helper activity in seronegative health care workers exposed to contaminated blood. *JAMA*. 1994 Jan;271(1):42–6.
 54. Clerici M, Giorgi J V, Chou CC, Gudeman VK, Zack JA, Gupta P, et al. Cell-mediated immune response to human immunodeficiency virus (HIV) type 1 in seronegative homosexual men with recent sexual exposure to HIV-1. *J Infect Dis*. 1992 Jun;165(6):1012–9.
 55. Mazzoli S, Trabattoni D, Lo Caputo S, Piconi S, Blé C, Meacci F, et al. HIV-specific mucosal and cellular immunity in HIV-seronegative partners of HIV-seropositive individuals. *Nat Med*. 1997 Nov;3(11):1250–7.
 56. Winchester R, Pitt J, Charurat M, Magder LS, Göring HHH, Landay A, et al. Mother-to-child transmission of HIV-1: strong association with certain maternal HLA-B alleles independent of viral load implicates innate immune mechanisms. *J Acquir Immune Defic Syndr*. 2004 Jun;36(2):659–70.
 57. Clerici M, Sison A V, Berzofsky JA, Rakusan TA, Brandt CD, Ellaurie M, et al. Cellular immune factors associated with mother-to-infant transmission of HIV. *AIDS*. 1993 Nov;7(11):1427–33.
 58. Tiemessen CT, Shalekoff S, Meddows-Taylor S, Schramm DB, Papathanasopoulos MA, Gray GE, et al. Cutting Edge: Unusual NK cell responses to HIV-1 peptides are associated with protection against maternal-infant transmission of HIV-1. *J Immunol*. 2009 May;182(10):5914–8.

59. Salkowitz JR, Purvis SF, Meyerson H, Zimmerman P, O'Brien TR, Aledort L, et al. Characterization of high-risk HIV-1 seronegative hemophiliacs. *Clin Immunol.* 2001 Feb;98(2):200–11.
60. Horton RE, McLaren PJ, Fowke K, Kimani J, Ball TB. Cohorts for the study of HIV-1-exposed but uninfected individuals: Benefits and limitations. *J Infect Dis.* 2010;202(SUPP.3):377–81.
61. Shearer G, Clerici M. Historical perspective on HIV-exposed seronegative individuals: Has nature done the experiment for us? *J Infect Dis.* 2010;202(SUPP.3):329–32.
62. Restrepo C, Rallón NI, del Romero J, Rodríguez C, Hernando V, López M, et al. Low-Level Exposure to HIV Induces Virus-Specific T Cell Responses and Immune Activation in Exposed HIV-Seronegative Individuals. *J Immunol.* 2010;185(2):982–9.
63. Fowke KR, Nagelkerke NJD, Kimani J, Simonsen JN, Anzala AO, Bwayo JJ, et al. Resistance to HIV-1 infection among persistently seronegative prostitutes in Nairobi, Kenya. *Lancet.* 1996;348(9038):1347–51.
64. Boileau C, Bruneau J, Al-Nachawati H, Lamothe F, Vincelette J. A prognostic model for HIV seroconversion among injection drug users as a tool for stratification in clinical trials. *J Acquir Immune Defic Syndr.* 2005;39(4):489–95.
65. Follézou JY, Lan NY, Lien TX, Lafon ME, Tram LT, Hung P V., et al. Clinical and biological characteristics of human immunodeficiency virus- infected and uninfected intravascular drug users in Ho Chi Minh City, Vietnam. *Am J Trop Med Hyg.* 1999;61(3):420–4.
66. Vivier E, Malissen B. Innate and adaptive immunity: Specificities and signaling hierarchies revisited. *Nat Immunol.* 2005;6(1):17–21.
67. Iwasaki A, Medzhitov R. Control of adaptive immunity by the innate immune system. *Nat*

- Immunol. 2015;16(4):343–53.
68. Janeway CA Jr, Walport M, et al. TP. Principles of innate and adaptive immunity - Immunobiology - NCBI Bookshelf. New York: Garland Science. 2001. p. 1–9.
 69. Kamm K, Schierwater B, Desalle R. Innate immunity in the simplest animals - Placozoans. BMC Genomics. 2019;20(1):1–12.
 70. Storey M, Jordan S. An overview of the immune system. Nurs Stand. 2008;23(15–17):1777–89.
 71. Delves PJ, Roitt IM. First of Two Parts Three Levels Of Defense. Adv Immunol. 2000;37–49.
 72. Delves PJ, Fred S Rosen. Advances in immunology: Complement (second of two parts). N Engl J Med. 2001;344(15):1140–114.
 73. Salio M, Gasser O, Gonzalez-Lopez C, Martens A, Veerapen N, Gileadi U, et al. Activation of Human Mucosal-Associated Invariant T Cells Induces CD40L-Dependent Maturation of Monocyte-Derived and Primary Dendritic Cells. J Immunol. 2017;199(8):2631–8.
 74. Ismaili J, Olislagers V, Poupot R, Fournié JJ, Goldman M. Human $\gamma\delta$ T cells induce dendritic cell maturation. Clin Immunol. 2002;103(3 I):296–302.
 75. Petrasca A, Doherty DG. Human $V\delta 2^+$ $\gamma\delta$ T cells differentially induce maturation, cytokine production, and alloreactive T cell stimulation by dendritic cells and B cells. Front Immunol. 2014;5(DEC):1–11.
 76. Gottschalk C, Mettke E, Kurts C. The role of invariant natural killer T cells in dendritic cell licensing, cross-priming, and memory CD8⁺ T cell generation. Front Immunol. 2015;6(JUL):2–9.

77. Bennett MS, Round JL, Leung DT. Innate-like lymphocytes in intestinal infections. *Curr Opin Infect Dis.* 2015;28(5):457–63.
78. Gary W Litman, Cannon JP, Dishaw LJ. Reconstructing immune phylogeny: new perspectives. *Nat Rev Immunol.* 2005;5(11):866–79.
79. Dean M, Carrington M, Winkler C, Huttley GA, Michael W, Allikmets R, et al. Genetic Restriction of HIV-1 Infection and Progression to AIDS by a Deletion Allele of the CKR5 Structural Gene. *Science* (80-). 1996;273(5283):1856-1862.
80. Samson M, Liber F, Doranz BJ, Rucker J, Liesnard C, Farber C-M, et al. Resistance to HIV-1 infection in caucasian individuals bearing mutant alleles of the CCR-5 chemokine receptor gene. *Nature.* 1996;382(August):722–5.
81. Liu R, Paxton WA, Choe S, Ceradini D, Martin SR, Horuk R, et al. Homozygous defect in HIV-1 coreceptor accounts for resistance of some multiply-exposed individuals to HIV-1 infection. *Cell.* 1996;86(3):367–77.
82. Martinson JJ, Chapman NH, Rees DC, Liu Y, Clegg JB. Global distribution of the CCR5 gene 32-basepair deletion. *Nature* [Internet]. 1997;16(may):100–3. Available from: <http://www.nature.com/naturegenetics>
83. Meyer L, Magierowska M, Hubert JB, Rouzioux C, Deveau C, Sanson F, et al. Early protective effect of CCR-5 Δ 32 heterozygosity on HIV-1 disease progression: Relationship with viral load. *Aids.* 1997;11:73–8.
84. Zimmerman PA, Buckler-White A, Alkhatib G, Spalding T, Kubofcik J, Combadiere C, et al. Inherited resistance to HIV-1 conferred by an inactivating mutation in CC chemokine receptor 5: Studies in populations with contrasting clinical phenotypes, defined racial background, and quantified risk. *Mol Med.* 1997;3(1):23–36.
85. Cocchi F, DeVico AL, Garzino-demo A, Arya SK, Gallo RC, Lusso P, et al. Identification

- of RANTES , MIP-1 α , and MIP-1 β as the Major HIV-Suppressive Factors Produced by CD8 +T Cells. *Science* (80-) [Internet]. 1995;270(5243). Available from: <https://www.jstor.org/stable/2888164>
86. Zagury D, Lachgar A, Chams V, Fall LS, Bernard J, Zagury JF, et al. C-C chemokines, pivotal in protection against HIV type 1 infection. *Proc Natl Acad Sci U S A*. 1998;95(7):3857–61.
 87. Gallo RC, Garzino-Demo A, DeVico AL. HIV infection and pathogenesis: What about chemokines? *J Clin Immunol*. 1999;19(5):293–9.
 88. Koning FA, Jansen CA, Dekker J, Kaslow RA, Dukers N, Van Baarle D, et al. Correlates of resistance to HIV-1 infection in homosexual men with high-risk sexual behaviour. *Aids*. 2004;18(8):1117–26.
 89. Gonzalez E, Kulkarni H, Bolivar H, Mangano A, Sanchez R, Catano G, et al. The influence of CCL3L1 gene-containing segmental duplications on HIV-1/AIDS susceptibility. *Science* (80-). 2005;307(5714):1434–40.
 90. Kuhn L, Schramm DB, Donninger S, Meddows-Taylor S, Coovadia AH, Sherman GG, et al. African infants' CCL3 gene copies influence perinatal HIV transmission in the absence of maternal nevirapine. *Aids*. 2007;21(13):1753–61.
 91. Modi WS, Goedert JJ, Strathdee S, Buchbinder S, Detels R, Donfield S, et al. MCP-1-MCP-3-Eotaxin gene cluster influences HIV-1 transmission. *Aids*. 2003;17(16):2357–65.
 92. Winkler C, Modi W, Smith MW, Nelson GW, Wu X, Carrington M, et al. Genetic restriction of AIDS pathogenesis by an SDF-1 chemokine gene variant. *Science* (80-). 1998;279(5349):389–93.
 93. Soriano A, Martínez C, García F, Plana M, Palou E, Lejeune M, et al. Plasma stromal cell-derived factor (SDF)-1 levels, SDF1-3'A genotype, and expression of CXCR4 on T

- lymphocytes: Their impact on resistance to human immunodeficiency virus type 1 infection and its progression. *J Infect Dis.* 2002;186(7):922–31.
94. Kovacs AAZ, Kono N, Wang C-H, Wang D, Frederick T, Operskalski E, et al. Association of HLA Genotype With T-Cell Activation in Human Immunodeficiency Virus (HIV) and HIV/Hepatitis C Virus-Coinfected Women. *J Infect Dis.* 2020 Mar;221(7):1156–66.
 95. Pegram HJ, Andrews DM, Smyth MJ, Darcy PK, Kershaw MH. Activating and inhibitory receptors of natural killer cells. *Immunol Cell Biol.* 2011;89(2):216–24.
 96. Walker BD, Yu XG. Unravelling the mechanisms of durable control of HIV-1. *Nat Rev Immunol.* 2013;13(7):487–98.
 97. Carrington M, Nelson GW, Martin MP, Kissner T, Vlahov D, Goedert JJ, et al. HLA and HIV-1 : Heterozygote Disadvantage. *Science (80-).* 1999;283(March):1748–52.
 98. Olvera A, Ganoza C, Pérez-Álvarez S, Hildebrand W, Sanchez J, Brander C. HLA-B*35-PX and HLA-B*35-PY subtype differentiation does not predict observed differences in level of HIV control in a Peruvian MSM cohort. Vol. 28, *AIDS (London, England).* England; 2014. p. 2323–5.
 99. Hardie RA, Luo M, Bruneau B, Knight E, Nagelkerke NJD, Kimani J, et al. Human leukocyte antigen-DQ alleles and haplotypes and their associations with resistance and susceptibility to HIV-1 infection. *Aids.* 2008;22(7):807–16.
 100. Sarah F Lockett, Robertson JR, Brettle RP, Yap PL, Middleton D, Brown AJL. Mismatched human leukocyte antigen alleles protect against heterosexual HIV transmission. *JAIDS.* 2001;27:277–80.
 101. Dorak MT, Tang J, Penman-Aguilar A, Westfall AO, Zulu I, Lobashevsky ES, et al. Transmission of HIV-1 and HLA-B allele-sharing within serodiscordant heterosexual

- Zambian couples. *Lancet*. 2004;363(9427):2137–9.
102. MacDonald KS, Embree J, Njenga S, Nagelkerke NJD, Ngatia I, Mohammed Z, et al. Mother-child class I HLA concordance increases perinatal human immunodeficiency virus type 1 transmission. *J Infect Dis*. 1998;177(3):551–6.
 103. Levy JA, Hsueh F, Blackbourn DJ, Wara D, Weintrub PS. CD8 cell noncytotoxic antiviral activity in human immunodeficiency virus-infected and -uninfected children. *J Infect Dis*. 1998;177(2):470–2.
 104. Matta B, Song S, Li D, Barnes BJ. Interferon regulatory factor signaling in autoimmune disease. *Cytokine* [Internet]. 2017;98:15–26. Available from: <http://dx.doi.org/10.1016/j.cyto.2017.02.006>
 105. Watanabe N, Sakakibara J, Hovanessian AG, Taniguchi T, Fujita T. Activation of IFN- β element by IRF-1 requires a post-translational event in addition to IRF-1 synthesis. *Nucleic Acids Res*. 1991;19(16):4421–8.
 106. Jefferies CA. Regulating IRFs in IFN driven disease. *Front Immunol*. 2019;10(MAR):1–15.
 107. Lee J, Chuang TH, Redecke V, She L, Pitha PM, Carson DA, et al. Molecular basis for the immunostimulatory activity of guanine nucleoside analogs: Activation of toll-like receptor 7. *Proc Natl Acad Sci U S A*. 2003;100(11):6646–51.
 108. Ji H, Ball TB, Ao Z, Kimani J, Yao X, Plummer FA. Reduced HIV-1 long terminal repeat transcription in subjects with protective interferon regulatory factor-1 genotype: A potential mechanism mediating resistance to infection by HIV-1. *Scand J Infect Dis*. 2010;42(5):389–94.
 109. Ball TB, Ji H, Kimani J, McLaren P, Marlin C, Hill AVS, et al. Polymorphisms in IRF-1 associated with resistance to HIV-1 infection in highly exposed uninfected Kenyan sex

- workers. *Aids*. 2007;21(9):1091–101.
110. Schneider WM, Chevillotte MD, Rice CM. Interferon-stimulated genes: a complex web of host defenses. *Annu Rev Immunol*. 2014;32:513–45.
 111. Pestka S, Krause CD, Walter MR. Interferons, interferon-like cytokines, and their receptors. *Immunol Rev*. 2004 Dec;202:8–32.
 112. Pestka S, Langer JA, Zoon KC, Samuel CE. Interferons and their actions. *Annu Rev Biochem*. 1987;56:727–77.
 113. Pestka S. The human interferon-alpha species and hybrid proteins. *Semin Oncol*. 1997 Jun;24(3 Suppl 9):S9-4-S9-17.
 114. Lee AJ, Ashkar AA. The dual nature of type I and type II interferons. *Front Immunol*. 2018;9(SEP):1–10.
 115. Bach EA, Aguet M, Schreiber RD. The IFN gamma receptor: a paradigm for cytokine receptor signaling. *Annu Rev Immunol*. 1997;15:563–91.
 116. Pestka S, Kotenko S V, Muthukumaran G, Izotova LS, Cook JR, Garotta G. The interferon gamma (IFN-gamma) receptor: a paradigm for the multichain cytokine receptor. *Cytokine Growth Factor Rev*. 1997 Sep;8(3):189–206.
 117. Kotenko S V, Gallagher G, Baurin V V, Lewis-Antes A, Shen M, Shah NK, et al. IFN-lambdas mediate antiviral protection through a distinct class II cytokine receptor complex. *Nat Immunol*. 2003 Jan;4(1):69–77.
 118. Darnell JEJ, Kerr IM, Stark GR. Jak-STAT pathways and transcriptional activation in response to IFNs and other extracellular signaling proteins. *Science*. 1994 Jun;264(5164):1415–21.

119. Ihle JN. The Janus protein tyrosine kinase family and its role in cytokine signaling. *Adv Immunol.* 1995;60:1–35.
120. Plataniias LC. Mechanisms of type-I- and type-II-interferon-mediated signalling. *Nat Rev Immunol.* 2005;5(5):375–86.
121. Haque SJ, Williams BR. Signal transduction in the interferon system. *Semin Oncol.* 1998 Feb;25(1 Suppl 1):14–22.
122. Sen GC, Sarkar SN. The interferon-stimulated genes: targets of direct signaling by interferons, double-stranded RNA, and viruses. *Curr Top Microbiol Immunol.* 2007;316:233–50.
123. Schoggins JW. Interferon-Stimulated Genes: What Do They All Do? *Annu Rev Virol.* 2019;6:567–84.
124. Colomer-Lluch M, Ruiz A, Moris A, Prado JG. Restriction Factors: From Intrinsic Viral Restriction to Shaping Cellular Immunity Against HIV-1. *Front Immunol.* 2018;9(December):2876.
125. Kane M, Yadav SS, Bitzegeio J, Kutluay SB, Zang T, Wilson SJ, et al. MX2 is an interferon-induced inhibitor of HIV-1 infection. *Nature.* 2013;502(7472):563–6.
126. Kobayashi M, Takaori-Kondo A, Shindo K, Abudu A, Fukunaga K, Uchiyama T. APOBEC3G Targets Specific Virus Species. *J Virol.* 2004;78(15):8238–44.
127. Shattock RJ, Moore JP. Inhibiting Sexual Transmission of I HIV-1 Infetcion. *Nat Publ Gr.* 2003;1(October).
128. Shen R, Richter HE, Clements RH, Novak L, Huff K, Bimczok D, et al. Macrophages in Vaginal but Not Intestinal Mucosa Are Monocyte-Like and Permissive to Human Immunodeficiency Virus Type 1 Infection □. *J Virol.* 2009;83(7):3258–67.

129. Shen R, Richter HE, Smith PD. Early HIV-1 Target Cells in Human Vaginal and Ectocervical Mucosa. *NIH*. 2012;65(3):261–7.
130. Bomsel M, Alfsen A. Entry of Viruses Through the Epithelial Barrier: Pathogenic Trickery. *Nat Publ Gr*. 2003;4(January).
131. Mccoombe SG, Short R V. Potential HIV-1 target cells in the human penis. *AIDS*. 2006;20(January):1491–5.
132. Hirbod T, Bailey RC, Agot K, Moses S, Ndinya-achola J, Murugu R, et al. Abundant Expression of HIV Target Cells and C-Type Lectin Receptors in the Foreskin Tissue of Young Kenyan Men. *Am J Pathol [Internet]*. 2010;176(6):2798–805. Available from: <http://dx.doi.org/10.2353/ajpath.2010.090926>
133. Sennepin A, Real F, Duvivier M, Ganor Y, Henry S, Damotte D, et al. The human Penis is a genuine immunological effector site. *Front Immunol*. 2017;8(December):1–18.
134. Liu A, Yang Y, Liu L, Meng Z, Li L, Qiu C, et al. Differential Compartmentalization of HIV-Targeting Immune Cells in Inner and Outer Foreskin Tissue. *PLoS One*. 2014;9(1):1–10.
135. Zhou Z, Longchamps NB De, Schmitt A, Zerbib M, Ganor Y, Bomsel M. HIV-1 Efficient Entry in Inner Foreskin Is Mediated by Elevated CCL5 / RANTES that Recruits T Cells and Fuels Conjugate Formation with Langerhans Cells. *PLoS Pathog*. 2011;7(6).
136. Ganor Y, Zhou Z, Bodo J, Tudor D, Leibowitch J, Mathez D, et al. The adult penile urethra is a novel entry site for HIV-1 that preferentially targets resident urethral macrophages. *Mucosal Immunol*. 2013;6(4).
137. Mills E, Cooper C, Anema A, Guyatt G. Male circumcision for the prevention of heterosexually acquired HIV infection : a meta-analysis of randomized trials involving 11 050 men *. *HIV Med*. 2008;9:332–5.

138. Dinh MH, Anderson MR, Mcraven MD, Cianci GC. Visualization of HIV-1 Interactions with Penile and Foreskin Epithelia : Clues for Female-to-Male HIV Transmission. *PLoS Pathog.* 2015;11:1–20.
139. Patel P, Borkowf CB, Brooks JT, Lasry A, Lansky A, Mermin J. Estimating per-act HIV transmission risk : a systematic review. *AIDS.* 2014;28(April):1509–1519.
140. Boily M, Baggaley RF, Wang L, Masse B, Richard G. Heterosexual risk of HIV-1 infection per sexual act: a systematic review and meta-analysis of observational studies. *Lancet Infect Dis.* 2009;9(2):118–29.
141. Tugizov S. Human immunodeficiency virus-associated disruption of mucosal barriers and its role in HIV transmission and pathogenesis of HIV / AIDS disease. *Tissue Barriers* [Internet]. 2016;4(3):1–19. Available from: <http://dx.doi.org/10.1080/21688370.2016.1159276>
142. Hladik F, McElrath MJ. Setting the stage: Host invasion by HIV. *Nat Rev Immunol.* 2008;8(6):447–57.
143. Godfrey Kigozi, Wawer M, Ssettuba A, Kagaayi J, Nalugoda F, Watya S, et al. Foreskin surface area and HIV acquisition in Rakai, Uganda (size matters). *AIDS.* 2009;23(16):2209–2213.
144. Telzak EE, Chiasson MA, Bevier PJ, Stoneburner RL, Castro KG, Jaffe HW. HIV-1 Seroconversion in Patients with and without Genital Ulcer Disease A Prospective Study. *Ann Intern Med.* 1993;119(12):1181–6.
145. Weiler AM, Li Q, Duan L, Kaizu M, Weisgrau KL, Friedrich TC, et al. Genital Ulcers Facilitate Rapid Viral Entry and Dissemination following Intravaginal Inoculation with Cell-Associated Simian Immunodeficiency Virus SIVmac239. *J Virol.* 2008;82(8):4154–8.

146. Bracq L, Maorong Xie SB, Bouchet J. Mechanisms for Cell-to-Cell Transmission of Hiv-1. *Front Immunol.* 2018;9(February):1–14.
147. Kolodkin-gal D, Hulot SL, Koriath-schmitz B, Gombos RB, Zheng Y, Owuor J, et al. Efficiency of Cell-Free and Cell-Associated Virus in Mucosal Transmission of Human Immunodeficiency Virus Type 1 and Simian. *J Virol.* 2013;87(24):13589–97.
148. Anderson DJ, Politch JA, Nadolski AM, Blaskewicz CD, Pudney J, Mayer KH. Targeting Trojan Horse leukocytes for HIV prevention. *AIDS.* 2010;24(2):163–87.
149. Tugizov S. Human immunodeficiency virus-associated disruption of mucosal barriers and its role in HIV transmission and pathogenesis of HIV / AIDS disease. *Tissue Barriers* [Internet]. 2016;4(3):1–19. Available from: <http://dx.doi.org/10.1080/21688370.2016.1159276>
150. Nazli A, Chan O, Dobson-belaire WN, Ouellet M, Tremblay MJ, Scott D, et al. Exposure to HIV-1 Directly Impairs Mucosal Epithelial Barrier Integrity Allowing Microbial Translocation. *PLoS Pathog.* 2010;6(4).
151. Sufiawati I, Tugizov SM. HIV-Associated Disruption of Tight and Adherens Junctions of Oral Epithelial Cells Facilitates HSV-1 Infection and Spread. *PLoS One.* 2014;9(2).
152. Dayanithi G, Yahil N, Baghdiguian S, Fantini J. Intracellular calcium release induced by human immunodeficiency virus type 1 (HIV-I) surface envelope glycoprotein in human intestinal epithelial cells : a putative mechanism for HIV-1 enteropathy. *Cell Calcium.* 1995;18:9–18.
153. Pu H, Tian J, Andras IE, Hayashi K, Flora G, Hennig B, et al. HIV-1 Tat protein-induced alterations of ZO-1 expression are mediated by redox-regulated ERK1 / 2 activation. *J Cereb Blood Flow Metab.* 2005;25:1325–35.
154. Nazli A, Kafka JK, Ferreira VH, Mueller K, Osborne BJ, Dizzell S, et al. HIV-1 gp120

- Induces TLR2- and TLR4-Mediated Innate Immune Activation in Human Female Genital Epithelium. *J Immunol.* 2013;191:4246–58.
155. Tugizov SM, Herrera R, Veluppillai P, Greenspan D, Greene WC, Levy JA, et al. HIV is inactivated after transepithelial migration via adult oral epithelial cells but not fetal epithelial cells. *J Virol.* 2012;409(2):211–22.
156. Bobardt MD, Chatterji U, Selvarajah S, Schueren B Van Der, David G, Kahn B, et al. Cell-Free Human Immunodeficiency Virus Type 1 Transcytosis through Primary Genital Epithelial Cells □. *J Virol.* 2007;81(1):395–405.
157. Cohen MS. Preventing Sexual Transmission of HIV. 2007;7030:287–92.
158. Shen R, Richter HE, Smith PD. Interactions between HIV-1 and Mucosal Cells in the Female Reproductive Tract. *NIH.* 2015;71(6):608–17.
159. Galvin SR, Cohen MS. The role of sexually transmitted diseases in HIV transmission. *Nat Rev Microbiol.* 2004;2(1):33–42.
160. Quinn TC, Wawer MJ, Sewankambo N, Serwadda D, Li C, Wabwire-Mangen F, et al. Viral load and heterosexual transmission of human immunodeficiency virus type 1. 2000;921–9.
161. Mole L, Ripich S, Margolis D, Holodniy M. The impact of active herpes simplex virus infection on human immunodeficiency virus load. *J Infect Dis.* 1997;176(3):766–70.
162. Coombs RW, Reichelderfer PS, Landay AL. Recent observations on HIV type-1 infection in the genital tract of men and women. *Aids.* 2003;17(4):455–80.
163. Sturm-Ramirez K, Gaye-Diallo A, Eisen G, Mboup S, Kanki PJ. High levels of tumor necrosis factor- α and interleukin-1 β in bacterial vaginosis may increase susceptibility to human immunodeficiency virus. *J Infect Dis.* 2000;182(2):467–73.

164. Montano MA, Nixon CP, Ndung'u T, Bussmann H, Novitsky VA, Dickman D, et al. Elevated tumor necrosis factor- α activation of human immunodeficiency virus type 1 subtype C in southern Africa is associated with an NF- κ B enhancer gain-of-function. *J Infect Dis.* 2000;181(1):76–81.
165. Masson L, Passmore JS, Liebenberg LJ, Werner L, Baxter C, Arnold KB, et al. Genital Inflammation and the Risk of HIV Acquisition in Women. *Clin Infect Dis.* 2015;61:260–9.
166. Kaul R, Prodger J, Joag V, Shannon B, Yegorov S, Galiwango R, et al. Inflammation and HIV Transmission in Sub-Saharan Africa. *Curr HIV/AIDS Rep.* 2015;12:216–22.
167. Card CM, McLaren PJ, Wachihi C, Kimani J, Plummer FA, Fowke KR. Decreased immune activation in resistance to HIV-1 infection is associated with an elevated frequency of CD4+CD25+FOXP3+ Regulatory T Cells. *J Infect Dis.* 2009;199(9):1318–22.
168. Gupta P, Collins KB, Ratner D, Watkins S, Naus GJ, Landers D V, et al. Memory CD4² T Cells Are the Earliest Detectable Human Immunodeficiency Virus Type 1 (HIV-1) - Infected Cells in the Female Genital Mucosal Tissue during HIV-1 Transmission in an Organ Culture System. *J Virol.* 2002;76(19):9868–76.
169. Mckinnon LR, Nyanga B, Chege D, Kimani M, Huibner S, Gelmon L, et al. Characterization of a Human Cervical CD4 + T Cell Subset Coexpressing Multiple Markers of HIV Susceptibility. *J Immunol.* 2011;187:6032–42.
170. Milush JM, Kosub D, Marthas M, Schmidt K, Scott F, Wozniakowski A, et al. Rapid dissemination of SIV following oral inoculation. *Aids.* 2004;18(18):2371–80.
171. Taborda N, Zapata-Builes W, Montoya C, Rugeles MT. Short communication: Increased expression of secretory leukocyte protease inhibitor in oral mucosa of colombian HIV type 1-exposed seronegative individuals. *AIDS Res Hum Retroviruses.* 2012;28(9):859–

62.

172. Novak RM, Donoval BA, Graham PJ, Boksa LA, Spear G, Hershov RC, et al. Cervicovaginal levels of lactoferrin, secretory leukocyte protease inhibitor, and RANTES and the effects of coexisting vaginoses in Human Immunodeficiency Virus (HIV)-seronegative women with a high risk of heterosexual acquisition of HIV infection. *Clin Vaccine Immunol.* 2007;14(9):1102–7.
173. Yang C, Boone L, Nguyen TX, Rudolph D, Limpakarnjanarat K, Mastro TD, et al. θ -defensin pseudogenes in HIV-1-exposed, persistently seronegative female sex-workers from Thailand. *Infect Genet Evol.* 2005;5(1):11–5.
174. Gonzalez SM, Taborda NA, Feria MG, Arcia D, Aguilar-Jiménez W, Zapata W, et al. High expression of antiviral proteins in mucosa from individuals exhibiting resistance to human immunodeficiency virus. *PLoS One.* 2015;10(6):1–13.
175. Burgener A, Rahman S, Ahmad R, Lajoie J, Ramdahin S, Mesa C, et al. Comprehensive proteomic study identifies serpin and cystatin antiproteases as novel correlates of HIV-1 resistance in the cervicovaginal mucosa of female Sex workers. *J Proteome Res.* 2011;10(11):5139–49.
176. Walker H, Hall W, Hurst J. *The White Blood Cell and Differential Count - Clinical Methods - NCBI Bookshelf.* 1990.
177. van Furth R, Cohn ZA. The origin and kinetics of mononuclear phagocytes. *J Exp Med.* 1968 Sep;128(3):415–35.
178. van Furth R. Monocyte production during inflammation. *Comp Immunol Microbiol Infect Dis.* 1985;8(2):205–11.
179. Liu Y, Wang R, Jiang J, Cao Z, Zhai F, Sun W, et al. A subset of CD1c(+) dendritic cells is increased in patients with tuberculosis and promotes Th17 cell polarization.

- Tuberculosis (Edinb). 2018 Dec;113:189–99.
180. Kadowaki N, Ho S, Antonenko S, De R, Malefyt W, Kastelein RA, et al. Brief Definitive Report Subsets of Human Dendritic Cell Precursors Express Different Toll-like Receptors and Respond to Different Microbial Antigens. *J Exp Med* [Internet]. 2001;098630700(6):863–9. Available from: <http://www.jem.org/cgi/content/full/194/6/863>
 181. Olingy CE, Dinh HQ, Hedrick CC. Monocyte heterogeneity and functions in cancer. *J Leukoc Biol*. 2019;106(2):309–22.
 182. Auffray C, Sieweke MH, Geissmann F. Blood monocytes: Development, heterogeneity, and relationship with dendritic cells. *Annu Rev Immunol*. 2009;27:669–92.
 183. Steinman RM. The dendritic cell system and its role in immunogenicity. *Annu Rev Immunol*. 1991;9:271–96.
 184. Banchereau J, Steinman RM. Dendritic cells and the control of immunity. [Review] [103 refs]. *Nature*. 1998;392(6673):245–52.
 185. Abbas A. K., and Lichtman, A. H. *Cellular and Molecular Immunology* (5th Ed. 2003).
 186. Parihar A, Eubank TD, Doseff AI. Monocytes and macrophages regulate immunity through dynamic networks of survival and cell death. *J Innate Immun*. 2010;2(3):204–15.
 187. Shey MS, Balfour A, Wilkinson KA, Meintjes G. Contribution of APCs to mucosal-associated invariant T cell activation in infectious disease and cancer. *Innate Immun*. 2018;24(4):192–202.
 188. Kjer-nielsen L, Mccluskey J, Rossjohn J, Awad W. Mucosal-associated invariant T cell receptor recognition of small molecules presented by MR1. 2018;588–97.

189. Lamichhane R, Schneider M, de la Harpe SM, Harrop TWR, Hannaway RF, Dearden PK, et al. TCR- or Cytokine-Activated CD8⁺ Mucosal-Associated Invariant T Cells Are Rapid Polyfunctional Effectors That Can Coordinate Immune Responses. *Cell Rep* [Internet]. 2019;28(12):3061-3076.e5. Available from: <https://doi.org/10.1016/j.celrep.2019.08.054>
190. Peng G, Greenwell-Wild T, Nares S, Jin W, Lei KJ, Rangel ZG, et al. Phagocytes_ Myeloid differentiation and susceptibility to HIV-1 are linked to APOBEC3 expression. 2007.
191. Berger A, Sommer AFR, Zwarg J, Hamdorf M, Welzel K, Esly N, et al. SAMHD1-deficient CD14⁺ cells from individuals with Aicardi-Goutières syndrome are highly susceptible to HIV-1 infection. *PLoS Pathog*. 2011;7(12):1–12.
192. Ivey NS, MacLean AG, Lackner AA. Acquired immunodeficiency syndrome and the blood-brain barrier. *J Neurovirol*. 2009;15(2):111–22.
193. Chayt KJ, Harper ME, Marselle LM, Lewin EB, Rose RM, Oleske JM, et al. Detection of HTLV-III RNA in Lungs of Patients With AIDS and Pulmonary Involvement. *JAMA J Am Med Assoc*. 1986;256(17):2356–9.
194. Brown A, Zhang H, Lopez P, Pardo CA, Gartner S. In vitro modeling of the HIV-macrophage reservoir. *J Leukoc Biol*. 2006;80(5):1127–35.
195. Koenig S, Gendelman HE, Orenstein JM, Canto MC, Pezeshkpour H, Yungbluth M, et al. Detection of AIDS Virus in Macrophages in Brain Tissue from AIDS Patients with Encephalopathy Stable. *Am Assoc Adv Sci* [Internet]. 2016; Available from: <http://www.jstor.org/stable/1697543>
196. Schrier RD, McCutchan JA, Venable JC, Nelson JA, Wiley CA. T-cell-induced expression of human immunodeficiency virus in macrophages. *J Virol*. 1990;64(7):3280–8.

197. Rich EA, Chen ISY, Zack JA, Leonard ML, O'Brien WA. Increased susceptibility of differentiated mononuclear phagocytes to productive infection with human immunodeficiency virus-1 (HIV-1). *J Clin Invest.* 1992;89(1):176–83.
198. Freudenthal PS, Bhardwaj N. Dendritic cells in human blood and synovial exudates. *Int Rev Immunol.* 1990;6(2–3):103–16.
199. Merad M, Manz MG. Dendritic cell homeostasis. *Blood.* 2009;113(15):3418–27.
200. Freudenthal PS, Steinman RM. The distinct surface of human blood dendritic cells, as observed after an improved isolation method. *Proc Natl Acad Sci U S A.* 1990;87(19):7698–702.
201. Brooks CF, Moore M. Differential MHC class II expression on human peripheral blood monocytes and dendritic cells. *Immunology* [Internet]. 1988;63(2):303–11. Available from:
<http://www.ncbi.nlm.nih.gov/pubmed/3350576><http://www.pubmedcentral.nih.gov/articlerender.fcgi?artid=PMC1454506>
202. Collin M, Mcgovern N, Haniffa M. Human dendritic cell subsets. Vol. 140, *Immunology.* 2013. p. 22–30.
203. Jarrossay D, Napolitani G, Colonna M, Sallusto F, Lanzavecchia A. Specialization and complementarity in microbial molecule recognition by human myeloid and plasmacytoid dendritic cells. *Eur J Immunol.* 2001;31(11):3388–93.
204. Szabo A, Rajnavolgyi E. Collaboration of Toll-like and RIG-I-like receptors in human dendritic cells: tRIGgering antiviral innate immune responses. *Am J Clin Exp Immunol* [Internet]. 2013;2(3):195–207. Available from:
<http://www.ncbi.nlm.nih.gov/pubmed/24179728><http://www.pubmedcentral.nih.gov/articlerender.fcgi?artid=PMC3808934>

205. Unterholzner L. The interferon response to intracellular DNA: Why so many receptors? *Immunobiology* [Internet]. 2013;218(11):1312–21. Available from: <http://dx.doi.org/10.1016/j.imbio.2013.07.007>
206. Lanzavecchia A, Sallusto F. Regulation of T cell immunity by dendritic cells. *Cell*. 2001;106(3):263–6.
207. Ferlazzo G, Münz C. NK Cell Compartments and Their Activation by Dendritic Cells. *J Immunol*. 2004;172(3):1333–9.
208. Hladik F, Sakchalathorn P, Ballweber L, Lentz G, Fialkow M, Eschenbach D, et al. Article Initial Events in Establishing Vaginal Entry and Infection by Human Immunodeficiency Virus Type-1. *Immunity* [Internet]. 2007;26(2):257–70. Available from: <http://dx.doi.org/10.1016/j.immuni.2007.01.007>
209. Merad M, Ginhoux F, Collin M. Origin , homeostasis and function of Langerhans cells and other langerin- expressing dendritic cells. *Nat Rev Immunol*. 2008;8:935–47.
210. Yu HJ, Reuter MA, McDonald D. HIV Traffics through a Specialized , Surface-Accessible Intracellular Compartment during trans-Infection of T Cells by Mature Dendritic Cells. *PLoS Pathog*. 2008;4(8).
211. Cameron PU, Freudenthal PS, Barker JM, Gezelter S, Inaba K, Steinman RM, et al. Dendritic Cells Exposed to Human Immunodeficiency Virus Type-1 Transmit a Vigorous Cytopathic Infection to CD4+ T Cells. *Science* (80-). 1992;257(5068):383–7.
212. Wong BR, Josien R, Lee SY, Sauter B, Li HL, Steinman RM, et al. TRANCE (tumor necrosis factor [TNF]-related activation-induced cytokine), a new TNF family member predominantly expressed in T cells, is a dendritic cell-specific survival factor. *J Exp Med*. 1997 Dec;186(12):2075–80.
213. De Witte L, Nabatov A, Pion M, Fluitsma D, De Jong MAWP, De Gruijl T, et al.

- Langerin is a natural barrier to HIV-1 transmission by Langerhans cells. *Nat Med.* 2007;13(3):367–71.
214. Kawamura T, Koyanagi Y, Nakamura Y, Ogawa Y, Yamashita A, Iwamoto T, et al. Significant Virus Replication in Langerhans Cells following Application of HIV to Abraded Skin: Relevance to Occupational Transmission of HIV. *J Immunol.* 2008;180(5):3297–304.
215. De Jong MAWP, De Witte L, Oudhoff MJ, Gringhuis SI, Gallay P, Geijtenbeek TBH. TNF- α and TLR agonists increase susceptibility to HIV-1 transmission by human Langerhans cells ex vivo. *J Clin Invest.* 2008;118(10):3440–52.
216. Akira S, Uematsu S, Takeuchi O. Pathogen recognition and innate immunity. *Cell.* 2006;124(4):783–801.
217. Gonzalez S, González-Rodríguez AP, Suárez-Álvarez B, López-Soto A, Huergo-Zapico L, Lopez-Larrea C. Conceptual aspects of self and nonself discrimination. *Self/Nonself - Immune Recognit Signal.* 2011;2(1):19–25.
218. Kubelkova K, Macela A. Innate Immune Recognition : An Issue More Complex Than Expected. *Front Cell Infect Microbiol.* 2019;9(July):1–19.
219. Smole U, Kratzer B. Soluble pattern recognition molecules : Guardians and regulators of homeostasis at airway mucosal surfaces. *Eur J Immunol.* 2020;50:624–42.
220. Kawai T, Akira S. The role of pattern-recognition receptors in innate immunity : update on Toll-like receptors. *Nat Publ Gr.* 2010;11(5):373–84.
221. Triantafilou M, Gamper FGJ, Haston RM, Mouratis MA, Morath S, Hartung T, et al. Membrane sorting of toll-like receptor (TLR)-2/6 and TLR2/1 heterodimers at the cell surface determines heterotypic associations with CD36 and intracellular targeting. *J Biol Chem.* 2006 Oct;281(41):31002–11.

222. Motoi Y, Shibata T, Takahashi K, Kanno A, Murakami Y, Li X, et al. Lipopeptides are signaled by Toll-like receptor 1, 2 and 6 in endolysosomes. *Int Immunol*. 2014 Oct;26(10):563–73.
223. Jin MS, Kim SE, Heo JY, Lee ME, Kim HM, Paik S, et al. Crystal Structure of the TLR1-TLR2 Heterodimer Induced by Binding of a Tri-Acylated Lipopeptide. *Cell*. 2007;1071–82.
224. Kang JY, Nan X, Jin MS, Youn S, Ryu YH, Mah S, et al. Article Recognition of Lipopeptide Patterns by Toll-like Receptor 2-Toll-like Receptor 6 Heterodimer. *Immunity* [Internet]. 2009;31(6):873–84. Available from: <http://dx.doi.org/10.1016/j.immuni.2009.09.018>
225. Akira S, Uematsu S, Takeuchi O. Pathogen Recognition and Innate Immunity. *Cell*. 2006;3:783–801.
226. Kawai T, Akira S. Toll-like Receptor and RIG-1-like Receptor Signaling. *Ann New York Acad Sci*. 2008;20:1–20.
227. Kawai T, Akira S. Innate immune recognition of viral infection. *Nat Immunol*. 2006;7(2):11–6.
228. Gordon KB, Gorski KS, Gibson SJ, Kedl RM, Kieper WC, Qiu X, et al. Synthetic TLR Agonists Reveal Functional Differences between Human TLR7 and TLR8. *J Immunol*. 2005;174(3):1259–68.
229. Shibata T, Ohto U, Nomura S, Kibata K, Motoi Y, Zhang Y, et al. Guanosine and its modified derivatives are endogenous ligands for TLR7. *Int Immunol*. 2016 May;28(5):211–22.
230. Oshiumi H, Sasai M, Shida K, Fujita T, Matsumoto M, Seya T. TIR-containing Adapter Molecule (TICAM) -2 , a Bridging Adapter Recruiting to Toll-like Receptor 4 TICAM-1

- That. *J Biol Chem* [Internet]. 2003;278(50):49751–62. Available from:
<http://dx.doi.org/10.1074/jbc.M305820200>
231. Yamamoto M, Sato S, Mori K, Hoshino K, Takeuchi O, Takeda K, et al. Cutting Edge: A Novel Toll/IL-1 Receptor Domain-Containing Adapter That Preferentially Activates the IFN- β Promoter in the Toll-Like Receptor Signaling. *J Immunol*. 2002;169:6668–72.
 232. Kagan JC, Su T, Horng T, Chow A, Akira S, Medzhitov R. TRAM couples endocytosis of Toll-like receptor 4 to the induction of interferon- β . *Nat Immunol*. 2008;9(4):361–8.
 233. Fitzgerald KA, Chen ZJ. Previews Sorting out Toll Signals. *Cell*. 2006;834–6.
 234. Li X, Yang Y, Ashwell JD. TNF-RII and c-IAP1 mediate ubiquitination and degradation of TRAF2. *Nat Immunol*. 2002;3378(1991):639–43.
 235. Wang C, Deng L, Hong M, Akkaraju GR. TAK1 is a ubiquitin-dependent kinase of MKK and IKK. *Nat Immunol*. 2001;412(July).
 236. Kawasaki T, Kawai T. Toll-like receptor signaling pathways. *Front Immunol*. 2014;5(September):1–8.
 237. Yamamoto M, Sato S, Hemmi H. Role of Adaptor TRIF in the. *Science* (80-). 2003;301(August):640–4.
 238. Doyle SE, Vaidya SA, Connell RO, Dadgostar H, Dempsey PW, Wu T, et al. IRF3 Mediates a TLR3 / TLR4-Specific Antiviral Gene Program. *Immunity*. 2002;17:251–63.
 239. Takeda K, Akira S. TLR signaling pathways. *Semin Immunol*. 2004;16:3–9.
 240. Silhavy TJ, Kahne D, Walker S. The Bacterial Cell Envelope1 T. J. Silhavy, D. Kahne and S. Walker, . *Cold Spring Harb Perspect Biol* [Internet]. 2010;2:1–16. Available from:
<https://www.ncbi.nlm.nih.gov/pmc/articles/PMC2857177/pdf/cshperspect-PRK->

241. Sizar O, Unakal CG. Gram Positive Bacteria. In Treasure Island (FL); 2022.
242. Ramachandran G. Gram-positive and gram-negative bacterial toxins in sepsis. *Landes Biosci.* 2014;5(1):213–8.
243. Lu Y-C, Yeh W-C, Ohashi PS. LPS/TLR4 signal transduction pathway. *Cytokine.* 2008 May;42(2):145–51.
244. Alexopoulou L, Thomas V, Schnare M, Yves L, Juan A, Robert, T S, et al. Hyporesponsiveness to vaccination with *Borrelia burgdorferi* OspA in humans and in TLR1- and TLR2-deficient mice. *Nat Med* •. 2002;8(8).
245. Ozinsky A, Underhill DM, Fontenot JD, Hajjar AM, Smith KD, Wilson CB, et al. The repertoire for pattern recognition of pathogens by the innate immune system is defined by cooperation between Toll-like receptors. *PNAS.* 2000;
246. Yonekura K, Maki-yonekura S, Namba K. Complete atomic model of the bacterial flagellar filament by electron cryomicroscopy. *Nature.* 2003;643–50.
247. Hayashi F, Smith KD, Ozinsky A, Hawn TR, Yi EC, Goodlett DR, et al. The innate immune response to bacterial flagellin is mediated by Toll-like receptor 5. *Nature.* 2001;410(April):1–5.
248. Hawn TR, Verbon A, Lettinga KD, Zhao LP, Li SS, Laws RJ, et al. A Common Dominant TLR5 Stop Codon Polymorphism Abolishes Flagellin Signaling and Is Associated with Susceptibility to Legionnaires ' Disease The Journal of Experimental Medicine. *J Exp Med.* 2003;198(10).
249. Andersen-nissen E, Smith KD, Strobe KL, Barrett SLR, Cookson BT, Logan SM, et al. Evasion of Toll-like receptor 5 by flagellated bacteria. *PNAS.* 2005;102(26):9247–52.

250. Redecke V, Hausmann S, Akira S, Bauer S, Kirschning CJ, Ha H, et al. Human TLR9 confers responsiveness to bacterial DNA via species-specific CpG motif recognition. *PNAS*. 2001;98(16):9237–42.
251. Dalpke A, Frank J, Peter M, Heeg K. Activation of Toll-Like Receptor 9 by DNA from Different Bacterial Species. *Infect Immun*. 2006;74(2):940–6.
252. Mancuso G, Gambuzza M, Midiri A, Biondo C, Papasergi S, Akira S, et al. Bacterial recognition by TLR7 in the lysosomes of conventional dendritic cells. *Nat Immunol*. 2009;10(6):587–94.
253. Hochrein H, Schlatter B, Keeffe MO, Wagner C, Schmitz F, Schiemann M, et al. Herpes simplex virus type-1 induces IFN- γ production via Toll-like receptor 9-dependent and -independent pathways. *PNAS*. 2004;101(31):1–6.
254. Krug A, Rothenfusser S, Hornung V, Jahrsdörfer B, Ballas ZK, Endres S, et al. Identification of CpG oligonucleotide sequences with high induction of IFN- α / β in plasmacytoid dendritic cells. *Eur J Immunol*. 2001;2154–63.
255. Choe J, Kelker MS, Wilson IA. Crystal Structure of Human Toll-Like Receptor 3 (TLR3) Ectodomain. *Science* (80-). 2005;309(July):581–6.
256. Alexopoulou L, Holt AC, Medzhitov R, Flavell RA. Recognition of double-stranded RNA and activation of NF- κ B by Toll-like receptor 3. *Nature*. 2001;413(1985).
257. Tabeta K, Georgel P, Janssen E, Du X, Hoebe K, Crozat K, et al. Toll-like receptors 9 and 3 as essential components of innate immune defense against mouse cytomegalovirus infection. *PNAS*. 2004;101(10):3516–3521.
258. Zhang S, Jouanguy E, Ugolini S, Smahi A, Puel A, Picard C, et al. TLR3 Deficiency in Patients with Herpes Simplex Encephalitis. *Science* (80-). 2007;317(September):1522–8.

259. Hemmi H, Kaisho T, Takeuchi O, Sato S, Sanjo H, Hoshino K, et al. Small-antiviral compounds activate immune cells via the TLR7 MyD88-dependent signaling pathway. *Nat Immunol.* 2002;3(2):196–200.
260. Barchet W, Krug A, Cella M, Newby C, Fischer JAA, Dzionek A, et al. Dendritic cells respond to influenza virus through TLR7- and PKR-independent pathways. *Eur J Immunol.* 2005 Jan;35(1):236–42.
261. Lee HK, Lund JM, Ramanathan B, Mizushima N, Iwasaki A. Autophagy-dependent viral recognition by plasmacytoid dendritic cells. *Science* (80-). 2007;315(5817):1398–401.
262. Heil F, Hemmi H, Hochrein H, Ampenberger F, Kirschning C, Akira S, et al. Species-Specific Recognition of Single-Stranded RNA via Toll-like Receptor 7 and 8. 2004. p. 1526–9.
263. Kolb-Mäurer A, Kämmerer U, Mäurer M, Gentschev I, Bröcker EB, Rieckmann P, et al. Production of IL-12 and IL-18 in human dendritic cells upon infection by *Listeria monocytogenes*. *FEMS Immunol Med Microbiol.* 2003;35(3):255–62.
264. Tsuda J, Li W, Yamanishi H, Yamamoto H, Okuda A, Kubo S, et al. Involvement of CD56 bright CD11c + Cells in IL-18–Mediated Expansion of Human $\gamma\delta$ T Cells . *J Immunol.* 2011;186(4):2003–12.
265. Lamichhane R, Schneider M, Harpe SM De, Tyndall JDA, Vernall AJ, Ussher JE, et al. Associated Invariant T Cells Are Rapid Polyfunctional Effectors That Can Coordinate Invariant T Cells Are Rapid Polyfunctional Effectors That Can Coordinate Immune Responses. *CellReports.* 2019;28(12):3061-3076.e5.
266. Scott-Algara D, Truong LX, Versmisse P, David A, Luong TT, Nguyen N V., et al. Cutting Edge: Increased NK Cell Activity in HIV-1-Exposed but Uninfected Vietnamese Intravascular Drug Users. *J Immunol.* 2003;171(11):5663–7.

267. Kahle EM, Bolton M, Hughes JP, Donnell D, Celum C, Lingappa JR, et al. Plasma cytokine levels and risk of HIV type 1 (HIV-1) transmission and acquisition: A nested case-control study among HIV-1-serodiscordant couples. *J Infect Dis.* 2015;211(9):1451–60.
268. Cooper MD, Alder MN. The evolution of adaptive immune systems. *Cell.* 2006;124(4):815–22.
269. Janeway CA, Medzhitov R. Innate Immune Recognition. *Annu Rev Immunol.* 2002;(2):197–216.
270. Takahama Y. Journey through the thymus: Stromal guides for T-cell development and selection. *Nat Rev Immunol.* 2006;6(2):127–35.
271. Fuxa M, Skok JA. Transcriptional regulation in early B cell development. *Curr Opin Immunol.* 2007;19(2):129–36.
272. LeBien TW, Tedder TF. B lymphocytes: How they develop and function. *Blood.* 2008;112(5):1570–80.
273. Richards S, Watanabe C, Santos L, Craxton A, Clark EA. Regulation of B-cell entry into the cell cycle. *Immunol Rev.* 2008;224(1):183–200.
274. Batista FD, Harwood NE. The who, how and where of antigen presentation to B cells. *Nat Rev Immunol.* 2009;9(1):15–27.
275. Adler LN, Jiang W, Bhamidipati K, Millican M, Macaubas C, Hung S chen, et al. The other function: Class II-restricted antigen presentation by B cells. *Front Immunol.* 2017;8(MAR):1–14.
276. Allen CDC, Okada T, Cyster JG. Germinal-Center Organization and Cellular Dynamics. *Immunity.* 2007;27(2):190–202.

277. Stavnezer J, Guikema JEJ, Schrader CE. Mechanism and regulation of class switch recombination. *Annu Rev Immunol.* 2008;26:261–92.
278. Oettgen HC. Regulation of the IgE isotype switch: New insights on cytokine signals and the functions of ϵ germline transcripts. *Curr Opin Immunol.* 2000;12(6):618–23.
279. Johansen FE, Brandtzaeg P. Transcriptional regulation of the mucosal IgA system. *Trends Immunol.* 2004;25(3):150–7.
280. Schnittman SM, Lane HC, Higgins SE, Folks T, Fauci AS. Direct Polyclonal activation of human b lymphocytes by the acquired immune deficiency syndrome virus. *J Clin Invest.* 2017;233(4768):1084–6.
281. Gras G, Richard Y, Roques P, Olivier R, Dormont D. Complement and virus-specific antibody-dependent infection of normal B lymphocytes by human immunodeficiency virus type 1. *Blood.* 1993;81(7):1808–18.
282. Moir BS, Malaspina A, Li Y, Chun T, Lowe T, Adelsberger J, et al. B Cells of HIV-1 – infected Patients Bind Virions through CD21 – Complement Interactions and Transmit Infectious Virus to Activated T Cells. *J Exp Med.* 2000;192(5).
283. Moir S, Malaspina A, Li Y, Chun TW, Lowe T, Adelsberger J, et al. B cells of HIV-1-infected patients bind virions through CD21-complement interactions and transmit infectious virus to activated T cells. *J Exp Med.* 2000;192(5):637–45.
284. Heath SL, Tew JG, Szakal AK, Burton GF. Follicular dendritic cells and human immunodeficiency virus infectivity. *Nature.* 1995;377(October):7814–8.
285. Garside P, Ingulli E, Merica RR, Johnson JG, Noelle RJ, Jenkins MK. Visualization of specific B and T lymphocyte interactions in the lymph node. *Science (80-).* 1998;281(5373):96–9.

286. Moir S, Fauci AS. Insights into B cells and HIV-specific B-cell responses in HIV-infected individuals. *Immunol Rev.* 2013;207–24.
287. Tomaras GD, Haynes BF. HIV-1-specific antibody responses during acute and chronic HIV-1 infection. *Curr Opin HIV AIDS.* 2009;4(5):373–9.
288. Mcmichael AJ, Borrow P, Tomaras GD, Goonetilleke N, Haynes BF. The immune response during acute HIV-1 infection: clues for vaccine development. *Nat Rev Immunol.* 2010;10(jAnuARy).
289. Tomaras GD, Yates NL, Liu P, Qin L, Fouda GG, Chavez LL, et al. Initial B-Cell Responses to Transmitted Human Immunodeficiency Virus Type 1: Virion-Binding Immunoglobulin M (IgM) and IgG Antibodies Followed by Plasma Anti-gp41 Antibodies with Ineffective Control of Initial Viremia. *J Virol.* 2008;82(24):12449–63.
290. Moldt B, Rakasz EG, Schultz N, Chan-Hui PY, Swiderek K, Weisgrau KL, et al. Highly potent HIV-specific antibody neutralization in vitro translates into effective protection against mucosal SHIV challenge in vivo. *Proc Natl Acad Sci U S A.* 2012;109(46):18921–5.
291. Shingai M, Donau OK, Plishka RJ, Buckler-White A, Mascola JR, Nabel GJ, et al. Passive transfer of modest titers of potent and broadly neutralizing anti-HIV monoclonal antibodies block SHIV infection in macaques. *J Exp Med.* 2014;211(10):2061–74.
292. Davis KL, Gray ES, Moore PL, Decker JM, Salomon A, Montefiori C, et al. High Titer HIV-1 V3-Specific Antibodies with Broad Reactivity but Low Neutralizing Potency in Acute Infection and Following Vaccination. *Virology.* 2010;387(2):414–26.
293. Williams KL, Stumpf M, Naiman NE, Ding S, Garrett M, Gobillot T, et al. Identification of HIV gp41-specific antibodies that mediate killing of infected cells. *PLoS Pathog.* 2019;15(2):1–27.

294. Riera NE, Galassi N, Barrera S de la, Rickard E, Muchnik G, Perez-Bianco R, et al. Anti-leukocyte antibodies as a consequence of HIV infection in HIV+ individuals. *Immunol Lett.* 1992;33:99–104.
295. Barrera SDELA, Fainboim L, Muchnik GR, Iihema MMEDEB, Aires B. Anti-class II antibodies in AIDS patients and AIDS-risk groups. *Immunology.* 1987;62:599–604.
296. Beretta A, Weiss SH, Rappocciolo G, Mayur R, De Santis C, Quirinale J, et al. Human immunodeficiency virus type 1 (HIV-1)-seronegative injection drug users at risk for HIV exposure have antibodies to HLA class I antigens and T cells specific for HIV envelope. *J Infect Dis.* 1996;173(2):472–6.
297. Callahan LN, Roderiquez G, Mallinson M, Norcross MA. Analysis of HIV-induced autoantibodies to cryptic epitopes on human CD4. *J Immunol* [Internet]. 1992;149(6):2194–202. Available from: <http://www.ncbi.nlm.nih.gov/pubmed/1381399>
298. Lopalco L, Barassi C, Pastori C, Longhi R, Burastero SE, Tambussi G, et al. CCR5-Reactive Antibodies in Seronegative Partners of HIV-Seropositive Individuals Down-Modulate Surface CCR5 In Vivo and Neutralize the Infectivity of R5 Strains of HIV-1 In Vitro. *J Immunol.* 2000;164(6):3426–33.
299. Lopalco L, Barassi C, Paolucci C, Breda D, Brunelli D, Nguyen M, et al. Predictive value of anti-cell and anti-human immunodeficiency virus (HIV) humoral responses in HIV-1 exposed seronegative cohorts of European and Asian origin. *J Gen Virol.* 2005;86(2):339–48.
300. Bentwich Z, Kalinkovich A, Weisman Z. Immune activation is a dominant factor in the pathogenesis of African AIDS. *Immunol Today.* 1995;16(4):187–91.
301. Rizzardini G, Piconi S, Ruzzante S, Fusi M-L, Lukwiya M, Demilich S, et al. Immunological activation markers in the serum of African and European HIV-seropositive and seronegative individuals. *AIDS.* 1996;10:1535–42.

302. Clerici M, Butto S, Lukwiya M, Saresella M, Declich S, Trabattoni D, et al. Immune activation in Africa is environmentally-driven and is associated with upregulation of CCR5. *Aids*. 2000;14(14):2083–92.
303. Mazzoli S, Lopalco L, Salvi A, Trabattoni D, Lo Caputo S, Semplici F, et al. Human immunodeficiency virus (HIV)-specific IgA and HIV neutralizing activity in the serum of exposed seronegative partners of HIV-seropositive persons. *J Infect Dis*. 1999;180(3):871–5.
304. Broliden K, Hinkula J, Devito C, Kiama P, Kimani J, Trabattoni D, et al. Functional HIV-1 specific IgA antibodies in HIV-1 exposed, persistently IgG seronegative female sex workers. *Immunol Lett*. 2001;79(1–2):29–36.
305. Kaul R, Trabattoni D, Bwayo JJ, Arienti D, Zagliani A, Mwangi FM, et al. HIV-1-specific mucosal IgA in a cohort of HIV-1-resistant Kenyan sex workers. *AIDS*. 1999;13(1):23–9.
306. Hirbod T, Kaul R, Reichard C, Kimani J, Ngugi E, Bwayo JJ, et al. HIV-neutralizing immunoglobulin A and HIV-specific proliferation are independently associated with reduced HIV acquisition in Kenyan sex workers. *Aids*. 2008;22(6):727–35.
307. Hasselrot K, Bratt G, Hirbod T, Saˆberg P, Ehnlund M, Lopalco L, et al. Orally exposed uninfected individuals have systemic anti-HIV responses associating with partners' viral load. *AIDS*. 2010;24(August 2009):35–43.
308. Farquhar C, Vancott T, Bosire R, Bermudez C, Mbori-Ngacha D, Lohman-Payne B, et al. Salivary human immunodeficiency virus (HIV)-1-specific immunoglobulin a in HIV-1-exposed infants in Kenya. *Clin Exp Immunol*. 2008;153(1):37–43.
309. Clerici M, Barassi C, Devito C, Pastori C, Piconi S, Trabattoni D, et al. Serum IgA of HIV-exposed uninfected individuals inhibit HIV through recognition of a region within the α -helix of gp41. *Aids*. 2002;16(13):1731–41.

310. Herr AB, White CL, Milburn C, Wu C, Bjorkman PJ. Bivalent binding of IgA1 to Fc α RI suggests a mechanism for cytokine activation of IgA phagocytosis. *J Mol Biol.* 2003;327(3):645–57.
311. Raghavan M, Bjorkman PJ. Fc receptors and their interactions with immunoglobulins. *Annu Rev Cell Dev Biol.* 1996;12:181–220.
312. Hedrick SM. Thymus Lineage Commitment: A Single Switch. *Immunity.* 2008;28(3):297–9.
313. Jenkinson EJ, Jenkinson WE, Rossi SW, Anderson G. Opinion - The thymus and T-cell commitment: The right niche for Notch? *Nat Rev Immunol.* 2006;6(7):551–5.
314. Hosokawa H, Rothenberg E V. How transcription factors drive choice of the T cell fate. *Nat Rev Immunol.* 2020;
315. Oltz EM, Osipovich O. Targeting V(D)J Recombinase: Putting a PHD to Work. *Immunity.* 2007;27(4):539–41.
316. Bonilla FA, Oettgen HC. Adaptive immunity. *J Allergy Clin Immunol* [Internet]. 2010;125(2 SUPPL. 2):S33–40. Available from: <http://dx.doi.org/10.1016/j.jaci.2009.09.017>
317. Tzachanis D, Freeman GJ, Hirano N, Van Puijenbroek AAFL, Delfs MW, Berezovskaya A, et al. Tob is a negative regulator of activation that is expressed in anergic and quiescent T cells. *Nat Immunol.* 2001;2(12):1174–82.
318. Yusuf I, Fruman DA. Regulation of quiescence in lymphocytes. *Trends Immunol.* 2003;24(7):380–6.
319. Weiss A, Littmant DR. Signal Transduction by Lymphocyte Antigen Receptors. *Cell.* 1994;76:263–74.

320. Schwartz RH. T cell clonal anergy. *Curr Opin Immunol*. 1997;9(3):351–7.
321. Mueller DL, Jenkins MK, Schwartz RH. An accessory cell-derived costimulatory signal acts independently of protein kinase C activation to allow T cell proliferation and prevent the induction of unresponsiveness. *J Immunol* [Internet]. 1989;142(8):2617–28. Available from: <http://www.ncbi.nlm.nih.gov/pubmed/2522963>
322. Vatakis DN, Nixon CC, Zack JA. Quiescent T cells and HIV : an unresolved relationship. *Immunol Res*. 2010;(August):110–21.
323. Lewis P, Hensel M, Emerman M. Human immunodeficiency virus infection of cells arrested in the cell cycle. *EMBO J*. 1992;11(8):3053–8.
324. Stevenson M. HIV-1 pathogenesis. *Nat Med* •. 2003;9(7):853–60.
325. Unutmaz D, KewalRamani VN, Marmon S, Littman DR. Cytokine signals are sufficient for HIV-1 infection of resting human T lymphocytes. *J Exp Med*. 1999;189(11):1735–46.
326. Ivanov S, Paget C. Role of Non-conventional T Lymphocytes in Respiratory Infections : The Case of the Pneumococcus. *PLoS Pathog*. 2014;10(10).
327. Meierovics AI, Cowley SC. MAIT cells promote inflammatory monocyte differentiation into dendritic cells during pulmonary intracellular infection. *J Exp Med*. 2016;213(12):2793–809.
328. Johnson Z, Schwarz M, Power CA, Wells TNC, Proudfoot AEI. Multi-faceted strategies to combat disease by interference with the chemokine system. *Trends Immunol*. 2005;26(5):268–74.
329. Hirota K, Yoshitomi H, Hashimoto M, Maeda S, Teradaira S, Sugimoto N, et al. Preferential recruitment of CCR6-expressing Th17 cells to inflamed joints via CCL20 in rheumatoid arthritis and its animal model. *J Exp Med*. 2007;204(12):2803–12.

330. Reboldi A, Coisne C, Baumjohann D, Benvenuto F, Bottinelli D, Lira S, et al. C-C chemokine receptor 6-regulated entry of TH-17 cells into the CNS through the choroid plexus is required for the initiation of EAE. *Nat Immunol.* 2009;10(5):514–23.
331. Yamazaki T, Yang XO, Chung Y, Fukunaga A, Nurieva R, Pappu B, et al. CCR6 Regulates the Migration of Inflammatory and Regulatory T Cells. *J Immunol.* 2008;181(12):8391–401.
332. Harper EG, Guo C, Rizzo H, Lillis J V, Kurtz SE, Skorcheva I, et al. Th17 Cytokines Stimulate CCL20 Expression in Keratinocytes In Vitro and In Vivo: Implications for Psoriasis Pathogenesis. 2009;129(9):2175–83.
333. Kaser A, Ludwiczek O, Holzmann S, Moschen AR, Weiss G, Enrich B, et al. Increased expression of CCL20 in human inflammatory bowel disease. *J Clin Immunol.* 2004 Jan;24(1):74–85.
334. Bromley SK, Peterson DA, Gunn MD, Dustin ML. Cutting Edge: Hierarchy of Chemokine Receptor and TCR Signals Regulating T Cell Migration and Proliferation. *J Immunol.* 2000;165(1):15–9.
335. Matloubian M, Lo CG, Cinamon G, Lesneski MJ, Xu Y, Brinkmann V, et al. Lymphocyte egress from thymus and peripheral lymphoid organs is dependent on S1P receptor 1. *Nature* [Internet]. 2004;427(6972):355–60. Available from: <https://doi.org/10.1038/nature02284>
336. van der Voort R, Verweij V, de Witte TM, Lasonder E, Adema GJ, Dolstra H. An alternatively spliced CXCL16 isoform expressed by dendritic cells is a secreted chemoattractant for CXCR6 + cells . *J Leukoc Biol.* 2010;87(6):1029–39.
337. Tabata S, Kadowaki N, Kitawaki T, Shimaoka T, Yonehara S, Yoshie O, et al. Distribution and kinetics of SR-PSOX/CXCL16 and CXCR6 expression on human dendritic cell subsets and CD4 + T cells . *J Leukoc Biol.* 2005;77(5):777–86.

338. Kim CH, Kunkel EJ, Boisvert J, Johnston B, Campbell JJ, Genovese MC, et al. Bonzo/CXCR6 expression defines type 1-polarized T-cell subsets with extralymphoid tissue homing potential. *J Clin Invest*. 2001;107(5):595–601.
339. Ashhurst AS, Flórido M, Lin LCW, Quan D, Armitage E, Stifter SA, et al. CXCR6-deficiency improves the control of pulmonary mycobacterium tuberculosis and influenza infection independent of T-lymphocyte recruitment to the lungs. *Front Immunol*. 2019;10(MAR):1–16.
340. Weseslindtner L, Görzer I, Küng E, Roedl K, Jaksch P, Klepetko W, et al. High CXCL-16 levels correlate with symptomatic disease in lung transplant recipients with human cytomegalovirus replication in the allograft. *Am J Transplant*. 2014;14(10):2406–11.
341. Simmons G, Reeves JD, Hibbitts S, Stine JT, Gray PW, Proudfoot AEI, et al. Co-receptor use by HIV and inhibition of HIV infection by chemokine receptor ligands. *Immunol Rev*. 2000;177(II):112–26.
342. Samson M, Labbe O, Mollereau C, Vassart G, Parmentier M. Molecular cloning and functional expression of a new human CC-chemokine receptor gene. *Biochemistry*. 1996;35(11):3362–7.
343. Ogilvie P, Bardi G, Clark-Lewis I, Baggiolini M, Uguccioni M. Eotaxin is a natural antagonist for CCR2 and an agonist for CCR5. *Blood* [Internet]. 2001;97(7):1920–4. Available from: <http://dx.doi.org/10.1182/blood.V97.7.1920>
344. Blanpain C, Migeotte I, Lee B, Vakili J, Doranz BJ, Govaerts C, et al. CCR5 Binds Multiple CC-Chemokines: MCP-3 Acts as a Natural Antagonist. *Blood*. 1999;94(6):1899–905.
345. Reynes J, Portales P, Segondy M, Baillat V, André P, Réant B, et al. CD4+ T cell surface CCR5 density as a determining factor of virus load in persons infected with human immunodeficiency virus type 1. *J Infect Dis*. 2000;181(3):927–32.

346. Signoret N, Pelchen-matthews A, Mack M, Proudfoot AEI, Marsh M. Endocytosis and Recycling of the HIV Coreceptor CCR5. *J Biol Chem*. 2000;275(16):1281–93.
347. Mueller A, Strange PG. Mechanisms of internalization and recycling of the chemokine receptor , CCR5. *J Biol Chem*. 2004;279(1):243–52.
348. Glatzel A, Wesch D, Schiemann F, Brandt E, Janssen O, Kabelitz D. Patterns of Chemokine Receptor Expression on Peripheral Blood $\gamma\delta$ T Lymphocytes: Strong Expression of CCR5 Is a Selective Feature of V δ 2/V γ 9 $\gamma\delta$ T Cells. *J Immunol*. 2002;168(10):4920–9.
349. Hammerich L, Bangen JM, Govaere O, Zimmermann HW, Nikolaus Gassler, Sebastian H, et al. Chemokine Receptor CCR6-Dependent Accumulation of $\gamma\delta$ T Cells in Injured Liver Restricts Hepatic Inflammation and Fibrosis. *Hepatology*. 2014;59(2):630–42.
350. Sharma PK, Wong EB, Napier RJ, Bishai WR, Ndung'u T, Kasprovicz VO, et al. High expression of CD26 accurately identifies human bacteria-reactive MR1-restricted MAIT cells. *Immunology*. 2015;145(3):443–53.
351. Chen P, Deng W, Li D, Zeng T, Huang L, Wang Q, et al. Circulating mucosal-associated invariant T Cells in a large cohort of chinese individuals from newborn to elderly. *Front Immunol*. 2019;10(FEB):1–12.
352. Qin S, Rottman JB, Myers P, Kassam N, Weinblatt M, Loetscher M, et al. The chemokine receptors CXCR3 and CCR5 mark subsets of T cells associated with certain inflammatory reactions. *J Clin Invest*. 1998;101(4):746–54.
353. Thomas SY, Hou R, Boyson JE, Means TK, Hess C, Olson DP, et al. CD1d-Restricted NKT Cells Express a Chemokine Receptor Profile Indicative of Th1-Type Inflammatory Homing Cells. *J Immunol*. 2003;171(5):2571–80.
354. Cella M, Jarrossay D, Facchetti F, Alebardi O, Nakajima H, Lanzavecchia A, et al.

- Plasmacytoid monocytes migrate to inflamed lymph nodes and produce large amounts of type I interferon. *Nat Med* [Internet]. 1999;5(8):919–23. Available from: <https://doi.org/10.1038/11360>
355. Nanki T, Takada K, Komano Y, Morio T, Kanegane H, Nakajima A, et al. Chemokine receptor expression and functional effects of chemokines on B cells: Implication in the pathogenesis of rheumatoid arthritis. *Arthritis Res Ther*. 2009;11(5):1–11.
 356. Loetscher M, Loetscher P, Brass N, Meese E, Moser B. Lymphocyte-specific chemokine receptor CXCR3: Regulation, chemokine binding and gene localization. *Eur J Immunol*. 1998;28(11):3696–705.
 357. Cole KE, Strick CA, Paradis TJ, Ogborne KT, Loetscher M, Gladue RP, et al. Interferon-inducible T cell alpha chemoattractant (I-TAC): A novel non-ELR CXC chemokine with potent activity on activated T cells through selective high affinity binding to CXCR3. *J Exp Med*. 1998;187(12):2009–21.
 358. Campanella GSVBDM, Manicea LA, A.Colvina R, Luster A and AD. Development of a novel chemokine-mediated in vivo T cell recruitment assay. 2009;331:127–39.
 359. Campanella GS V., Grimm J, Manice LA, Colvin RA, Medoff BD, Wojtkiewicz GR, et al. Oligomerization of CXCL10 Is Necessary for Endothelial Cell Presentation and In Vivo Activity. *J Immunol*. 2006;177(10):6991–8.
 360. Kroemer G, Zitvogel L. Harnessing gd T cells in anticancer immunotherapy. 2012;33(5):199–206.
 361. Zhuo W, Jia L, Song N, Lu XA, Ding Y, Wang X, et al. The CXCL12 -CXCR4 chemokine pathway: A novel axis regulates lymphangiogenesis. *Clin Cancer Res*. 2012;18(19):5387–98.
 362. Daniel SK, Seo YD, Pillarisetty VG. The CXCL12-CXCR4/CXCR7 axis as a mechanism

- of immune resistance in gastrointestinal malignancies. *Semin Cancer Biol* [Internet]. 2020;65(September 2019):176–88. Available from: <https://doi.org/10.1016/j.semcancer.2019.12.007>
363. Ullah TR. The role of CXCR4 in multiple myeloma: Cells' journey from bone marrow to beyond. *J Bone Oncol* [Internet]. 2019;17(June):100253. Available from: <https://doi.org/10.1016/j.jbo.2019.100253>
364. Bleul CC, Wu L, Hoxie JA, Springer TA, Mackay CR. The HIV coreceptors CXCR4 and CCR5 are differentially expressed and regulated on human T lymphocytes. *Proc Natl Acad Sci U S A*. 1997;94(5):1925–30.
365. Wong EB, Akilimali NA, Govender P, Sullivan ZA, Cosgrove C, Pillay M, et al. Low levels of peripheral CD161⁺⁺CD8⁺ Mucosal Associated Invariant T (MAIT) cells are found in HIV and HIV/TB co-infection. *PLoS One*. 2013;8(12):1–9.
366. Dusseaux M, Martin E, Serriari N, Pe I, Premel V, Louis D, et al. Human MAIT cells are xenobiotic-resistant, tissue-targeted, CD161^{hi} IL-17 – secreting T cells. *Blood* [Internet]. 2011;117(4):1250–9. Available from: <http://dx.doi.org/10.1182/blood-2010-08-303339>
367. Campbell JJ, Pan J, Butcher EC. Cutting edge: developmental switches in chemokine responses during T cell maturation. *J Immunol* [Internet]. 1999;163(5):2353–7. Available from: <http://www.ncbi.nlm.nih.gov/pubmed/10452965>
368. Roth SJ, Diacovo TG, Brenner MB, Rosat JP, Buccola J, Morita CT, et al. Transendothelial chemotaxis of human α/β and γ/δ T lymphocytes to chemokines. *Eur J Immunol*. 1998;28(1):104–13.
369. Legoux F, Gilet J, Procopio E, Echasserieau K, Bernardeau K, Lantz O. Molecular mechanisms of lineage decisions in metabolite-specific T cells. *Nat Immunol* [Internet]. 2019;20(9):1244–55. Available from: <http://dx.doi.org/10.1038/s41590-019-0465-3>

370. Dieli F, Poccia F, Lipp M, Sireci G, Caccamo N, Di Sano C, et al. Differentiation of effector/memory V δ 2 T cells and migratory routes in lymph nodes or inflammatory sites. *J Exp Med*. 2003;198(3):391–7.
371. Luckheeram RV, Zhou R, Verma AD, Xia B. CD4 +T cells: Differentiation and functions. *Clin Dev Immunol*. 2012;
372. Stieh DJ, Matias E, Xu H, Fought AJ, Blanchard JL, Marx PA, et al. Th17 cells are preferentially infected very early after vaginal transmission of SIV in macaques. *Cell Host Microbe*. 2016;19(4):529–40.
373. Vatakis DN, Nixon CC, Jerome A, Zack. Quiescent T cells and HIV: an unresolved relationship. *Immunol Res*. 2010;48(0):1–13.
374. Zhang Z-Q, Schuler T, Zupancic M, Wietgreffe S, Staskus KA, Reimann KA, et al. Sexual Transmission and Propagation of SIV and HIV in Resting and Activated. *Science* (80-). 1999;286(November):1353–8.
375. Card CM, Ball TB, Fowke KR. Immune Quiescence: A model of protection against HIV infection. *Retrovirology*. 2013;10(1):1–8.
376. Vatakis DN, Nixon CC, Zack JA. Quiescent T cells and HIV: An unresolved relationship. *Immunol Res*. 2010;48(1–3):110–21.
377. Lajoie J, Juno J, Burgener A, Rahman S, Mogk K, Wachihi C, et al. A distinct cytokine and chemokine profile at the genital mucosa is associated with HIV-1 protection among HIV-exposed seronegative commercial sex workers. *Mucosal Immunol* [Internet]. 2012;5(3):277–87. Available from: <http://dx.doi.org/10.1038/mi.2012.7>
378. Yao XD, Omenge RW, Henrick BM, Lester RT, Kimani J, Ball TB, et al. Acting locally: Innate mucosal immunity in resistance to HIV-1 infection in Kenyan commercial sex workers. *Mucosal Immunol*. 2014;7(2):268–79.

379. Chege D, Chai Y, Huibner S, Kain T, Wachihi C, Kimani M, et al. Blunted IL17/IL22 and pro-inflammatory cytokine responses in the genital tract and blood of HIV-exposed, seronegative female sex workers in Kenya. *PLoS One*. 2012;7(8):1–9.
380. McLaren PJ, Ball TB, Wachihi C, Jaoko W, Kelvin DJ, Danesh A, et al. HIV-Exposed Seronegative Commercial Sex Workers Show a Quiescent Phenotype in the CD4 + T Cell Compartment and Reduced Expression of HIV-Dependent Host Factors . *J Infect Dis*. 2010;202(S3):S339–44.
381. Prodger J, Hirbod T, Kigozi G, Nalugoda F, Reynolds S, Galiwango R, et al. Immune correlates of HIV exposure without infection in foreskins of men from Rakai, Uganda. 2014;7(3):634–44.
382. Card CM, Rutherford WJ, Ramdahin S, Yao X, Kimani M, Wachihi C, et al. Reduced Cellular Susceptibility to In Vitro HIV Infection Is Associated with CD4+ T Cell Quiescence. *PLoS One*. 2012;7(9):1–7.
383. Card CM, McLaren PJ, Wachihi C, Kimani J, Plummer FA, Fowke KR. Decreased Immune Activation in Resistance to HIV-1 Infection Is Associated with an Elevated Frequency Cells. *JID*. 2009;199(9):1318–22.
384. Bégaud E, Chartier L, Marechal V, Ipero J, Léal J, Versmisse P, et al. Reduced CD4 T cell activation and in vitro susceptibility to HIV-1 infection in exposed uninfected Central Africans. *Retrovirology*. 2006;9:1–9.
385. Camara M, Dieye TN, Seydi M, Diallo AA, Fall M, Diaw PA, et al. Low-Level CD4 + T Cell Activation in HIV-Exposed Seronegative Subjects : Influence of Gender and Condom Use. *J Infect Dis*. 2010;201:835–42.
386. El-Zayat SR, Sibaii H, Manna FA. Toll-like receptors activation, signaling, and targeting: an overview. *Bull Natl Res Cent*. 2019;43(1).

387. Osborn L, Kunkel S, Nabel GJ. Tumor necrosis factor α and interleukin 1 stimulate the human immunodeficiency virus enhancer by activation of the nuclear factor κ B. *Proc Natl Acad Sci U S A*. 1989;86(7):2336–40.
388. Fowke KR, Kaul R, Rosenthal KL, Oyugi J, Kimani J, Rutherford WJ, et al. HIV-1-specific cellular immune responses among HIV-1-resistant sex workers. *Immunol Cell Biol*. 2000;78(6):586–95.
389. Ciccone EJ, Read SW, Mannon PJ, Yao MD, Hodge JN, Dewar R, et al. Cycling of gut mucosal CD4 T cells decreases after prolonged anti-retroviral therapy and is associated with plasma LPS levels. *Mucosal Immunol*. 2010;3(2):172–81.
390. Lu X, Li Z, Li Q, Jiao Y, Ji Y, Zhang H, et al. Preferential loss of gut-homing α 4 β 7 CD4⁺ T cells and their circulating functional subsets in acute HIV-1 infection. *Cell Mol Immunol*. 2016;13(6):776–84.
391. Laher F, Ranasinghe S, Porichis F, Mewalal N, Pretorius K, Ismail N, et al. HIV Controllers Exhibit Enhanced Frequencies of Major Histocompatibility Complex Class II Tetramer_ Gag-Specific CD4⁺ T Cells in Chronic Clade C HIV-1 Infection. *J Virol*. 2017;91(7):1–17.
392. Singh A, Vajpayee M, Ali SA, Mojumdar K, Chauhan NK, Singh R. HIV-1 diseases progression associated with loss of Th17 cells in subtype “C” infection. *Cytokine* [Internet]. 2012;60(1):55–63. Available from: <http://dx.doi.org/10.1016/j.cyto.2012.06.288>
393. Saxena V, Patil A, Tayde R, Bichare S, Chinchkar V, Bagul R, et al. HIV-specific CD4⁺Th17 cells from HIV infected long-term non-progressors exhibit lower CTLA-4 expression and reduced apoptosis. *Immunobiology* [Internet]. 2018;223(11):658–62. Available from: <https://doi.org/10.1016/j.imbio.2018.07.011>
394. Zhang N, Bevan MJ. CD8⁺ T Cells: Foot Soldiers of the Immune System. *Immunity*.

- 2011;35(2):161–8.
395. Curtsinger JM, Johnson CM, Mescher MF. CD8 T Cell Clonal Expansion and Development of Effector Function Require Prolonged Exposure to Antigen, Costimulation, and Signal 3 Cytokine. *J Immunol*. 2003;171(10):5165–71.
396. Curtsinger JM, Valenzuela JO, Agarwal P, Lins D, Mescher MF. Cutting Edge: Type I IFNs Provide a Third Signal to CD8 T Cells to Stimulate Clonal Expansion and Differentiation. *J Immunol*. 2005;174(8):4465–9.
397. Miller JD, van der Most RG, Akondy RS, Glidewell JT, Albott S, Masopust D, et al. Human Effector and Memory CD8⁺ T Cell Responses to Smallpox and Yellow Fever Vaccines. *Immunity*. 2008;28(5):710–22.
398. Hamann D, Baars PA, Rep MHG, Hooibrink B, Kerkhof-Garde SR, Klein MR, et al. Phenotypic and functional separation of memory and effector human CD8⁺ T cells. *J Exp Med*. 1997;186(9):1407–18.
399. Wolint P, Betts MR, Koup RA, Oxenius A. Immediate Cytotoxicity but Not Degranulation Distinguishes Effector and Memory Subsets of CD8⁺ T Cells. *J Exp Med*. 2004;199(7):925–36.
400. Bachmann MF, Barner M, Viola A, Kopf M. Distinct kinetics of cytokine production and cytolysis in effector and memory T cells after viral infection. *Eur J Immunol*. 1999;29(1):291–9.
401. Promadej N, Costello C, Wernett MM, Kulkarni PS, Robison VA, Nelson KE, et al. Broad Human Immunodeficiency Virus (HIV)– Specific T Cell Responses to Conserved HIV Proteins in HIV-Seronegative Women Highly Exposed to a Single HIV-Infected Partner. *J Infect Dis*. 2003;30341:1053–64.
402. Addo MM, Altfeld M, Brainard DM, Rathod A, Piechocka-trocha A, Fideli U, et al. Lack

- of Detectable HIV-1 – Specific CD8⁺ T Cell Responses in Zambian HIV-1 – Exposed Seronegative Partners of HIV-1 – Positive Individuals. *J Infect Dis.* 2011;203.
403. Ruiz-riol M, Llano A, Ibarrodo J, Zamarreño J, Yusim K, Bach V, et al. Alternative Effector-Function Profiles Identify Broad HIV-Specific T-Cell Responses in Highly HIV-Exposed Individuals Who Remain Uninfected. *J Infect Dis.* 2015;211:936–946.
404. Hladik F, Desbien A, Lang J, Wang L, Ding Y, Holte S, et al. Most Highly Exposed Seronegative Men Lack HIV-1-Specific, IFN- γ -Secreting T Cells. *J Immunol.* 2003;171:2671–83.
405. Ritchie AJ, Champion SL, Kopycinski J, Moodie Z, Wang ZM, Pandya K, et al. Differences in HIV-Specific T Cell Responses between HIV-Exposed and -Unexposed HIV-Seronegative Individuals. *J Virol.* 2011;85(7):3507–16.
406. Alimonti JB, Koesters SA, Kimani J, Matu L, Wachihi C, Plummer FA, et al. CD4⁺ T Cell Responses in HIV-Exposed Seronegative Women Are Qualitatively Distinct from Those in HIV-Infected Women. *J Infect Dis.* 2005;191:2–6.
407. Card CM, McLaren PJ, Wachihi C, Kimani J, Plummer FA, Fowke KR. Decreased Immune Activation in Resistance to HIV-1 Infection Is Associated with an Elevated Frequency of CD4⁺ CD25⁺ FOXP3⁺ Regulatory T Cells. *J Infect Dis.* 2009;199(9):1318–22.
408. Legrand FA, Nixon DF, Loo CP, Ono E, Chapman JM, Miyamoto M, et al. Strong HIV-1-Specific T Cell Responses in HIV-1-Exposed Uninfected Infants and Neonates Revealed after Regulatory T Cell Removal. *PLoS One.* 2006;e102(1).
409. Koning FA, Otto SA, Hazenberg MD, Dekker L, Prins M, Miedema F, et al. Low-Level CD4⁺ Activation is Associated with Low Susceptibility to HIV-1 Infection 1. *J Immunol.* 2005;175:6117–22.

410. McLaren PJ, Ball TB, Wachihi C, Jaoko W, Kelvin DJ, Danesh A, et al. HIV-Exposed Seronegative Commercial Sex Workers Show a Quiescent Phenotype in the CD4 + T Cell Compartment and Reduced Expression of HIV-Dependent Host Factors. *JID*. 2010;3(Suppl 3):339–44.
411. Chege D, Chai Y, Huibner S, Kain T, Wachihi C, Kimani M, et al. Blunted IL17/IL22 and pro-inflammatory cytokine responses in the genital tract and blood of HIV-exposed, seronegative female sex workers in Kenya. *PLoS One*. 2012;7(8):1–9.
412. Furci BL, Scarlatti G, Burastero S, Tambussi G, Colognesi C, Quillent C, et al. Antigen-driven C-C Chemokine-mediated HIV-1 Suppression by CD4+ T cells from Exposed Uninfected Individuals Expressing the Wild-type CCR-5 Allele. *J Exp Med*. 1997;186(3):455–60.
413. Dalod M, Dupuis M, Deschemin J-C, Sicard D, Salmon D, Delfraissy J-F, et al. Broad, Intense Anti-Human Immunodeficiency Virus (HIV) Ex Vivo CD8+ Responses in HIV Type 1-Infected Patients: Comparison with Anti-Epstein-Barr Virus Responses and Changes during Antiretroviral Therapy. *J Virol*. 1999;73(9):7108–16.
414. Gea-Banacloche JC, Migueles SA, Martino L, Shupert WL, McNeil AC, Sabbaghian MS, et al. Maintenance of Large Numbers of Virus-Specific CD8 + T Cells in HIV-Infected Progressors and Long-Term Nonprogressors . *J Immunol*. 2000;165(2):1082–92.
415. Betts MR, Ambrozak DR, Douek DC, Bonhoeffer S, Brenchley JM, Casazza JP, et al. Analysis of Total Human Immunodeficiency Virus (HIV)-Specific CD4+ and CD8+ T-Cell Responses: Relationship to Viral Load in Untreated HIV Infection. *J Virol*. 2001;75(24):11983–91.
416. Migueles SA, Connors M. Frequency and function of HIV-specific CD8+ T Cells. *Immunol Lett*. 2001;79(1–2):141–50.
417. Addo MM, Yu XG, Rathod A, Cohen D, Eldridge RL, Strick D, et al. Comprehensive

- Epitope Analysis of Human Immunodeficiency Virus Type 1 (HIV-1)-Specific T-Cell Responses Directed against the Entire Expressed HIV-1 Genome Demonstrate Broadly Directed Responses, but No Correlation to Viral Load. *J Virol.* 2003;77(3):2081–92.
418. Buckheit RW, Salgado M, Silciano RF, Blankson JN. Inhibitory Potential of Subpopulations of CD8⁺ T Cells in HIV-1-Infected Elite Suppressors. *J Virol.* 2012;86(24):13679–88.
419. M. Genescà, M.B. McChesney and CJM. Antiviral CD8⁺ T cells in the genital tract control viral replication and delay progression to AIDS after vaginal SIV challenge in rhesus macaques immunized with virulence attenuated SHIV 89.6. *J Intern Med.* 2009;265(1):67–77.
420. Ogg GS, Jin X, Bonhoeffer S, Dunbar PR, Nowak MA, Monard S, et al. Quantitation of HIV-1-specific cytotoxic T lymphocytes and plasma load of viral RNA. *Science.* 1998 Mar;279(5359):2103–6.
421. Edwards BH, Bansal A, Sabbaj S, Bakari J, Mulligan MJ, Goepfert PA. Magnitude of functional CD8⁺ T-cell responses to the gag protein of human immunodeficiency virus type 1 correlates inversely with viral load in plasma. *J Virol.* 2002 Mar;76(5):2298–305.
422. Varadarajan N, Julg B, Yamanaka YJ, Chen H, Ogunniyi AO, McAndrew E, et al. A high-throughput single-cell analysis of human CD8⁺ T cell functions reveals discordance for cytokine secretion and cytotoxicity. *J Clin Invest.* 2011;121(11):4322–31.
423. Betts MR, Nason MC, West SM, Rosa SC De, Migueles SA, Abraham J, et al. HIV nonprogressors preferentially maintain highly functional HIV-specific CD8⁺ T cells. *Blood.* 2006;107(12):4781–9.
424. Hersperger AR, Pereyra F, Nason M, Demers K, Sheth P, Shin LY, et al. Perforin expression directly ex vivo by HIV-specific CD8⁺ T-cells is a correlate of HIV elite control. *PLoS Pathog.* 2010;6(5):1–13.

425. Noel N, Peña R, David A, Avettand-Fenoel V, Erkizia I, Jimenez E, et al. Long-Term Spontaneous Control of HIV-1 Is Related to Low Frequency of Infected Cells and Inefficient Viral Reactivation. *J Virol*. 2016;90(13):6148–58.
426. Lecuroux C, Saez-Cirion A, Girault I, Versmisse P, Boufassa F, Avettand-Fenoel V, et al. Both HLA-B*57 and Plasma HIV RNA Levels Contribute to the HIV-Specific CD8+ T Cell Response in HIV Controllers. *J Virol*. 2014;88(1):176–87.
427. Migueles SA, Laborico AC, Shupert WL, Sabbaghian MS, Rabin R, Hallahan CW, et al. HIV-specific CD8+ T cell proliferation is coupled to perforin expression and is maintained in nonprogressors. *Nat Immunol*. 2002;3(11):1061–8.
428. Migueles SA, Osborne CM, Royce C, Compton AA, Joshi RP, Weeks KA, et al. Lytic Granule Loading of CD8+ T Cells Is Required for HIV-Infected Cell Elimination Associated with Immune Control. *Immunity*. 2008;29(6):1009–21.
429. Monel B, McKeon A, Lamothe-Molina P, Jani P, Boucau J, Pacheco Y, et al. HIV Controllers Exhibit Effective CD8 + T Cell Recognition of HIV-1-Infected Non-activated CD4 + T Cells. *Cell Rep [Internet]*. 2019;27(1):142-153.e4. Available from: <https://doi.org/10.1016/j.celrep.2019.03.016>
430. Cheynier R, Langlade-Demoyen P, Marescot M -R, Blanche S, Blondin G, Wain-Hobson S, et al. Cytotoxic T lymphocyte responses in the peripheral blood of children born to human immunodeficiency virus-1-infected mothers. *Eur J Immunol*. 1992;22(9):2211–7.
431. Rowland-Jones SL, Nixon DF, Aldhous MC, Gotch F, Ariyoshi K, Hallam N, et al. HIV-specific cytotoxic T-cell activity in an HIV-exposed but uninfected infant Transmural myocardial infarction with sumatriptan For sumatriptan , tightness in the chest caused by. *Lancet*. 1993;341:860–1.
432. Biasin M, Caputo S Lo, Speciale L, Colombo F, Racioppi L, Zagliani A, et al. Mucosal and Systemic Immune Activation Is Present in Human Immunodeficiency Virus –

- Exposed Seronegative Women. *J Infect Dis.* 2000;182:1365–74.
433. Skurnick JH, Palumbo P, Devico A, Shacklett BL, Valentine FT, Merges M, et al. Correlates of Nontransmission in US Women at High Risk of Human Immunodeficiency Virus Type 1 Infection through Sexual Exposure. *J Infect Dis.* 2002;428–38.
434. ALimonti JB, Kimani J, Matu L, Wachii CS, Kaul R, Plummer FA, et al. Characterization of CD8 + T-cell responses in HIV-1-exposed seronegative commercial sex workers from Nairobi , Kenya. *Immunol Cell Biol.* 2006;84(March):482–5.
435. Rowland-jones SL, Dong T, Fowke KR, Kimani J, Krausa P, Newell H, et al. Cytotoxic T Cell Responses to Multiple Conserved HIV Epitopes in HIV-Resistant Prostitutes in Nairobi. *J Clin Invest.* 1998;102:1758–65.
436. Godfrey DI, Uldrich AP, Mccluskey J, Rossjohn J, Moody DB. The burgeoning family of unconventional T cells. 2015;(October).
437. Salio M, Silk JD, Jones EY, Cerundolo V. Biology of CD1- and MR1-Restricted T Cells.
438. Godfrey DI, Uldrich AP, Mccluskey J, Rossjohn J, Moody DB. The burgeoning family of unconventional T cellsGodfrey, D.I. et al., 2015. The burgeoning family of unconventional T cells. , 16(11). *Nat Immunol.* 2015;16(11):1114–24.
439. Bourhis L Le, Martin E, Péguillet I, Guihot A, Froux N, Coré M, et al. Antimicrobial activity of mucosal-associated invariant T cells. *Nat Immunol.* 2010;11(8).
440. Gherardin NA, Souter MNT, Koay HF, Mangas KM, Seemann T, Stinear TP, et al. Human blood MAIT cell subsets defined using MR1 tetramers. *Immunol Cell Biol.* 2018;96(5):507–25.
441. Dusseaux M, Martin E, Serriari N, Pe I, Premel V, Louis D, et al. Human MAIT cells are xenobiotic-resistant , tissue-targeted , CD161 hi IL-17 – secreting T cells.

- 2011;117(4):1250–9.
442. Tilloy BF, Treiner E, Park S, Garcia C, Lemonnier F, Salle D, et al. An Invariant T Cell Receptor α Chain Defines a Novel TAP-independent Major Histocompatibility Complex Class Ib–restricted α/β T Cell Subpopulation in Mammals. 1999;189(12).
443. Treiner E, Duban L, Bahram S, Radosavljevic M, Wanner V, Tilloy F, et al. Selection of evolutionarily conserved mucosal-associated invariant T cells by MR1. *Nature*. 2003;423(6943):1018.
444. Lamichhane R, Ussher JE. Expression and trafficking of MR1. *Immunology*. 2017;151(3):270–9.
445. Keiichiro Hashimoto, Momoki Hirai YK. A Gene Outside the Human MHC Related to Classical HLA Class I Genes. *Science* (80-). 1995;269(5224):693–5.
446. Lamichhane R, Ussher JE. Expression and trafficking of MR1. *Immunology*. 2017;151(3):270–9.
447. Harrieff MJ, Cansler ME, Toren KG, Canfield ET, Kwak S, Gold MC, et al. Human lung epithelial cells contain *Mycobacterium tuberculosis* in a late endosomal vacuole and are efficiently recognized by CD8⁺ T Cells. *PLoS One*. 2014;9(5):1–12.
448. McWilliam HEG, Eckle SBG, Theodossis A, Liu L, Chen Z, Wubben JM, et al. The intracellular pathway for the presentation of Vitamin B-related antigens by the antigen-presenting molecule MR1. *Nat Immunol*. 2016;17(5):531–7.
449. Treiner E, Duban L, Bahram S, Radosavljevic M, Wanner V, Tilloy F. Selection of evolutionarily conserved mucosal-associated invariant T cells by MR1. 2003;422(March):1–7.
450. Meyer-bahlburg A, Bandaranayake AD, Sarah F, Rawlings DJ. Reduced c- myc

- Expression Levels Limit Follicular Mature B Cell Cycling in Response to TLR Signals. *J Immunol.* 2009;182:4065–75.
451. Gururajan M, Jacob J, Pulendran B. Toll-Like Receptor Expression and Responsiveness of Distinct Murine Splenic and Mucosal B-Cell Subsets. *PLoS One.* 2007;057266(9).
452. Ussher JE, van Wilgenburg B, Hannaway RF, Ruustal K, Phalora P, Kurioka A, et al. TLR signaling in human antigen-presenting cells regulates MR1-dependent activation of MAIT cells. *Eur J Immunol.* 2016;46(7):1600–14.
453. Maleki KT, Tauriainen J, García M, Kerkman PF, Christ W, Dias J, et al. MAIT cell activation is associated with disease severity markers in acute hantavirus infection. *Cell Reports Med.* 2021;2(3).
454. Juno JA, Waruk JLM, Wragg KM, Mesa C, Lopez C, Bueti J, et al. Mucosal-associated invariant T cells are depleted and exhibit altered chemokine receptor expression and elevated granulocyte macrophage-colony stimulating factor production during end-stage renal disease. *Front Immunol.* 2018;9(MAY).
455. Godfrey DI, Koay H, Mccluskey J, Gherardin NA. The biology and functional importance of MAIT cells. *Nat Immunol.* 2019;20(September).
456. Martin E, Treiner E, Duban L, Guerri L, Laude H, Toly C, et al. Stepwise development of mait cells in mouse and human. *PLoS Biol.* 2009;7(3):0525–36.
457. Koay HF, Gherardin NA, Enders A, Loh L, Mackay LK, Almeida CF, et al. A three-stage intrathymic development pathway for the mucosal-associated invariant T cell lineage. *Nat Immunol.* 2016;17(11):1300–11.
458. Leeansyah E, Ganesh A, Quigley MF, Sönnnerborg A, Andersson J, Hunt PW, et al. Activation, exhaustion, and persistent decline of the antimicrobial MR1-restricted MAIT-cell population in chronic HIV-1 infection. *Blood.* 2013;121(7):1124–35.

459. Sobkowiak MJ, Davanian H, Heymann R, Gibbs A, Emgård J, Dias J, et al. Tissue-resident MAIT cell populations in human oral mucosa exhibit an activated profile and produce IL-17. *Eur J Immunol.* 2019;49(1):133–43.
460. Koppejan H, Jansen DTSL, Hameetman M, Thomas R, Toes REM, Van Gaalen FA. Altered composition and phenotype of mucosal-associated invariant T cells in early untreated rheumatoid arthritis. *Arthritis Res Ther.* 2019;21(1):1–7.
461. Gherardin NA, McCluskey J, Rossjohn J, Godfrey DI. The Diverse Family of MR1-Restricted T Cells. *J Immunol.* 2018;201(10):2862–71.
462. Dias J, Boulouis C, Gorin J, Biggelaar RHGA Van Den, Lal KG. functionally distinct subset developmentally related to the main CD8 + MAIT cell pool. 2018;
463. Leeansyah E, Loh L, Nixon DF, Sandberg JK. Acquisition of innate-like microbial reactivity in mucosal tissues during human fetal MAIT-cell development. *Nat Commun.* 2014;5.
464. Meierovics A, Yankelevich WJC, Cowley SC. MAIT cells are critical for optimal mucosal immune responses during in vivo pulmonary bacterial infection. *Proc Natl Acad Sci U S A.* 2013;110(33):3119–28.
465. Georgel P, Radosavljevic M, Macquin C, Bahram S. The non-conventional MHC class I MR1 molecule controls infection by *Klebsiella pneumoniae* in mice. *Mol Immunol* [Internet]. 2011;48(5):769–75. Available from: <http://dx.doi.org/10.1016/j.molimm.2010.12.002>
466. Wang H, D'Souza C, Lim XY, Kostenko L, Pediongco TJ, Eckle SBG, et al. MAIT cells protect against pulmonary *Legionella longbeachae* infection. *Nat Commun* [Internet]. 2018;9(1). Available from: <http://dx.doi.org/10.1038/s41467-018-05202-8>
467. Wilgenburg B van, Loh L, Chen Z, Pediongco TJ, Wang H, Shi M, et al. MAIT cells

- contribute to protection against lethal influenza infection in vivo. *Nat Commun.* 2018;9(1).
468. Loh L, Wang Z, Sant S, Koutsakos M, Jegaskanda S, Corbett AJ, et al. Human mucosal-associated invariant T cells contribute to antiviral influenza immunity via IL-18-dependent activation. *Proc Natl Acad Sci U S A.* 2016;113(36):10133–8.
469. Wong EB, Ndung'u T, Kasprovicz VO. The role of mucosal-associated invariant T cells in infectious diseases. *Immunology.* 2017;150(1):45–54.
470. Gold MC, Napier RJ and LDM. MR1-restricted mucosal associated invariant T (MAIT) cells in the immune response to *Mycobacterium tuberculosis*. 2016;264(1):154–66.
471. Chua W, Truscott SM, Eickhoff CS, Blazevic A, Hoft DF, Hansen TH. Polyclonal Mucosa-Associated Invariant T Cells Have Unique Innate. 2012;80(9):3256–67.
472. Salou M, Franciszkiewicz K, Lantz O. MAIT cells in infectious diseases. *Curr Opin Immunol [Internet].* 48:7–14. Available from: <http://dx.doi.org/10.1016/j.coi.2017.07.009>
473. Fernandez CS, Amarasena T, Kelleher AD, Rossjohn J, Mccluskey J, Godfrey DI, et al. MAIT cells are depleted early but retain functional cytokine expression in HIV infection. *Immunol Cell Biol.* 2015;93(2):177–88.
474. Saeidi A, Tien Tien VL, Al-Batran R, Al-Darraj HA, Tan HY, Yong YK, et al. Attrition of TCR V α 7.2+ CD161++ MAIT cells in HIV-tuberculosis co-infection is associated with elevated levels of PD-1 expression. *PLoS One.* 2015;10(4):1–14.
475. Cosgrove C, Ussher JE, Rauch A, Gärtner K, Kurioka A, Hühn MH, et al. Early and nonreversible decrease of CD161++/MAIT cells in HIV infection. *Blood.* 2013;121(6):951–61.
476. Leeansyah E, Ganesh A, Quigley MF, Sönnnerborg A, Andersson J, Hunt PW, et al.

- Activation, exhaustion, and persistent decline of the antimicrobial MR1-restricted MAIT-cell population in chronic HIV-1 infection. *Blood*. 2013;121(7):1124–35.
477. Leeansyah E, Svärd J, Dias J, Buggert M, Nyström J, Quigley MF, et al. Arming of MAIT Cell Cytolytic Antimicrobial Activity Is Induced by IL-7 and Defective in HIV-1 Infection. *PLoS Pathog*. 2015;11(8):1–23.
478. Lal KG, Kim D, Costanzo MC, Creegan M, Leeansyah E, Dias J, et al. Dynamic MAIT cell response with progressively enhanced innateness during acute HIV-1 infection. *Nat Commun* [Internet]. 2020;1–13. Available from: <http://dx.doi.org/10.1038/s41467-019-13975-9>
479. Brenchley JM, Price DA, Schacker TW, Asher TE, Silvestri G, Rao S, et al. Microbial translocation is a cause of systemic immune activation in chronic HIV infection. 2006;12(12):1365–71.
480. Solders M, Gorchs L, Tiblad E, Gidlöf S, Leeansyah E, Kaibe H. Recruitment of MAIT Cells to the Intervillous Space of the Placenta by. *Front Immunol*. 2019;10(June):1–16.
481. Juno JA, Wragg KM, Amarasena T, Meehan BS, Mak JYW, Liu L, et al. MAIT Cells Upregulate $\alpha 4\beta 7$ in Response to Acute Simian Immunodeficiency Virus/Simian HIV Infection but Are Resistant to Peripheral Depletion in Pigtail Macaques. 2020;
482. Sivo A, Su RC, Plummer FA, Ball TB. Interferon responses in HIV infection: From protection to disease. *AIDS Rev*. 2014;16(1):43–51.
483. Hirano M, Guo P, McCurley N, Schorpp M, Das S, Boehm T, et al. Evolutionary implications of a third lymphocyte lineage in lampreys. 2014;501(7467):435–8.
484. Saito H, Kranz DM, Takagaki Y, Hayday AC, Eisen HN, Tonegawa S. Complete primary structure of a heterodimeric T-cell receptor deduced from cDNA sequences. *Nature*. 1984;309(5971):757–62.

485. Vantourout P, Hayday A. Six - of - the-best : unique contributions of $\gamma\delta$ T cells to immunology. *Nat Rev Immunol*. 2013;13(February).
486. Serre K, Silva-santos B. Molecular mechanisms of differentiation of murine pro-inflammatory $\gamma\delta$ T cell subsets. 2013;4(December):1–7.
487. Chien Y, Meyer C, Bonneville M. $\gamma\delta$ T Cells : First Line of Defense and Beyond. 2014;
488. Hoft DF, Brown RM, Roodman ST. Bacille Calmette-Guérin Vaccination Enhances Human $\gamma\delta$ T Cell Responsiveness to Mycobacteria Suggestive of a Memory-Like Phenotype. 2021;
489. Deroost K, Langhorne J. Gamma / Delta T Cells and Their Role in Protection Against Malaria. 2018;9(December):1–9.
490. Ramsey JM, Tello A, Contreras CO, Ordon R, Chirino N, Rojo J, et al. Plasmodium falciparum and p. Vivax gametocyte-specific exoantigens stimulate proliferation of TCR $\gamma\delta$ lymphocytes. 2002;88(1):59–68.
491. Khairallah C, Déchanet-merville J, Capone M, Déchanet-merville J. $\gamma\delta$ T Cell-Mediated immunity to Cytomegalovirus infection. 2017;8(February).
492. Déchanet J, Merville P, Lim A, Retière C, Pitard V, Lafarge X, et al. Implication of $\gamma\delta$ T cells in the human immune response to cytomegalovirus. 1999;103(10):1437–49.
493. Wallace M, Bartz SR, Chang W, Mackenzie DA, Pauza CD. T lymphocyte responses to HIV.
494. Sebestyen Z, Prinz I, Déchanet-merville J, Silva-santos B, Kuball J. Translating gammadelta ($\gamma\delta$) T cells and their receptors into cancer cell therapies. *Nat Rev Drug Discov* [Internet]. Available from: <http://dx.doi.org/10.1038/s41573-019-0038-z>

495. Hayday AC, Pennington DJ. Key factors in the organized chaos of early T cell development. 2007;8(2):137–44.
496. Zarin P, Chen ELY, In TSH, Anderson MK, Zúñiga-pflücker JC. Gamma delta T-cell differentiation and effector function programming , TCR signal strength , when and how much ? Cell Immunol [Internet]. 2015;296(1):70–5. Available from: <http://dx.doi.org/10.1016/j.cellimm.2015.03.007>
497. Adams EJ, Gu S, Luoma AM. Human gamma delta T cells : Evolution and ligand recognition. Cell Immunol [Internet]. 2015;296(1):31–40. Available from: <http://dx.doi.org/10.1016/j.cellimm.2015.04.008>
498. Pang DJ, Neves JF, Sumaria N, Daniel J. Understanding the complexity of $\gamma\delta$ T-cell subsets in mouse and human.
499. Kabelitz D, Bender A, Schondelmaier S, Lobo MLS, Kabelitz D, Bender A, et al. Human cytotoxic lymphocytes . V . Frequency and specificity of gamma delta + cytotoxic lymphocyte precursors activated by allogeneic or autologous stimulator cells . J Immunol [Internet]. 1990;145(1550–6606):2827–32. Available from: <https://www.jimmunol.org/>
500. Brenner MB, McLean J, Dialynas DP, Strominger JL, Smith JA, Owen FL, et al. Identification of a putative second T-cell receptor. Nature. 1986;322(6075):145–9.
501. Ferrarini M, Ferrero E, Dagna L, Poggi A, Zocchi MR. Human $\gamma\delta$ T cells: A nonredundant system in the immune-surveillance against cancer. Trends Immunol. 2002;23(1):14–8.
502. Martino A, Meraviglia S, El Daker S, Dieli F, Martini F. T cells cross-link innate and adaptive immunity in mycobacterium tuberculosis infection. Clin Dev Immunol. 2011;2011.
503. Chen ZW, Letvin NL. $V\gamma 2V\delta 2^+$ T cells and anti-microbial immune responses. Microbes

- Infect. 2003;5(6):491–8.
504. Rajoriya N, Fergusson J, Leithead JA, Klenerman P. Gamma delta T-lymphocytes in hepatitis C and chronic liver disease. *Front Immunol.* 2014;5(AUG):1–9.
505. David Pauza C, Poonia B, Li H, Cairo C, Chaudhry S. $\gamma\delta$ T cells in HIV disease: Past, present, and future. *Front Immunol.* 2015;6(JAN):1–11.
506. Chen Zheng W. Immune biology of Ag-specific $\gamma\delta$ T cells in infections. *CellMol Life Sci.* 2011;68(1):2409–17.
507. Paul S, Shilpi, Lal G. Role of gamma-delta ($\gamma\delta$) T cells in autoimmunity . *J Leukoc Biol.* 2015;97(2):259–71.
508. Gogoi D, Chiplunkar S V. Targeting gamma delta T cells for cancer immunotherapy: Bench to bedside. *Indian J Med Res.* 2013;138(NOV):755–61.
509. Deniger DC, Moyes JS, Cooper LJN. Clinical applications of gamma delta T cells with multivalent immunity. *Front Immunol.* 2014;5(DEC):1–10.
510. Siegers GM, Lamb LS. Cytotoxic and Regulatory Properties of Circulating $V\delta 1 + \gamma\delta$ T Cells : A New Player on the Cell Therapy Field ? 2014;22(8):1416–22.
511. Kazen AR, Adams EJ. Evolution of the V , D , and J gene segments used in the primate $\gamma\delta$ T-cell receptor reveals a dichotomy of conservation and diversity. 2011;108(29).
512. Wang H, Lee HK, Bukowski JF, Li H, Mariuzza RA, Chen ZW, et al. Conservation of Nonpeptide Antigen Recognition by Rhesus Monkey $V\gamma 2V\delta 2$ T Cells. *J Immunol.* 2003;170:3696–706.
513. Karunakaran MM, Göbel TW. $V\gamma 9$ and $V\delta 2$ Tcell antigen receptor genes and butyrophilin 3 (*BTN3*) emerged with placental mammals and are concomitantly

- preserved in selected species like alpaca (*Vicugna pacos*). Immunogenetics. 2014;66:243–54.
514. Triebel F, Hercend T. Subpopulations of human peripheral T gamma delta lymphocytes. Immunol Today. 1989;10(6):186–8.
515. Schirmer L, Rothhammer V, Hemmer B, Korn T. Enriched CD161^{high} CCR6+ $\gamma\delta$ T cells in the cerebrospinal fluid of patients with multiple sclerosis. JAMA Neurol. 2013;70(3):345–51.
516. Morita CT, Jin C, Sarikonda G, Wang H. Nonpeptide antigens , presentation mechanisms , and immunological memory of human V g 2V d 2 T cells : discriminating friend from foe through the recognition of prenyl pyrophosphate antigens. 2007;1986(1):59–76.
517. Liuzzi AR, McLaren JE, Price DA, Eberl M. Early innate responses to pathogens : pattern recognition by unconventional human T-cells. Curr Opin Immunol [Internet]. 2015;36:31–7. Available from: <http://dx.doi.org/10.1016/j.coi.2015.06.002>
518. Harly C, Guillaume Y, Nedellec S, Peigne C, Li J, Adams EJ, et al. Key implication of CD277 / butyrophilin-3 (BTN3A) in cellular stress sensing by a major human $\gamma\delta$ T-cell subset. 2012;120(11):1–3.
519. Palakodeti A, Sandstrom A, Sundaresan L, Harly C, Nedellec S, Olive D, et al. The Molecular Basis for Modulation of HumanV γ 9V2 T Cell Responses by CD277 / Butyrophilin-3 (BTN3A) -specific. 2012;287(39):32780–90.
520. Rhodes DA, Reith W, Trowsdale J. Regulation of Immunity by Butyrophilins. Annu Rev Immunol. 2016;34:151–72.
521. Miyawaki T, Kasahara Y, Taga K, Akihiro Yachie A, Taniguchi N. Differential expression of CD45RO (UCHLI) and its Functional Relevance in two subpopulations of circulating TCR- $\gamma\delta$ + lymphocytes. 1990;171(May).

522. Lawand M, Déchanet-Merville J, Dieu-Nosjean MC. Key features of gamma-delta T-cell subsets in human diseases and their immunotherapeutic implications. *Front Immunol.* 2017;8(JUN).
523. Wesch D, Peters C, Pietschmann K, Kabelitz D. Modulation of $\gamma\delta$ T cell responses by TLR ligands. *Cell Mol Life Sci.* 2011;2357–70.
524. Pietschmann K, Beetz S, Welte S, Martens I, Gruen J, H.-H. Oberg DW, et al. Toll-Like Receptor Expression and Function in Subsets of Human cd T Lymphocytes. 2009;245–55.
525. Domae E, Hirai Y, Ikeo T, Goda S, Shimizu Y. Cytokine-mediated activation of human ex vivo-expanded V γ 9V δ 2 T cells. *Oncotarget.* 2017;8(28):45928–42.
526. Born WK, Kemal Aydintug M, O'brien RL. Diversity of $\gamma\delta$ T-cell antigens. *Cell Mol Immunol.* 2013;10(1):13–20.
527. Dimova T, Brouwer M, Gosselin F, Tassignon J, Leo O, Donner C, et al. Effector v γ 9v δ 2 t cells dominate the human fetal $\gamma\delta$ t-cell repertoire. *Proc Natl Acad Sci U S A.* 2015;112(6):E556–65.
528. Strbo N, Romero L, Alcaide M, Fischl M. Isolation and flow cytometric analysis of human endocervical gamma delta T cells. *J Vis Exp.* 2017;2017(120):1–5.
529. Falini B, Flenghi L, Pileri S, Pelicci P, Fagioli M, Martelli MF, et al. Distribution of T cells bearing different forms of the T cell receptor γ/δ in normal and pathological human tissues. *J Immunol.* 1989;143(8):2480–8.
530. Chowers BY, Holtmeier W, Harwood J, Morzycka-wroblewska E, Kagnoff MF. The Vd1 T Cell Receptor Repertoire in Human Small Intestine and Colon By Yehuda Chowers, Wolfgang Holtmeier, Julia Harwood, Ewa Morzycka-Wroblewska, and Martin F. Kagnoff. *J Exp Med.* 1994;180(July):183–90.

531. Wu J, Groh V, Spies T. T Cell Antigen Receptor Engagement and Specificity in the Recognition of Stress-Inducible MHC Class I-Related Chains by Human Epithelial $\gamma\delta$ T Cells. *J Immunol.* 2002;169(3):1236–40.
532. Stephens HAF. MICA and MICB genes: Can the enigma of their polymorphism be resolved? *Trends Immunol.* 2001;22(7):378–85.
533. Groh V, Bahram S, Bauer S, Herman A, Beauchamp M, Spies T. Cell stress-regulated human major histocompatibility complex class I gene expressed in gastrointestinal epithelium. *Proc Natl Acad Sci U S A.* 1996;93(22):12445–50.
534. Fichtner AS, Karunakaran MM, Gu S, Boughter CT, Borowska MT. Alpaca (*Vicugna pacos*), the first nonprimate species with a phosphoantigen-reactive V γ 9V δ 2 T cell subset. 2020;117(12).
535. Belmant C, Espinosa E, Poupot R, Peyrat MA, Guiraud M, Poquet Y, et al. 3-Formyl-1-butyl pyrophosphate a novel mycobacterial metabolite- activating human $\gamma\delta$ T cells. *J Biol Chem.* 1999;274(45):32079–84.
536. Hintz M, Reichenberg A, Altincicek B, Bahr U, Gschwind RM, Kollas AK, et al. Identification of (E)-4-hydroxy-3-methyl-but-2-enyl pyrophosphate as a major activator for human $\gamma\delta$ T cells in *Escherichia coli*. *FEBS Lett.* 2001;509(2):317–22.
537. Mangan BA, Dunne MR, O'Reilly VP, Dunne PJ, A. ME, O'Shea D, et al. CD1d restriction and Th1/Th2/Th17 cytokine secretion by human V δ 3 T cells. *J Immunol.* 2008;23(1):1–7.
538. Blink SE, Caldis MW, Goings GE, Harp CT, Malissen B, Prinz I, et al. $\gamma\delta$ T cell subsets play opposing roles in regulating experimental autoimmune encephalomyelitis. *Cell Immunol.* 2014 Jul;290(1):39–51.
539. Martin B, Hirota K, Cua DJ, Stockinger B, Veldhoen M. Interleukin-17-producing

- gammadelta T cells selectively expand in response to pathogen products and environmental signals. *Immunity*. 2009 Aug;31(2):321–30.
540. Petermann F, Rothhammer V, Claussen MC, Haas JD, Blanco LR, Heink S, et al. $\gamma\delta$ T cells enhance autoimmunity by restraining regulatory T cell responses via an interleukin-23-dependent mechanism. *Immunity*. 2010 Sep;33(3):351–63.
541. Riol-Blanco L, Lazarevic V, Awasthi A, Mitsdoerffer M, Wilson BS, Croxford A, et al. IL-23 receptor regulates unconventional IL-17-producing T cells that control bacterial infections. *J Immunol*. 2010 Feb;184(4):1710–20.
542. Roark CL, French JD, Taylor MA, Bendele AM, Born WK, O'Brien RL. Exacerbation of collagen-induced arthritis by oligoclonal, IL-17-producing gamma delta T cells. *J Immunol*. 2007 Oct;179(8):5576–83.
543. Welte T, Lamb J, Anderson JF, Born WK, O'Brien RL, Wang T. Role of two distinct gammadelta T cell subsets during West Nile virus infection. *FEMS Immunol Med Microbiol*. 2008 Jul;53(2):275–83.
544. Girardi M, Oppenheim DE, Steele CR, Lewis JM, Glusac E, Filler R, et al. Regulation of cutaneous malignancy by gammadelta T cells. *Science*. 2001 Oct;294(5542):605–9.
545. Jameson J, Havran WL. Skin gammadelta T-cell functions in homeostasis and wound healing. *Immunol Rev*. 2007 Feb;215:114–22.
546. Shibata K, Yamada H, Hara H, Kishihara K, Yoshikai Y. Resident Vdelta1+ gammadelta T cells control early infiltration of neutrophils after *Escherichia coli* infection via IL-17 production. *J Immunol*. 2007 Apr;178(7):4466–72.
547. Chen Y, Chou K, Fuchs E, Havran WL, Boismenu R. Protection of the intestinal mucosa by intraepithelial gamma delta T cells. *Proc Natl Acad Sci U S A*. 2002 Oct;99(22):14338–43.

548. Tsuchiya T, Fukuda S, Hamada H, Nakamura A, Kohama Y, Ishikawa H, et al. Role of gamma delta T cells in the inflammatory response of experimental colitis mice. *J Immunol*. 2003 Nov;171(10):5507–13.
549. Pietschmann K, Beetz S, Welte S, Martens I, Gruen J, Oberg H-H, et al. Toll-Like Receptor Expression and Function in Subsets of Human $\gamma\delta$ T Lymphocytes. *BASIC Immunol*. 2009;245–55.
550. Tyler CJ, Doherty DG, Moser B, Eberl M. Human V γ 9/V δ 2 T cells: Innate adaptors of the immune system. *Cell Immunol* [Internet]. 2015;296(1):10–21. Available from: <http://dx.doi.org/10.1016/j.cellimm.2015.01.008>
551. Leslie DS, Vincent MS, Spada FM, Das H, Sugita M, Morita CT, et al. CD1-mediated $\gamma\delta$ T cell maturation of dendritic cells. *J Exp Med*. 2002;196(12):1575–84.
552. McCarthy NE, Jones HA, Marks NA, Shiner RJ, Ind PW, Al-Hassi HO, et al. Inhaled allergen-driven CD1c up-regulation and enhanced antigen uptake by activated human respiratory-tract dendritic cells in atopic asthma. *Clin Exp Allergy*. 2007;37(1):72–82.
553. Lahn M, Kalataradi H, Mittelstadt P, Pflum E, Vollmer M, Cady C, et al. Early preferential stimulation of $\gamma\delta$ T cells by TNF- α . *J Immunol*. 1998;160(11):5221–30.
554. Li H, Luo K, Pauza CD. TNF- α Is a Positive Regulatory Factor for Human V γ 2V δ 2 T Cells. *J Immunol*. 2008;181(10):7131–7.
555. Do J, Visperas A, Dong C, Baldwin WM, Min B. Cutting Edge: Generation of Colitogenic Th17 CD4 T Cells Is Enhanced by IL-17 + $\gamma\delta$ T Cells. *J Immunol*. 2011;186(8):4546–50.
556. Do J, Kim S, Keslar K, Jang E, Huang E, Fairchild RL, et al. $\gamma\delta$ T Cells Coexpressing Gut Homing α 4 β 7 and α E Integrins Define a Novel Subset Promoting Intestinal Inflammation. *J Immunol*. 2017;198(2):908–15.

557. Cheung AKL, Kwok HY, Huang Y, Chen M, Mo Y, Wu X, et al. Gut-homing $\Delta 42PD1+V\delta 2$ T cells promote innate mucosal damage via TLR4 during acute HIV type 1 infection. *Nat Microbiol* [Internet]. 2017;2(10):1389–402. Available from: <http://dx.doi.org/10.1038/s41564-017-0006-5>
558. Laggner U, Di Meglio P, Perera GK, Hundhausen C, Lacy KE, Ali N, et al. Identification of a Novel Proinflammatory Human Skin-Homing $V\gamma 9V\delta 2$ T Cell Subset with a Potential Role in Psoriasis. *J Immunol*. 2011;187(5):2783–93.
559. Tyler CJ, McCarthy NE, Lindsay JO, Stagg AJ, Moser B, Eberl M. Antigen-Presenting Human $\gamma\delta$ T Cells Promote Intestinal CD4 + T Cell Expression of IL-22 and Mucosal Release of Calprotectin . *J Immunol*. 2017;198(9):3417–25.
560. Kabelitz D, Pechhold K, Bender A, Wesselborg S. Activation and Activation-Driven Death of Human γ/δ T Cells. *Immunol Rev*. 1991;(120).
561. Bryant NL, Suarez-cuervo C, Gillespie GY, Markert JM, Nabors LB, Meleth S, et al. Characterization and immunotherapeutic potential of $\gamma\delta$ T-cells in patients with glioblastoma. *Neuro Oncol*. 2009;2.
562. Argentati K, Re F, Serresi S, Tucci MG, Bartozzi B, Bernardini G. Reduced Number and Impaired Function of Circulating $\gamma\delta$ T Cells in Patients with Cutaneous Primary Melanoma. *J Invest Dermatol* [Internet]. 2003;120(5):829–34. Available from: <http://dx.doi.org/10.1046/j.1523-1747.2003.12141.x>
563. Li H, Chaudry S, Poonia B, Shao Y, Pauza CD. Depletion and dysfunction of $V\gamma 2V\delta 2$ T cells in HIV disease: Mechanisms, impacts and therapeutic implications. *Cell Mol Immunol*. 2013;10(1):42–9.
564. Wallace M, Gan Y -H, Pauza CD, Malkovsky M. Antiviral activity of primate $\gamma\delta$ T lymphocytes isolated by magnetic cell sorting. *J Med Primatol*. 1994;23(2–3):131–5.

565. Boudová S, Li H, Sajadi MM, Redfield RR, David Pauza C. Impact of persistent HIV replication on CD4 negative V γ 2V δ 2 T cells. *J Infect Dis.* 2012;205(9):1448–55.
566. Devilder M, Maillet S, Donnadieu E, Bonneville M, Scotet E, Bouyge-moreau I. Potentiation of antigen-stimulated V gamma 9V delta 2 T cell cytokine production by immature dendritic cells (DC) and reciprocal effect on DC maturation. *J Immunol.* 2006;176:1386–93.
567. Wilgenburg B Van, Scherwitzl I, Hutchinson EC, Leng T, Kurioka A, Kulicke C, et al. MAIT cells are activated during human viral infections. *Nat Publ Gr.* 2016;
568. Ussher JE, Bilton M, Attwod E, Shadwell J, Richardson R, Lara C De, et al. CD161 ++ CD8 + T cells , including the MAIT cell subset , are specifically activated by IL-12 + IL-18 in a TCR-independent manner. *Eur J Immunol.* 2014;195–203.
569. Sattler A, Dang-heine C, Reinke P, Babel N. IL-15 dependent induction of IL-18 secretion as a feedback mechanism controlling human MAIT-cell effector functions. *Eur J Immunol.* 2015;2286–98.
570. Hornung V, Rothenfusser S, Britsch S, Jahrsdörfer B, Giese T, Endres S, et al. Quantitative Expression of Toll-Like Receptor 1 – 10 mRNA in Cellular Subsets of Human Peripheral Blood Mononuclear Cells and Sensitivity to CpG Oligodeoxynucleotides. *J Immunol.* 2002;168:4531–7.
571. Zarembler KA, Godowski PJ, Alerts E. This information is current as of January 29, 2021. *J Immunol.* 2002;168:554–61.
572. Dolganiuc A, Garcia C, Kodys K, Szabo G, Dolganiuc A, Garcia C, et al. Distinct toll-like receptor expression in monocytes and T cells in chronic HCV infection. 2006;12(8):1198–204.
573. Betts MR, Brenchley JM, Kuruppu J, Khojasteh S, Perfetto S, Roederer M, et al. Toll-

- Like Receptor Ligands Modulate Dendritic Cells to Augment Cytomegalovirus- and HIV-1-Specific T Cell Responses 1. *J Immunol.* 2003;171(8):4320-4328.
574. Ueta C, Kawasumi H, Hjiwara H, Miyagawa T, Kida H, Ohmoto Y, et al. Interleukin-12 activates human $\gamma\delta$ T cells : synergistic effect of tumor necrosis factor- α . *Eur J Immunol.* 1996;30:66-73.
575. Wen L, Kubo S, Okuda A, Yamamoto H, Ueda H, Tanaka T, et al. Effect of IL-18 on Expansion of $\gamma\delta$ T Cells. *Immunotherapy.* 2010;33(3):287-96.
576. Devilder M, Allain S, Dousset C, Bonneville M, Scotet E, Cells D, et al. Early Triggering of Exclusive IFN- γ Responses of Human V γ 9V δ 2 T Cells by TLR-Activated Myeloid and Plasmacytoid Dendritic Cells. *J Immunol.* 2009;183:3625-3633;
577. Lafont V, Sanchez F, Laprevotte E, Michaud HA, Gros L, Eliaou JF, et al. Plasticity of $\gamma\delta$ T cells: Impact on the anti-tumor response. *Front Immunol.* 2014;5(DEC):1-13.
578. Wesch D, Glatzel A, Kabelitz D. Differentiation of resting human peripheral blood $\gamma\delta$ T cells toward Th1- or Th2-phenotype. *Cell Immunol.* 2001;212(2):110-7.
579. Zhao Y, Niu C, Cui J. Gamma-delta ($\gamma\delta$) T Cells: Friend or Foe in Cancer Development. *J Transl Med [Internet].* 2018;16(1):1-13. Available from: <https://doi.org/10.1186/s12967-017-1378-2>
580. Kuhl AA, Pawlowski N, Grollich K, Blessenohl M, Westermann J, Zeitz M, et al. Human peripheral $\gamma\delta$ T cells possess regulatory potential. 2009;580-8.
581. Dar AA, Patil RS, Chiplunkar SV. Insights into the relationship between toll like receptors and gamma delta T cell responses. *Front Immunol.* 2014;5(July):1-12.
582. Tang X-Z, Jo J, Tan AT, Sandalova E, Chia A, Tan KC, et al. IL-7 Licenses Activation of Human Liver Intrahepatic Mucosal-Associated Invariant T Cells. *J Immunol.*

- 2013;190(7):3142–52.
583. Billerbeck E, Kang YH, Walker L, Lockstone H, Grafmueller S, Fleming V, et al. Analysis of CD161 expression on human CD8+ T cells defines a distinct functional subset with tissue-homing properties. *Proc Natl Acad Sci U S A*. 2010;107(7):3006–11.
584. Wehrly K, Chesebro B. p24 antigen capture assay for quantification of human immunodeficiency virus using readily available inexpensive reagents. *Methods*. 1997 Aug;12(4):288–93.
585. Reantragoon R, Corbett AJ, Sakala IG, Gherardin NA, Furness JB, Chen Z, et al. Antigen-loaded MR1 tetramers define T cell receptor heterogeneity in mucosal-associated invariant T cells. *J Exp Med*. 2013;210(11):2305–20.
586. Tilloy F, Treiner E, Park SH, Garcia C, Lemonnier F, De La Salle H, et al. An invariant T cell receptor α chain defines a novel TAP-independent major histocompatibility complex class Ib-restricted α/β T cell subpopulation in mammals. *J Exp Med*. 1999;189(12):1907–21.
587. Booth JS, Salerno-Goncalves R, Blanchard TG, Patil SA, Kader HA, Safta AM, et al. Mucosal-associated invariant T cells in the human gastric mucosa and blood: Role in *Helicobacter pylori* infection. *Front Immunol*. 2015;6(SEP):1–14.
588. Bister J, Crona Guterstam Y, Strunz B, Dumitrescu B, Haij Bhattarai K, Özenci V, et al. Human endometrial MAIT cells are transiently tissue resident and respond to *Neisseria gonorrhoeae*. *Mucosal Immunol* [Internet]. 2021;14(2):357–65. Available from: <http://dx.doi.org/10.1038/s41385-020-0331-5>
589. Keller AN, Corbett AJ, Wubben JM, McCluskey J, Rossjohn J. ScienceDirect MAIT cells and MR1-antigen recognition. *Curr Opin Immunol* [Internet]. 2017;46:66–74. Available from: <http://dx.doi.org/10.1016/j.coi.2017.04.002>

590. Tynan FE, Reid HH, Kjer-Nielsen L, Miles JJ, Wilce MCJ, Kostenko L, et al. A T cell receptor flattens a bulged antigenic peptide presented by a major histocompatibility complex class I molecule. *Nat Immunol.* 2007;8(3):268–76.
591. Miles JJ, Elhassen D, Borg NA, Silins SL, Tynan FE, Burrows JM, et al. CTL Recognition of a Bulged Viral Peptide Involves Biased TCR Selection. *J Immunol.* 2005;175(6):3826–34.
592. Van Rhijn I, Kasmar A, De Jong A, Gras S, Bhati M, Doorenspleet ME, et al. A conserved human T cell population targets mycobacterial antigens presented by CD1b. *Nat Immunol.* 2013;14(7):706–13.
593. Dias J, Boulouis C, Gorin JB, Van Den Biggelaar RHGA, Lal KG, Gibbs A, et al. The CD4–CD8– MAIT cell subpopulation is a functionally distinct subset developmentally related to the main CD8+ MAIT cell pool. *Proc Natl Acad Sci U S A.* 2018;115(49):E11513–22.
594. Chien YH, Bonneville M. Gamma delta T cell receptors. *Cell Mol Life Sci.* 2006;63(18):2089–94.
595. Walker LJ, Kang Y-H, Smith MO, Tharmalingham H, Ramamurthy N, Fleming VM, et al. Human MAIT and CD8 α cells develop from a pool of type-17 precommitted CD8+ T cells. *Blood.* 2012 Jan;119(2):422–33.
596. Kurioka A, Cosgrove C, Simoni Y, van Wilgenburg B, Geremia A, Björkander S, et al. CD161 defines a functionally distinct subset of pro-inflammatory natural killer cells. *Front Immunol.* 2018;9(APR):1–14.
597. Yokobori N, Schierloh P, Geffner L, Balboa L, Romero M, Musella R, et al. CD3 expression distinguishes two $\gamma\delta$ T cell receptor subsets with different phenotype and effector function in tuberculous pleurisy. *Clin Exp Immunol.* 2009;157(3):385–94.

598. Dusseaux M, Martin E, Serriari N, Péguillet I, Premel V, Louis D, et al. Human MAIT cells are xenobiotic-resistant, tissue-targeted, CD161 hi IL-17-secreting T cells. *Blood*. 2011;117(4):1250–9.
599. Novak J, Dobrovolny J, Novakova L, Kozak T. The Decrease in Number and Change in Phenotype of Mucosal-Associated Invariant T cells in the Elderly and Differences in Men and Women of Reproductive Age. *Scand J Immunol*. 2014;80(4):271–5.
600. Parker CM, Groh V, Band H, Porcelli SA, Morita C, Fabbi M, et al. Evidence for extrathymic changes in the T cell receptor γ/δ repertoire. *J Exp Med*. 1990;171(5):1597–612.
601. Ribeiro ST, Ribot JC, Silva-Santos B. Five layers of receptor signaling in $\gamma\delta$ T-cell differentiation and activation. *Front Immunol*. 2015;6(JAN):1–9.
602. Hinton G, Roweis S. Stochastic neighbor embedding. *Adv Neural Inf Process Syst*. 2003;
603. Maaten L van der, Hinton G. Visualizing data using t-SNE. 2017;(November 2008).
604. Wallach I, Lilien R. The protein-small-molecule database, a non-redundant structural resource for the analysis of protein-ligand binding. *Bioinformatics*. 2009;25(5):615–20.
605. McInnes L, Healy J, Melville J. UMAP: Uniform Manifold Approximation and Projection for Dimension Reduction. 2018; Available from: <http://arxiv.org/abs/1802.03426>
606. Amid E, Warmuth MK. TriMap: Large-scale Dimensionality Reduction Using Triplets. 2019;1–13. Available from: <http://arxiv.org/abs/1910.00204>
607. Roelofs AJ, Jauhainen M, Mönkkönen H, Rogers MJ, Mönkkönen J, Thompson K. Peripheral blood monocytes are responsible for $\gamma\delta$ T cell activation induced by zoledronic acid through accumulation of IPP/DMAPP. *Br J Haematol*. 2009;144(2):245–50.

608. Morita CT, Lee HK, Wang H, Li H, Mariuzza RA, Tanaka Y. Structural Features of Nonpeptide Prenyl Pyrophosphates That Determine Their Antigenicity for Human $\gamma\delta$ T Cells. *J Immunol*. 2001;167(1):36–41.
609. Serrano R, Wesch D, Kabelitz D. cells Activation of Human $\gamma\delta$ T Cells : Modulation by Toll-Like Receptor 8 Ligands and Role of Monocytes. 2020;
610. Heron M, Grutters JC, van Moorsel CHM, Ruven HJT, Huizinga TWJ, van der Helm-van Mil AHM, et al. Variation in IL7R predisposes to sarcoid inflammation. *Genes Immun*. 2009;10(7):647–53.
611. MacKall CL, Fry TJ, Gress RE. Harnessing the biology of IL-7 for therapeutic application. *Nat Rev Immunol*. 2011;11(5):330–42.
612. Rochman Y, Spolski R, Leonard WJ. New insights into the regulation of T cells by $\gamma\epsilon$ family cytokines. *Nat Rev Immunol*. 2009;9(7):480–90.
613. Sarah R. Pickens, Nathan D. Chamberlain, Michael V. Volin RMP, Nicholas E Talarico, Arthur M. Mandelin II and SS. Characterization of IL-7 and IL-7R in the pathogenesis of Rheumatoid Arthritis. 2011;63(10):2884–93.
614. Penaranda C, Kuswanto W, Hofmann J, Kenefeck R, Narendran P, Walker LSK, et al. IL-7 receptor blockade reverses autoimmune diabetes by promoting inhibition of effector/memory T cells. *Proc Natl Acad Sci U S A*. 2012;109(31):12668–73.
615. Lee LF, Logronio K, Tu GH, Zhai W, Ni I, Mei L, et al. Anti-IL-7 receptor- α reverses established type 1 diabetes in nonobese diabetic mice by modulating effector T-cell function. *Proc Natl Acad Sci U S A*. 2012;109(31):12674–9.
616. Lawson BR, Gonzalez-quintial R, Eleftheriadis T, Michael A, Miller SD, Sauer K, et al. Interleukin-7 is required for CD4⁺ T cell activation and autoimmune neuroinflammation. *Publ Final Ed form as Clin Immunol*. 2015;161(2):260–9.

617. Totsuka T, Kanai T, Nemoto Y, Makita S, Okamoto R, Tsuchiya K, et al. IL-7 Is Essential for the Development and the Persistence of Chronic Colitis. *J Immunol.* 2007;178(8):4737–48.
618. Yamazaki M, Yajima T, Tanabe M, Fukui K, Okada E, Okamoto R, et al. Mucosal T Cells Expressing High Levels of IL-7 Receptor Are Potential Targets for Treatment of Chronic Colitis. *J Immunol.* 2003;171(3):1556–63.
619. Gonzalez-Quintial R, Lawson BR, Scatizzi JC, Craft J, Kono DH, Baccala R, et al. Systemic autoimmunity and lymphoproliferation are associated with excess IL-7 and inhibited by IL-7R α blockade. *PLoS One.* 2011;6(11).
620. Jin JO, Kawai T, Cha S, Yu Q. Interleukin-7 enhances the Th1 response to promote the development of Sjögren’s syndrome-like autoimmune exocrinopathy in mice. *Arthritis Rheum.* 2013;65(8):2132–42.
621. Hubrack S, Al-Nesf MA, Agrebi N, Raynaud C, Khattab MA, Thomas M, et al. In vitro Interleukin-7 treatment partially rescues MAIT cell dysfunction caused by SARS-CoV-2 infection. *Sci Rep [Internet].* 2021;11(1):1–7. Available from: <https://doi.org/10.1038/s41598-021-93536-7>
622. Hinks TSC, Zhang X. MAIT Cell Activation and Functions. *Front Immunol.* 2020;11(May):1–10.
623. Sortino O, Richards E, Dias J, Leeansyah E, Johan K, Sereti I, et al. IL-7 treatment supports CD8+ MAIT cell restoration in HIV-1 infected patients on ART. *AIDS.* 2019;
624. Fergusson JR, Smith KE, Fleming VM, Rajoriya N, Newell EW, Simmons R, et al. CD161 defines a transcriptional and functional phenotype across distinct human T cell lineages. *Cell Rep.* 2014;9(3):1075–88.
625. Fergusson J, MHHu“hn, Swadling L, Walker L, Kurioka1 A, Llibre1 A, et al.

- CD161^{int}CD8⁺ T cells: a novel population of highly functional, memory CD8⁺ T cells enriched within the gut. *Mucosal Immunol.* 2016;9(2):401–13.
626. Billerbeck E, Kang Y, Walker L, Lockstone H, Grafmueller S, Fleming V, et al. Analysis of CD161 expression on human CD8⁺ T cells defines a distinct functional subset with tissue-homing properties. 2010;107(7).
627. Galletti G, De Simone G, Mazza EMC, Puccio S, Mezzanotte C, Bi TM, et al. Two subsets of stem-like CD8⁺ memory T cell progenitors with distinct fate commitments in humans. *Nat Immunol* [Internet]. 2020;21(12):1552–62. Available from: <http://dx.doi.org/10.1038/s41590-020-0791-5>
628. Klessig DF, Dean M, Carrington M, Winkler C, Huttley GA, Smith MW, et al. Genetic Restriction of HIV-1 Infection and Progression to AIDS by a Deletion Allele of the CKR5 Structural Gene Cohort Study , Multicenter Hemophilia Cohort Study , San. 1996;(September).
629. Hashimoto K, Hirai M, Kurosawa Y. A Gene Outside the Human MHC Related to Classical HLA Class I Genes Author (s): Keiichiro Hashimoto , Momoki Hirai and Yoshikazu Kurosawa Published by : American Association for the Advancement of Science Stable URL : <http://www.jstor.org/stable/2888972>. *Science* (80-). 1995;269(5224):693–5.
630. Abós B, Gómez del Moral M, Gozalbo-López B, López-Relaño J, Viana V, Martínez-Naves E. Human MR1 expression on the cell surface is acid sensitive, proteasome independent and increases after culturing at 26°C. *Biochem Biophys Res Commun.* 2011;411(3):632–6.
631. Williams Martin, Ginhoux F, Jakubzick C, Naik SH, Onai N, Schraml BU, et al. Dendritic cells, monocytes and macrophages: a unified nomenclature based on ontogeny. *Physiol Behav.* 2014;14(8)(1):571–578.

632. León B, López-Bravo M, Ardavín C. Monocyte-derived dendritic cells. *Semin Immunol.* 2005;17(4):313–8.
633. Naik SH. *Dendritic Cell Protocols - Second Edition* [Internet]. Vol. 2. 2009. 388 p. Available from: www.springer.com/series/7651
634. Chometon TQ, Da Silva Siqueira M, Sant'anna JC, Almeida MR, Gandini M, De Almeida Nogueira ACM, et al. A protocol for rapid monocyte isolation and generation of singular human monocytederived dendritic cells. *PLoS One.* 2020;15(4):1–16.
635. Bhattacharjee J, Das B, Mishra A, Sahay P, Upadhyay P. Monocytes isolated by positive and negative magnetic sorting techniques show different molecular characteristics and immunophenotypic behaviour. *F1000Research.* 2017;6(0):2045.
636. Kasinrek W, Baumruker T, Majdic O, Knapp W, Stockinger H. CD1 molecule expression on human monocytes induced by granulocyte- macrophage colony-stimulating factor. *J Immunol.* 1993;150(2):579–84.
637. Sallusto F, Lanzavecchia A. Efficient presentation of soluble antigen by cultured human dendritic cells is maintained by granulocyte/macrophage colony-stimulating factor plus interleukin 4 and downregulated by tumor necrosis factor alpha. *J Exp Med.* 1994 Apr;179(4):1109–18.
638. Caux C, Dezutter-Dambuyant C, Schmitt D, Banchereau J. GM-CSF and TNF- α cooperate in the generation of dendritic Langerhans cells. *Nature.* 1992;360(6401):258–61.
639. Romani N, Gruner S, Brang D, Käimpfen E, Lenz A, Trockenbacher B, et al. Proliferating dendritic cell progenitors in human blood. *J Exp Med.* 1994;180(1):83–93.
640. Schuler G, Romani N. Generation of mature dendritic cells from human blood: An improved method with special regard to clinical applicability. *Adv Exp Med Biol.*

- 1997;417(96):7–13.
641. Banchereau J, Steinman RM. Dendritic cells and the control of immunity. *Nature*. 1998;392(March):245–52.
642. Steinman RM. Dendritic cells: Understanding immunogenicity. *Eur J Immunol*. 2007;37(SUPPL. 1):53–60.
643. Banchereau J, Klechevsky E, Schmitt N, Morita R, Palucka K, Ueno H. Harnessing human dendritic cell subsets to design novel vaccines. *Ann N Y Acad Sci*. 2009;1174:24–32.
644. Gozalbo-López B, Gómez del Moral M, Campos-Martín Y, Setién F, Martín P, Bellas C, et al. The MHC-related protein 1 (MR1) is expressed by a subpopulation of CD38+, IgA+ cells in the human intestinal mucosa. *Histol Histopathol*. 2009 Nov;24(11):1439–49.
645. Assier E, Marin-Esteban V, Haziot A, Maggi E, Charron D, Mooney N. TLR7/8 agonists impair monocyte-derived dendritic cell differentiation and maturation. *J Leukoc Biol*. 2007;81(1):221–8.
646. Banchereau J, Briere F, Caux C, Davoust J, Lebecque S, Liu YJ, et al. Immunobiology of dendritic cells. *Annu Rev Immunol*. 2000;18:767–811.
647. Yrlid U, Svensson M, Johansson C, Wick MJ. Salmonella infection of bone marrow-derived macrophages and dendritic cells: influence on antigen presentation and initiating an immune response. *FEMS Immunol Med Microbiol*. 2000 Apr;27(4):313–20.
648. González-Amaro R, Cortés JR, Sánchez-Madrid F, Martín P. Is CD69 an effective brake to control inflammatory diseases? *Trends Mol Med*. 2013;19(10):625–32.
649. Gibbs A, Leeansyah E, Introini A, Paquin-Proulx D, Hasselrot K, Andersson E, et al. MAIT cells reside in the female genital mucosa and are biased towards IL-17 and IL-22

- production in response to bacterial stimulation. *Mucosal Immunol.* 2017;10(1):35–45.
650. Hinks TSC, van Wilgenburg B, Wang H, Loh L, Koutsakos M, Kedzierska K, et al. Study of MAIT Cell Activation in Viral Infections In Vivo. *Methods Mol Biol.* 2020;2098:261–81.
651. Stranford SA, Joan S, Donald L, Dennis O, Sheng-Yung C, Sninsky J, et al. Lack of infection in HIV-exposed individuals is associated with a strong CD8⁺ cell noncytotoxic anti-HIV response. *Proc Natl Acad Sci USA.* 1999;96(February):1030–5.
652. Koay H-F, Godfrey DI, Pellicci DG. Development of mucosal-associated invariant T cells. *Immunol Cell Biol.* 2018 Jul;96(6):598–606.
653. Paquin-Proulx D, Avelino-Silva VI, Santos BAN, Silveira Barsotti N, Siroma F, Fernandes Ramos J, et al. MAIT cells are activated in acute Dengue virus infection and after in vitro Zika virus infection. *PLoS Negl Trop Dis.* 2018;12(1):1–15.
654. UNAIDS. Women and On, A Spotlight Girls, Adolescent Women, Young. 2019;
655. Fernandez CS, Amarasena T, Kelleher AD, Rossjohn J, McCluskey J, Godfrey DI, et al. MAIT cells are depleted early but retain functional cytokine expression in HIV infection. *Immunol Cell Biol.* 2015 Feb;93(2):177–88.
656. Dillon SM, Frank DN, Wilson CC. The gut microbiome and HIV-1 pathogenesis: a two-way street. *AIDS.* 2016 Nov;30(18):2737–51.
657. Pietschmann K, Beetz S, Welte S, Martens I, Gruen J, Oberg H-H, et al. Toll-like receptor expression and function in subsets of human gammadelta T lymphocytes. *Scand J Immunol.* 2009 Sep;70(3):245–55.
658. Reynolds JM, Dong C. Toll-like receptor regulation of effector T lymphocyte function. *Trends Immunol [Internet].* 2013;34(10):511–9. Available from:

<http://dx.doi.org/10.1016/j.it.2013.06.003>

659. Testi R, Ambrosio DD, Maria R De, Santoni A. The CD69 receptor: a multipurpose cell-surface trigger for hematopoietic cells. *Immunol Today*. 1994;69:2–6.
660. Ussher JE, Wilgenburg B Van, Hannaway RF. TLR signaling in human antigen-presenting cells regulates MR1-dependent activation of MAIT cells. 2016;1600–14.
661. Huang S, Martin E, Kim S, Yu L, Soudais C, Fremont DH, et al. MR1 antigen presentation to mucosal-associated invariant T cells was highly conserved in evolution. *Proc Natl Acad Sci U S A*. 2009 May;106(20):8290–5.
662. Fergusson JR, Smith KE, Fleming VM, Rajoriya N, Newell EW, Simmons R, et al. CD161 defines a transcriptional and functional phenotype across distinct human T cell lineages. *Cell Rep*. 2014 Nov;9(3):1075–88.
663. Lepore M, Kalinichenko A, Colone A, Paleja B, Singhal A, Tschumi A, et al. Parallel T-cell cloning and deep sequencing of human MAIT cells reveal stable oligoclonal TCR β repertoire. *Nat Commun*. 2014 May;5:3866.
664. Savage AK, Constantinides MG, Han J, Picard D, Martin E, Li B, et al. The transcription factor PLZF directs the effector program of the NKT cell lineage. *Immunity*. 2008 Sep;29(3):391–403.
665. Kaech SM, Cui W. Transcriptional control of effector and memory CD8⁺ T cell differentiation. *Nat Rev Immunol*. 2012 Nov;12(11):749–61.
666. Akimova T, Beier UH, Wang L, Levine MH, Hancock WW. Helios expression is a marker of T cell activation and proliferation. *PLoS One*. 2011;6(8):e24226.
667. Kjer-Nielsen L, Patel O, Corbett AJ, Nours LJ, Meehan B, Liu L, et al. MR1 presents microbial vitamin B metabolites to MAIT cells. *Nature*. 2012;(V).

668. Wyrożemski Ł, Sollid LM, Qiao S-W. C-type lectin-like CD161 is not a co-signalling receptor in gluten-reactive CD4 + T cells. *Scand J Immunol.* 2021 Jun;93(6):e13016.
669. Pavlovic M, Gross C, Chili C, Secher T, Treiner E. MAIT Cells Display a Specific Response to Type 1 IFN Underlying the Adjuvant Effect of TLR7/8 Ligands. *Front Immunol.* 2020;11(September):1–16.
670. Saxena V, Ghate M, Bichare S, Khan I, Majumdar R, Angadi M, et al. Increased degranulation of immune cells is associated with higher cervical viral load in HIV-infected women. *Aids.* 2018;32(14):1939–49.
671. McInally S, Wall K, Yu T, Tirouvanziam R, Kilembe W, Gilmour J, et al. Elevated levels of inflammatory plasma biomarkers are associated with risk of HIV infection. *Retrovirology* [Internet]. 2021;18(1):1–11. Available from: <https://doi.org/10.1186/s12977-021-00552-6>
672. Ishikawa Y, Yamada M, Wada N, Takahashi E, Imadome K-I. Mucosal-associated invariant T cells are activated in an interleukin-18-dependent manner in Epstein–Barr virus-associated T/natural killer cell lymphoproliferative diseases. *Clin Exp Immunol.* 2022;207(2):141–8.
673. Lamichhane R, Galvin H, Hannaway RF, de la Harpe SM, Munro F, Tyndall JDA, et al. Type I interferons are important co-stimulatory signals during T cell receptor mediated human MAIT cell activation. *Eur J Immunol.* 2020;50(2):178–91.
674. Cole S, Murray J, Simpson C, Okoye R, Tyson K, Griffiths M, et al. Interleukin (IL)-12 and IL-18 Synergize to Promote MAIT Cell IL-17A and IL-17F Production Independently of IL-23 Signaling. *Front Immunol.* 2020;11(November):1–14.
675. van Wilgenburg B, Loh L, Chen Z, Pediongco TJ, Wang H, Shi M, et al. MAIT cells contribute to protection against lethal influenza infection in vivo. *bioRxiv.* 2018;1–32.

676. Ussher JE, Bilton M, Attwod E, Shadwell J, Richardson R, de Lara C, et al. CD161⁺⁺CD8⁺ T cells, including the MAIT cell subset, are specifically activated by IL-12+IL-18 in a TCR-independent manner. *Eur J Immunol*. 2014;44(1):195–203.
677. Jo J, Tan AT, Ussher JE, Sandalova E, Tang XZ, Tan-Garcia A, et al. Toll-Like Receptor 8 Agonist and Bacteria Trigger Potent Activation of Innate Immune Cells in Human Liver. *PLoS Pathog*. 2014;10(6):1–13.
678. Leng T, Akther HD, Hackstein CP, Powell K, King T, Friedrich M, et al. TCR and Inflammatory Signals Tune Human MAIT Cells to Exert Specific Tissue Repair and Effector Functions. *Cell Rep*. 2019;28(12):3077-3091.e5.
679. Bender AT, Tzvetkov E, Pereira A, Wu Y, Kasar S, Przetak MM, et al. TLR7 and TLR8 Differentially Activate the IRF and NF- κ B Pathways in Specific Cell Types to Promote Inflammation. *ImmunoHorizons*. 2020;4(2):93–107.
680. Franciszkiewicz K, Salou M, Legoux F, Zhou Q, Cui Y, Bessoles S, et al. MHC class I-related molecule, MR1, and mucosal-associated invariant T cells. *Immunol Rev*. 2016 Jul;272(1):120–38.
681. Di Domizio J, Blum A, Gallagher-Gambarelli M, Molens JP, Chaperot L, Plumas J. TLR7 stimulation in human plasmacytoid dendritic cells leads to the induction of early IFN-inducible genes in the absence of type I IFN. *Blood*. 2009;114(9):1794–802.
682. Takagi H, Arimura K, Uto T, Fukaya T, Nakamura T, Chojjookhuu N, et al. Plasmacytoid dendritic cells orchestrate TLR7-mediated innate and adaptive immunity for the initiation of autoimmune inflammation. *Sci Rep*. 2016;6(November 2015):1–18.
683. Sakata K, Nakayamada S, Miyazaki Y, Kubo S, Ishii A, Nakano K, et al. Up-Regulation of TLR7-Mediated IFN- α Production by Plasmacytoid Dendritic Cells in Patients With Systemic Lupus Erythematosus. *Front Immunol*. 2018;9(August):1–11.

684. Lamichhane R, Galvin H, Hannaway RF, de la Harpe SM, Munro F, Tyndall JDA, et al. Type I interferons are important co-stimulatory signals during T cell receptor mediated human MAIT cell activation. *Eur J Immunol*. 2020 Feb;50(2):178–91.
685. van Wilgenburg B, Scherwitzl I, Hutchinson EC, Leng T, Kurioka A, Kulicke C, et al. MAIT cells are activated during human viral infections. *Nat Commun*. 2016 Jun;7:11653.
686. Berghöfer B, Frommer T, Haley G, Fink L, Bein G, Hackstein H. TLR7 Ligands Induce Higher IFN- α Production in Females. *J Immunol*. 2006;177(4):2088–96.
687. Nkwanyana NN, Gumbi PP, Roberts L, Denny L, Hanekom W, Soares A, et al. Impact of human immunodeficiency virus 1 infection and inflammation on the composition and yield of cervical mononuclear cells in the female genital tract. *Immunology*. 2009 Sep;128(1 Suppl):e746-57.
688. Arnold KB, Burgener A, Birse K, Romas L, Dunphy LJ, Shahabi K, et al. Increased levels of inflammatory cytokines in the female reproductive tract are associated with altered expression of proteases, mucosal barrier proteins, and an influx of HIV-susceptible target cells. *Mucosal Immunol*. 2016 Jan;9(1):194–205.
689. Wira CR, Fahey J V., Sentman CL, Pioli PA, Shen L. Innate and adaptive immunity in female genital tract: Cellular responses and interactions. *Immunol Rev*. 2005;206:306–35.
690. Li Q, Estes JD, Schlievert PM, Duan L, Brosnahan AJ, Southern PJ, et al. Glycerol monolaurate prevents mucosal SIV transmission. *Nature*. 2009;458(7241):1034–8.
691. Haase AT. Early events in sexual transmission of HIV and SIV and opportunities for interventions. *Annu Rev Med*. 2011;62:127–39.
692. Phalke SP, Chiplunkar S V. Activation status of $\gamma\delta$ T cells dictates their effect on osteoclast generation and bone resorption. *Bone Reports* [Internet]. 2015;3:95–103. Available from: <http://dx.doi.org/10.1016/j.bonr.2015.10.004>

693. Wu D, Wu P, Qiu F, Wei Q, Huang J. Human $\gamma\delta$ T-cell subsets and their involvement in tumor immunity. *Cell Mol Immunol*. 2017;14(3):245–53.
694. Adams EJ, Gu S, Luoma AM. Human gamma delta T cells: Evolution and ligand recognition. *Cell Immunol* [Internet]. 2015;296(1):31–40. Available from: <http://dx.doi.org/10.1016/j.cellimm.2015.04.008>
695. Nian H, Shao H, O'Brien RL, Born WK, Kaplan HJ, Sun D. Activated $\gamma\delta$ T cells promote the activation of uveitogenic t cells and exacerbate EAU development. *Investig Ophthalmol Vis Sci*. 2011;52(8):5920–7.
696. Serrano R, Wesch D, Kabelitz D. Activation of Human $\gamma\delta$ T Cells: Modulation by Toll-Like Receptor 8 Ligands and Role of Monocytes. *Cells*. 2020;9(713).
697. Serrano R, Wesch D, Kabelitz D. Activation of Human $\gamma\delta$ T Cells: Modulation by Toll-Like Receptor 8 Ligands and Role of Monocytes. *Cells*. 2020 Mar;9(3).
698. Domae E, Hirai Y, Ikeo T, Goda S, Shimizu Y. Cytokine-mediated activation of human ex vivo-expanded V γ 9V δ 2 T cells. *Oncotarget*. 2017 Jul;8(28):45928–42.
699. Guimond M, Veenstra RG, Grindler DJ, Zhang H, Cui Y, Murphy RD, et al. Interleukin 7 signaling in dendritic cells regulates the homeostatic proliferation and niche size of CD4+ T cells. *Nat Immunol*. 2009 Feb;10(2):149–57.
700. Sortino O, Richards E, Dias J, Leeansyah E, Sandberg JK, Sereti I. IL-7 treatment supports CD8+ mucosa-associated invariant T-cell restoration in HIV-1-infected patients on antiretroviral therapy. *AIDS*. 2018 Mar;32(6):825–8.
701. Laterre PF, François B, Collienne C, Hantson P, Jeannet R, Remy KE, et al. Association of Interleukin 7 Immunotherapy With Lymphocyte Counts Among Patients With Severe Coronavirus Disease 2019 (COVID-19). *JAMA Netw open*. 2020 Jul;3(7):e2016485.

702. Kabelitz D, Marischen L, Oberg H-H, Holtmeier W, Wesch D. Epithelial defence by gamma delta T cells. *Int Arch Allergy Immunol*. 2005 May;137(1):73–81.
703. Willcox CR, Pitard V, Netzer S, Couzi L, Salim M, Silberzahn T, et al. Cytomegalovirus and tumor stress surveillance by binding of a human $\gamma\delta$ T cell antigen receptor to endothelial protein C receptor. *Nat Immunol*. 2012;13(9):872–9.
704. Michel M-L, Pang DJ, Haque SFY, Potocnik AJ, Pennington DJ, Hayday AC. Interleukin 7 (IL-7) selectively promotes mouse and human IL-17-producing $\gamma\delta$ cells. *Proc Natl Acad Sci U S A*. 2012 Oct;109(43):17549–54.
705. Annibali V, Ristori G, Angelini DF, Serafini B, Mechelli R, Cannoni S, et al. CD161^{high}CD8⁺T cells bear pathogenetic potential in multiple sclerosis. *Brain*. 2011;134(2):542–54.
706. Oo YH, Banz V, Kavanagh D, Liaskou E, Withers DR, Humphreys E, et al. CXCR3-dependent recruitment and CCR6-mediated positioning of Th-17 cells in the inflamed liver. *J Hepatol* [Internet]. 2012;57(5):1044–51. Available from: <http://dx.doi.org/10.1016/j.jhep.2012.07.008>
707. Flament H, Rouland M, Beaudoin L, Toubal A, Bertrand L, Lebourgeois S, et al. Outcome of SARS-CoV-2 infection is linked to MAIT cell activation and cytotoxicity. *Nat Immunol* [Internet]. 2021;22(March). Available from: <http://dx.doi.org/10.1038/s41590-021-00870-z>
708. Kaplan AP. Chemokines, chemokine receptors and allergy. *Int Arch Allergy Immunol*. 2001 Apr;124(4):423–31.
709. Vilgelm AE, Richmond A. Chemokines Modulate Immune Surveillance in Tumorigenesis , Metastasis , and Response to Immunotherapy. *Front Immunol*. 2019;10(February):6–8.
710. Nagarsheth N, Wicha MS, Zou W. Chemokines in the cancer microenvironment and their

- relevance in cancer immunotherapy. *Nat Rev Immunol.* 2017 Sep;17(9):559–72.
711. Voillet V, Buggert M, Slichter CK, Berkson JD, Mair F, Addison MM, et al. Human MAIT cells exit peripheral tissues and recirculate via lymph in steady state conditions. *JCI insight.* 2018;3(7):1–10.
712. Glatzel A, Wesch D, Schiemann F, Brandt E, Janssen O, Kabelitz D. Patterns of Chemokine Receptor Expression on Peripheral Blood $\gamma\delta$ T Lymphocytes: Strong Expression of CCR5 Is a Selective Feature of V δ 2/V γ 9 $\gamma\delta$ T Cells. 2002;(16).
713. Lee CH, Zhang HH, Singh SP, Koo L, Kabat J, Tsang H, et al. C/EBP δ drives interactions between human MAIT cells and endothelial cells that are important for extravasation. *Elife.* 2018;7:1–31.
714. Patel O, Kjer-Nielsen L, Le Nours J, Eckle SBG, Birkinshaw R, Beddoe T, et al. Recognition of vitamin B metabolites by mucosal-associated invariant T cells. *Nat Commun.* 2013;4(May):1–9.
715. Toubal A, Nel I, Lotersztajn S, Lehuen A. Mucosal-associated invariant T cells and disease. *Nat Rev Immunol.* 2019 Oct;19(10):643–57.
716. Provine NM, Klenerman P. MAIT Cells in Health and Disease. *Annu Rev Immunol.* 2020 Apr;38:203–28.
717. Rahimpour A, Koay HF, Enders A, Clanchy R, Eckle SBG, Meehan B, et al. Identification of phenotypically and functionally heterogeneous mouse mucosal-associated invariant T cells using MR1 tetramers. *J Exp Med.* 2015 Jun;212(7):1095–108.
718. Chen Z, Wang H, D’Souza C, Sun S, Kostenko L, Eckle SBG, et al. Mucosal-associated invariant T-cell activation and accumulation after in vivo infection depends on microbial riboflavin synthesis and co-stimulatory signals. *Mucosal Immunol.* 2017;10(1):58–68.

719. Magalhaes I, Pingris K, Poitou C, Bessoles S, Venteclef N, Kiaf B, et al. Mucosal-associated invariant T cell alterations in obese and type 2 diabetic patients. *J Clin Invest.* 2015 Apr;125(4):1752–62.
720. Miyawaki T, Kasahara Y, Taga K, Yachie A, Taniguchi N. Differential expression of CD45RO (UCHL1) and its functional relevance in two subpopulations of circulating TCR-gamma/delta+ lymphocytes. *J Exp Med.* 1990 May;171(5):1833–8.
721. Braakman E, Sturm E, Vijverberg K, van Krimpen BA, Gratama JW, Bolhuis RLH. Expression of CD45 isoforms by fresh and activated human $\gamma\delta$ T lymphocytes and natural killer cells. *Int Immunol* [Internet]. 1991;3(7):691–7. Available from: <https://doi.org/10.1093/intimm/3.7.691>
722. Sallusto F, Kremmer E, Palermo B, Hoy A, Ponath P, Qin S, et al. Switch in chemokine receptor expression upon TCR stimulation reveals novel homing potential for recently activated T cells. *Eur J Immunol.* 1999;29(6):2037–45.
723. Juno JA, Wragg KM, Kristensen AB, Lee WS, Selva KJ, van der Sluis RM, et al. Modulation of the CCR5 Receptor/Ligand Axis by Seminal Plasma and the Utility of In Vitro versus In Vivo Models. *J Virol.* 2019 Jun;93(11).
724. Geissmann F, Dieu-Nosjean MC, Dezutter C, Valladeau J, Kayal S, Leborgne M, et al. Accumulation of immature Langerhans cells in human lymph nodes draining chronically inflamed skin. *J Exp Med.* 2002 Aug;196(4):417–30.
725. Randolph GJ, Inaba K, Robbiani DF, Steinman RM, Muller WA. Differentiation of phagocytic monocytes into lymph node dendritic cells in vivo. *Immunity.* 1999 Dec;11(6):753–61.
726. Liu YJ, Kanzler H, Soumelis V, Gilliet M. Dendritic cell lineage, plasticity and cross-regulation. *Nat Immunol.* 2001 Jul;2(7):585–9.

727. Harrieff MJ, Cansler ME, Toren KG, Canfield ET, Kwak S, Gold MC, et al. Human lung epithelial cells contain Mycobacterium tuberculosis in a late endosomal vacuole and are efficiently recognized by CD8⁺ T cells. *PLoS One*. 2014;9(5):e97515.
728. Larange A, Antonios D, Pallardy M, Kerdine-Romer S. TLR7 and TLR8 agonists trigger different signaling pathways for human dendritic cell maturation. *J Leukoc Biol*. 2009;85(4):673–83.
729. Kadowaki N, Ho S, Antonenko S, De Waal Malefyt R, Kastelein RA, Bazan F, et al. Subsets of human dendritic cell precursors express different toll-like receptors and respond to different microbial antigens. *J Exp Med*. 2001;194(6):863–9.
730. Ito T, Amakawa R, Kaisho T, Hemmi H, Tajima K, Uehira K, et al. Interferon- α and interleukin-12 are induced differentially by toll-like receptor 7 ligands in human blood dendritic cell subsets. *J Exp Med*. 2002;195(11):1507–12.
731. Towarowski A, Krug A, Britsch S, Rothenfusser S, Hornung V, Bals R, et al. Toll-like receptor expression reveals CpG DNA as a unique microbial stimulus for plasmacytoid dendritic cells which synergizes with CD40L to induce high amounts of IL-12. *Eur J Cancer*. 2001;37(SUPPL. 1):3026–37.
732. Iwasaki A, Medzhitov R. Toll-like receptor control of the adaptive immune responses. *Nat Immunol*. 2004;5(10):987–95.
733. Krug A, Towarowski A, Britsch S, Rothenfusser S, Hornung V, Bals R, et al. Toll-like receptor expression reveals CpG DNA as a unique microbial stimulus for plasmacytoid dendritic cells which synergizes with CD40 ligand to induce high amounts of IL-12. *Eur J Immunol*. 2001 Oct;31(10):3026–37.
734. Renn CN, Sanchez DJ, Ochoa MT, Legaspi AJ, Oh C-K, Liu PT, et al. TLR Activation of Langerhans Cell-Like Dendritic Cells Triggers an Antiviral Immune Response. *J Immunol*. 2006;177(1):298–305.

735. Shey MS, Balfour A, Wilkinson KA, Meintjes G. Contribution of APCs to mucosal-associated invariant T cell activation in infectious disease and cancer. *Innate Immun.* 2018 May;24(4):192–202.
736. Sriram U, Xu J, Chain RW, Varghese L, Chakhtoura M, Bennett HL, et al. IL-4 suppresses the responses to TLR7 and TLR9 stimulation and increases the permissiveness to retroviral infection of murine conventional dendritic cells. *PLoS One.* 2014;9(1).
737. Tel J, Torensma R, Figdor CG, de Vries IJM. IL-4 and IL-13 alter plasmacytoid dendritic cell responsiveness to CpG DNA and herpes simplex virus-1. *J Invest Dermatol.* 2011 Apr;131(4):900–6.
738. Phetsouphanh C, Phalora P, Hackstein C-P, Thornhill J, Munier CML, Meyerowitz J, et al. Human MAIT cells respond to and suppress HIV-1. *Elife.* 2021 Dec;10.
739. Nel I, Bertrand L, Toubal A, Lehuen A. MAIT cells, guardians of skin and mucosa? *Mucosal Immunol* [Internet]. 2021;14(4):803–14. Available from: <http://dx.doi.org/10.1038/s41385-021-00391-w>
740. Fulcher JA, Romas L, Hoffman JC, Elliott J, Saunders T, Burgener AD, et al. Highly Human Immunodeficiency Virus-Exposed Seronegative Men Have Lower Mucosal Innate Immune Reactivity. *AIDS Res Hum Retroviruses.* 2017 Aug;33(8):788–95.
741. Bai L, Yokoyama K, Watanuki S, Ishizaki H, Takeshima S nosuke, Aida Y. Development of a new recombinant p24 ELISA system for diagnosis of bovine leukemia virus in serum and milk. *Arch Virol* [Internet]. 2019;164(1):201–11. Available from: <https://doi.org/10.1007/s00705-018-4058-5>
742. Sáez-Ciri3n A, Shin SY, Versmisse P, Barr3-Sinoussi F, Pancino G. Ex vivo T cell-based HIV suppression assay to evaluate HIV-specific CD8⁺ T-cell responses. *Nat Protoc.* 2010;5(6):1033–41.

743. Passaes CPB, Bruel T, Decalf J, David A, Angin M, Monceaux V, et al. Ultrasensitive HIV-1 p24 Assay Detects Single Infected Cells and Differences in Reservoir Induction by Latency Reversal Agents. *J Virol*. 2017 Mar;91(6).
744. John-Stewart GC, Mbori-Ngacha D, Payne BL, Farquhar C, Richardson BA, Emery S, et al. HIV-1-specific cytotoxic T lymphocytes and breast milk HIV-1 transmission. *J Infect Dis*. 2009;199(6):889–98.
745. Poccia F, Gioia C, Martini F, Sacchi A, Piacentini P, Tempestilli M, et al. Zoledronic acid and interleukin-2 treatment improves immunocompetence in HIV-infected persons by activating V γ 9V δ 2 T cells. *Aids*. 2009;23(5):555–65.
746. Sabo MC, Lehman DA, Wang B, Richardson BA, Srinivasan S, Osborn L, et al. Associations between vaginal bacteria implicated in HIV acquisition risk and proinflammatory cytokines and chemokines. *Sex Transm Infect*. 2020;96(1):3–9.
747. Paul S, Lal G. Regulatory and effector functions of gamma-delta ($\gamma\delta$) T cells and their therapeutic potential in adoptive cellular therapy for cancer. *Int J Cancer*. 2016;139(5):976–85.
748. Pattacini L, Murnane PM, Kahle EM, Bolton MJ, Delrow JJ, Lingappa JR, et al. Differential regulatory T cell activity in HIV type 1-exposed seronegative individuals. *AIDS Res Hum Retroviruses*. 2013 Oct;29(10):1321–9.
749. Camara M, Dieye TN, Seydi M, Diallo AA, Fall M, Diaw PA, et al. Low-Level CD4 + T Cell Activation in HIV-Exposed Seronegative Subjects : Influence of Gender and Condom Use. 2010;835–42.
750. Rowland-Jones S, Sutton J, Ariyoshi K, Dong T, Gotch F, McAdam S, et al. HIV-specific cytotoxic T-cells in HIV-exposed but uninfected Gambian women. *Nat Med*. 1995 Jan;1(1):59–64.

751. Bulitta B, Zuschmitter W, Bernal I, Bruder D, Klawonn F, von Bergen M, et al. Proteomic definition of human mucosal-associated invariant T cells determines their unique molecular effector phenotype. *Eur J Immunol.* 2018 Aug;48(8):1336–49.

Appendix 1: List of Abbreviations

ADCC	Antibody-dependent cellular cytotoxicity
Ags	Antigens
AIDS	Acquired immunodeficiency syndrome
AP-1	Activator protein 1
APCs	Antigen presenting cells
APOBEC3	Apolipoprotein B editing complex 3
BCR	B cell receptor
BST-2	Bone marrow stromal antigen 2
BTN2A1	Butyrophilin 2A1
BTN3A1	Butyrophilin 3A
BV	Bacterial vaginosis
CCL3L1	C-C motif chemokine ligand 3 like 1
CCL3	C-C chemokine ligand 3
CCL4	C-C motif ligand 4
CCL5	C-C chemokine ligand 5
CCR4	C-C chemokine receptor 4
CCR5	C-C chemokine receptor 5
CD4	Cluster of differentiation 4
CD38	Cluster of differentiation 38
CD40L	Cluster of differentiation 40 ligand
CD69	Cluster of differentiation 69
CD70	Cluster of differentiation 70
CG	Cytosine and Guanine
CLA1+	Cutaneous Lymphocyte associated antigen 1 positive
CMC	Cervical mononuclear cells
CMV	Cytomegalovirus
CpG	Cytidine-phosphate guanosine
CTL	Cytotoxic T lymphocyte
CFLA-4	Cytotoxic T lymphocyte-associated protein 4
CR2	Complimentary receptor 2
CSW	Commercial sex worker
CXCR4	CXC chemokine receptor 4
DC	Dendritic cell
DMSO	Dimethyl sulphoxide
DN	Double negative
DNA	Deoxyribonucleic acid
dNTPs	Deoxynucleoside triphosphate
DP	Double positive
dsRNA	Double stranded RNA
ERK1/2	Extracellular signal-regulated protein kinases 1 and 2
FBS	Fetal bovine serum
FDCs	Follicular dendritic cells
FMO	Florescence minus one
Foxp3	Forkhead fox P3
FSW	Female sex worker

GalCer	Galactosylceramide
GM-CSF	Granulocyte macrophage colony stimulating factor
GP	Glycoprotein
GPI	Glycosylphosphatidylinositol
GrzB	Granzyme B
6-FP	6-formyl pterin
HESN	Highly exposed HIV-seronegative (person/individual)
HIV	Human immunodeficiency virus
HLA	Human leukocyte antigen
HMBPP	(E)-4 Hydroxy-3-methyl-but-2-enyl pyrophosphate
HPV	Human papilloma virus
HSPGs	Heparan sulfate proteoglycans
HSV	Herpes simplex virus
IDU	Intra drug users
IFNs	Interferons
IFN- γ	Interferon gamma
IgG	Immunoglobulin
IKB	I kappa B
IKK	IKB kinase
IL-1 β	Interleukin 1 beta
IL-1R	Interleukin 1 receptor
IL-7R	Interleukin 7 receptor
IL-12	Interleukin 12
IL-18	Interleukin 18
IL-12R	Interleukin 12 receptor
IL-18R	Interleukin 18 receptor
IL-23R	Interleukin 23 receptor
ILC	Innate lymphoid cells
IN	Integrase
iNKT	Invariant natural killer T cells
IP-10	Interferon gamma-induced protein 10
IPP	Isopentenyl pyrophosphate
IRAK	IL-1R associated kinase
IRF	Interferon regulatory factor
ISGs	Interferon-stimulated genes
JNK	c-Jun N-terminal kinase
Ki67	Antigen KI-67
KIRs	Killer cell immunoglobulin-like receptors
KPs	Key populations
LB	Lysogeny broth
LBP	LPS binding protein
LPS	Lipopolysaccharide
LRR	Leucine-rich repeat
LTA	Lipoteichoic acid
LTNPs	Long term non-progressors
LTR	Long terminal repeat

MA	Matrix
MAdCAM-1	Mucosal addressin cellular adhesion molecule-1
MAIT	Mucosal associated invariant T cells
MAL	MyD88 adapter-like
MAPK	Mitogen-activated Protein kinase
MCMV	Murine cytomegalovirus
MD2	Myeloid differentiation factor2
mDC	Myeloid dendritic cells
MDDC	Monocyte-derived dendritic cells
MDMs	Monocyte-derived macrophages
MHC	Major histocompatibility complex
MIC	MHC class I chain-related proteins
MIP-1 α	Macrophage inflammatory protein 1 α
MIP-1 β	Macrophage inflammatory protein one beta
mRNA	Messenger RNA
MR1	MHC class I related protein 1
MSM	Men who have sex with men
MX2	Myxovirus resistance 2
MyD88	Myeloid differentiation primary response 88
Nef	Negative regulatory factor
NEMO	Nuclear factor kappa B modulator
NF-kB	Nuclear factor kappa B
NK	Natural killer (cell)
NKG2D	Natural killer group 2D
NLRs	NOD-like receptors
NOD	Nucleotide binding oligomerization domain
5-OP-RU	5-(2-oxopropylideneamino)-6-D-ribityl amino uracil
ORF	Open reading frame
P6	Protein 6
P13K	Phosphoinositide 3-kinase
P17	Protein 17
P24	Protein 24
PAMPs	Pathogen associated molecular pattern
PAX5	Paired box gene 5
PBMCs	Peripheral blood mononuclear cells
PCR	Polymerase chain reaction
PD1	Programmed cell death protein 1
pDC	Plasmacytoid dendritic cells
PFA	Paraformaldehyde
PMA/Iono	Phorbol 12-myristate 13-acetate/ ionomycin
Poly I:C	Polyinosinedeoxycytidylic acid
PR	Protease
Pro-B cells	Progenitor B cells
PRR	Pathogen recognition receptors
PLZF	Promyelocytic leukemia zinc finger
RAG	Recombinase-activating genes

RANTES	Regulated upon activation normal T cell expressed and presumably secreted
RBCC	Ring box coiled coil domain
rGM CSF	Recombinant granulocyte macrophage colony stimulating factor
RHIM	Receptor-interacting serine/threonine-protein homotypic interaction motif domains
RIG1	Retinoic acid inducible gene 1
rIL4	Recombinant interleukin 4
RIPK1	Receptor-interacting serine/threonine-protein kinase 1
RNA	Ribonucleic acid
ROR γ	Retinoic acid-related Orphan Receptor gamma
RPM	Revolution per minute
RSV	Respiratory syncytial virus
RT	Reverse transcriptase
SAMHD1	Sterile alpha motif histidine aspartate domain containing protein 1
SDF	Stromal cell derived factor-1
SERINGS	Serine incorporator 5
SHIV	Simian human immunodeficiency virus
SIV	Simian immunodeficiency virus
SIVmac	Simian immunodeficiency virus
SLPI	Secretory leukocyte protease inhibitor
SNP	Single nucleotide polymorphism
ssRNA	Single-stranded RNA
STDs	Sexually transmitted diseases
TAB	TAK1 binding protein
TAK	TGF associated kinase
TANK	TRAF family member-associated NF-kB
Tat	Transactivator of transcription
TBK1	TANK-binding kinase 1
TCR	T-cell receptor
TGF- β	Transforming growth factor beta
Th1	helper T cell 1
Th2	helper T cell 2
Th17	helper T cell 17
Treg	Regulatory T cell
TfH	Follicular helper T cell
Th9	helper T cell 9
TICAM	TIR-domain containing molecule
TIM3	T-cell immunoglobulin domain and mucin domain 3
TIR	Toll/IL-1R homology
TIRAP	Toll/interleukin-1 domain containing adaptor protein
TLR4	Toll-like receptor
TNF- α	Tumor necrosis factor alpha
TRAF	TNF-receptor-associated factor 6
TRAM	TRIF-related adaptor molecule
TRIF	TIR-domain-containing adaptor protein-inducing IFN- β
TRIM5 α	Tripartite motif 5 alpha
Ub	Ubiquitin

ULBP	UL16 binding protein
UNAIDS	United Nations programme on HIV/AIDS
Vif	Viral infectivity protein
VIPERIN	Virus inhibitory protein, endoplasmic reticulum-associated, interferon-inducible
Vpr	Viral protein
Vpu	Viral protein u

Appendix 2 : IL-12p70 ELISA Analysis



Data Report

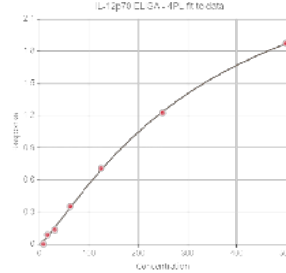


$$y = d + \frac{a - d}{1 + \left(\frac{x}{c}\right)^b}$$

a	b	c	d
0.0	1.216135	342.353617	3.048519

R² = 0.999

- a: Theoretical response at zero concentration
- b: Slope factor
- c: Inflection point (EC50/IC50)
- d: Theoretical response at infinite concentration



ID	Well(s)	Raw data	Average	Conc.	SD
U1	A3, A4	-0.086, -0.065	-0.075	Out of range	0.01
U2	B3, B4	-0.042, -0.041	-0.042	Out of range	0.001
U3	C3, C4	1.72, 0.033	0.876	162.226	0.843
U4	D3, D4	nan, nan	nan	nan	nan
U5	E3, E4	-0.074, -0.075	-0.074	Out of range	0.001
U6	F3, F4	-0.09, -0.085	-0.087	Out of range	0.002
U7	G3, G4	0.095, 0.145	0.12	24.751	0.025
U8	H3, H4	2.669, 2.645	2.657	1653.149	0.012
U9	A5, A6	-0.025, -0.022	-0.024	Out of range	0.002
U10	B5, B6	-0.09, -0.085	-0.087	Out of range	0.002
U11	C5, C6	0.806, 0.805	0.806	147.589	0.001
U12	D5, D6	3.007, 3.005	3.006	11355.228	0.001
U13	E5, E6	-0.09, -0.089	-0.089	Out of range	0.001
U14	F5, F6	-0.001, -0.005	-0.003	Out of range	0.002
U15	G5, G6	2.058, 2.06	2.059	625.388	0.001
U16	H5, H6	2.313, 2.31	2.312	876.971	0.002
U17	A7, A8	1.361, 1.362	1.361	286.868	0.001
U18	B7, B8	0.785, 0.885	0.835	153.577	0.05
C1	H1, H2	-0.064, -0.06	-0.062	Out of range	0.002
S1	A1, A2	1.515, 2.231	1.873	500.0	0.358
S2	B1, B2	1.064, 1.382	1.223	250.0	0.159
S3	C1, C2	0.593, 0.818	0.706	125.0	0.112
S4	D1, D2	0.238, 0.466	0.352	62.5	0.114
S5	E1, E2	0.103, 0.162	0.133	31.25	0.03
S6	F1, F2	0.054, 0.12	0.087	15.625	0.033
S7	G1, G2	-0.027, 0.027	0.0	7.812	0.027

This report is generated by GainData® (arigo's ELISA Calculator). <https://www.arigobio.com/ELISA-calculator>

Appendix 3: IL-18 ELISA analysis



Data Report

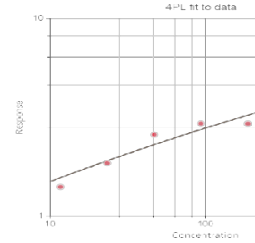


$$y = d + \frac{a - d}{1 + \left(\frac{x}{c}\right)^b}$$

a	b	c	d
0.0	0.348632	1212.794734	9.426848

R² = 0.959

- a: Theoretical response at zero concentration
- b: Slope factor
- c: Inflection point (EC50/IC50)
- d: Theoretical response at infinite concentration



ID	Well(s)	Raw data	Average	Conc.	SD
U1	A3, A4	0.147, 0.09	0.118	0.004	0.028
U2	B3, B4	0.152, 0.151	0.151	0.009	0.001
U3	C3, C4	0.131, 0.101	0.116	0.004	0.015
U4	D3, D4	0.175, 0.176	0.175	0.014	0.001
U5	E3, E4	0.12, 0.119	0.119	0.004	0.001
U6	F3, F4	0.208, 0.2	0.204	0.022	0.004
U7	G3, G4	0.072, 0.071	0.071	0.001	0.001
U8	H3, H4	0.126, 0.183	0.154	0.01	0.028
U9	A5, A6	0.133, 0.134	0.134	0.006	0.001
U10	B5, B6	0.334, 0.333	0.334	0.093	0.001
U11	C5, C6	0.142, 0.143	0.142	0.008	0.001
U12	D5, D6	0.426, 0.429	0.427	0.193	0.002
U13	E5, E6	0.127, 0.117	0.122	0.005	0.005
U14	F5, F6	0.169, 0.168	0.169	0.012	0.001
U15	G5, G6	0.32, 0.329	0.325	0.086	0.005
U16	H5, H6	0.191, 0.197	0.194	0.019	0.003
U17	A7, A8	0.1, 0.099	0.1	0.003	0.001
U18	B7, B8	0.128, 0.127	0.128	0.006	0.001
U19	C7, C8	0.077, 0.073	0.075	0.001	0.002
U20	D7, D8	0.191, 0.197	0.194	0.019	0.003
U21	E7, E8	0.113, 0.074	0.093	0.002	0.02
U22	F7, F8	0.292, 0.19	0.241	0.035	0.051
U23	G7, G8	0.179, 0.19	0.184	0.016	0.006
U24	H7, H8	0.292, 0.368	0.33	0.09	0.038
C1	H1	0.648	0.648	0.687	0.0
C2	H2	0.899	0.899	1.911	0.0
S1	A1, A2	3.55, 5.304	4.427	750.0	0.877
S2	B1, B2	3.447, 3.906	3.676	375.0	0.23
S3	C1, C2	3.048, 2.811	2.929	188.0	0.119
S4	D1, D2	2.881, 2.99	2.936	93.8	0.055
S5	E1, E2	2.851, 2.306	2.579	46.9	0.272
S6	F1, F2	1.8, 1.898	1.849	23.4	0.049
S7	G1, G2	1.46, 1.343	1.401	11.7	0.058

This report is generated by GainData® (arigo's ELISA Calculator). <https://www.arigobio.com/ELISA-calculator>

Appendix 4 : HIV-1 p24 ELISA analysis



Data Report

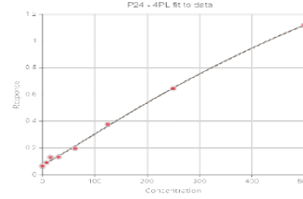


$$y = d + \frac{a - d}{1 + \left(\frac{x}{c}\right)^b}$$

a	b	c	d
0.075336	1.132035	1008.353763	3.426977

R² = 0.999

- a: Theoretical response at zero concentration
- b: Slope factor
- c: Inflection point (EC50/IC50)
- d: Theoretical response at infinite concentration



ID	Well(s)	Raw data	Average	Conc.	SD
U1	E4, E5, E6, E7	0.072, 0.109, 0.084, 0.109	0.093	9.844	0.016
U2	F4, F5, F6, F7	0.08, 0.115, 0.096, 0.147	0.11	17.939	0.025
U3	G4, G5, G6, G7	0.097, 0.104, 0.124, 0.127	0.113	19.319	0.013
U4	H4, H5, H6, H7	0.073, 0.085, 0.222, 0.147	0.132	27.853	0.059
U5	A3, H8, H9, H10, H11	0.132, 0.15, 0.181, 0.013, 0.011	0.097	11.802	0.071
U6	B3, C3, D3, E3	0.207, 0.14, 0.096, 0.057	0.125	24.744	0.056
U7	F3, G3, H2, H3	0.144, 0.107, 0.367, 0.085	0.176	46.827	0.112
U8	A12, B12, C12, H1	0.114, 0.13, 0.109, 0.278	0.158	39.156	0.07
U9	D12, E12, F12, G12	0.109, 0.09, 0.114, 0.124	0.109	17.476	0.012
U11	A8, A9, A10, A11	1.841, 1.903, 1.895, 1.997	1.909	191.508	0.056
U12	B8, B9, B10, B11	1.718, 1.827, 1.888, 1.692	1.781	1040.587	0.08
U13	C8, C9, C10, C11	1.298, 1.349, 1.341, 1.306	1.324	636.252	0.022
U14	D8, D9, D10, D11	0.409, 0.593, 0.505, 0.538	0.511	188.052	0.067
U15	E8, E9, E10, E11	0.271, 0.228, 0.23, 0.177	0.226	67.787	0.033
U16	F8, F9, F10, F11	0.153, 0.123, 0.129, 0.156	0.14	31.367	0.014
U17	G8, G9, G10, G11	0.166, 0.215, 0.131, 0.145	0.164	41.724	0.032
U18	A4, A5, A6, A7	0.077, 0.224, 0.242, 0.098	0.16	40.013	0.073
U19	B4, B5, B6, B7	0.088, 0.151, 0.121, 0.087	0.112	18.86	0.026
U20	C4, C5, C6, C7	0.184, 0.101, 0.115, 0.104	0.126	25.191	0.034
U21	D4, D5, D6, D7	0.103, 0.144, 0.082, 0.116	0.111	18.4	0.022
BL	H12	0.138	0.138	0.0	0.0
S1	A1, A2	1.165, 1.072	1.119	500.0	0.046
S2	B1, B2	0.601, 0.69	0.645	250.0	0.044
S3	C1, C2	0.354, 0.4	0.377	125.0	0.023
S4	D1, D2	0.142, 0.247	0.195	62.5	0.053
S5	E1, E2	0.124, 0.139	0.132	31.25	0.008
S6	F1, F2	0.121, 0.138	0.13	15.625	0.009
S7	G1	0.09	0.09	7.812	0.0
S8	G2	0.065	0.065	0.0	0.0

This report is generated by GainData[®] (arigo's ELISA Calculator). <https://www.arigobio.com/ELISA-calculator>

Appendix 5 : MAIT and CD4+ T cells sorting

Experiment : zippy 2019-10-24		Sort Report		Report Date : 2019.10.24 at 17:01:35	
Specimen : Specimen_001				Device : 2 Tube	
Tube : J27				User ID : Administrator	
Sort Layout : Sort Layout_001				Cytometer : FACSAriaIII (P65670000021)	
Application : FACSDiva Version 8.0.1					
Sort Settings					
Sort Setup	70 micron	Precision		4-Way Purity	
Frequency	87.0	Yield Mask			0
Amplitude	12.5	Purity Mask			32
Phase	0.00	Phase Mask			0
Drop Delay	48.55	Single Cell			Off
Attenuation	Off	Plates Voltage			4,500
Sweet Spot	On	Voltage Centering			34
First Drop	185	Sheath Pressure			70.00
Target Gap	9				
Side Stream Voltage (%)					
Far Left		Left		Right	Far Right
0.00		47.00		44.00	0.00
Neighboring Drop Charge (%)					
2nd		3rd		4th	
16.00		7.00		0.00	
Acquisition Counters					
Threshold Count					11238875
Processed Events Count(evt)					12748527
Electronic Aborts Count(evt)					229838
Sort Elapsed Time(hh:mm:ss)					00:10:15
Sort Counters					
		Left		Right	
Sort Rate(evt/s)		563		19	
Conflicts Count(evt)		90268		3276	
Conflicts Rate(evt/s)		146		5	
Efficiency(%)		79		78	
Sort Layout					
		Left		Right	
		CD4 SORT : 346403		MAIT SORT : 12249	

Appendix 5 : MAIT and CD4+ T cells sorting

Experiment : zippy 2019-10-24		Sort Report		Report Date : 2019.10.24 at 16:43:47	
Specimen : Specimen_001				Device : 2 Tube	
Tube : D165				User ID : Administrator	
Sort Layout : Sort Layout_001				Cytometer : FACSAriaIII (P65670000021)	
Application : FACSDiva Version 8.0.1					
Sort Settings					
Sort Setup	70 micron	Precision		4-Way Purity	
Frequency	87.0	Yield Mask			0
Amplitude	12.6	Purity Mask			32
Phase	0.00	Phase Mask			0
Drop Delay	48.55	Single Cell			Off
Attenuation	Off	Plates Voltage			4,500
Sweet Spot	On	Voltage Centering			34
First Drop	185	Sheath Pressure			70.00
Target Gap	9				
Side Stream Voltage (%)					
Far Left	Left	Right		Far Right	
0.00	47.00	44.00		0.00	
Neighboring Drop Charge (%)					
2nd		3rd		4th	
16.00		7.00		0.00	
Acquisition Counters					
Threshold Count					43487285
Processed Events Count(evt)					43778262
Electronic Aborts Count(evt)					1348576
Sort Elapsed Time(hh:mm:ss)					00:28:15
Sort Counters					
		Left		Right	
Sort Rate(evt/s)		943		109	
Conflicts Count(evt)		606896		73541	
Conflicts Rate(evt/s)		358		43	
Efficiency(%)		72		71	
Sort Layout					
		Left		Right	
		CD4 SORT : 1598469		MAIT SORT : 185443	

Appendix 6 : MAIT and CD4+ T cells sorting

Experiment : zippy 2019-10-24		Sort Report		Report Date : 2019.10.24 at 16:13:27	
Specimen : Specimen_001				Device : 2 Tube	
Tube : D165				User ID : Administrator	
Sort Layout : Sort Layout_001				Cytometer : FACSAriaIII (P65670000021)	
Application : FACSDiva Version 8.0.1					
Sort Settings					
Sort Setup	70 micron	Precision		4-Way Purity	
Frequency	87.0	Yield Mask			0
Amplitude	12.7	Purity Mask			32
Phase	0.00	Phase Mask			0
Drop Delay	48.55	Single Cell			Off
Attenuation	Off	Plates Voltage			4,500
Sweet Spot	On	Voltage Centering			34
First Drop	185	Sheath Pressure			70.00
Target Gap	9				
Side Stream Voltage (%)					
Far Left		Left		Right	
0.00		47.00		44.00	0.00
Neighboring Drop Charge (%)					
2nd		3rd		4th	
16.00		7.00		0.00	
Acquisition Counters					
Threshold Count				106459461	
Processed Events Count(evt)				104496928	
Electronic Aborts Count(evt)				2631462	
Sort Elapsed Time(hh:mm:ss)				01:26:39	
Sort Counters					
		Left		Right	
Sort Rate(evt/s)		645		68	
Conflicts Count(evt)		1072501		117876	
Conflicts Rate(evt/s)		206		22	
Efficiency(%)		75		75	
Sort Layout					
		Left		Right	
		CD4 SORT : 3355291		MAIT SORT : 355931	

Appendix 7: MAIT and CD4+ T cells sorting

Experiment : zippy 2019-10-24		Sort Report		Report Date : 2019.10.24 at 14:44:54	
Specimen : Specimen_001				Device : 2 Tube	
Tube : D207				User ID : Administrator	
Sort Layout : Sort Layout_001				Cytometer : FACSAriaIII (P65670000021)	
Application : FACSDiva Version 8.0.1					
Sort Settings					
Sort Setup	70 micron	Precision		4-Way Purity	
Frequency	87.0	Yield Mask			0
Amplitude	12.9	Purity Mask			32
Phase	0.00	Phase Mask			0
Drop Delay	48.55	Single Cell			Off
Attenuation	Off	Plates Voltage			4,500
Sweet Spot	On	Voltage Centering			34
First Drop	185	Sheath Pressure			70.00
Target Gap	9				
Side Stream Voltage (%)					
Far Left		Left		Right	Far Right
0.00		47.00		44.00	0.00
Neighboring Drop Charge (%)					
2nd		3rd		4th	
16.00		7.00		0.00	
Acquisition Counters					
Threshold Count				106435878	
Processed Events Count(evt)				105062787	
Electronic Aborts Count(evt)				3538363	
Sort Elapsed Time(hh:mm:ss)				01:13:07	
Sort Counters					
		Left		Right	
Sort Rate(evt/s)		1397		31	
Conflicts Count(evt)		2410875		58352	
Conflicts Rate(evt/s)		549		13	
Efficiency(%)		71		70	
Sort Layout					
		Left		Right	
		CD4 SORT : 6131806		MAIT SORT : 136251	

Appendix 8: MAIT and CD4+ T cells sorting

Experiment : zippy 2019-10-24		Sort Report		Report Date : 2019.10.24 at 13:23:05	
Specimen : Specimen_001				Device : 2 Tube	
Tube : D207				User ID : Administrator	
Sort Layout : Sort Layout_001				Cytometer : FACSAriaIII (P65670000021)	
Application : FACSDiva Version 8.0.1					
Sort Settings					
Sort Setup	70 micron	Precision		4-Way Purity	
Frequency	87.0	Yield Mask			0
Amplitude	13.1	Purity Mask			32
Phase	0.00	Phase Mask			0
Drop Delay	48.55	Single Cell			Off
Attenuation	Off	Plates Voltage			4,500
Sweet Spot	On	Voltage Centering			34
First Drop	185	Sheath Pressure			70.00
Target Gap	9				
Side Stream Voltage (%)					
Far Left		Left		Right	Far Right
0.00		47.00		44.00	0.00
Neighboring Drop Charge (%)					
2nd		3rd		4th	
16.00		7.00		0.00	
Acquisition Counters					
Threshold Count				120598550	
Processed Events Count(evt)				120787096	
Electronic Aborts Count(evt)				2954627	
Sort Elapsed Time(hh:mm:ss)				01:44:18	
Sort Counters					
		Left		Right	
Sort Rate(evt/s)		1161		25	
Conflicts Count(evt)		2141442		51754	
Conflicts Rate(evt/s)		342		8	
Efficiency(%)		77		75	
Sort Layout					
		Left		Right	
		CD4 SORT : 7265783		MAIT SORT : 161307	